



<https://theses.gla.ac.uk/>

Theses Digitisation:

<https://www.gla.ac.uk/myglasgow/research/enlighten/theses/digitisation/>

This is a digitised version of the original print thesis.

Copyright and moral rights for this work are retained by the author

A copy can be downloaded for personal non-commercial research or study, without prior permission or charge

This work cannot be reproduced or quoted extensively from without first obtaining permission in writing from the author

The content must not be changed in any way or sold commercially in any format or medium without the formal permission of the author

When referring to this work, full bibliographic details including the author, title, awarding institution and date of the thesis must be given

Enlighten: Theses

<https://theses.gla.ac.uk/>  
[research-enlighten@glasgow.ac.uk](mailto:research-enlighten@glasgow.ac.uk)

# **Studies of the Function and Regulation of Vasodilator-Stimulated Phosphoprotein**

A thesis submitted to the University of Glasgow  
for the degree of

Doctor of Philosophy

by

Susan Margaret CRAIL, B.Sc, MB BS, MRCP

Division of Immunology, Infection and Inflammation  
Faculty of Medicine  
University of Glasgow

**October 2005**

ProQuest Number: 10753978

All rights reserved

INFORMATION TO ALL USERS

The quality of this reproduction is dependent upon the quality of the copy submitted.

In the unlikely event that the author did not send a complete manuscript and there are missing pages, these will be noted. Also, if material had to be removed, a note will indicate the deletion.



ProQuest 10753978

Published by ProQuest LLC (2018). Copyright of the Dissertation is held by the Author.

All rights reserved.

This work is protected against unauthorized copying under Title 17, United States Code  
Microform Edition © ProQuest LLC.

ProQuest LLC.  
789 East Eisenhower Parkway  
P.O. Box 1346  
Ann Arbor, MI 48106 – 1346

GLASGOW  
UNIVERSITY  
LIBRARY:

## Summary

Sepsis-induced renal failure is associated with damage to the proximal epithelial tubule and is associated with disruption of the actin cytoskeleton and cell shedding. Nitric oxide is associated with the changes induced by pro-inflammatory cytokines in early sepsis. We hypothesised that it acts via phosphorylation of vasodilator-stimulated phosphoprotein (VASP) altering its ability to act as a link between cell:cell and cell:matrix junctions and the actin cytoskeleton.

Transfection of iNOS into epithelial cells was associated with a loss of VASP from its normal location at the cell membrane and with disruption of the actin cytoskeleton. Immunoblotting revealed that iNOS transfection was associated with a rise in the cGMP-dependent protein kinase preferred phosphorylation site at Ser239, a region close to G-actin binding and F-actin polymerising domains. We also showed that Ser239 phosphorylation was only seen when Ser157 phosphorylation had already occurred, that it was a transient effect and that it was nitric oxide dependent. We hypothesised that this was due to a conformational change in VASP and that Ser239 phosphorylation was dependent on the level of Ser157-phosphorylated VASP available. This was demonstrated in RAW 264.7 macrophages in which very high levels of Ser157 are achievable.

Given the permissive effect of Ser157 phosphorylation on Ser239 phosphorylation, we investigated the effects of cAMP on this as the Ser157 site has been demonstrated to be preferentially phosphorylated via cAMP-dependent protein kinase. The addition of cAMP alone was not associated with an increase in Ser239 phosphorylation. However, when given to iNOS transfected cells, prolongation of the presence of the dually

phosphorylated form of VASP was seen. We therefore proposed that the interaction of both cyclic nucleotide-dependent protein kinase pathways is important in the control of VASP phosphorylation.

VASP is present at highly dynamic areas of the cell membrane such as lamellopodia and is important in cell motility. We hypothesised that it would be important in the formation of new epithelial sheets following injury. To investigate this we used a dominant-negative form of VASP (DN-VASP) consisting of amino acids 277-383 of the full-length protein. Expression of DN-VASP in a preformed epithelial monolayer did not appear to be associated with breakdown of the sheet even though it did disrupt actin fibres. However, expression of DN-VASP in a newly forming sheet did appear to be involved with cell loss and a reduced ability to adhere to the sub-stratum. Therefore, VASP may be of greater importance in the formation of an epithelial sheet than in maintenance of its integrity.

The ability of the actin cytoskeleton to reorganise in response to external stimuli is also of crucial importance in T cell activation. A T cell adaptor protein, ADAP contains an EVH 1 binding domain and is therefore capable of binding VASP. ADAP and VASP are amongst a group of proteins that are localised to the T cell: antigen presenting cell interface. ADAP knockouts show a decreased ability to cluster the integrin LFA-1 to the immunological synapse following stimulation. We investigated the effects of disrupting VASP function in T cells via the use of DN-VASP.

Transfection of DN-VASP into T cells was associated with an inability to polarise actin in response to TCR ligation and a significant decrease in interleukin-2 production.

However it was not associated with a decrease in the ability to bind to beads coated with the LFA-1 ligand, ICAM-1. We further investigated the effects of DN-VASP transfection on signal transduction pathways and demonstrated that it appears to disrupt MAP kinase activation though not through phosphorylation of early steps of the cascade. It did not appear to have as great an effect on NFAT and NF- $\kappa$ B pathways. We hypothesised that VASP is important in T cell activation via its effects on signal transduction and that, *in vivo* these effects may be modulated through phosphorylation of VASP.

In summary, this work shows that VASP is affected by NO-induced phosphorylation and that appears to be more complex than first expected, involving cAMP-dependent pathways also. VASP appears to be important in the formation of new epithelial sheets but is of less importance in a pre-formed monolayer. VASP also appears crucial to T cell activation and DN-VASP appears to induce T cell anergy, specifically disrupting MAP kinase pathways.

## **Acknowledgements**

First and foremost, I would like to thank my supervisor, Professor Tom Evans, for his unflagging patience, enthusiasm and support during this project. I would also like to thank the other members of the group, Jo Picot, Rick Fielding, Katie Darling, Fi Stirling, Susan Lindsay and Michelle Bellingham for their help at all times. I am also grateful to Dr Alison Michie and Professor Allan Mowat for their advice about the immunological aspects of this work. This work would not have been possible without the financial support of the Wellcome Trust. Finally I would like to thank my Mum and Dad for their love and support. They always knew I could achieve this, even when I had doubts.

## **Index**

	<b>Page</b>
<b>Summary</b>	<b>2</b>
<b>Acknowledgments</b>	<b>5</b>
<b>Index</b>	<b>6</b>
<b>List of Figures</b>	<b>14</b>
<b>List of Tables</b>	<b>18</b>
<b>List of publications arising from the present study</b>	<b>19</b>
<b>Abbreviations</b>	<b>20</b>

## **Chapter 1 General Introduction**

<b>1.1 Introduction</b>	<b>24</b>
<b>1.2 The Kidney</b>	<b>25</b>
1.2.1 Anatomy of the proximal tubule	25
1.2.2 Proximal tubule epithelial cells (PTEC)	26
<b>1.3 Tubulogenesis</b>	<b>28</b>
<b>1.4 Sepsis-associated acute renal failure</b>	<b>33</b>
1.4.1 Definition of sepsis and septic shock	33
1.4.2 Acute renal failure and sepsis	33
1.4.3 Pathophysiology of sepsis-associated ARF	35
<b>1.5 Nitric Oxide</b>	<b>37</b>
1.5.1 Nitric oxide and the kidney	37
1.5.2 The nitric oxide synthases	38
<b>1.6 The actin cytoskeleton</b>	<b>41</b>
1.6.1 Function of the actin cytoskeleton	41

1.6.2	The actin cytoskeleton in epithelial cell motility and migration	42
1.6.3	Control of actin polymerisation	42
1.7	Vasodilator-stimulated phosphoprotein	43
1.7.1	Localisation and role of VASP	43
1.7.2	VASP and the kinetics of actin polymerisation	46
1.7.3	Structure of Ena/VASP proteins	48
1.7.3.1	Ena/VASP homology domain 1 (EVH 1)	48
1.7.3.2	Central proline-rich domain	51
1.7.3.3	Ena/VASP homology domain 2 (EVH 2)	51
1.7.4	Cyclic nucleotide-dependent sites in VASP	52
1.8	VASP in non-epithelial cells	58
1.8.1	VASP and phagocytosis	58
1.8.2	VASP in T cell activation	59
1.8.2.1	T cell adhesion, integrins and actin cytoskeleton reorganisation	60
1.8.2.2	Adhesion and degranulation-promoting protein (ADAP)	62
1.8.2.3	A potential role for VASP in T cell activation	65
1.9	Aims of the project	68

## **Chapter 2 Nitric Oxide and VASP phosphorylation in epithelial cells and macrophages**

2.1	Introduction	71
2.2	Methods	74
2.2.1	Cell culture of normal human bronchial epithelial (NHBE) cells	74
2.2.2	Cell culture of RAW 264.7 macrophages	74

2.2.3 Cell culture of MDCK TetOff cells	75
2.2.4 Preparation and characterisation of primary human PTEC	75
2.2.4.1 Reagents	75
2.2.4.2 Preparation of matrix substrate	75
2.2.4.3 Serum-free, hormonally defined media	76
2.2.4.4 Preparation, culture and passage of HPTEC	76
2.2.4.5 Immunofluorescent staining of HPTEC	77
2.2.4.5.1 Cytokeratin staining	78
2.2.4.5.2 iNOS induction and staining	78
2.2.5 Distribution of VASP and actin in HPTEC	78
2.2.6 The effects of iNOS transfection on VASP localisation in HPTEC	79
2.2.6.1 Transfection protocol	79
2.2.6.2 Immunostaining protocol	79
2.2.7 Effects of iNOS transfection on VASP phosphorylation in bronchial epithelial cells and HPTEC	80
2.2.7.1 Transfection and lysis	80
2.2.7.2 Measurement of NO production	81
2.2.7.3 Sodium dodecyl sulfate (SDS)-polyacrylamide gel electrophoresis and immunoblotting	82
2.2.7.4 Membrane stripping	83
2.2.8 Induction of iNOS in RAW cells by pro-inflammatory cytokines: The effects on VASP phosphorylation	83
2.2.9 Effects of nitric oxide donors on VASP phosphorylation in HPTEC	84
2.2.10 Effects of a cell permeable cGMP analog on VASP phosphorylation in NHBEs	84

2.2.11 Effects of addition of a cell permeable cAMP analog to iNOS	
transfected NHBEs	85
2.2.12 Production of a Ser239-Ala VASP mutant	85
2.2.12.1 Extraction of VASP cDNA	86
2.2.12.2 Site-directed mutagenesis of Ser239 residue to alanine	86
2.2.13 Localisation of VASP and VASP Ser239-Ala mutant in HPTEC:	
Effects of iNOS cotransfection	87
2.2.13.1 Transfection protocol	87
2.2.13.2 Immunostaining protocol	88
2.2.14 Transfection and production of a stable pTRE2hyg/iNOS clone of	
MDCK TetOff cells	88
2.2.14.1 Production of pTRE2hyg/iNOS construct	89
2.2.14.2 Electrical transformation of bacteria with	
pTRE2hyg/iNOS	89
2.2.14.3 Transfection of MDCK TetOff cells with	
pTRE2hyg/iNOS	90
2.2.14.4 Cloning of pTRE2hyg/iNOS transfected MDCK	
TetOff cells	90
2.2.14.5 Construction of a hygromycin kill curve	91
2.3 Results	92
2.3.1 HPTEC in culture demonstrate epithelial pattern cytokeratin staining	
and iNOS staining following cytokine stimulation	92
2.3.2 VASP localisation in HPTEC	92
2.3.4 iNOS expression causes loss of VASP from focal sites at the	

cell membrane	94
2.3.5 Nitric oxide, cGMP and VASP phosphorylation	98
2.3.6 The effects of addition of a cAMP analog to iNOS-transfected cells	108
2.3.7 Distribution of His-tagged VASP and Ser239-Ala VASP in HPTEC	110
2.3.8 Transfection and cloning of pTRE2hyg/iNOS in MDCK	
TetOff cells	112
2.4 Discussion	114

### **Chapter 3. The effects of dominant-negative VASP on epithelial sheet formation**

3.1 Introduction	122
3.2 Methods	127
3.2.1 Immunofluorescent staining of native VASP in MDCK TetOff cells	127
3.2.2 Production of dominant-negative VASP (DN-VASP)	127
3.2.2.1 Polymerase chain reaction (PCR) protocol	127
3.2.2.2 Insertion of DN-VASP into a regulatable plasmid	128
3.2.3 Expression of DN-VASP in MDCK TetOff cells	130
3.2.3.1 Detection with immunoblotting	130
3.2.3.2 Detection with Immunofluorescence	131
3.2.4 The effects of DN-VASP transfection on the formation of an epithelial sheet and the presence of actin fibres	132
3.2.5 Establishment of a 3-dimensional model to investigate VASP distribution	134
3.2.5.1 Culture of tubules	134
3.2.5.2 Immunostaining of tubules in collagen matrices	134

3.2.6 Cloning of pTRE2hyg/DN-VASP stable transfectants	135
3.2.7 DN-VASP expression by stable transfectants	136
3.3 Results	137
3.3.1 DNA sequencing of DN-VASP	137
3.3.2 Distribution of native VASP in MDCK TetOff cells	137
3.3.3 Expression of DN-VASP in MDCK TetOff cells	139
3.3.4 Detection of DN-VASP by immunoblotting	142
3.3.5 DN-VASP expression decreases actin fibre formation	144
3.3.6 Effects of DN-VASP transfection on the ability of cells to readhere to the cell sub-stratum	146
3.3.7 The effects of DN-VASP transfection on the formation of an epithelial sheet	149
3.3.8 Establishment of a 3D tubule model to investigate tubule formation and breakdown	153
3.4 Discussion	157

## **Chapter 4. The effects of dominant-negative VASP on T cell activation**

4.1 Introduction	162
4.2 Methods	167
4.2.1 Culture of Jurkat TetOff cells	167
4.2.2 Optimisation of Jurkat TetOff cell transfection	167
4.2.3 Time course of expression of DN-VASP in Jurkat TetOff cells	168
4.2.4 The effects of DN-VASP transfection on interleukin-2 and interferon- $\gamma$ expression in Jurkat TetOff cells	169
4.2.4.1 Transfection and stimulation	169

4.2.4.2 IL-2 and IFN- $\gamma$ enzyme-linked immunosorbent assay (ELISA)	170
4.2.5 The effects of DN-VASP transfection on CD69 and CD25 expression by Jurkat TetOff cells	171
4.2.6 The effects of DN-VASP Transfection on signal transduction pathways in Jurkat TetOff cells	172
4.2.6.1 Transfection protocols	176
4.2.6.2 Extraction of luciferase	178
4.2.6.3 Luciferase activity assay	178
4.2.7 The effects of DN-VASP on calcium flux in Jurkat TetOff cells	179
4.2.8 The effects of DN-VASP transfection on phosphorylation of early MAP kinase signal pathways	180
4.2.9 The effects of DN-VASP on actin polymerisation in Jurkat TetOff cells	181
4.2.10 The effects of DN-VASP transfection on primary T cell binding	184
4.2.10.1 Isolation of human T cells	184
4.2.10.2 Transfection of primary T cells	185
4.2.10.3 Binding assay	186
4.3 Results	187
4.3.1 Optimisation of transfection	187
4.3.2 Time course of DN-VASP expression	189
4.3.3 The effects of DN-VASP transfection on IL-2 and IFN- $\gamma$ production by Jurkat TetOff cells	192
4.3.4 The effects of DN-VASP transfection on CD69 and CD25 expression by Jurkat TetOff cells	197

4.3.5 The effects of DN-VASP transfection on signal transduction pathways in Jurkat TetOff cells	200
4.3.6 The effects of DN-VASP transfection on calcium flux in Jurkat TetOff cells	204
4.3.7 The effects of DN-VASP on early signal transduction pathways	206
4.3.8 DN-VASP transfection reduces actin collar formation and actin polarisation in Jurkat TetOff cells	208
4.3.9 DN-VASP transfection reduces the contact between CD3/CD28 coated beads and Jurkat TetOff cells	210
4.3.10 The effects of DN-VASP on primary T cell adhesion	212
4.4 Discussion	215
<b>Chapter 5 Conclusions</b>	
5.1 Summary of results	224
5.2 Biological implications and future work	225
<b>References</b>	230
<b>Appendix</b>	
Appendix 1. Plasmids used in signal transduction pathway experiments in Jurkat TetOff cells	272

## List of Figures

### Chapter One

Figure 1.1	The nephron	26
Figure 1.2	Basic epithelial cell structure	27
Figure 1.3	Development of tubules by MDCK cells following HGF stimulation	32
Figure 1.4	Renal histology	36
Figure 1.5	Domain structure of the nitric oxide synthases	40
Figure 1.6	Structure of an epithelial adherens junction	45
Figure 1.7	Three domain structure of VASP	49
Figure 1.8	Structure and homology of the Ena/VASP proteins	53
Figure 1.9	Possible pathways of cyclic nucleotide-controlled VASP phosphorylation	56
Figure 1.10	ADAP domain structure and protein binding affinities	64
Figure 1.11	Potential role for VASP in T cell activation	67

### Chapter Two

Figure 2.1	Cytokeratin staining in HPTEC	93
Figure 2.2	iNOS expression in HPTEC following cytokine stimulation	93
Figure 2.3	Co-localisation of VASP and actin in HPTEC	94
Figure 2.4	The effects of iNOS expression on VASP localisation in HPTEC	96
Figure 2.5	iNOS expression leads to a decrease in the mean	

	number of focal adhesion sites in VASP	97
Figure 2.6	VASP phosphorylation following the administration of NO donors to bronchial epithelial cells	99
Figure 2.7	VASP phosphorylation at Ser239 in bronchial epithelial Cells following the administration of 8 Br-cGMP	100
Figure 2.8	VASP phosphorylation following iNOS transfection	102
Figure 2.9	Inhibition of nitrite production by iNOS inhibitors	103
Figure 2.10	VASP phosphorylation in RAW cells following iNOS induction	105
Figure 2.11	VASP phosphorylation in HPTEC following iNOS transfection	107
Figure 2.12	iNOS transfection with or without costimulation with 8 Br-cAMP: Effects on VASP phosphorylation	109
Figure 2.13	Distribution of VASP and the Ser239-Ala mutant in HPTEC	111
Figure 2.14	Expression of iNOS in MDCK TetOff cells following transfection with pTRE2hyg/iNOS: Effects of doxycycline suppression	113

### **Chapter Three**

Figure 3.1	The TetOff system	124
Figure 3.2	Protocol for investigating the effects of replating DN-VASP transfected cells	133
Figure 3.3	Distribution of native VASP in MDCK TetOff cells	138
Figure 3.4	Detection of DN-VASP by immunofluorescence	141

Figure 3.5	DN-VASP expression in MDCK TetOff cells	143
Figure 3.6	The presence of DN-VASP expression inhibits actin fibre formation	145
Figure 3.7	The effects of replating cells transfected with DN-VASP	148
Figure 3.8	Distribution of MDCK TetOff cells transfected <i>in situ</i> with DN-VASP	151
Figure 3.9	Distribution of DN-VASP expressing MDCK TetOff cells subjected to detachment and reattachment	152
Figure 3.10	MDCK cells in collagen gels following HGF stimulation	154
Figure 3.11	Confocal images of MDCK cells in collagen gels	
 <b>Chapter Four</b>		
Figure 4.1	T cell receptor signalling pathways	165
Figure 4.2	PathDetect <i>cis</i> -reporter system	174
Figure 4.3	PathDetect <i>trans</i> -reporter system	175
Figure 4.4	Calculation of contact between cell and bead	183
Figure 4.5	Electroporation of Jurkat TetOff cells with pMaxGFP using the Amaxa Nucleofector	188
Figure 4.6	Expression of DN-VASP following transfection in Jurkat TetOff cells	191
Figure 4.7	The effects of DN-VASP transfection on interleukin-2 and interferon- $\gamma$ production by Jurkat TetOff cells	193
Figure 4.8	The effects of doxycycline on IL-2 production by Jurkat TetOff cells following CD3/CD28 stimulation	196

<b>Figure 4.9</b>	<b>The effects of DN-VASP transfection (V) vs empty vector transfection on CD69 and CD25 expression</b>	<b>198</b>
<b>Figure 4.10</b>	<b>Flow cytometry data: Effects of DN-VASP transfection on CD69 and CD 25 expression</b>	<b>199</b>
<b>Figure 4.11</b>	<b>The effects of DN-VASP transfection on the activation of NF-<math>\kappa</math>B and CREB pathways</b>	<b>201</b>
<b>Figure 4.12</b>	<b>The effects of DN-VASP transfection on NFAT and AP-1 signal transduction pathway activation</b>	<b>203</b>
<b>Figure 4.13</b>	<b>The effects of DN-VASP transfection on calcium flux in Jurkat TetOff cells</b>	<b>205</b>
<b>Figure 4.14</b>	<b>The effects of DN-VASP on early MAPK phosphorylation</b>	<b>207</b>
<b>Figure 4.15</b>	<b>The effects of DN-VASP transfection on actin cuff formation and cytoskeleton polarisation in Jurkat TetOff cells</b>	<b>209</b>
<b>Figure 4.16</b>	<b>The effects of DN-VASP transfection on the length of anti-CD3/CD28 coated bead: cell contact</b>	<b>211</b>
<b>Figure 4.17</b>	<b>ICAM-1 coated bead binding by primary T cells</b>	<b>213</b>
<b>Figure 4.18</b>	<b>The effects of DN-VASP on the ability of primary T cells to bind to ICAM-1 coated beads</b>	<b>214</b>
<b>Figure 4.19</b>	<b>Potential site of VASP involvement in signal transduction in T cells following TCR ligation</b>	<b>220</b>

## List of Tables

### Chapter One

Table 1.1	Classification of sepsis syndromes	33
Table 1.2	Percentage identity between members of the Ena/VASP family	48
Table 1.3	Phosphodiesterase substrate specificity and regulation	55

### Chapter Four

Table 4.1	<i>cis</i> -reporting system plasmids	176
Table 4.2	Protocol for <i>cis</i> -system transfections	176
Table 4.3	<i>trans</i> -reporting system plasmids	176
Table 4.4	Protocol for <i>trans</i> system transfections	177
Table 4.5	Transfection and stimulation conditions for signal transduction pathway experiments	177
Table 4.6	Transfection efficiency of Jurkat TetOff cells	188

## **Publications arising from this work**

### **Meeting Posters and Abstracts**

1. **Susan M Crail & Thomas J. Evans. (2005).** The role of vasodilator-stimulated phosphoprotein in renal tubule epithelial sheet formation. Poster presentation at the World Congress of Nephrology, Singapore.
2. **Susan M Crail & Thomas J Evans (2003)** The effects of iNOS induction on the phosphorylation of VASP in human proximal tubule epithelial cells. Abstract and poster presentation at the World Congress of Nephrology, Berlin. *Nephrol. Dial. Transplant.* 18 S4: 574.
3. **Susan M Crail & Thomas J Evans. (2003)** The role of VASP in epithelial sheet formation. Poster presentation at the Medical Research Society Meeting for Clinician Scientists in Training, London

### **Oral Presentations**

1. Acute Renal Failure in Sepsis. Brighton School of Pharmacy, May 2003
2. VASP, iNOS and epithelial cell shedding: A role in ATN? Scottish Renal Association, November 2004

## **Abbreviations**

<b>Abl</b>	<b>Abelson tyrosine kinase</b>
<b>ADAP</b>	<b>Adhesion and degranulation adaptor protein</b>
<b>AKAP</b>	<b>A-kinase anchoring protein</b>
<b>ALL</b>	<b>Acute lymphoblastic leukaemia</b>
<b>AP-1</b>	<b>Activating Protein-1</b>
<b>ARF</b>	<b>Acute renal failure</b>
<b>ATN</b>	<b>Acute tubular necrosis</b>
<b>ATP</b>	<b>Adenosine triphosphate</b>
<b>cAMP</b>	<b>cyclic adenosine monophosphate</b>
<b>cGMP</b>	<b>cyclic guanosine monophosphate</b>
<b>CREB</b>	<b>cAMP-response element binding factor</b>
<b>DAPI</b>	<b>4,6-Diaminidino-2-phenylindole</b>
<b>DNA</b>	<b>Deoxyribose nucleic acid</b>
<b>DN-VASP</b>	<b>Dominant-negative VASP</b>
<b>EBP50</b>	<b>Ezrin-radixin-moesin binding phosphoprotein 50</b>
<b>ECM</b>	<b>Extracellular matrix</b>
<b>EGF</b>	<b>Epidermal growth factor</b>
<b>eNOS</b>	<b>endothelial nitric oxide synthase</b>
<b>ERK</b>	<b>Extracellular signal regulated kinase</b>
<b>EVH</b>	<b>Ena/VASP homology domain</b>
<b>EVL</b>	<b>Ena/VASP-like protein</b>
<b>FACS</b>	<b>Fluorescence activated cell sorter</b>
<b>GFP</b>	<b>Green fluorescent protein</b>

HGF	Hepatocyte growth factor
HPTEC	Human proximal tubule epithelial cells
IFN	Interferon- $\gamma$
IL-1	Interleukin-1
iNOS	inducible nitric oxide synthase
JGA	Juxta-glomerular apparatus
JNK	c-Jun N terminal kinase
kDa	kilodaltons
LFA	Lymphocyte function associated molecule
LPS	Lipopolysaccharide
MAPK	Mitogen-activated protein kinase
MDCK	Madin-Darby canine kidney
MEK	MAP or ERK kinase
Mena	Mammalian Ena
NFAT	Nuclear factor of activated T cells
NF- $\kappa$ B	Nuclear factor - $\kappa$ B
nNOS	neuronal nitric oxide synthase
NO	Nitric oxide
NOS	Nitric oxide synthase
PCT	Proximal convoluted tubule
PDE	Phosphodiesterase
PKA	Protein kinase A
PKG	Protein kinase G
PP	Protein phosphatases
PP-VASP	bis-phosphorylated VASP

<b>PTEC</b>	<b>Proximal tubule epithelial cells</b>
<b>P-VASP</b>	<b>Phosphorylated VASP</b>
<b>RNA</b>	<b>Ribose nucleic acid</b>
<b>RSK</b>	<b>Ribosomal S6 kinase</b>
<b>Ser</b>	<b>Serine</b>
<b>SH3</b>	<b>Src homology 3</b>
<b>SIRS</b>	<b>Systemic inflammatory response syndrome</b>
<b>TCR</b>	<b>T cell receptor</b>
<b>TGF</b>	<b>Transforming growth factor</b>
<b>Thr</b>	<b>Threonine</b>
<b>TLM</b>	<b>Thymosin-like motif</b>
<b>TNF</b>	<b>Tumour necrosis factor</b>
<b>TRE</b>	<b>Tetracycline response element</b>
<b>VASP</b>	<b>Vasodilator-stimulated phosphoprotein</b>

## **Chapter 1. General Introduction**

## 1.1 Introduction

Severe sepsis is a major risk factor for the development of acute renal failure (ARF). A patient requiring admission to an Intensive Care Unit because of sepsis has a 50% risk of death. If acute renal failure develops in this setting, the mortality risk rises to approximately 70% (Neveu *et al.*, 1996). Even a moderate decline in renal function, not resulting in the need for renal replacement therapy, increases the risk of death by a factor of 5 (Levy *et al.*, 1996). However, if the patient survives the infection, they have a 95% chance of regaining independent renal function. The predominant pathological change seen in the kidneys occurs in proximal tubule epithelial cells (PTEC) and is termed acute tubular necrosis (ATN) (Racusen, 1995; Solez *et al.*, 1979). In ATN flattening of proximal tubules, loss of the epithelial brush border and cell shedding are seen but necrosis is actually an uncommon feature. At a subcellular level, the changes seen include alterations in the cytoskeleton, loss of cell polarity and redistribution of  $\beta_1$  integrins to the cell apex (Glynn and Evans, 1999b; Kellerman and Bogusky, 1992). The proximal tubules normally survive at a much lower oxygen tension than other parts of the kidney (3-4 kPa compared to 9kPa) and are therefore much more prone to damage when any reduction in blood flow or pressure is seen, as in the vasodilatation and hypovolaemia associated with severe sepsis. However, renal function can deteriorate before hypotension develops (Walker *et al.*, 1998), possibly via the actions of pro-inflammatory cytokines Interferon- $\gamma$  (IFN- $\gamma$ ), Interleukin-1 (IL-1) and Tumour Necrosis Factor- $\alpha$  (TNF $\alpha$ ) (Groeneveld *et al.*, 1991) One of the effects of these cytokines is the generation of nitric oxide (NO) via the upregulation of inducible nitric oxide synthase (iNOS) (McLay *et al.*, 1994) NO appears to contribute to the development of ARF (Yaqoob *et al.*, 1996) (Ling *et al.*, 1998), though the mechanism by which this occurs is unclear.

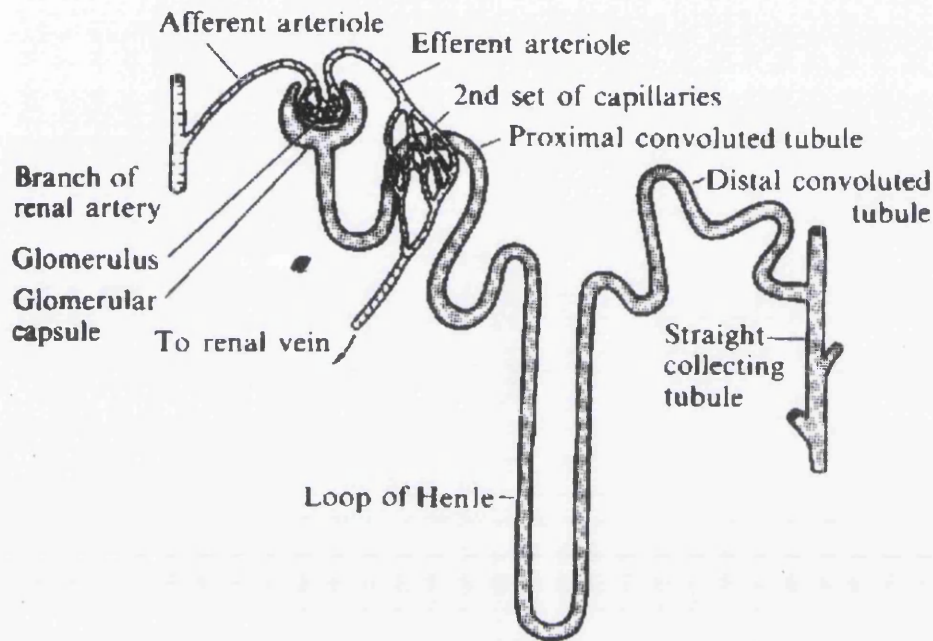
The purpose of this study is to determine the mechanisms by which acute renal failure may occur in sepsis. Nitric oxide induced damage to the actin cytoskeleton and the potential role of the cytoskeletal protein vasodilator-stimulated phosphoprotein (VASP) as a mediator of these effects will be examined. Additional potential roles of VASP in defence against infection via phagocytosis and modification of T cell activation with implications in developments of new types of immunosuppressive agents will also be examined.

## **1.2 The Kidney**

### **1.2.1 Anatomy of the proximal tubule**

The functional unit of the kidney is the nephron. Normal kidneys contain approximately 1 million nephrons each. The nephron consists of the renal corpuscle (glomerulus and Bowman's capsule), the proximal convoluted tubule (PCT), the loop of Henle, the distal convoluted tubule and the collecting ducts (figure 1.1). The proximal tubule consists of a cortical convoluted segment (pars convoluta) starting at the glomerulus and a straight part (pars recta) ending at the loop of Henle in the outer medulla. Morphologically, the PCT can be divided into three segments – S1, forming approximately the first two thirds of the pars convoluta, S2, forming the remaining third of the convoluted segment and the initial portion of the pars recta and S3 forming the more distal portions of the PCT (Kaissling and Kriz, 1979; Tisher *et al.*, 1969). These three segments have different functional characteristics. The S1 segment has a higher transport capacity than later segments of the proximal tubule for a number of solutes including chloride, glucose, sodium and bicarbonate (Maddox and Gennari, 1987). The S2 segment has much higher tubular secretion by organic anion and cation secretory pumps (Woodhall *et al.*, 1978). The cells in the earlier portions of the PCT have a greater luminal surface membrane

area due to a brush border with long cilia. These become shorter in the more distal segments. S1 segment cells have a greater number of lysosomes and endocytic vacuoles than more distal segments (Madsen and Park, 1987). The lysosomal-vacuolar system in the PCT is responsible for the reabsorption and degradation of filtered proteins.



A nephron and the blood vessels associated with it.

**Figure 1.1 The Nephron**

### 1.2.2 Proximal Tubule Epithelial Cells (PTEC)

The cells of the proximal tubule have a basic polarised structure similar to that of other transporting epithelial cells (Figure 1.2). This consists of an apical (luminal) membrane, containing a number of vectorial, transmembrane carriers (Schnermann, 1998), facilitating the entry of solutes from the tubular lumen into the cell. The basolateral membrane contains the Na-K-ATPase pump as well as other transporters (Burrow *et al.*, 1999) and ion channels to allow the return of filtered solutes into the systemic circulation.

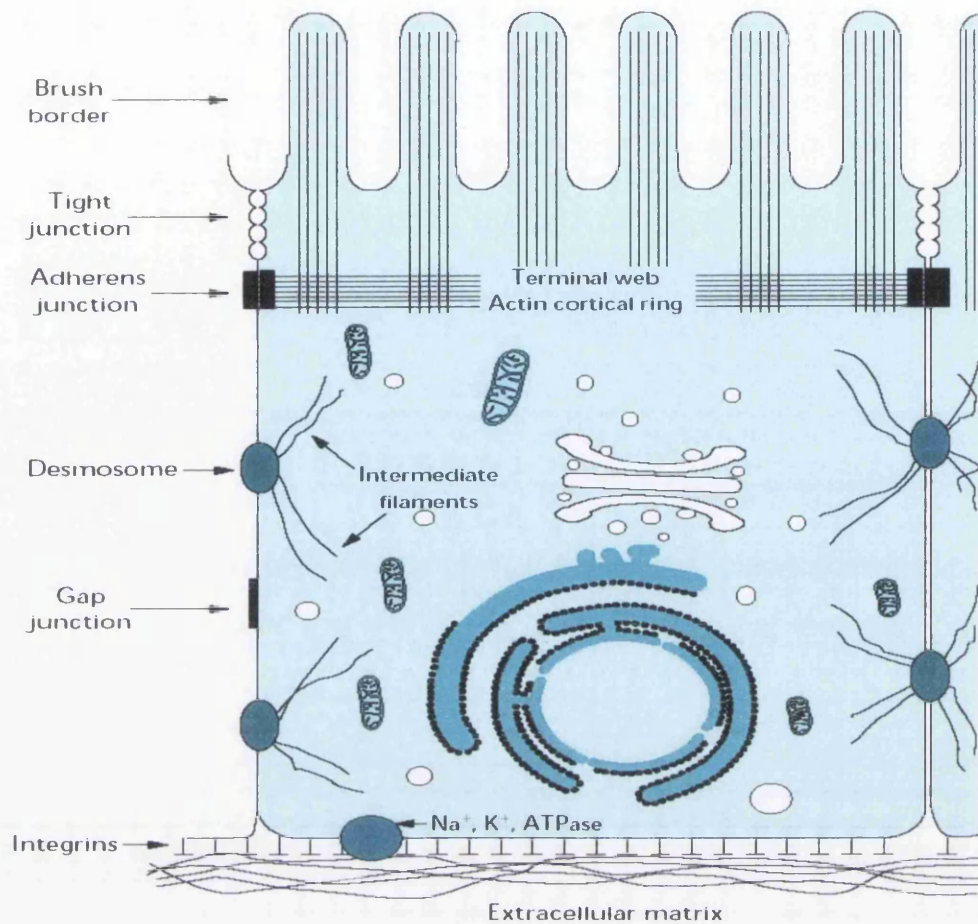


**Figure 1.2. Basic epithelial cell structure.** The polarised nature of the cell is demonstrated, with a web of actin connecting the cells to each other via adherens junctions.

The polarity of the cell is essential for function and is maintained by a highly organised actin cytoskeleton (Piepenhagen and Nelson, 1998). The cytoskeleton plays a vital role in the regulation of cell shape, polarity and maintenance of cell: cell and cell: matrix interactions (Schmidt and Hall, 1998).

### **1.3 Tubulogenesis**

The proximal tubules of the kidney are 3- dimensional (3D) tubular structures with an inward-facing apical surface where the brush border is located, and a basolateral surface, surrounded by extracellular matrix. Although two-dimensional models of epithelia have provided much information, culture of epithelial cells in a 3-D matrix has revealed additional signalling pathways not evident in 2-dimensional (2D) culture systems (Santos and Nigam, 1993; Wang et al., 1998). Tubulogenesis is the process by which epithelial cells form 3 dimensional branching structures. It is a process seen within many organs of the body including the lungs, mammary glands (Berdichevsky *et al.*, 1994), salivary glands (Nogawa and Mizuno, 1981) and the kidney (Saxen and Sariola, 1987) and involves complex interactions between the cells, their extracellular matrix (ECM), cell surface receptors and various growth factors such as epidermal growth factor (EGF), transforming growth factor (TGF) (Kjelsberg *et al.*, 1997; Taub *et al.*, 1990) and hepatocyte growth factor (HGF) (Pollack *et al.*, 1998; Santos and Nigam, 1993).

It is not unreasonable to expect different processes to be involved in the breakdown and formation of tubular epithelial sheets when compared to monolayers. Several ways have been identified as to how a 3D model more closely resembles the *in vivo* situation than cells grown in a 2D culture (Zegers *et al.*, 2003). These include

- In 3D culture, cells can migrate and maintain contact with the ECM in 3 dimensions. In 2D culture, in order to migrate away from the support, they must crawl over adjacent cells, losing contact with the ECM
- The support used in 2D culture is more rigid and inflexible than a normal ECM. Cells respond to and exert mechanical forces on the ECM so the rigidity of the support is likely to influence behaviour.
- Cells grown in 3D culture are more resistant to apoptosis
- The polarised location of certain proteins depends on whether they are grown in 2D or 3D culture – galectin 3 (a promoter of epithelial cell differentiation) is located basolaterally in 3D cultures and apically in 2D cultures (Hikita *et al.*, 2000)

A 3D model may be able to give us more useful insight into the effects of actin cytoskeletal arrangement, responses to disruption and recovery after injury. Madin-Darby Canine Kidney (MDCK) are an epithelial cell line that will spontaneously form hollow fluid-filled cysts when grown in a collagen gel matrix (Barros *et al.*, 1995; Mangoo-Karim *et al.*, 1989) and, on exposure to conditioned media, undergo branching tubulogenesis (Montesano *et al.*, 1991b).

Various growth factors have since been implicated in the induction of branching morphogenesis. Hepatocyte growth factor (HGF) (also known as Scatter Factor) is a morphogenic growth factor (Montesano *et al.*, 1991a) involved in the development of

various organs in the body including the kidneys and mammary glands. It also is involved in the recovery from injury of many organs such as kidneys, lung, stomach and liver. (Matsumoto K & Nakamura T, 2001) It acts via the c-met receptor (Rosario M & Birchmeier W, 2003; Montesano et al., 1991a; Weidner et al., 1993) which activates a number of signalling pathways including SHP2 tyrosine kinase, Ras-ERK-MAP kinase and phosphoinositide-3-kinase (PI3K) involved in cytoskeletal and cell adhesion, reorganisation and motility. TGF- $\beta$ , in contrast, appears to inhibit the formation of tubular structures and to decrease branching in pre-formed tubules (Santos and Nigam, 1993). TGF- $\alpha$  and EGF have been shown to act as promoters of tubulogenesis (Taub *et al.*, 1990). It is probable that the growth factors work together to determine the length and degree of branching of tubules via their conflicting enhancing and inhibiting activities.

The extracellular matrix also appears to play an important role in the control of tubulogenesis. Fibronectin deposition by MDCK cells enhances cell proliferation and migration thereby facilitating branching tubulogenesis (Jiang *et al.*, 2000) as do laminin and entactin (Santos and Nigam, 1993). Fibronectin is a major component of ECM and interacts with cells via integrin receptors. High turnover of ECM proteins, particularly proteoglycans is seen at the tips of budding branches, areas in which the greatest cell proliferation is seen (Gumbiner, 1996). Alterations in integrin expression and avidity may also play a role in tubulogenesis (Jiang *et al.*, 2001) and the interaction of  $\beta_1$  integrins (the major receptor family for collagen) with the ECM appears to be necessary for cyst and tubule formation (Zuk and Matlin, 1996).

Several models have been proposed to explain the mechanisms of cell rearrangement in tubulogenesis. The first suggests a 2 stage process in which cells initially dissociate from the cyst, losing polarity, migrate out into the ECM, proliferate and then re-coalesce into a tubule (Thiery and Boyer, 1992). A second model hypothesises tubules forming as outpouchings from the cyst. In this model, in contrast to the first, cells do not lose cell: cell contact or normal polarity at any time (Sariola and Sainio, 1997). In a third model cells temporarily lose polarity but not cell: cell contact. This model has been demonstrated in MDCK cells (Pollack *et al.*, 1998). Cells appear to undergo a 4-stage process following cyst formation. The cyst polarises forming a single cell extension which then develops into a chain of cells. Cells in the chain then divide to form a cord and then develop a lumen that eventually joins with the original cyst lumen (Figure 1.3). Cells redevelop polarity in the tubular structure. Rho kinase signal transduction factors appear to have an important role in actin cytoskeleton remodelling during tubulogenesis (Eisen *et al.*, 2004; Rogers *et al.*, 2003).

The 3- dimensional model is a potentially interesting way to study the effects of disrupting the actin cytoskeleton both in preformed tubules and newly forming tubules at varying stages of development.

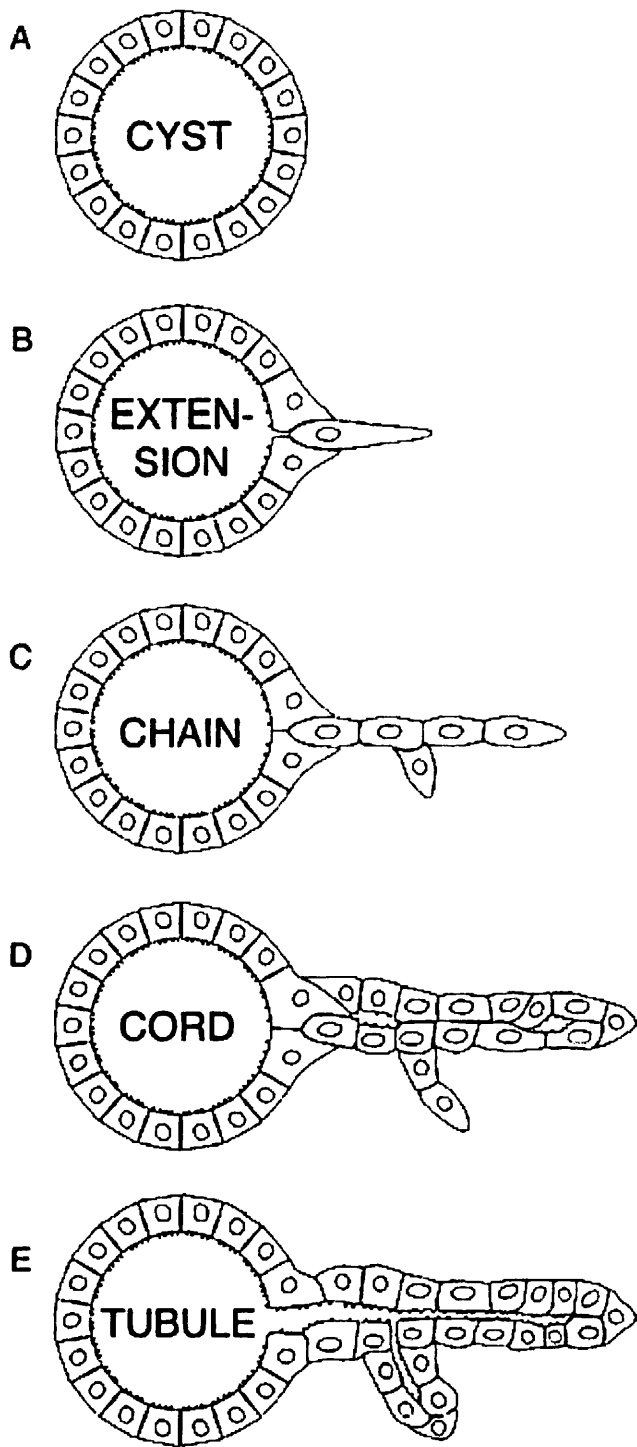


**Figure 1.3. Development of tubules by MDCK cells following HGF stimulation.**

(Pollack et al., 1998)

## 1.4 Sepsis-Associated Acute Renal Failure

### 1.4.1 Definition of Sepsis and Septic Shock

Sepsis is defined as evidence of infection, combined with a systemic inflammatory response and can either be self-limiting or progress to severe sepsis or septic shock. A system used for classification is shown in table 1.1.

	<b>Criteria</b>
Sepsis	Clinical infection plus 2 or more of the following <ul style="list-style-type: none"><li>• Pulse rate &gt; 90 beats/minute</li><li>• Temperature either &gt;38°C or &lt; 36°C</li><li>• Respiratory rate &gt; 20 breaths/minute</li><li>• White cell count &gt; 12x10<sup>9</sup>/ml or &lt; 4x10<sup>9</sup>/ml</li></ul>
Severe Sepsis	Sepsis plus organ dysfunction (e.g. confusion, hypotension, hypoxia)
Septic Shock	Sepsis-induced hypotension resistant to adequate intravascular fluid replacement

**Table 1.1 Classification of Sepsis Syndromes** (Bone *et al.*, 1992)

Septic shock carries a high risk of death. Death rates in the intensive care unit due to septic shock still remain at nearly 60% (Annane *et al.*, 2003; Rangel-Frausto *et al.*, 1995) with most of the deaths seen, unsurprisingly, in those with markers of increased severity of organ dysfunction (Pittet *et al.*, 1995). Following infection, an intense pro-inflammatory response occurs, induced by microbial products such as lipopolysaccharide (LPS). This activates a complex pathway of cellular and cytokine cascades (Blank *et al.*, 1997; Dinarello, 1992; Sriskandan and Cohen, 1995) and this response plays a major role in the multi-organ dysfunction and circulatory collapse seen.

### **1.4.2 Acute Renal Failure and Sepsis**

Acute renal failure (ARF) occurs in over 50% of patients with blood culture positive-septic shock (Rangel-Frausto *et al.*, 1995). Sepsis-associated acute renal failure (ARF) has a higher mortality rate than ARF due to non-septic causes (Neveu *et al.*, 1996). The combination of ARF and sepsis is associated with a 70% mortality rate compared to 45% in those with ARF due to non-septic causes.

In sepsis, generalized arterial vasodilatation with a decrease in systemic vascular resistance is a common feature (Groeneveld, 1994). Upregulation of iNOS in the vasculature by pro-inflammatory cytokines is an important mediator of this effect and has a much sustained and profound response than that caused by constitutive eNOS release alone (Thiemermann *et al.*, 1993). The renal circulation is capable of autoregulating blood flow to maintain perfusion pressure however, when arterial blood pressure declines, renal vessels will constrict in an effort to maintain pressure which can lead to a reduction in renal blood flow (Lucas, 1976; van Lambalgen *et al.*, 1991). Vasoconstriction is partly offset by eNOS and vasodilating endothelins (Groeneveld, 1994; Groeneveld *et al.*, 1994) but the overall result is hypoperfusion of the kidneys with the development of ARF.

Whilst circulatory failure with accompanying hypotension, hypoxia and hypoperfusion of the kidney undoubtedly play a major role in sepsis-associated ARF (Groeneveld *et al.*, 1991; Myers and Moran, 1986), experimental models of sepsis demonstrate that renal function may decline without a fall in renal blood flow (Walker *et al.*, 1998). Nitric oxide within the kidney has been identified as a mediator in sepsis-associated ARF.

### 1.4.3 Pathophysiology of Sepsis-associated ARF

The main pathological features of ARF in sepsis are seen in the proximal tubule and are termed acute tubular necrosis (ATN). Early features of ATN are loss of the tubular epithelial brush border, dilatation of the tubules and interstitial oedema and progress to show flattening of the epithelial cells lining the tubule, shedding of these cells into the lumen and subsequent obstruction of the tubule (Figure 1.4) (Solez *et al.*, 1979). Widespread necrosis is an uncommon feature (Lieberthal *et al.*, 1998). The damage is usually sub-lethal and signs of regeneration such as nuclear enlargement and mitotic figures may be seen. In fact, many patients who survive their sepsis syndrome regain significant renal function and are able to discontinue renal replacement therapy (Sponsel *et al.*, 1994).

At a subcellular level, the changes seen in response to sepsis with associated hypoxia and hypoperfusion include major alterations in the actin cytoskeleton of proximal tubule cells (Kellerman and Bogusky, 1992). Loss of cell polarity due to hypoxia and ATP-depletion actin microfilament disruption is seen with redistribution of basolateral integrins and Na/K-ATPase transporters to the apex (Molitoris *et al.*, 1991; Molitoris and Marrs, 1999; Molitoris and Wagner, 1996). Cell shedding into the tubule lumen is seen as a consequence of dissolution of  $\beta_1$  integrin: extracellular matrix interactions. Shed cells aggregate and form casts that can cause obstruction and increase back pressure into the glomerulus (Molitoris and Marrs 1999), further reducing renal function.

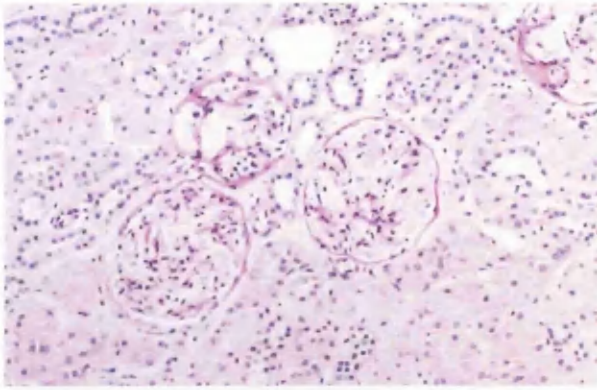


Figure 1.4a. Normal kidney

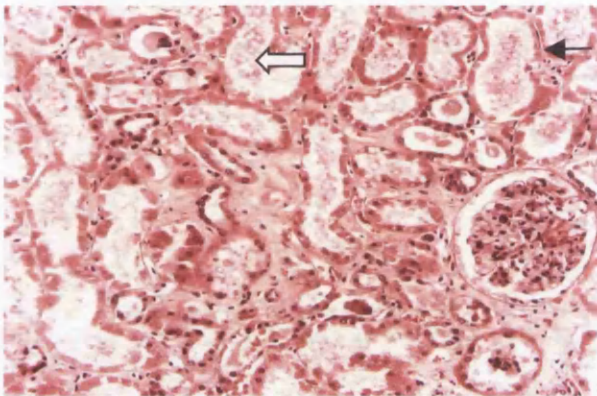


Figure 1.4b. Acute tubular necrosis

**Figure 1.4. Renal Histology.** Figure 1.4a is a biopsy taken from normal kidney, showing 2 normal glomeruli and cuboidal cells lining the tubules. In Figure 1.4b, the glomerulus retains a normal appearance but the tubule epithelium is flattened (arrow) and there is debris within the tubule lumen (open arrow).

## **1.5 Nitric Oxide**

### **1.5.1 Nitric Oxide and the Kidney**

Nitric oxide induction has multiple effects in the kidney. NO is synthesised in the endothelial cells of the macula densa and the pre- and post-glomerular capillaries where it acts as a vasodilator in response to shear stress, playing an important part in the control of renal vascular tone (Kone, 1997). It is also involved in the regulation of glomerular haemodynamics via tubuloglomerular feedback and modulation of renin release from the juxtaglomerular apparatus (JGA). Whilst in sepsis-related renal failure, hypotension with hypoperfusion of the kidneys undoubtedly plays a role in the development of ATN if left untreated (van Lambalgen *et al.*, 1991), blocking NO actions are not necessarily beneficial and can lead to infarction (Shultz and Rajj, 1992). Constitutive NO production by eNOS, is important for maintenance of renal perfusion. eNOS plays an important role in ameliorating renal vasoconstriction in response to a baroreflex-mediated rise in sympathetic activity and activation of the renin-angiotensin-aldosterone system (Groeneveld *et al.*, 1994; Nath and Norby, 2000).

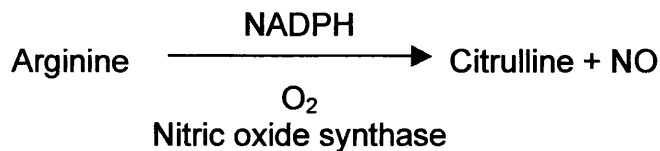
In addition to eNOS, there are other sources of NO in the kidney during sepsis. Infiltrating macrophages express iNOS following LPS stimulation (Buttery *et al.*, 1994). iNOS is induced in proximal tubule epithelial cells in response to combinations of LPS and pro-inflammatory cytokines. This is associated with epithelial cell shedding and can at least be partially blocked by selective iNOS inhibitors. Cytoskeletal disruption is seen after pro-inflammatory cytokine release and is associated with cell shedding. (Glynn and Evans, 1999a; Glynn *et al.*, 2001). Infiltrating neutrophils are also a source of NO in the kidney in sepsis as they too upregulate iNOS following cytokine stimulation

*et al.*, 1996). The release of NO and reactive oxygen species by neutrophils has been implicated in direct damage to the cells of renal tubules (Nath and Norby, 2000).

The cells of the proximal tubule constitutively express iNOS mRNA (Markewitz *et al.*, 1993) yet under basal conditions, the enzyme is not detected. Proximal tubule epithelial cells (PTEC) are able to produce high levels of NO following stimulation with combinations of lipopolysaccharide (LPS), and the pro-inflammatory cytokines, interferon- $\gamma$ , interleukin-1 and Tumour necrosis factor- $\alpha$  (McLay *et al.*, 1994; Nathan, 1997). Hypoxia also stimulates NO production in the proximal tubule with administration of the selective iNOS inhibitor L-NIL shown to ameliorate renal damage in a rat model (Noiri *et al.*, 2001).

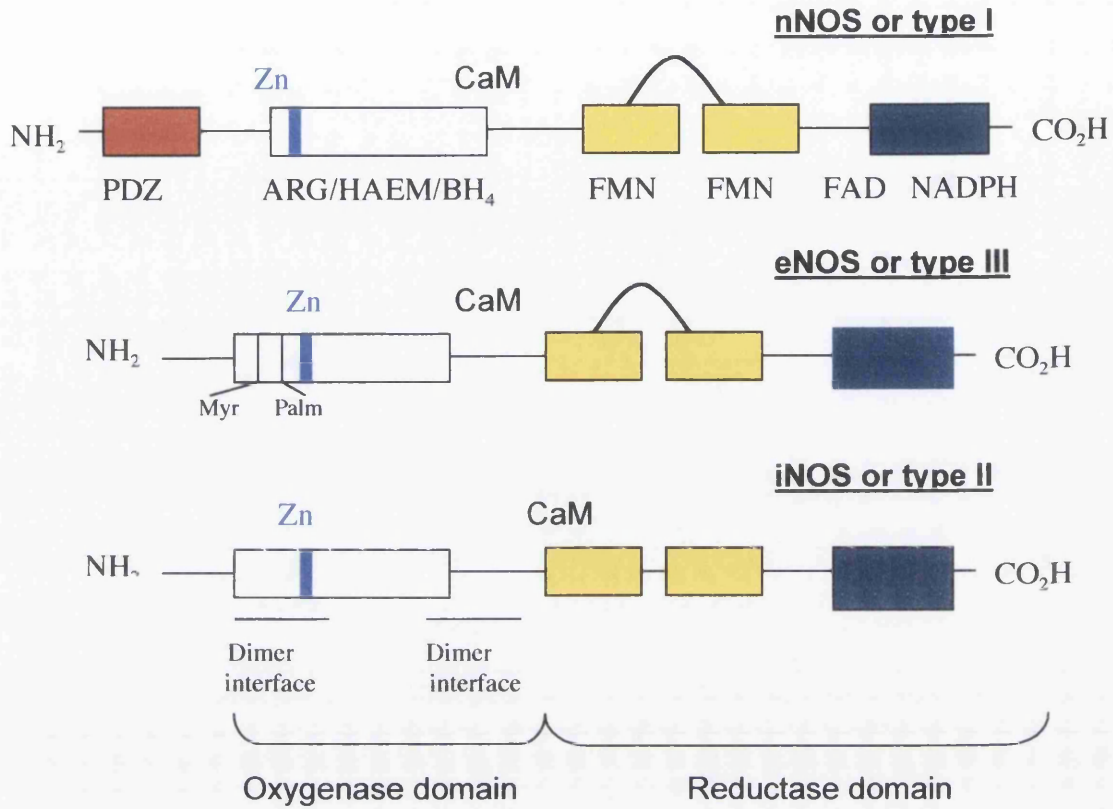
### 1.5.2 Nitric Oxide and the Nitric Oxide Synthases

Endothelium-derived relaxing factor was identified as the labile gas nitric oxide (NO) in the late 1980s (Ignarro *et al.*, 1987; Palmer *et al.*, 1987). Three nitric oxide synthases have been identified since then - type I, nNOS (neuronal nitric oxide synthase), type II, iNOS (inducible nitric oxide synthase) and type III, eNOS (endothelial nitric oxide synthase) with 51-57% identity between the human isoforms (Nathan, 1992). All of these enzymes catalyse a reaction of l-arginine, NADPH and oxygen to produce citrulline, NADP and the free radical NO (Knowles and Moncada, 1994).



The enzyme isoforms have been differentiated in various ways including by the tissues in which they predominate (Forstermann *et al.*, 1995), by function (Forstermann *et al.*, 1994), whether they are constitutive (nNOS and eNOS) or inducible (iNOS) in their expression (Forstermann and Kleinert, 1995) and by whether they are calcium dependent (nNOS and eNOS) (Bredt and Snyder, 1994) or not. None of these systems are completely satisfactory, as many features, initially thought to be unique to a particular isoform, have been demonstrated in other isoforms.

The enzymes exist in a dimeric structure in their active forms, associated with two molecules of calmodulin each. Each nitric oxide synthase molecule exhibits a bi-domain structure (figure 1.5) with an N-terminal oxygenase domain linked by a calmodulin (CaM)-recognition site to a C-terminal reductase domain (Alderton *et al.*, 2001; Stuehr, 1997). The structures of the constitutive synthases eNOS and nNOS contain auto-inhibitory loops to produce autoregulation of their function so they only cause NO production for very brief time periods in response to physiological stimuli (Bredt and Snyder, 1994; Forstermann and Kleinert, 1995; Salerno *et al.*, 1997). Inducible NOS is usually only induced in response to stimuli such as the pro-inflammatory cytokines and contains no such regulatory loop (Forstermann *et al.*, 1994; Xie *et al.*, 1992). Once induced, iNOS continues to catalyse a high level of production of NO for a sustained period of time (Nathan and Xie, 1994). Down-regulation of iNOS is via ubiquitination and caveolin-1 (reviewed in Kone, 2000). Caveolin-1 co-segregates with iNOS in a detergent-insoluble membrane fraction of the cell and degradation occurs there via the proteasome pathway.



<b>Key</b>	
<b>CaM</b>	Calmodulin recognition site
	Autoinhibitory loop (eNOS and nNOS)
<b>Myr</b>	Myristoylation site (eNOS)
<b>Zn</b>	Zinc-ligating cysteines
<b>Palm</b>	Palmitoylation site (eNOS)
<b>PDZ</b>	Protein interaction domain

**Figure 1.5. Domain structure of the nitric oxide synthases**  
(adapted from (Alderton et al., 2001).

## 1.6 The Actin Cytoskeleton

### 1.6.1 Function of the actin cytoskeleton

Actin is a highly conserved cytoskeletal protein which is able to form 5-9nm diameter filaments (F-actin) in the presence of salt and ATP. This is a dynamic process with actin monomers being constantly added to and subtracted from the filament, regulated by ATP hydrolysis and is important for cell motility (Lauffenburger and Horwitz, 1996) and the generation of cell-surface processes such as lamellopodia and filopodia (Rottner *et al.*, 1999). The actin cytoskeleton allows transduction of signals between the extracellular matrix and the cell and between cells via complex protein structures – focal adhesions and adherens junctions, containing proteins with intra and extracellular domains (Hazan *et al.*, 1997). The adherens junction in epithelial sheets forms a continuous belt located close to the cell apex, just below the tight junction. The cells are held together at the adherens junction by the transmembrane protein E-cadherin (Adams and Nelson, 1998). The intracellular domains of this protein bind to the proteins  $\alpha$  and  $\beta$  catenin (Aberle *et al.*, 1994) which in turn bind to proteins such as Zyxin and Vinculin (Brindle *et al.*, 1996; Bubeck *et al.*, 1997; Hazan *et al.*, 1997; Lozano and Cano, 1998). These both contain a consensus binding sequence (D/E FPPPPX D/E (Niebuhr *et al.*, 1997) for the cytoskeletal protein **V**asodilator-**S**timulated **P**hosphoprotein (VASP) which in turn associates with polymerised actin. A similar protein bundle is found at points of contact with the extracellular matrix (Fillingham *et al.*, 2005). The main transmembrane proteins at these focal contacts are the integrins which, in renal PTECs, are predominantly of the  $\beta_1$  integrin family (Rahilly and Fleming, 1993). These in turn are complexed to intracellular proteins, including Zyxin and Vinculin and via these to VASP and F-actin (Critchley *et al.*, 1999).

### **1.6.2 The Actin Cytoskeleton in Epithelial Cell Motility and Migration**

Changes in epithelial cell motility, shape and movement are associated with dynamic reorganisation of the actin cytoskeleton. Three main organisational arrays of actin are seen: lamellipodia, filopodia and stress fibres (Small *et al.*, 1999b). Stress fibres require substrate anchorage and are constructed of bipolar bundles of actin and type II myosin. They are therefore able to contract and exert tension. Substrate contact sites undergo turnover and recreation to allow cell crawling (Small *et al.*, 1999a). Lamellipodia are composed of unipolar actin filaments and filopodia are loose bundles of actin filaments either embedded within or extending from lamellipodia. Filopodia and lamellipodia do not require substrate adhesion to form. They protrude from the leading edge of a cell due to actin polymerisation and form focal adhesions with the cell substrate. This protrusive ruffling of cells is part of the mechanism by which cells move (Mitchison and Cramer, 1996).

### **1.6.3 Control of Actin Polymerisation**

Regulation of the actin cytoskeleton is under the control of the Rho GTPase family of proteins (Rho, Rac and CDC42) (Arthur *et al.*, 2002; Hall, 1998) which are members of the p21 Ras superfamily of small GTPases. Rho-family proteins act as molecular switches and are activated by GTPase-activating proteins (GAPs) and GDP-GTP exchange factors (GEFs) (Machesky and Hall, 1996). A variety of processes are triggered including formation of protein-protein complexes, rearrangement of the actin cytoskeleton, protein phosphorylation and synthesis and turnover of phospholipids. Rho activation by lysophosphatidic acid, for example, mediates actin stress fibre formation and focal adhesion formation in fibroblasts (Ridley and Hall, 1992). Rho also appears to be important in integrin clustering in T cell activation which can be blocked by

ribosylation of Rho (Tominaga *et al.*, 1993). Rac activation leads to the formation of lamellopodia and membrane ruffles, leading to forward cell movement and CDC42 is required for filopodia formation and to maintain cell polarity (Nobes and Hall, 1999). The Rho GTPase family also appear to be important in cyst and tubule formation by MDCK cells. Rho, Rac and CDC42 appear to act in concert to allow formation of cysts and tubules and to maintain normal cyst polarity (Rogers *et al.*, 2003).

Actin will polymerise under normal physiological salt conditions (Hannappel and Wartenberg, 1993). In order to maintain a pool of monomeric actin and to regulate the sites within the cell where polymerisation occurs, a group of regulatory proteins exist within the cell which include the actin-monomer binding proteins, thymosin and profilin (Bear *et al.*, 2001). Profilin is a 14kDa protein, usually found associated with the plasma membrane. When bound to monomeric actin, it accelerates the exchange of ATP for ADP, promoting actin polymerisation via the addition of actin monomers to the free barbed ends of actin filaments. A profilin-binding site is found in the cytoskeletal protein vasodilator-stimulated phosphoprotein (Reinhard *et al.*, 1995), discussed below.

## **1.7 Vasodilator-Stimulated Phosphoprotein (VASP)**

### **1.7.1 Localisation and role of VASP**

VASP was first described in human platelets (Halbrugge and Walter, 1989; Halbrugge and Walter, 1990) where its phosphorylation status has been linked to platelet activation and aggregation (Halbrugge *et al.*, 1990). It is part of a family of proteins known as the Ena/VASP proteins that include the Drosophila protein enabled (Ena) (Gertler *et al.*, 1995), and the mammalian orthologs Mena (mammalian Ena) (Gertler *et al.*, 1996) and Ena/VASP-like (EVL) protein (Lambrechts *et al.*, 2000). VASP is localised to sites of

cell:matrix interaction at focal adhesion sites and cell:cell interaction at the adherens junction (figure 1.6) and focal contacts where it is associated with actin filaments (Reinhard *et al.*, 1992). It is also present at sites of dynamic actin turnover such as the protruding edge of lamellopodia and in filopodial tips (Gomez and Robles, 2004). VASP has been shown to be important in the regulation of actin polymerisation in cell:cell and cell:matrix interactions. Ena/VASP proteins are found in epithelial contacts as part of complexes containing F-actin, E-cadherin, vinculin and zyxin in a distribution termed the adhesion zipper, thought to be an early stage in cell: cell contact formation (Vasioukhin *et al.*, 2000). A dominant negative form of the VASP protein (Bachmann *et al.*, 1999) has been used to demonstrate the essential position of VASP in the sealing of cells into epithelial sheets Over-expression of the dominant-negative VASP fraction appears to disrupt epithelial sheet formation.

As well as its role in cell shape, interactions between cells and the matrix and in cell motility, the cytoskeleton may have other functions in other cells. Ena/VASP proteins are a potential pathway through which modification of the actin cytoskeleton can occur and allow control of these functions. T cells polarise when in contact with antigen-presenting cells (APCs) by remodelling their cytoskeleton towards the APC to allow contact to be maintained (Krause *et al.*, 2000). Ena/VASP proteins are recruited to the T cell receptor (TCR) complex. Blocking this recruitment inhibits activation-induced T cell polarisation. (Bear *et al.*, 2001). VASP proteins are also required for remodelling of the actin cytoskeleton in macrophages to allow pseudopodial extension and internalisation of particles (Coppolino *et al.*, 2001).

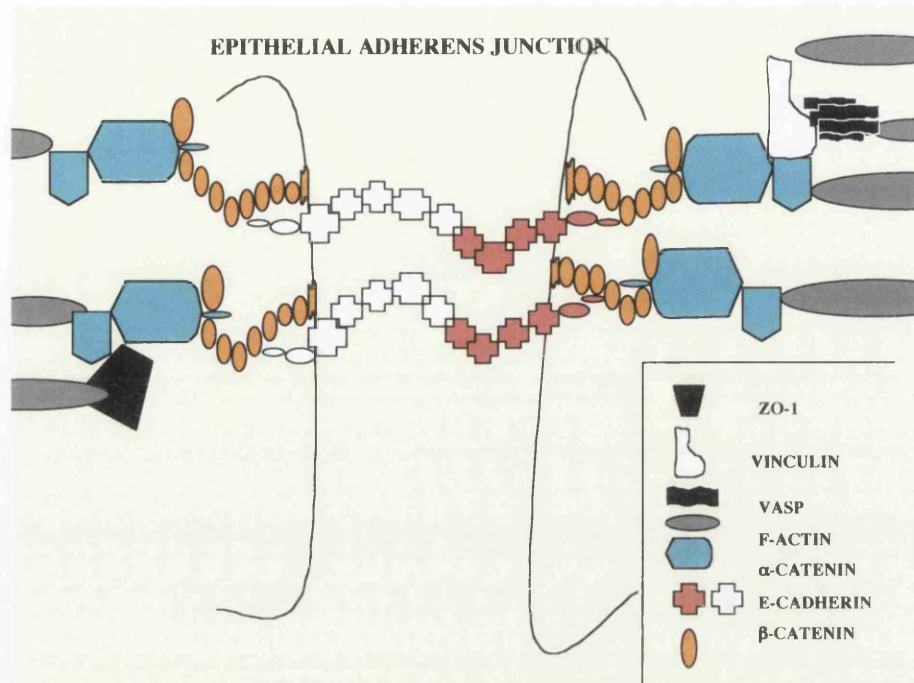


**Figure 1.6. Structure of an epithelial adherens junction**

Representation of an adherens junction between two epithelial cells showing E-cadherins bridging the cell: cell divide and connecting to the intracellular actin cytoskeleton by means of a complex of proteins.

The bacterium *Listeria monocytogenes* uses VASP to harness the host actin cytoskeleton to move through the cell (Geese *et al.*, 2002).

### **1.7.2 VASP and the Kinetics of Actin Polymerisation**

The mechanisms by which VASP may promote actin polymerisation are still unclear. Whilst some reports have suggested it is a direct nucleator of F-actin, this was only seen at low, non-physiological salt concentrations (Bachmann *et al.*, 1999). Actin is able to polymerise from both ends *in vitro* though the rate differs between the two ends. Slow polymerisation occurs at the pointed end and more rapid polymerisation at the barbed end. There appears to be a constant treadmilling of actin monomers being added to and removed from actin filaments under the control of Actin Depolymerising Factor (ADF or cofilin), profilin (supplying actin monomers) and capping proteins (Carlier *et al.*, 2003). The localisation of Ena/VASP proteins within the cell may suggest the mechanisms by which they act. Ena/VASP proteins are concentrated in areas containing free barbed ends of actin filaments at the cell membrane. Treatment with cytochalasin D (a fungal metabolite that binds barbed ends and inhibits actin polymerisation) causes loss of VASP from these areas (Lebrand *et al.*, 2004). Ena/VASP proteins appear to antagonise the actions of actin capping proteins. It is possible that they localise at or near the end of a growing actin filament and prevent capping by capping proteins (Bear *et al.*, 2002). The EVH2 domain alone, including its F-actin and G-actin binding domains and the tetramerisation domain, is sufficient to prevent barbed ends from capping actin fibres (Barzik *et al.*, 2005; Sechi and Wehland, 2004).

Ena/VASP proteins also appear to regulate branching of actin filaments. These proteins suppress Arp 2/3 complex-induced actin filament branching (Krause *et al.*, 2002;

Krause *et al.*, 2000). *Listeria* require both VASP and Arp2/3 to use actin polymerisation to move through a cell (Bear *et al.*, 2001).

These two mechanisms of control of actin filament elongation and branching density may be a method by which cell motility rates are controlled. Long filaments with few branches due to excessive inhibition of capping proteins by VASP would be too flexible to counteract membrane tension. An absence of Ena/VASP proteins would lead to highly branched, short, rigid filaments that would promote persistence of protrusions and increase the chances of formation of attachments to the extracellular matrix (Krause *et al.*, 2002). However, more flexible filaments may be needed for active cell movement. Experimental data (Bear *et al.*, 2002) shows that the optimal free-actin filament length for effective lamellipodial protrusion (distance beyond the last cross-link) is 70-200nm, with a maximal protrusive force at 120nm (seen in lamellipodia in which Ena/VASP has been over-expressed). In Ena/VASP- depleted lamellipodia, the free-filament length drops to approximately 50nm with an accompanying decrease in instantaneous protrusion rate. However, at the higher protrusion rate of 120nm, retraction of the lamellipodia by membrane tension leads to an overall slower rate of protrusion when compared to the Ena/VASP-depleted situation. It is suggested that Ena/VASP-accelerated actin filament assembly may temporarily deplete the lamellipodia of G-actin leading to retraction until more monomeric actin can be provided through the breakdown of other filaments (Cramer, 1999). Cell motility is therefore likely to involve a balance between the actions of these, and other proteins. Regulation of this may involve processes such as VASP phosphorylation and new evidence suggests that protein kinase A phosphorylation at the Ser235 residue of murine

VASP (equivalent to Ser239 in human VASP) *in vitro* is sufficient to prevent the normal anti-capping actions of VASP (Barzik *et al.*, 2005).

### 1.7.3 Structure of Ena/VASP Proteins

The Ena/VASP family of proteins are tetramers (Haffner *et al.*, 1995) and share a highly conserved (table 1.2), three-domain structure (figure 1.7) (Reinhard M *et al* 2001). The Ena-VASP homology domain 1 (EVH1) has the highest level of conservation within the family, whilst the central, proline-rich domain is the least highly conserved (table 1.2). The domains have distinct functions and are discussed below.

	<b>EVL</b>	<b>VASP</b>	<b>Ena</b>
<b>Mena</b>	73%	67%	73%
<b>EVL</b>		61%	62%
<b>VASP</b>			58%

**Table 1.2. Percentage identity between members of the Ena/VASP protein family.** (Adapted from Gertler *et al.*, 1996)

#### 1.7.3.1 Ena-VASP Homology Domain1 (EVH1)

The N-terminal EVH1 domain (approx 111-113 amino acid residues) binds to the focal adhesion proteins vinculin and zyxin, and to the *Listeria* protein ActA via a consensus motif (D/E)-FPPPP-X(D/E)(D/E) (Carl *et al* 1999, Reinhard *et al* 1995, (Ahern-Djamali *et al.*, 1998). Binding is established by electrostatic interactions forming between the positively charged aromatic and basic residues of the EVH1 domain with the negatively charged motifs in vinculin, zyxin and ActA (Carl *et al.*, 1999). This interaction appears to be important in cell morphogenesis, especially during the formation of adherens junctions (Vashioukin *et al* 2000).

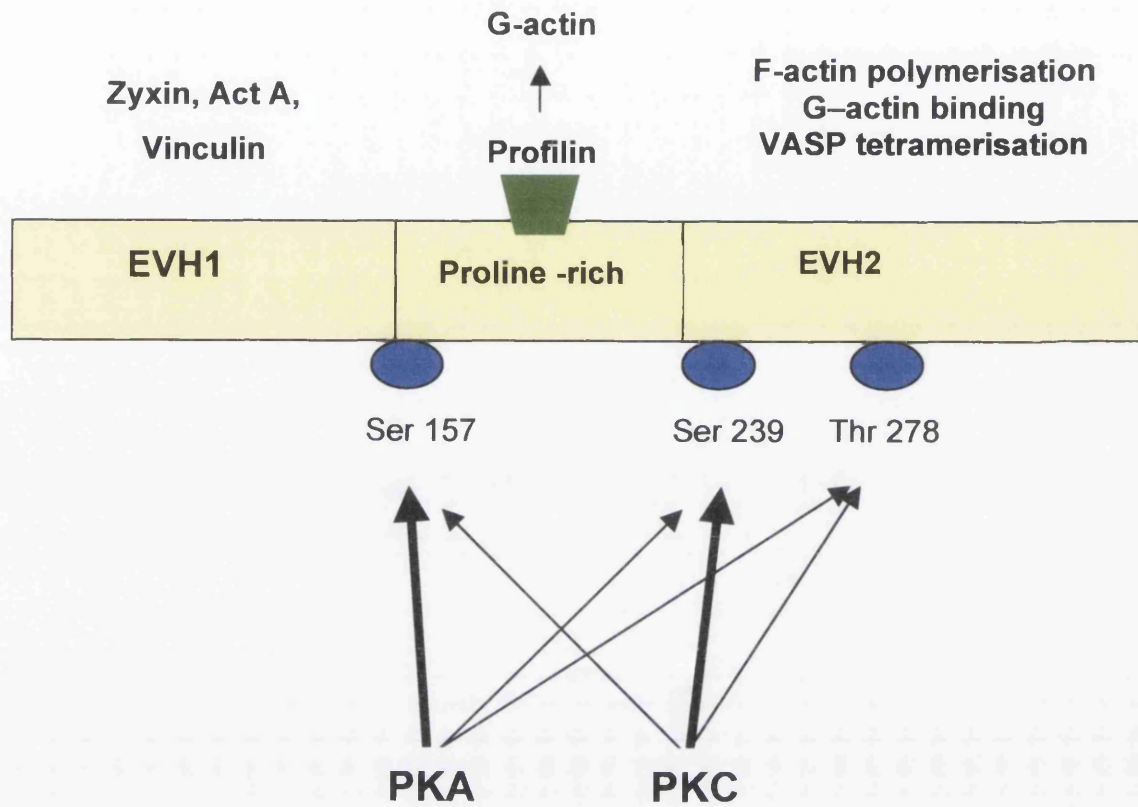


Figure 1.7. Tri-domain structure of VASP.

The EVH1 domain is comprised of a high proportion of aromatic and aliphatic residues. The structure of the domain is of seven  $\beta$  strands packed together to form an anti-parallel  $\beta$  sandwich with a long C-terminal  $\alpha$  helix along one side (Ball *et al.*, 2000). There is a hydrophobic core with 3 highly conserved non-core aromatic residues on the protein surface forming a peptide recognition groove.

The ability of *Listeria* to bind VASP via its ActA surface protein (Niebuhr *et al.*, 1997) has been an important tool in the study of VASP and its interactions with other proteins. *Listeria* use this ability to bind VASP to form a comet tail of actin polymerisation, moving the bacterium through the cell. ActA is essential for actin-based motility in *Listeria*. (Auerbuch *et al.*, 2003; Pistor *et al.*, 1995). It locates VASP to the bacterial surface where it promotes the rapid polymerisation of an actin comet that is able to propel the bacteria through the cell (Laurent *et al.*, 1999). ActA recruits and binds the host protein complex Arp 2/3 (actin related proteins 2 and 3) and Ena/VASP proteins (Machner *et al.*, 2001). This provides a bridge between the actin tail and the bacterium (Skoble *et al.*, 2001; Welch *et al.*, 1998). The combination of ActA and the Arp 2/3 complex appear to allow branching of actin fibres with VASP appearing to be delivering actin filaments to this process.

The EVH1 domain of VASP appears to also be involved in the linking of actin fibres to the extracellular matrix through integrins at focal adhesion sites (Critchley *et al.*, 1999; Walter *et al.*, 1995). Integrins bind talin which in turn is able to bind vinculin. Vinculin contains the consensus binding domain for the EVH1 domain of VASP as mentioned previously (Critchley *et al.*, 1999). Alterations in the ability of VASP to bind to F-actin

are therefore a potential site by which signals between the extracellular matrix and the cell may be modulated.

### **1.7.3.2 Proline-Rich Central Domain**

The central proline-rich domain of VASP is the least conserved domain. It binds the monomeric actin-binding protein Profilin via polyproline (GP<sub>3</sub>) binding sites (Haffner *et al.*, 1995; Reinhard *et al.*, 1995). Deletion of this site does not appear to affect fibroblast motility but does affect the ability of *Listeria* to move through the cell (Geese *et al.*, 2000; Grenklo *et al.*, 2003). This domain is also able to bind to the src homology 3 (SH3) binding domain of Abelson tyrosine kinase (Abl) which is important in control of the actin cytoskeleton in the developing *Drosophila* embryo (Ahern-Djamali *et al.*, 1998).

Profilin is thought to enhance actin nucleation by raising local levels of monomeric actin to sufficiently high concentrations to induce actin polymerisation (Witke *et al.*, 2001) and as such may be important at sites of high turnover as in lamellipodia and filopodia.

### **1.7.3.3 Ena-VASP Homology Domain 2 (EVH2)**

The C-terminal EVH2 domain is the hallmark of this family of proteins and differentiates them from other EVH1 domain-containing proteins. The EVH2 domain, approximately 160-190 amino acids in length, has three conserved sub-domains. Closest to the amino terminus is a monomeric G-actin binding site, (a thymosin-like motif KLRK) (Walders-Harbeck *et al* 2002) essential for the *in vitro* actin nucleation properties of VASP. The second block is responsible for polymerisation of actin (residues 259-276) and the third block is a coiled-coil region (residues 343-380),

essential for tetramerisation of proteins of the Ena/VASP family (Bachmann *et al* 1999). The actin-binding properties of VASP are confined to the EVH2 domain which can be shown to associate with actin stress fibres (Huttelmaier *et al.*, 1999). Interactions with F-actin are enhanced by tetramerisation of VASP. There is evidence to show that other members of the Ena/VASP family are able to form hetero-oligomers with VASP (Ahern-Djamali *et al.*, 1998; Gertler *et al.*, 1996). Expression of this region alone, acts as a dominant-negative form of VASP and has been used to delineate the functions of this domain (Bachmann *et al.*, 1999).

Of note is the finding that the EVH2 domain contains a Serine residue close to the sites of G-actin binding and F actin polymerisation (Ser239), that is capable of being phosphorylated in response to cyclic-nucleotide-dependent protein kinases (Huttelmaier *et al.*, 1999).

#### **1.7.4 Cyclic Nucleotide – Dependent Phosphorylation sites in VASP**

A variable number of cyclic nucleotide dependent phosphorylation sites have been identified within the proteins of the Ena/VASP family (Butt E *et al.*, 1994). Ena has none, Ena/VASP-like protein (EVL) has one, mammalian Ena (Mena) has two and VASP three (Figure 1.8). The human VASP phosphorylation sites are at Serine 157, Serine 239 and Threonine 278, the first two of which are close to ligand-binding sites – the Serine 157 site is adjacent to the G-actin binding site of the central domain of VASP and Serine 239 is close to the G-actin binding domain and the actin polymerisation region of the EVH2 domain (Bachmann *et al.*, 1999; Butt *et al.*, 1994; Smolenski *et al.*, 1998). These sites are phosphorylated by cAMP and cGMP dependent protein

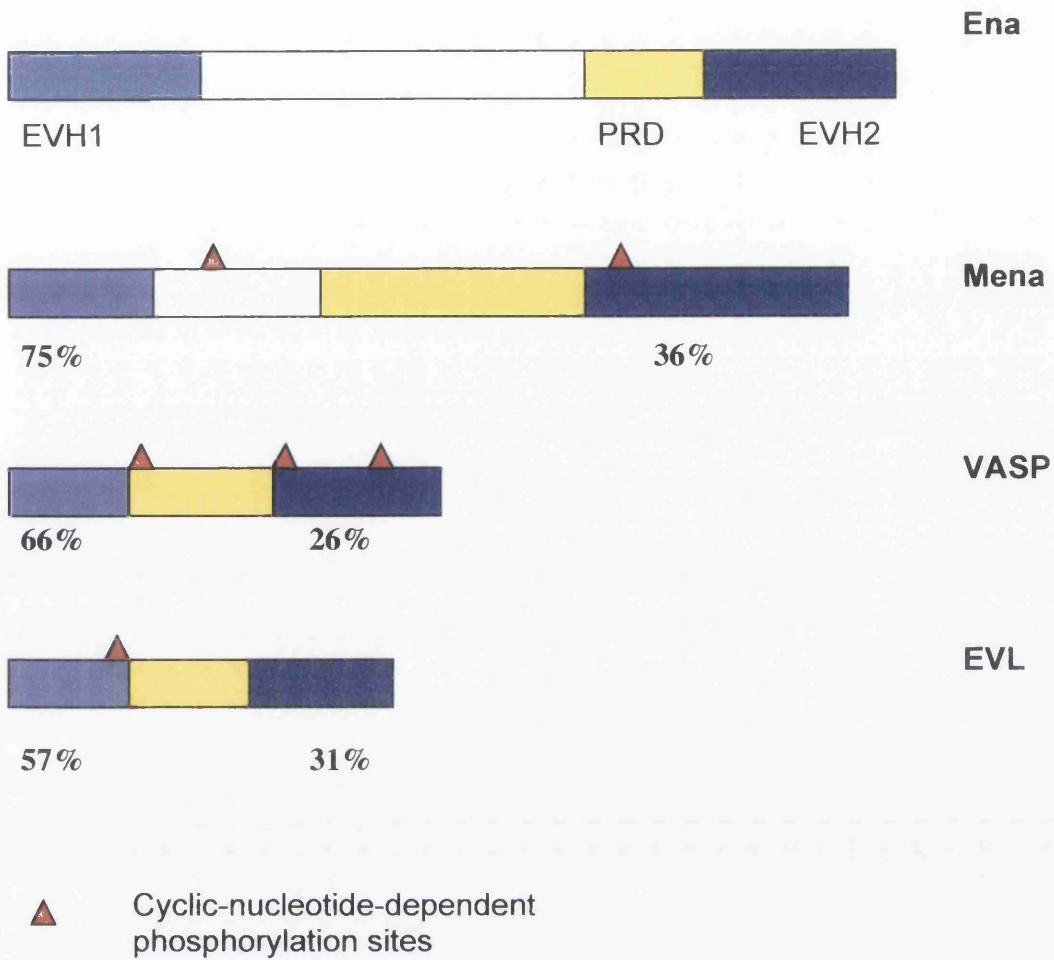


**Figure 1.8. Structure and homology of the Ena/VASP proteins**

kinases (Halbrugge *et al*, 1990) which have been shown *in vitro* to demonstrate different affinities for the different sites (Halbrugge *et al*, 1989). Cyclic AMP-dependent kinase appears to act primarily at the Ser157 site, and leads to an apparent mass shift of VASP from 46 to 50kDa when analysed by SDS-Page electrophoresis suggesting that this may cause a change in the secondary structure of the protein molecule (Halbrugge & Walter 1989). Phosphorylation of Mena and EVL at the equivalent sites also cause a similar band motility shift (Gertler *et al* 1996, Lambrechts *et al* 2000). Cyclic-GMP-dependent kinase acts primarily at the Ser239 site, with the Thr278 site only being phosphorylated after other sites have been phosphorylated and at comparatively low levels. *In vivo* the situation may be different. Experiments in platelets suggested that cGMP-dependent kinase might in fact phosphorylate both serine residues with a similar time course but with incomplete Ser157 phosphorylation where only a 50% shift from 46kDa to 50kDa VASP is seen (Butt *et al*, 1994). The Ser239 site is adjacent to the region of the EVH2 domain associated with actin polymerisation. (Hauser *et al*, 1999). In platelets, VASP phosphorylation has been shown to alter activation and integrin-mediated adhesion (Horstrup *et al.*, 1994; Walter *et al.*, 1993). The use of VASP knockout mutant mice showed that VASP is required for PKA-inhibited platelet aggregation (Aszodi *et al* 1999) and that for this process, Ser157 phosphorylation appears to be the key regulatory process.

Phosphorylation at the Ser239 site in the EVH2 domain of VASP has been shown to be a sensitive indicator of the activation of the nitric oxide (NO)/guanylate cyclase pathway ((Butt *et al.*, 1994; Eigenthaler *et al.*, 1992; Ibarra-Alvarado *et al.*, 2002), NO binds to the haem moiety of guanylate cyclase, increasing its activity (Hobbs, 1997). Binding of the EVH2 domain to G-actin appears to be reduced by phosphorylation at

the Ser239 residue (Walders-Harbeck *et al*, 2002). Activation of guanylate cyclase is limited via phosphodiesterase V which causes the breakdown of cGMP to GMP (Koesling and Friebe, 1999; Mullershausen *et al.*, 2005; Mullershausen *et al.*, 2001). cGMP also inhibits phosphodiesterase III which normally dephosphorylates cAMP and may therefore also upregulate this pathway (figure 1.9) (Feijge *et al.*, 2004). Therefore, induction of iNOS may not only activate the cGMP-dependent pathway but may also activate cAMP-dependent pathways (figure 1.9). The different phosphodiesterases have different specificities for the cyclic nucleotides (Table 1.3) and as such may be a target for therapeutic modification of these paths.

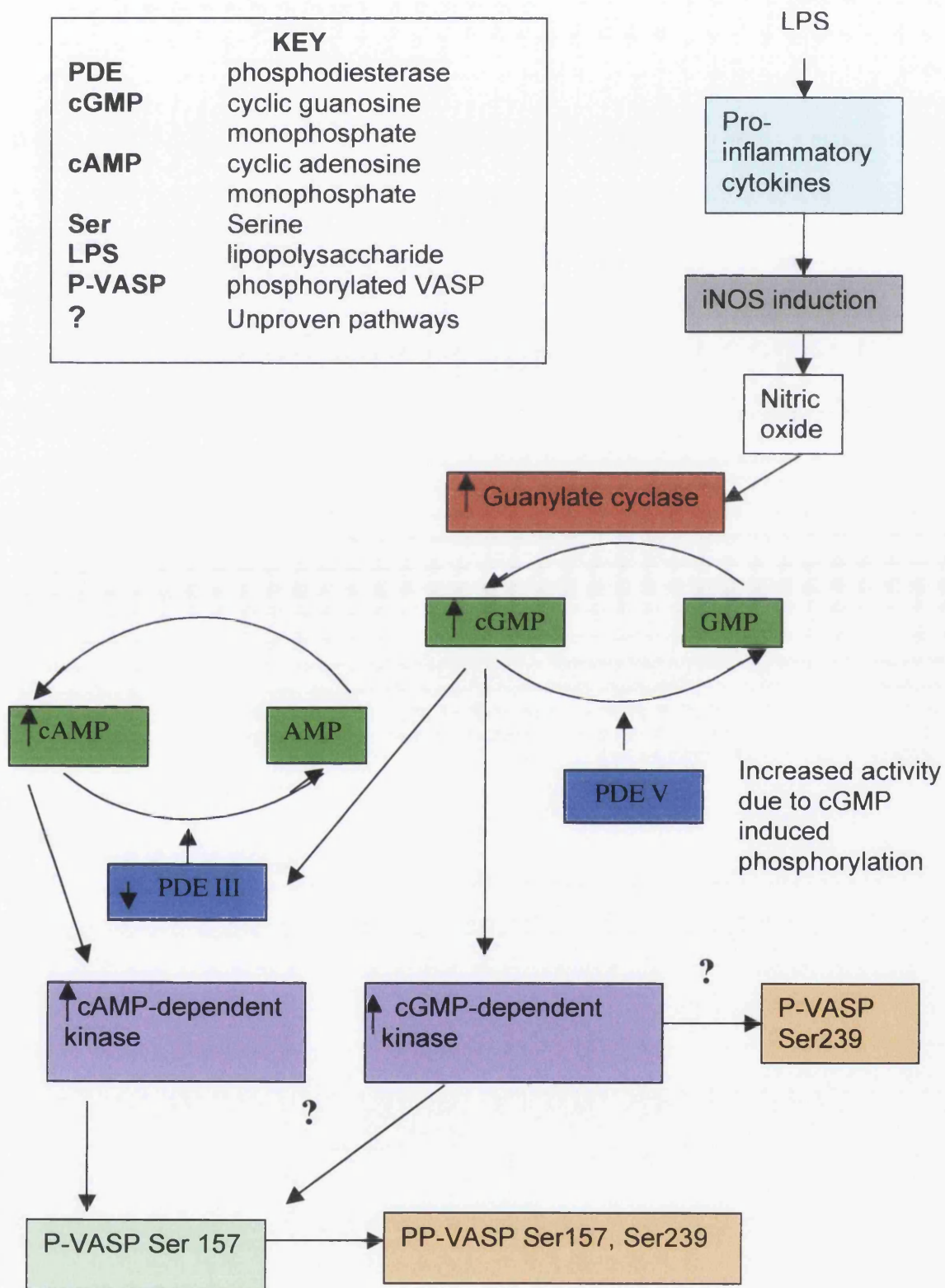
<b>Phosphodiesterase</b>	<b>Regulatory Mechanisms</b>	<b>Substrate</b>
III	cGMP-inhibited	cAMP
IV	cAMP-specific	cAMP
V	cGMP-specific	cGMP

**Table 1.3. Phosphodiesterase substrate specificity and regulation.**

(Conti and Jin, 1999)

The phosphorylation state of the Ena/VASP proteins is also regulated by dephosphorylation by protein phosphatases (PP). In human platelets, dephosphorylation of VASP (assessed by band shift of VASP from 50kDa back to 46kDa) occurs within minutes of removal of physiological or pharmacological stimuli (Halbrugge *et al* 1990). Different PPs have different selectivities for the different phosphorylation sites. *In vitro* studies show phosphorylated VASP as a substrate for the protein phosphatases PP2A,

**Figure 1.9. Possible pathways of cyclic nucleotide-controlled VASP phosphorylation**



PP2B and PP2C. PP2A appears to be selective for the Ser157 residue, whereas PP2B preferentially dephosphorylates Ser239 (Abel *et al.*, 1995). There is experimental evidence to suggest that binding of VASP to monomeric actin is regulated by its phosphorylation state. Murine VASP mutants of a putative G-actin binding site (KLRK) located within the EVH2 domain have been used to demonstrate that VASP and G-actin do indeed interact physically and that KLRK is involved in formation of the complex (Walders-Harbeck *et al.*, 2002). Mutation of this motif to KLGE or KLEE led to failure of G-actin binding and F-actin polymerisation. The VASP Ser235 (murine) and Ser239 (human) phosphorylation sites lie adjacent to the KLRK motif. Phosphorylation at this site via cAMP-dependent kinase abolishes VASP-directed actin polymerisation. Evidence for how VASP phosphorylation may alter both actin binding and nucleation comes mainly from *in vitro* studies. Two studies investigated the effects of VASP phosphorylation on F-actin binding and came to opposite conclusions. The first (Laurent *et al.*, 1999), concludes that the affinity of VASP for F-actin is controlled by phosphorylation at the Ser157 residue. The second study (Harbeck *et al.*, 2000) suggests that phosphorylation of the murine Ser153 residue (equivalent to the human Ser157 residue) has little or a reduced effect on F-actin binding unless there is additional phosphorylation at Ser235 (equivalent to Ser239 in human VASP). Different experimental conditions were used in the two studies which makes them difficult to compare. Both of these studies were carried out before phospho-specific antibodies were available which means it was not possible to examine the effects of Ser239 phosphorylation alone. Further work is therefore needed to elucidate the role of VASP phosphorylation in F-actin binding.

Actin nucleation *in vitro* also appears to be influenced by VASP phosphorylation. By looking at other members of the Ena/VASP family of proteins, it can be shown that the N-terminal Ser157 site appears to be the important residue. EVL does not have an equivalent Ser239 site. Phosphorylation of EVL at the Ser157 site reduces actin nucleation (Harbeck *et al.*, 2000; Lambrechts *et al.*, 2000). Phosphorylation at other sites in VASP may add extra levels of regulation of actin nucleation.

The reduction of actin nucleation with phosphorylation alternatively could be due to a decreased ability to bind G-actin. The EVH2 domain of VASP contains a thymosin like motif (TLM) related to a G-actin binding site in thymosin and has been demonstrated to bind monomeric actin (Walders-Harbeck *et al.*, 2002). Both mutation at this site and PKA-induced phosphorylation reduce G-actin binding.

Overall, the exact roles of phosphorylation in the regulation of VASP functions remain unclear. Further work is required in this field, in particular to study the effects *in vivo* rather than *in vitro* where control of phosphorylation and the effects of the different cyclic nucleotide-dependent protein kinases may be very different.

## **1.8 VASP in non-epithelial cells**

### **1.8.1 VASP and Phagocytosis**

Phagocytosis is the process by which specialised cell types recognise and engulf foreign extracellular material. It is a central component of the innate immune response. Foreign materials are coated with opsonins such as complement and immunoglobulins (Allen and Aderem, 1996a). Immunoglobulin-coated particles are recognised by the Fc family of cell surface receptors. Binding to these receptors triggers a cascade of intracellular

signals leading to engulfment of the particle. Remodelling of the actin cytoskeleton is an essential part of this process as it allows the extension of pseudopodia to engulf the particle (Allen and Aderem, 1996b; Greenberg *et al.*, 1990). A phagosome is thus formed in which the particle is destroyed.

It has been shown that Ena/VASP proteins are recruited to phagosomes forming around an ingested particle and that this coincides spatially and temporally with actin filament reorganisation (Coppolino *et al.*, 2001) A multimolecular complex consisting of Ena/VASP proteins, Fyb/SLAP (also known as ADAP – see section 1.8.2.2), SLP-76 and Wiskott-Aldrich Syndrome protein (WASP) forms and links the cytoskeleton to Fc-mediated signalling pathways during phagocytosis. It is not yet known which proteins are responsible for the localisation of VASP to these sites of actin remodelling but ADAP (Krause *et al.*, 2000) and vinculin (Allen and Aderem, 1996b) have been proposed.

### **1.8.2 VASP in T Cell Activation**

Interaction of a T cell with antigen presented by an antigen-presenting cell (APC) results in the triggering of intracellular signalling cascades leading to T cell activation and differentiation (Wange and Samelson, 1996). When this interaction occurs a massive reorganisation of the actin cytoskeleton is seen (Barda-Saad *et al.*, 2005; Valitutti *et al.*, 1995). Polymerisation of F-actin at the site of cell:cell contact stabilises the interaction between the lymphocyte and the APC via an increase in integrin avidity. A supramolecular activation cluster (SMAC) forms at the immunological synapse consisting of a central zone containing the T-cell receptor (TCR), CD3, CD28 and other receptors, surrounded by a peripheral zone (pSMAC) containing the integrin LFA-1

(leukocyte function-associated antigen-1) (Grakoui *et al.*, 1999) and cytoskeletal elements such as talin (Krawczyk and Penninger, 2001; Monks *et al.*, 1998). Integrins are not constitutively adhesive but are activated by extracellular stimuli to trigger intracellular signalling pathways which lead to changes in ligand binding activity without increasing levels of cell surface expression (Griffiths and Penninger, 2002b). The mechanism by which this occurs has not yet been ascertained. The adapter protein ADAP (adhesion and degranulation adaptor protein) has been postulated as a potential mechanism by which the TCR and integrins may be linked (Peterson *et al.*, 2001a). ADAP contains an EVH-1 binding domain and can therefore potentially interact with the Ena/VASP family of proteins.

Reorganisation of the actin cytoskeleton is also required for T cell activation. Interruption of the actin cytoskeleton with cytochalasin D (a cell permeable fungal toxin that inhibits actin polymerisation) inhibits T cell receptor (TCR) mediated interleukin 2 gene transcription (Holsinger *et al.*, 1998), suggesting that cytoskeletal reorganisation is a necessary event in T cell activation.

#### **1.8.2.1 T Cell Adhesion, Integrins and Actin Cytoskeleton Reorganisation**

Lymphocyte function-associated molecule-1 (LFA-1) is a member of the  $\beta_2$  integrin family and is expressed on the surface of most leukocytes where it acts as an adhesion receptor. LFA-1, in common with other integrins, is a heterodimeric transmembrane receptor consisting of an  $\alpha$  subunit ( $\alpha_L$  or CD11a) and a  $\beta_2$  subunit (CD18) (Larson *et al.*, 1989; Stanley *et al.*, 1994). It interacts with its ligand intercellular adhesion molecule-1 (ICAM-1) to bring about responses such as leukocyte adhesion to endothelial cells and antibody-dependent, monocyte mediated cytotoxicity. (Springer,

1990). LFA-1 is generally non-functional until stimulated by TCR/CD3 activation which induces intracellular signals, activating LFA-1:ligand binding (inside-out signalling) (Miyamoto *et al.*, 2003). These intercellular signals lead to an increase in integrin avidity for its ligand. Clustering of integrins is thought to enhance avidity (Griffiths *et al.*, 2001). In its non-active state, LFA-1 is tethered to the actin cytoskeleton. Release from this appears to allow motility, leading to LFA-1 clustering. Newly formed clusters then form stronger links with the actin cytoskeleton via proteins such as  $\alpha$ -actinin (Sampath *et al.*, 1998) and recruit other molecules to form a functional adhesive unit, capable of transducing outside-in signals (van Kooyk *et al.*, 1994). Whilst the cytoplasmic domains of integrins have been shown to be important in linkage to the actin cytoskeleton, they do not demonstrate enzymatic features themselves. They are thought to transduce their signals by associating with adaptor proteins. This then allows coupling with the cytoskeleton, cytoplasmic kinases and G-receptor proteins.

The molecular mechanisms by which TCR stimulation leads to alterations in integrin avidity is unclear. The TCR-proximal kinase  $\zeta$ -associated protein of 70kDa (ZAP-70) appears to be required for anti-CD3 induced integrin adhesion in Jurkat cells (Goda *et al.*, 2004). A ZAP-70 mutant unable to induce adhesion was unable to fully activate gene transcription. Many other signal intermediates appear to play a role in inside-out signalling to integrins, including calcium, the small GTPases, protein kinase C (PKC) and phosphoinositide 3-OH kinase (PI 3-kinase) (Kolanus and Seed, 1997; Woods and Shimizu, 2001).

The adaptor protein ADAP appears to be an important intermediate in the coupling of TCR-induced cytoskeleton rearrangements with alterations in integrin avidity. ADAP

deficient T cells exhibit reduced LFA-1 clustering in response to anti-CD3 stimulation though they are still able to cluster their TCRs. (Griffiths *et al.*, 2001; Peterson *et al.*, 2001a).

### **1.8.2.2 Adhesion and degranulation-promoting protein (ADAP)**

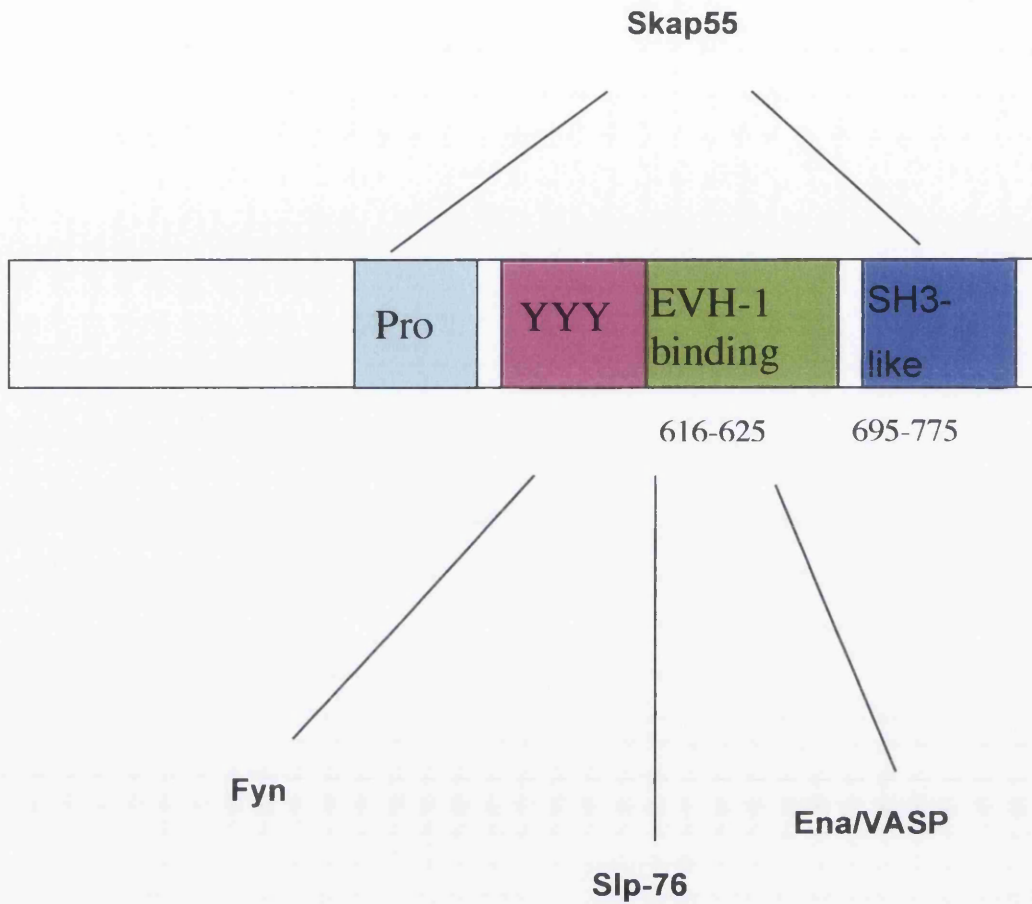
ADAP (formerly known as Fyb (fyn-binding protein)/Slap (Slp-76-associated protein)) is an adaptor protein expressed in T and myeloid cells and is phosphorylated in response to TCR stimulation. Upon TCR stimulation, ADAP is phosphorylated by Fyn (a tyrosine-binding kinase) and binds to Slp-76 (da Silva *et al.*, 1997). Slp-76 (SH2-domain-containing leukocyte protein 76) is a haematopoietic multi-domain adaptor protein required for T cell development, TCR-dependent mitogen-activated protein kinase (MAPK) activation and calcium flux (Wilkinson *et al.*, 2004).

ADAP-deficient T cells show defective proliferation and cytokine production in response to TCR stimulation (Peterson *et al.*, 2001a). This appears to be due to deficiencies in  $\beta_1$  integrin clustering whilst TCR signalling pathways are unaffected, suggesting that ADAP is a regulator of T cell activation by coupling of TCR stimulation to integrin avidity modulation. ADAP-deficient T cells are still able to cluster TCRs in response to stimulation and actin polymerisation appears to be grossly normal in these cells. The alteration appears to be specifically in the clustering of integrins in response to TCR stimulation. (Griffiths *et al.*, 2001) The molecular mechanism by which this occurs is unknown.

ADAP contains a proline-rich region and an SH3-like domain both of which bind the SH2 domains of Fyn and Slp-76. It also contains an EVH-1-binding domain (Figure

1.10) which is able to bind members of the Ena/VASP family of cytoskeletal proteins (Krause *et al.*, 2000) . A potential mechanism by which ADAP may regulate integrin adhesion is via modulation of the cytoskeleton, possibly through binding to Ena/VASP proteins which are known to be involved in G-actin binding and F-actin polymerisation (Walders-Harbeck *et al.*, 2002). ADAP has been shown to co-localise with F-actin, Ena/VASP proteins, the Arp 2/3 complex, Vav-I and WASP (Wiskott-Aldrich syndrome protein) at the interface between Jurkat T cells and anti-CD3 coated beads. Blocking this interaction by using transfected ActA repeats (the Listeria protein that binds EVH1 domains), inhibited TCR-induced actin rearrangement (Krause *et al.*, 2000). However, mutation of the EVH1 binding domain of ADAP, abolishing the ability to bind VASP, appears to have no effect on LFA-1 avidity (Wang *et al.*, 2004). Whilst ADAP does not in fact appear to be necessary for gross actin polymerisation (Griffiths *et al.*, 2001; Peterson *et al.*, 2001a) it may be required for more subtle actin rearrangements, not visible by phalloidin staining, specifically targeted to integrin but not TCR clustering. ADAP-VASP may be involved in extending the interface between the T cell and the APC following LFA-1 or have a non-essential, supplementary role in ADAP function (Wang *et al.*, 2004).

As well as the interactions with ADAP discussed above, the phosphorylation status of VASP may also be important in T cell proliferation and IL-2 production. cGMP -



<b>KEY to domains and binding partners</b>	
<b>Pro</b>	Proline-rich
<b>EVH</b>	Ena/VASP homology
<b>YYY</b>	Fyn binding tyrosine residues
<b>SH3</b>	Src homology 3
<b>Slp-76</b>	Src homology 2 domain-containing Leukocyte protein of 76kDa
<b>Fyn</b>	src kinase p59fyn

**Figure 1.10. ADAP Domain Structure and Protein Binding Affinities.**

ADAP contains an EVH-1 binding domain capable of binding to Ena/VASP family proteins. Slp-76 is an adaptor protein required for T cell development, MAP Kinase activation and calcium flux

dependent kinase inhibits CD3-induced IL-2 production (Fischer *et al.*, 2001). This enzyme is known to phosphorylate VASP, with a preference for its Ser239 site as discussed previously. Phosphorylation of VASP is known to alter its ability to polymerise actin (Walders-Harbeck *et al.*, 2002).

### **1.2.8.3 A Potential Role for VASP in T Cell Activation**

In order for regulated T cell signal transduction to occur, the physical organisation of these molecules in space is likely to be important. For example, if all components of a signal pathway are required to be assembled before full signal propagation occurs, this would allow a T cell to ignore transient signals and only respond to a sustained signal lasting for a threshold duration (McKeithan, 1995). Adaptor proteins such as ADAP can form part of a scaffold within a cell and thereby hold molecules at specific sub-cellular sites, regulate movement of signalling proteins to specific compartments during signalling and enhance the specificity of signal pathways by stopping them interacting with other paths (Burack *et al.*, 2002; Weston and Davis, 2001). Adaptors may allow two different proteins or pathways to be linked.

VASP is a molecule potentially involved in the link between T cell receptor stimulation and signal transduction pathways. It is a known part of the actin cytoskeleton (Reinhard *et al.*, 1992) and its interactions with actin may be altered by its phosphorylation state (Kwiatkowski *et al.*, 2003; Loureiro *et al.*, 2002). It has been found co-localised with the scaffold protein ADAP (Griffiths and Penninger, 2002a; Krause *et al.*, 2000) and is known in epithelial and platelet models to interact with integrins. We propose that it is a potential target for modulation of T cell activation.

VASP may be involved in many aspects of T cell activation (figure 1.11). As an EVH-1 domain containing protein, it may be involved in the clustering of integrins via interactions with the scaffold protein ADAP. Integrin clustering appears to be associated with an increase in avidity (van Kooyk *et al.*, 1999; Woods and Shimizu, 2001). Release of integrins from their normal distribution on the T cell membrane possibly by modulation of VASP phosphorylation and hence its ability to polymerise actin, could be involved in permitting the clustering to occur. This may then lead to prolongation of the T cell activation signal if the actin cytoskeleton reassembles to hold the integrins in their new location. Transient phosphorylation and dephosphorylation of VASP in response to cyclic nucleotide-dependent protein kinases are a potential mechanism by which this cytoskeletal reorganisation could occur. VASP-mediated rearrangements of the cytoskeleton could also be involved in signal transduction pathways by allowing involved proteins and kinases to move into the correct location and interact. Again, physiological transient phosphorylation/dephosphorylation is a possible pathway by which this may be modulated. This could affect both initiation and duration of a signal.

A potential method for examination of the role of VASP in integrin clustering and actin cytoskeleton rearrangements with their subsequent effects on signal transduction is by the use of a dominant-negative form of the protein. Amino acid residues 277-380 of the EVH2 domain of VASP act as a dominant-negative form of the protein (Bachmann *et al.*, 1999). It is able to take up its normal tetrameric structure but is unable to bind actin as these binding-sites are not present in this terminal portion of the protein. Neither can it link to other cytoskeletal proteins such as zyxin via the EVH-1 domain. Transfection of dominant negative VASP (DN-VASP) into T cells with investigation of

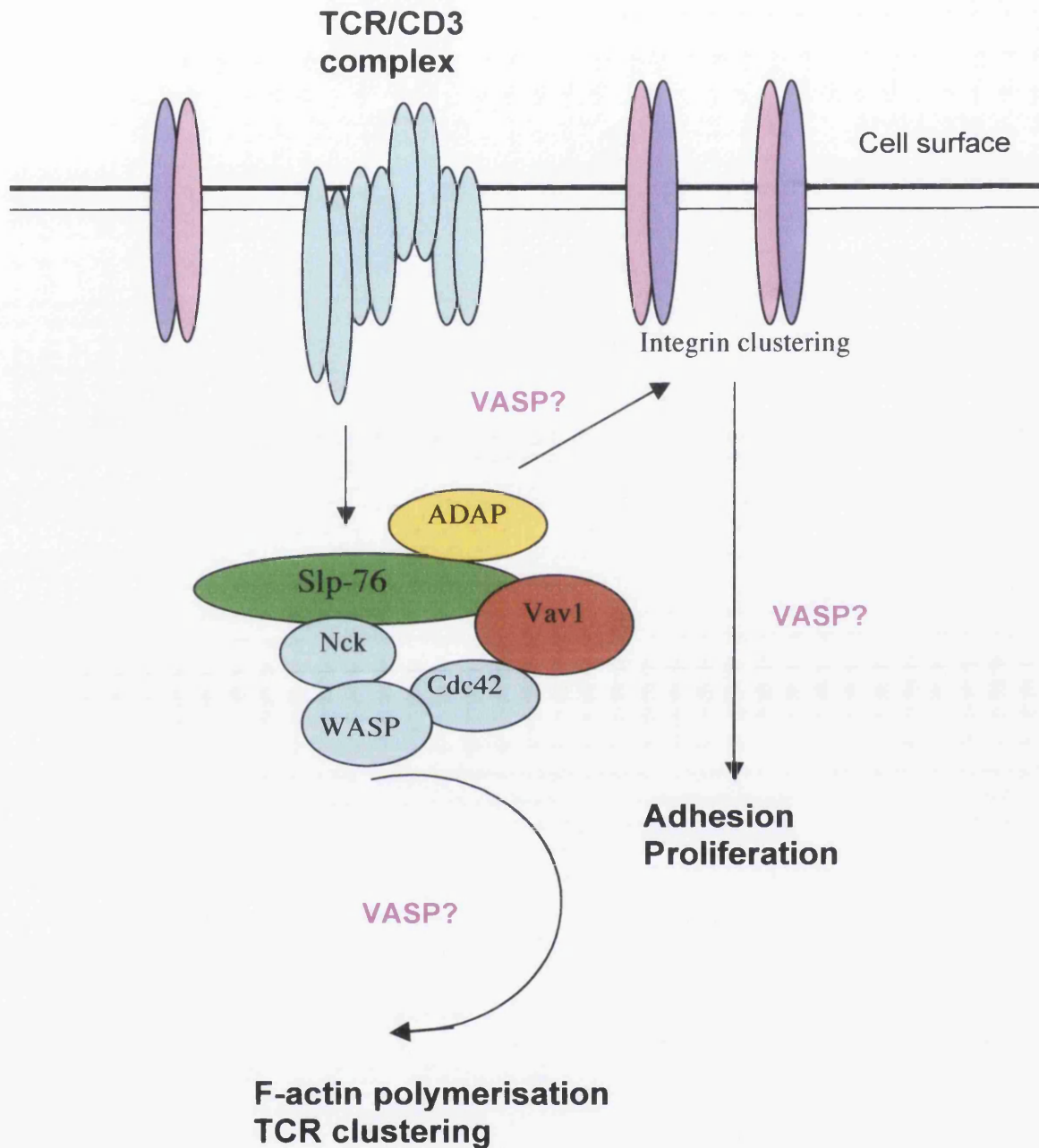


**Figure 1.11. Potential Role for VASP in T cell activation.** (Griffiths and Penninger, 2002b). The exact positions at which VASP is involved in T cell activation are not yet clear but may involve actin polymerisation, cytoskeletal polarisation, integrin clustering and signal transduction pathways.

cell morphology, polarisation and activation of signal transduction pathways is potentially very interesting and has not been carried out previously. DN-VASP is a more useful technique in this situation than either the use of knockout mice or siRNAs as it will block the function of other members of the Ena/VASP family (Vasioukhin *et al.*, 2000). Both siRNA and knockout animal techniques would specifically disrupt VASP function but would still allow Mena and Evl to function and substitute for VASP in the cells (Kwiatkowski *et al.*, 2003; Lambrechts *et al.*, 2000).

### **1.9 Aims of the Project**

The central theme of this project was an investigation into the roles of the cytoskeletal protein VASP and its function in the modulation of the actin cytoskeleton in epithelial cells and T lymphocytes. The following objectives are addressed

- Identification of the effects of iNOS on VASP phosphorylation and distribution in epithelial cells and the effects on the actin cytoskeleton as a model of sepsis-induced renal failure. Given that we know nitric oxide is involved in proximal tubule epithelial cell shedding and that VASP contains a cGMP-dependent kinase phosphorylation site, close to a domain associated with actin binding and polymerisation, we investigated whether phosphorylation at this site was a potential mechanism by which NO disrupted the actin cytoskeleton. We also investigated the effects of NO on VASP phosphorylation in macrophages as VASP is involved in actin filament reorganisation in phagocytosis.
- The use of a dominant-negative form of VASP as a method for investigating the effects of actin cytoskeletal disruption on formation and breakdown of epithelial sheets. VASP is implicated in the formation of both cell:cell and cell:matrix

junctions. We examined the effect of disrupting normal VASP function with DN-VASP to see whether it affected the ability of epithelial cells to both maintain a pre-formed epithelial sheet and to form new sheets.

- Investigation of the role of VASP in T cell activation and signal transduction by the use of DN-VASP. Little is known of the role of VASP in T cells and investigations of its role in integrin clustering are unclear. The objective of this area of work was to use DN-VASP to interfere with normal VASP function and look at the effects on ligand binding and actin polymerisation. We also looked at T cell activation via assays of markers of activation and activation of signal transduction pathways in order to try and identify what roles VASP plays.

**Chapter 2. Nitric Oxide and VASP Phosphorylation in Epithelial Cells and Macrophages.**

## 2.1 Introduction

Nitric oxide is a free radical gas produced by the oxygenation of L-arginine by the enzyme nitric oxide synthase (NOS) (Knowles and Moncada, 1994). Three isoforms of this enzyme have been identified, neuronal NOS (nNOS), endothelial NOS (eNOS) and inducible NOS (iNOS) (Nathan, 1992). Two of these isoforms, nNOS and eNOS are constitutively expressed (Bredt and Snyder, 1994) but the third, iNOS, is usually up-regulated following pro-inflammatory cytokine stimulation as seen in severe sepsis (Forstermann et al., 1994). Nitric oxide produced by renal proximal tubule epithelial cells (PTECs) has been implicated in cell shedding (Glynn and Evans, 1999a). A key feature seen in experimental models of sepsis in epithelial and other cells is disruption of the actin cytoskeleton and loss of normal cell polarity (Koukouritaki et al., 1999; Puls et al., 1999). Given that nitric oxide stimulates cGMP-dependent protein kinase, the actions of this enzyme on cytoskeletal proteins present a potential mechanism by which the actin cytoskeleton may be altered.

VASP is an attractive target by which NO-dependent mechanisms may affect the actin cytoskeleton. As reviewed in section 1.7.4, it contains 3 cyclic-nucleotide-dependent phosphorylation sites, one of which is found in close proximity to G- and F- actin binding sites (Butt et al., 1994; Halbrugge et al., 1992). VASP is localised to cell membranes at sites of dynamic turnover (Drees et al., 2000; Reinhard et al., 1996; Renfranz and Beckerle, 2002) via a consensus motif (D/E)-FPPPP-X(D/E)(D/E) to cytoskeletal proteins including zyxin and vinculin (Carl et al 1999, Reinhard *et al* 1995, (Ahern-Djamali et al., 1998) through its EVH1 domain (discussed further in Chapter One). VASP localises at cell: cell and cell: extracellular matrix contacts and therefore

provides a potential role in cyclic-nucleotide dependent protein kinase-induced alterations of contacts between these sites and the actin cytoskeleton.

The role of VASP and the effects of NO on VASP in this setting have not previously been investigated. VASP plays an important role in the mediation of both cAMP and cGMP-dependent pathways (Aszodi et al., 1999). NO may affect not only cGMP dependent pathways via activation of guanylate cyclase but, through actions on phosphodiesterases (Manns et al., 2002), may also affect cAMP activated pathways. cGMP, as well as activating cGMP-dependent kinase (PKG), also decreases activity of phosphodiesterase III, the enzyme that normally breaks down cAMP to AMP (Main introduction, figure 1.9). This should therefore lead to an increase in activity of the cAMP-dependent protein kinase (PKA) pathway as cAMP is present for a longer duration (Osinski and Schror, 2000). The importance of this in epithelial cells has not been determined.

The two major cyclic-nucleotide-dependent protein kinase phosphorylation sites in human VASP are at residues Ser157 and Ser239 (Butt et al., 1994) with PKG demonstrating specificity for the Ser239 site and PKA for the Ser157 site *in vitro*. The role of phosphorylation at these sites and the effects on actin binding are unclear. In previous investigations, conflicting results concerning the ability of phosphorylation to influence actin binding have been seen (Harbeck et al., 2000; Laurent et al., 1999). In one study an increase in binding was seen and in the other a decrease when phosphorylation occurred. The second study suggested that the effects are different when dual phosphorylation binding at Ser157 and 239 is seen rather than mono-phosphorylation. These studies were both carried out *in vitro* and the situation *in vivo*

may be very different. Also, the two studies used very different conditions and are not really comparable.

To examine the hypothesis that nitric oxide-induced phosphorylation of VASP is a mechanism by which the actin cytoskeleton is disrupted following iNOS induction, this study pursued several different pathways. In this section, we demonstrate that VASP is found at cell:cell and cell:matrix contacts in primary proximal renal tubule cells and bronchial epithelial cells. We show that iNOS expression was associated with a loss of VASP from focal adhesions and disruption actin fibres. We demonstrate that Ser239 VASP phosphorylation is an iNOS-dependent event and that blocking iNOS action, stops this phosphorylation step. We also show that this appears to be a two-step process and that phosphorylation at the Ser157 residue appeared to be permissive step for Ser239 phosphorylation. Stimulation of both the cAMP and cGMP pathways seems to show a synergistic effect on the presence and duration of VASP Ser239 phosphorylation. Work carried out in mouse macrophages suggests that the level of Ser157-phosphorylated VASP was critical to the production of Ser239 phosphorylated VASP. In order to investigate this further we have attempted to produce mutants of VASP in which the phosphorylation sites have been altered.

## **2.2 Methods**

### **2.2.1 Cell Culture of Normal Human Bronchial Epithelial (NHBE) Cells.**

The 16HBE (or NHBE) cell line is a human transformed bronchial epithelial (HBE) cell line (Cozens et al., 1994). We also used an HBE cell line, homozygous for the  $\Delta 508$  mutation in the cystic fibrosis transmembrane receptor (CFTR) (CFBEs) (Goncz et al., 1999). Culture conditions are the same for both cell types.

NHBE and CFBE cells were grown in RPMI media (Gibco, UK) supplemented with 10% FBS (Biowhittaker Europe, UK), penicillin-streptomycin (10u/ml to 10mg/ml) and 2mM glutamine (both from Gibco) at 37°C, 5% CO<sub>2</sub>. Stock cultures of the cell line were passaged when 100% confluence was reached. To passage cells, media was removed, and the cells were washed in HBSS which was then removed. Sufficient 0.05% trypsin- 0.02% ethylenediaminetetraacetate (trypsin-EDTA, Gibco, UK) was added to cover the cells which were then incubated at 37°C until cell detachment occurred. The action of trypsin was terminated by the addition of fresh, FBS-containing media. Cells were split at a 1:3 dilution to maintain stocks.

### **2.2.2 Cell Culture of RAW 264.7 Macrophages**

Mouse macrophage RAW 264.7 cells (European Cell Culture Collection, Porton Down, UK) were cultured in RPMI media supplemented with 10% FBS, 2mM glutamine and penicillin-streptomycin (10u/ml to 10mg/ml). They were passaged when cells had reached 70% confluence. To passage cells, media was removed from the flask and the cells were scraped from the flask. Cells were split at a 1 in 3 dilution to maintain stocks.

### **2.2.3 Cell Culture of MDCK TetOff Cells**

MDCK TetOff cells (BD Clontech) were grown in Dulbecco's modified Eagle's media (DMEM) (Gibco, UK) supplemented with glutamine and penicillin-streptomycin as for RAW cells. Puromycin (10µg/ml) (BD Clontech) was added to the media to maintain the clone. Cells were passaged as described for NHBEs. The MDCK TetOff clone will be described further in Chapter 3.1.

### **2.2.4 Preparation and Characterisation of Primary Human PTEC**

(method adapted from Glynn PA, 2000)

All procedures were performed in a laminar flow hood using sterile tissue culture grade plastic ware and sterile dissection equipment.

#### **2.2.4.1 Reagents**

The following additional materials were used; DMEM/Ham's F-12 (1:1 mixture); insulin-selenium-transferrin supplement (IST, stock 100x) (Gibco, Paisley, UK); type II collagenase from *Clostridium histolyticum*, hydrocortisone, tri-iodothyronine and 10% dimethyl sulfoxide (DMSO) (Sigma-Aldrich Co. Poole, UK); recombinant human epidermal growth factor (hEGF) (Peprotech, London, UK); collagen S (Roche Molecular Biochemicals, East Sussex, UK); 0.1% soybean trypsin inhibitor (Boehringer Mannheim), in sterile phosphate-buffered saline (PBS) (140mM NaCl, 2.7mM KCl, 10mM Na<sub>2</sub>HPO<sub>4</sub>, 1.8 mM KH<sub>2</sub>PO<sub>4</sub>);

#### **2.2.4.2 Preparation of matrix substrate**

Flasks, plates and titertek slides used in the culture of HPTEC were coated with collagen S (0.25mg/l in PBS) and allowed to dry and in the laminar flow hood. FBS was

then added to coat the entire surface and incubated for 6 hours at 37°C. The flasks were then washed 3 times with HBSS and stored for up to 2 weeks at 4°C before use.

#### **2.2.4.3 Serum-free, hormonally defined media**

The following media was used to culture HPTEC: DMEM/Ham's F-12 (1:1 mixture) supplemented with glutamine (2mM), penicillin-streptomycin (50U/ml to 50mcg/ml), insulin 10mcg/ml, transferrin (5mcg/ml), selenium 5ng/ml, hydrocortisone 36ng/ml, tri-iodothyronine (4pg/ml), and Epidermal growth factor (EGF) (10ng/ml).

#### **2.2.4.4 Preparation, culture & passage of HPTEC**

Sections of fresh normal kidney were obtained from nephrectomy specimens performed for the resection of tumours. Patients were counselled appropriately by the surgical staff and written consent for the use of material for research obtained. Cores of outer cortex were taken. Tissue was transported to the laboratory on ice in HBSS containing penicillin-streptomycin (50U/ml to 50mg/ml) and on arrival was placed in HBSS with penicillin-streptomycin, prewarmed to 37°C in a Petri dish in a tissue-culture laminar flow hood. The outer fibrous capsule was stripped away using sterile forceps and discarded. The outer cortex was dissected away from the inner cortical regions and the medulla. The outer cortex was then cut into fragments of approximately 1mm<sup>3</sup> and transferred into a sterile 50ml centrifuge tube. The sample was washed with HBSS three times by spinning at 200g for 5 minutes, pouring off the supernatant and resuspending in fresh HBSS. Collagenase (1mg/ml) was then added to cover the tissue fragments. This was then incubated at 37°C with occasional agitation for 60 minutes. Following this, the cells were sedimented by centrifuging at 200g for 5 minutes. The supernatant was discarded and the cells resuspended in serum free, hormonally defined media. The

cells were counted and then transferred to coated 25cm<sup>2</sup> tissue culture plates. These were then incubated at 37°C in a 5% CO<sub>2</sub>, 95% air incubator. The media was changed approximately 24 hours after initial plating.

Cells were passaged at approximately 100% confluence. Cells were washed with HBSS and incubated with a thin layer of prewarmed trypsin-EDTA at 37°C until cells detachment was observed. Trypsin action was terminated by adding an equal volume of 0.1% soybean trypsin inhibitor. Detached cells were resuspended in serum-free media and subcultured at a 1:3 subculture ratio.

#### **2.2.4.5 Immunofluorescent Staining of HPTEC**

In order to show that the cells showed characteristics of HPTEC, they were stained for specific cytokeratins (4, 5, 6, 8 and 13) found within human epithelial cells. Cells were also exposed to pro-inflammatory cytokines to induce iNOS expression, another characteristic of proximal tubule cells.

The following reagents were used: anti-pan cytokeratin monoclonal antibody (1:100 dilution) (Mouse ascites fluid Clone C-11; Sigma); AlexaFluor 488 goat anti-rabbit IgG (H+L) 2mg/ml and AlexaFluor 488 goat anti-mouse IgG 2mg/ml (H+L)(Molecular probes, Leiden, Netherlands), TNF $\alpha$  (10ng/ml), IFN $\gamma$  (200i.u/ml) and IL-1 (10ng/ml) (Peprotech); iNOS/NOS Type II mAb 250 $\mu$ g/ml (Transduction Laboratories); TitreTek 2 chamber tissue culture slides (Nalge Nunc, USA); Vectashield (Vector Laboratories, USA); normal goat serum (NGS), Triton X-100 and 4,6-Diaminidino-2-phenylindole (DAPI)(Sigma, UK). 4% paraformaldehyde (PFA) solution (4g paraformaldehyde, 1ml 1M NaOH in PBS, pH7.4)

#### **2.2.4.5.1 Cytokeratin Staining**

Cells were grown on collagen and FCS coated-Titrettek 2 chamber slides to approximately 100% confluence. They were then fixed and stained for cytokeratins. All incubations were carried out at room temperature. Cells were fixed in 1% paraformaldehyde (PFA) in PBS for 30 minutes, permeabilised in 0.2% Triton-X 100 in PBS for 20 minutes and blocked in 10% NGS in PBS for 1 hour. Cells were incubated with the primary cytokeratin antibody diluted 1:100 in 10% NGS for 1 hour. Following washing in PBS, the secondary fluorochrome-conjugated antibody was added at a 1:500 dilution in 10% NGS in PBS for a further hour. Nuclei were counterstained with DAPI 1:3000 dilution in PBS for 10 minutes. Slides were mounted in Vectashield and examined using fluorescence microscopy.

#### **2.2.4.5.2 iNOS Induction and staining**

Cells were grown to approximately 90% confluence on Titrettek 2 chamber slides before exposure to TNF $\alpha$  (10ng/ml), IFN $\gamma$  (200i.u/ml) and IL-1 (10ng/ml) for 24 hours to induce iNOS expression. They were then fixed and stained as above using a mouse iNOS mAb (1:200 dilution in NGS for 1 hour) and an anti-mouse fluorochrome-conjugated secondary antibody (1:500 dilution as before).

#### **2.2.5 Distribution of VASP and Actin in HPTEC**

HPTEC were grown in 2-chamber titrettek tissue culture slides. When the cells reached approximately 60% confluence, the media was removed, the cells washed in HBSS and then fixed, stained and permeabilised as before. They were stained with VASP antibody (M4 Antiserum (polyclonal) to VASP (human) (Alexis Biochemicals). (1:500 dilution in 10% NGS) for 1 hour before washing. A secondary fluorochrome-conjugated

antibody was then added and FITC labelled phalloidin to stain F-actin for a further hour. Cell nuclei were counterstained with DAPI and the slides were mounted and examined using conventional immunofluorescent microscopy.

### **2.2.6 The Effects of iNOS Transfection on VASP Localisation in HPTEC**

The following additional reagents were used: Lipofectamine 2000 (Invitrogen); Optimem media (Gibco) and pCI vector (Promega). The pCI/iNOS construct was kindly donated by Dr K.E.A Darling.

#### **2.2.6.1 Transfection protocol**

Human PTEC were grown to 80% confluence in treated 2 chamber Titretek slides in hormonally defined media. In half of the slides, a plasmid/iNOS construct (pCI/iNOS), already available in the laboratory, was transfected into the cells using the following protocol. 1.6µg of DNA in serum-free Optimem was combined with 10µl of Lipofectamine 2000 in serum-free Optimem and added to the tissue culture media in the slide chamber. The media was changed 4 hours post transfection. The cells were incubated overnight at 37°C, 5% CO<sub>2</sub> before being fixed for immunostaining. The other half of the cells were transfected using the same protocol but with empty pCI vector.

#### **2.2.6.2 Immunostaining protocol**

24 hours following transfection, media was removed, the cells washed and then fixed, permeabilised and blocked as before. The cells were stained for iNOS using a mouse monoclonal antibody (1:200 dilution) and for VASP using a rabbit polyclonal antibody at a 1:500 dilution, both for 1 hour at room temperature in 10% NGS. Following washing, the cells were incubated for 1 hour at room temperature with anti rabbit and

anti-mouse fluorochrome-conjugated secondary antibodies. The cell nuclei were counterstained with DAPI. The cells were mounted in Vectashield and visualised using immunofluorescent microscopy. Pictures were taken using Magnafire software.

The number of focal adhesions seen per cell were counted in 10 cells expressing iNOS and 10 cells not expressing iNOS. The number of focal adhesions seen in iNOS-expressing cells was then compared to the number seen in non-iNOS expressing cells using the Mann-Whitney test for non-parametric data. A p value <0.05 was considered significant.

### **2.2.7 Effects of iNOS transfection on VASP phosphorylation in Bronchial Epithelial Cells and HPTEC**

The following additional materials were used: Laemmelli lysis buffer (100mM Tris Cl (pH 6.8), 200mM Dithiothreitol (DTT), 4% sodium dodecyl sulfate (SDS) (both from Sigma, UK), 0.2% bromophenol blue and 20% glycerol); L-N<sup>6</sup>-(1-Iminoethyl)lysine, HCl (L-NIL), (Calbiochem) and N-(3-Aminoethyl) benzyl acetamide.2HCl (1400W) (Alexis Biochemicals)

#### **2.2.7.1 Transfection and lysis**

NHBE cells were grown to 80% confluence in 6 well plates and transfected using the transfection agent Lipofectamine 2000 following a standard protocol. Briefly, for each well 4µg pCI/iNOS DNA was added to 250µl Optimem and 20µl Lipofectamine 2000 was added to 250µl Optimem and incubated at room temperature for 5 minutes. The two mixtures were then combined and incubated at room temperature for a further 20 minutes before being added to the cell media in the 6 well plates.

The samples were then lysed at time points up to 24 hours post transfection, directly into 200µl Laemmli buffer containing 1mM sodium orthovanadate as a phosphatase inhibitor. They were denatured by heating at 105°C for 5 minutes. The samples were analysed by SDS-Page electrophoresis.

HPTEC were also investigated using the same method. They were grown to 80% confluence in pre-coated 6 well plates (See section 2.3.4.2), transfected with iNOS using Lipofectamine 2000 as for NHBEs (section 2.3.6.1), lysed and analysed as above.

In order to investigate control of the pathway further, the selective iNOS inhibitors L-NIL or 1400W at a concentration of 1mM were also added to some samples. These were added immediately prior to transfection of pCI/iNOS at a final concentration of 1mM. The ability of L-NIL and 1400W to block nitric oxide production was assessed with a Griess reaction (see below).

#### **2.2.7.2 Measurement of NO production**

In order to follow the production of nitric oxide in iNOS transfected cells, nitrite production was used as indirect measurement via a standard Griess reaction. Nitrite is an oxidation product of the short-lived free radical NO.

100µl of supernatant was added to an equal volume of Griess reagent (0.1% N(1-naphthyl)ethylenediamine in double-distilled water (DDW) with 1% sulfanilic acid in 5% phosphoric acid) and incubated at room temperature for 10 minutes. A standard curve was produced with NaNO<sub>2</sub>. A colorimetric reaction occurred and was assayed using a microplate reader at 550nm. The nitrite level was determined by comparing

100µl of supernatant was added to an equal volume of Griess reagent (0.1% N(1-naphthyl)ethylenediamine in double-distilled water (DDW) with 1% sulfanilic acid in 5% phosphoric acid) and incubated at room temperature for 10 minutes. A standard curve was produced with NaNO<sub>2</sub>. A colorimetric reaction occurred and was assayed using a microplate reader at 550nm. The nitrite level was determined by comparing values obtained for samples from a standard curve established by adding known quantities of sodium nitrite to the media used in the experiment.

### **2.2.7.3 Sodium dodecyl sulfate (SDS)-polyacrylamide gel electrophoresis and immunoblotting**

The following additional materials were used: polyvinylidene difluoride (PVDF) membrane (Amersham Pharmacia Biotech), VASP activated ser239 clone 16C2 monoclonal antibody, 1µg/ml, (Upstate Biotechnology); Rabbit VASP antiserum M4, 1:3000 dilution, (Alexis Biochemicals); Biotinylated Rabbit IgG H+L and biotinylated mouse IgG H+L, both 1.5mg/ml, (Vector Laboratories, 1:1000 dilution); horseradish peroxidase (HRP) conjugated streptavidin, 1mg/ml (Biosource International); ECL Plus detection kit (Amersham Pharmacia Biotech)

50µl of each sample was loaded and run on a 10% SDS-Page gel at 40mA, transferred onto a PVDF membrane (100mA overnight then 1000mA for 1 hour at 4°C), blocked in 5% milk in PBS for 1 hour and immunoblotted, for P-VASP Ser239 (2 hours, room temperature, 1:100 dilution in 5% milk in PBS) using a commercially available monoclonal antibody against P-VASP Ser239. Membranes were then incubated with a secondary biotinylated anti-mouse antibody for 1 hour following washing in 0.1% Tween 20 in PBS. Following further washes, HRP-conjugated streptavidin diluted

1:5,000 in 5% milk in PBS was added to the membranes (30 minutes at room temperature). Results were visualised using the ECL Plus detection kit.

Following stripping, (see below) the membranes were reblocked and re-stained with pan-VASP antibody (1:500 dilution) for 1 hour at room temperature and a secondary ant-rabbit biotinylated antibody to probe for all forms of VASP.

The same immunoblotting methods were used to look at the effects of the competitive iNOS inhibitors L-NIL and 1400W on VASP phosphorylation.

#### **2.2.7.4 Membrane Stripping**

Membranes were stripped for reprobing by submerging in stripping buffer (100mM 2-mercaptoethanol, 2%SDS, 62.5mM Tris-Cl pH6.7) at 50°C with intermittent agitation for 30 minutes. They were then washed in PBS with 0.1% Tween-20 and reblocked in 5% non-fat milk in PBS.

#### **2.2.8 Induction of iNOS in RAW Cells by pro-inflammatory cytokines and the Effects on VASP Phosphorylation**

RAW 264.7 cells were cultured in 6 well tissue culture flasks in the presence and absence of the selective iNOS-inhibitor, L-NIL. Cells were stimulated with 10ng/ml murine interferon- $\gamma$  (IFN- $\gamma$ ) (Peprotech, UK) and 2 $\mu$ g/ml Lipopolysaccharide (LPS) (10mg/ml from E.coli serotype 0111:B4 (Sigma, UK)) or left unstimulated as a control. Samples were taken at 0, 8, 16, 24 and 28 hours after stimulation to assay for VASP phosphorylation. Cells were harvested by removing media, washing twice in PBS and

lysing in 200µl of Laemmli lysis buffer before transferring to a microfuge tube. Samples were boiled for 5 minutes at 95°C before being analysed using immunoblotting as described in section 2.2.7.3. Membranes were stained initially with the P-VASP Ser239 (Clone 16C2) antibody before being stripped and reprobed with a pan VASP antibody as before.

### **2.2.9 Effects of Nitric Oxide Donors on VASP phosphorylation in HPTEC**

Human PTEC were grown to 90% confluence in 6 well plates as before. The nitric oxide donor spermine NONOate ( $T_{1/2}$  39 minutes at 37°C) (Calbiochem) was used as a nitric oxide donor at a final concentration of 200µM which will release 400µM of NO. The cells were lysed at time points from 15 minutes to 8 hours following the addition of the nitric oxide donor as before and analysed for the presence of P-VASP Ser239 and pan VASP using immunoblotting techniques as described above. A longer acting NO donor DetaNONOate ( $T_{1/2}$  1200mins at 37°C) also used in bronchial epithelial cells at a 200µM concentration with cells lysed at time points from 2 minutes to 28 hours and analysed by SDS-Page electrophoresis as before. Membranes were blotted for both P-VASP Ser239 and (after stripping) pan-VASP as described previously.

### **2.2.10 Effects of a cell permeable cGMP analog on VASP phosphorylation in NHBEs**

The cell permeable cGMP analog Guanosine 3', 5'-cyclic Monophosphate, 8-Bromo-, Sodium salt (8-Br-cGMP) (Calbiochem) was used throughout unless otherwise stated.

Bronchial epithelial cells were grown to approximately 90% confluence in 6 well plates. 8-Br-cGMP was administered at final concentrations of 200 and 500µM. Cells were

### **2.2.11 Effects of addition of a cell-permeable cAMP analog to iNOS-transfected NHBEs**

The following cell permeable cAMP analog was used in all experiments unless otherwise stated: 8-Bromoadenosine 3',5'-cyclic monophosphate. Sodium salt (8-Br-cAMP) (Alexis Biochemicals).

NHBE cells were grown to 70% confluence in 6-well plates and transfected with iNOS as described previously. At 4 hours post transfection, the media was changed and half the cells had 8-Br-cAMP added at a final concentration of 100mM. In wells treated with 8-Br-cAMP in addition to iNOS. As a control, some wells had 8 Br-cAMP alone added, with no iNOS transfection. Samples were taken at time points from 5 minutes to 4 hours post administration (8 hours post-iNOS transfection), directly into Laemelli buffer. The samples were analysed by immunoblotting for VASP and P-VASP Ser239 as before as described in section 2.2.7.3.

### **2.2.12 Production of a Ser239-Ala VASP mutant**

The following additional reagents were used:- VASP cDNA GeneStorm Expression Ready Clone RG00084 in pcDNA3.1/GS (Resgen); Qiagen Miniprep Kit and Midiprep Kit, Qiagen Gel Purification Kit (Qiagen); Zeocin, EcoR1, Mlu-1, Not-1, Bam-H1 restriction endonucleases and Luria-Bertani (LB) low salt medium (Invitrogen); Agarose (electrophoresis grade) (Sigma, UK); Stratagene QuikChange site-directed mutagenesis kit;); X-gal and Isopropyl  $\beta$ -D-1-thiogalactopyranoside (IPTG) (Invitrogen, UK); 6x His-tag rabbit polyclonal antibody (AbCam)

mutagenesis kit); X-gal and Isopropyl  $\beta$ -D-1-thiogalactopyranoside (IPTG) (Invitrogen, UK); 6x His-tag rabbit polyclonal antibody (AbCam)

#### **2.2.12.1 Extraction of VASP cDNA**

VASP cDNA was supplied in the pcDNA3.1/GS plasmid as an expression-ready bacterial clone in chemically competent *E.coli*. The plasmid contains a Zeocin resistance gene to allow selection of clones. It also contains a V5 epitope and a 6xHis tag to allow detection of the plasmid. The bacteria were streaked onto low salt LB containing 25 $\mu$ g/ml of zeocin and grown overnight at 37°C. A single colony was inoculated into 5ml liquid low salt LB medium containing zeocin (25 $\mu$ g/ml) and grown at 37° C in a shaking incubator at 200rpm for 2 hours. 1ml of this culture was then inoculated into 100ml of the same medium and grown overnight under the same conditions. The following day, the culture medium was centrifuged at 6,000g to give a bacterial pellet. Plasmid DNA was then extracted using a Qiagen MidiPrep kit. The amount of DNA was quantified spectrophotometrically. To check the DNA was present, it was digested with the restriction endonuclease Mlu-1 (which cuts at 228 and 983 in the plasmid) at 37° for 3 hours. The DNA digest was then run on a 1% agarose gel containing ethidium bromide, at 70v for approximately 1 hour before being visualised with a UV camera.

#### **2.2.12.2 Site-Directed Mutagenesis of Serine 239 residue to Alanine**

A VASP Ser239Ala mutant was constructed using the Stratagene QuikChange site-directed mutagenesis kit. The following oligonucleotide primers were used

5' CAAACTCAGGAAAGTCGCGAAGCAGGAGGAGG 3'

5' CCTCCTCCTGCTTCGCGACTTTCCTGAGTTTG 3'

(from (Smolenski et al., 1998).

This method allows site-specific mutagenesis in double stranded DNA plasmids. The steps involved are denaturing of plasmid and annealing of the oligonucleotide primer, temperature cycling with non-strand-displacing Pfu Turbo polymerase to extend and incorporate the mutagenic primers resulting in nicked circular strands, digestion of methylated, non-mutated parental DNA with Dpn I, followed by chemical transformation into XL-1 Blue supercompetent cells (all supplied in QuikChange Kit). The cells then repair the nicks in the mutated plasmid. The cells are spread onto low salt LB agar containing 25µg/ml Zeocin, spread with X-gal and IPTG to allow colour-screening identification of colonies (blue = contain mutation). Blue colonies were picked and grown up overnight in 4ml of media (as before). Plasmid DNA was then isolated using a Qiagen miniprep kit. The concentration of DNA was checked spectrophotometrically and DNA sequenced using the primer 5' AGGTGGAGCAGCAGAAAAG 3', to look for site-specific mutation.

### **2.2.13 Localisation of VASP and VASP Ser239-Ala mutant in HPTEC:**

#### **Effects of iNOS cotransfection**

##### **2.2.13.1 Transfection protocol**

Human PTEC were grown to 80% confluence in collagen S and FCS-treated 2-chamber Titretrek slides. Lipofectamine 2000 was used as a transfection agent. 1.6µg/well total of DNA (either 1.6µg of a single DNA or 0.8µg of each DNA if cotransfection was carried out) in 200µl Optimem was combined with 10µl of Lipofectamine 2000 in 200µl Optimem for 20 minutes before being added to the slide chamber. The media was changed 4 hours post-transfection. The cells were then incubated for a further 20 hours before being fixed and stained. The transfections carried out were

### **2.2.13.2 Immunostaining protocol**

24 hours post-transfection, media was removed from the cell chamber and the cells were washed, fixed, permeabilised and blocked as described previously. To stain for VASP or the VASP mutant, the cells were incubated with a 6x His-tag rabbit polyclonal antibody (1:500 dilution) for one hour at room temperature, washed and then stained with a secondary anti-rabbit fluorochrome-conjugated antibody (AlexaFluor 568 anti-rabbit IgG 2mg/ml). AlexaFluor FITC-conjugated phalloidin 488 (1:50 dilution) was used to visualise filamentous actin and was added at the same time as the secondary antibody. For iNOS staining, a mouse monoclonal antibody was used (Transduction Laboratories 250µg/ml, 1:200) as the primary antibody and a secondary anti-mouse antibody (AlexaFluor 568 anti mouse IgG) was used as before. The slides were visualised using confocal microscopy (Biorad MRC 1024, Zeiss Axiovert microscope and LaserSharp software).

### **2.2.14 Transfection and Production of a Stable pTRE2hyg/iNOS Clone of MDCK TetOff Cells**

The following additional reagents were used:- pTRE2hyg plasmid, Tet-system-approved foetal bovine serum (Tet-free FBS) and hygromycin were all obtained from BD Clontech. pCI/iNOS was donated by Dr K.E.A Darling. Restriction enzymes (Mlu-1 and Not-1) were obtained from Invitrogen. T4 DNA ligase and buffer were obtained from Promega.

#### **2.2.14.1 Production of pTRE2hyg/iNOS Construct**

The pCI/iNOS plasmid construct and pTRE2hyg were digested with Mlu-1 and Not-1 restriction enzymes for 2 hours at 37°C in a water bath. The products were then run on a 1% agarose gel containing 0.5µg/ml ethidium bromide to separate the plasmid and insert bands. Bands representing pTRE2hyg and iNOS were cut from the gel and gel purified using a Qiagen gel purification kit. The iNOS insert and pTRE2hyg were ligated using T4 DNA ligase overnight at 16°C. Following ligation, an aliquot was re-digested with Mlu-1 and Not-1 and run on a 1% agarose gel to check for insertion of iNOS into the plasmid.

#### **2.2.14.2 Electrical Transformation of Bacteria with pTRE2hyg/iNOS**

Chemically competent bacteria (TOPO One Shot, Invitrogen) were transformed with pTRE2hyg or pTRE2hyg/iNOS. Cells were defrosted on ice before the addition of 1µl of DNA solution. Bacteria were electroporated using an Electrocell Manipulator 600 at 2.5kV resistance voltage, 2.45kV charging voltage and 129 ohms resistance. 450µl of SOC media was added immediately to each bacterial aliquot. The bacteria were shaken for 1 hour at 37°C before aliquots were spread on LB agar plates containing 50µg/ml ampicillin (selective antibiotic for pTRE2hyg). Plates were incubated at 37°C overnight.

The following day, 12 colonies were picked from the pTRE2hyg/iNOS transformant plate and plasmid DNA extracted using a Qiagen DNA miniprep kit. DNA samples were digested once more with Mlu-1 and Not-1 before being run on a 1% agarose gel. 6 out of the 12 samples expressed pTRE2hyg containing the appropriately sized (1.14 kbp) band for iNOS insertion. One sample was chosen and used for all further experiments.

kbp) band for iNOS insertion. One sample was chosen and used for all further experiments.

#### **2.2.14.3 Transfection of MDCK TetOff Cells with pTRE2hyg/iNOS**

MDCK TetOff cells were grown on 2 chamber Titretek cell culture slides and transfected with pTRE2hyg/iNOS using Lipofectamine 2000 using a standard protocol. Briefly, 1.6µg of DNA and 10µl of Lipofectamine 2000 were used to transfect each well. Following transfection, half the cells were grown in the presence of 2µg/ml doxycycline and the other half in the absence of the antibiotic. 24 hours after transfection, cells were fixed, blocked and permeabilised. They were then stained for iNOS (method as section 2.3.6.2) and the nuclei stained with DAPI. Slides were then examined using standard immunofluorescent microscopy.

#### **2.2.14.4 Cloning of pTRE2hyg/iNOS Transfected MDCK TetOff Cells**

Attempts were made to produce a stable clone of pTRE2/hyg/iNOS transfected cells. (For an explanation of the TetOff system see Chapter 3, Section 3.1). MDCK TetOff cells were grown to 90% confluence before being transfected with pTRE2hyg/iNOS. Cells were grown in the presence of 2µg/ml of doxycycline unless otherwise stated.

24 hours after transfection, hygromycin (100µg/ml) was added as a selective antibiotic. In order to assess the concentration of hygromycin needed to act as a selective antibiotic, a kill curve experiment was carried out for each new attempt at production of a stable clone (section 2.3.14.5). Within 48 hours after hygromycin addition, massive cell death occurred. The remaining cells continued to be cultured in the presence of doxycycline and hygromycin until 100% confluence was reached. At this point, cells

were subjected to trypsin-EDTA to cause cell detachment. Cells were counted using a haemocytometer and diluted to a concentration of  $1 \times 10^4$  cells/ml. Cells were then transferred into a tissue culture 96 well plate. Column 1 contained cells at a concentration of  $1 \times 10^4$  cells/ml. Doubling dilutions were then carried out across the plate so the final column contained cells at a theoretical concentration of 7 cells/ml. Each well held 200 $\mu$ l so theoretically, the final column would be expected to hold approximately 1 cell. Cells continued to be cultured in selective antibiotics as before.

The 96 well plate was checked daily for cell growth. Only wells that appeared to contain single clones were allowed to continue growing. Once confluence was achieved in these wells, they were moved sequentially into 24 well plates, 6 well plates and T25 tissue culture flasks.

The ability of the clones to express iNOS was assessed by the culture of an aliquot of a clone on 2 chamber slides in the presence and absence of doxycycline.

#### **2.2.14.5 Construction of a Hygromycin Kill Curve**

MDCK TetOff cells were grown to 90% confluence in a 6 well plate. Hygromycin was added to the wells at concentrations from 0 – 800 $\mu$ g/ml. The cells were allowed to continue growing and assessed for cell death daily. The media was changed every 4 days, unless need earlier (indicated by a colour change from red to yellow). Hygromycin was added every 4 days or with a change in media. The end point was massive cell death at 5-7 days to give the most appropriate selection concentration.

## **2.3 Results**

### **HPTEC in Culture Demonstrate Epithelial Pattern Cytokeratin Staining and iNOS Expression following Cytokine Simulation**

Positive immunostaining for pan-cytokeratin using an antibody against human cytokeratins 4, 5, 6, 8, 10 and 13 was uniformly seen throughout the cells (figure 2.1). This antibody is a broad spectrum antibody that reacts with a wide variety of epithelial cells and is useful in staining cultured epithelial cells. The cells also demonstrate iNOS expression following cytokine stimulation in approximately 50% of cells. iNOS positive cells often appeared in aggregates (Figure 2.2). These cells were suitable for further experimental use.

#### **2.3.2 VASP Localisation in HPTEC**

VASP staining in individual HPTEC revealed its distribution at the cell membrane in focal sites. These sites were co-localised with the ends of actin fibres seen stretching across the cell cytoplasm (Figure 2.3). This is consistent with VASP's abilities to bind to integrins and also to actin as a focus of F-actin nucleation and polymerisation.

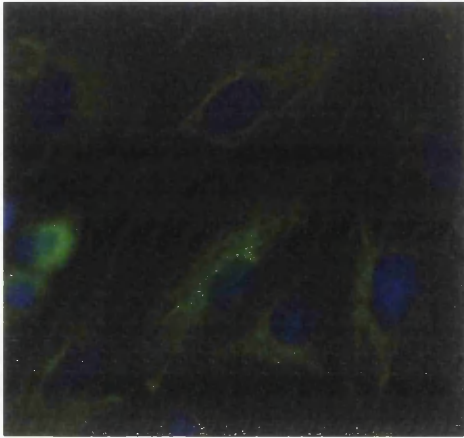


**Figure 2.1 Cytokeratin staining in HPTEC (green).** Cell nuclei are counterstained with DAPI. (Magnification x400)

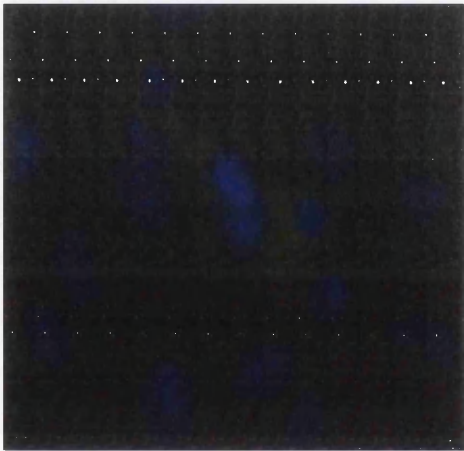
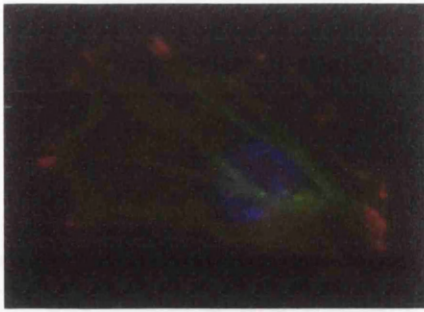


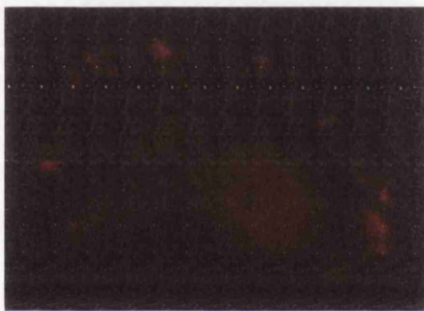
**Figure 2.2 iNOS expression in HPTEC following cytokine stimulation.** iNOS (green) expression is seen distributed throughout the aggregate of iNOS-expressing cells (Magnification x 400)



**MERGED**



**ACTIN**



**VASP**

**Figure 2.3 Co-localisation of VASP and actin in HPTEC.**  
VASP (red) localises at the ends of F-actin (green) fibres at focal adhesions (Nuclei stained with DAPI (blue) (magnification x 1000)

### **2.3.4 iNOS Expression Causes Loss of VASP from Focal Sites at the Cell Membrane**

The effects of iNOS expression on the distribution of VASP in human PTEC were examined using immunofluorescent microscopy to visualise native VASP and the effects of iNOS transfection on its location within the cell.

Following iNOS transfection in HPTEC, a large amount of cell death was seen (70-90%). In cells not expressing iNOS, VASP staining (Figure 2.4) was seen to localise to the cell periphery at what appear to be focal adhesions. This is consistent with its known distribution with  $\beta_1$  integrin associated protein complexes. Some low level, non-specific, cytoplasmic staining was seen. In cells expressing iNOS (Figure 2.4) focal adhesions were less common or not present at all. The cells also demonstrated a more rounded morphology that suggests that these cells were less firmly attached to the extracellular matrix (ECM), having fewer sites of contact and therefore more likely to shed.

The number of focal adhesions present was counted in 10 cells expressing iNOS and 10 cells not expressing iNOS. In surviving cells, the mean number of focal adhesions seen in iNOS-expressing cells was lower compared to cells not expressing iNOS. iNOS-expressing cells showed a mean of 3.1 focal adhesions (range 0-9, median 1.5) per cell (figure 2.5) In cells not expressing iNOS, the mean number of focal adhesions was 18.3 (5-39, median 16) per cell. This was significantly different ( $P < 0.01$ ) when analysed using the Mann-Whitney test. These results show that iNOS induction is associated with the loss of VASP from focal adhesion sites.

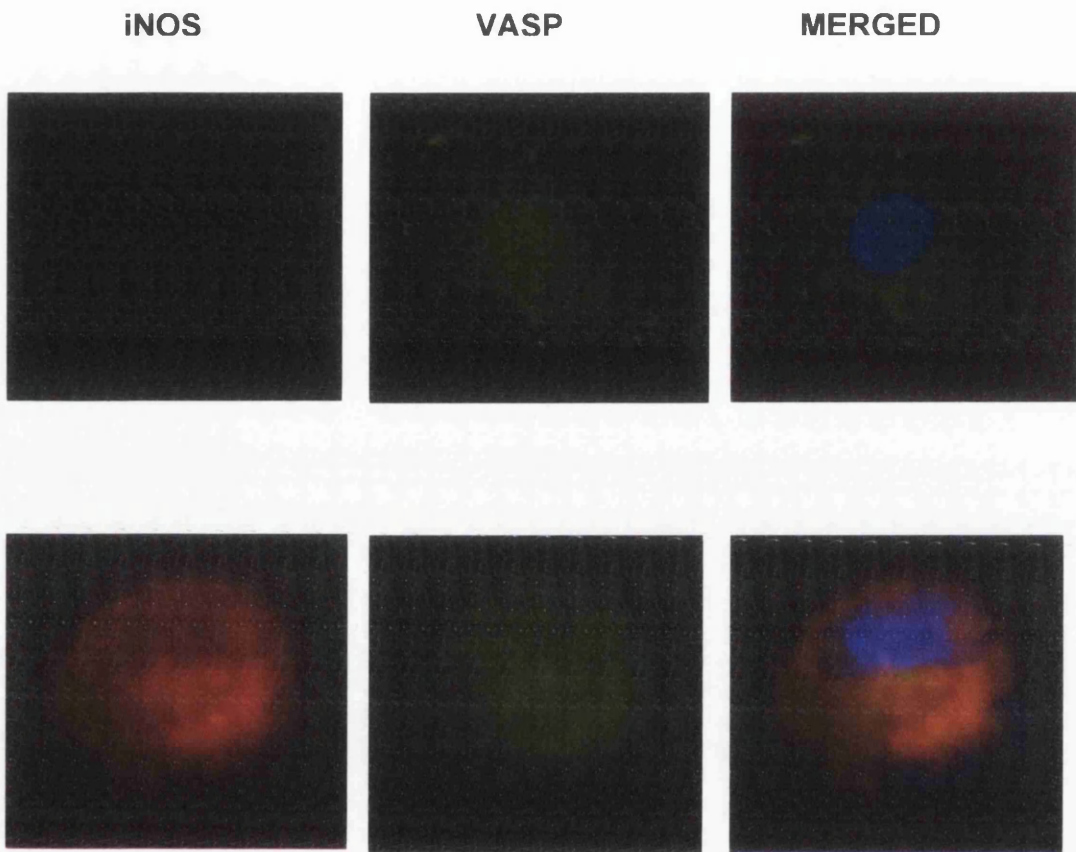


**Figure 2.4 The effects of iNOS expression on VASP localisation in HPTEC.** The upper panel of cells demonstrates the peripheral location of VASP (green) in a single HPTEC. The lower panel demonstrate the effects of iNOS (red) expression on this localisation. (Magnification x 1000)

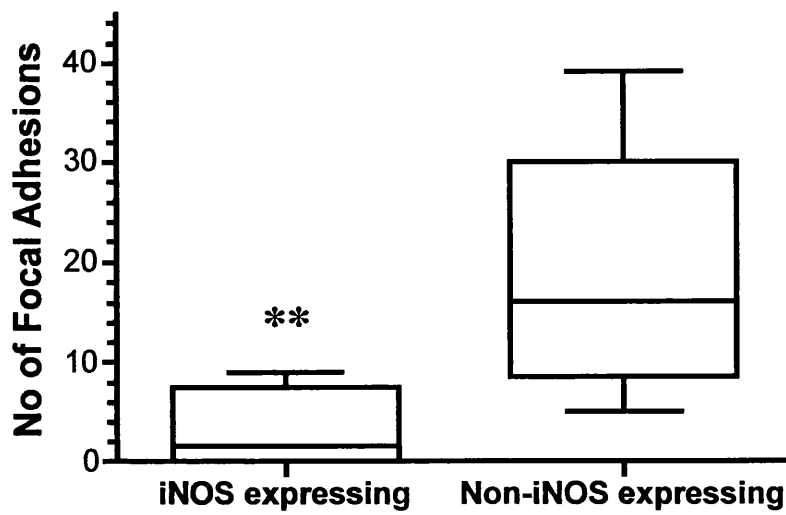


**Figure 2.5** iNOS expression leads to a decrease in the mean number of focal VASP adhesion sites in HPTEC. Mann-Whitney analysis shows a highly significant difference in the number of focal sites (\*\*  $p < 0.01$ ).

### **2.3.5 Nitric Oxide, cGMP and VASP Phosphorylation**

The nitric oxide donors, spermine NONOate and DetaNONOate were used to investigate the effect of a steady level of NO production on VASP phosphorylation in NHBEs. These molecules release NO over a sustained period of time when made into solution. They were used in order to try and look at the direct effects of treating the cells with NO. No Ser239 phosphorylation was detectable with either of these compounds (Figure 2.6). This lack of phosphorylation was also seen when 8-Br-cGMP was used as a cell-permeable analog of cGMP to try and stimulate cGMP-dependent kinase directly (Figure 2.7). Both of these methods have been used previously to stimulate VASP phosphorylation in platelets ((Horstrup et al., 1994; Li et al., 2003). It is unclear why these methods did not succeed. It is possible that in epithelial cells, NO needs to be produced in very close proximity to its target enzyme and that it is rapidly broken down in other locations within the cell, before it is able to have a detectable effect.

The effects of transfection of the iNOS gene were also investigated. Primary HPTEC are difficult to obtain, have a limited duration of usefulness prior to de-differentiation and are difficult to transfect. An alternative cell line was therefore also used to allow further investigations to be carried out. 16HBEs (or NHBEs, normal human bronchial epithelial cells) are a well-characterised human bronchial epithelial cell line ((Kelley TJ, 1995; Puddicombe et al., 2000) which display normal features of epithelial cells such as polarity and a well - defined actin cytoskeleton. They are more easily transfected than primary PTECs ((Wiseman et al., 2003) and as such are a useful tool in this work. The CF variant of this cell line was also used (CFBE)– these contain the cystic fibrosis transmembrane receptor mutant (CFTR) and were available within the laboratory).

**Figure 2.6a.** VASP phosphorylation following the administration of DetaNONOate demonstrating an absence of Ser239 phosphorylation

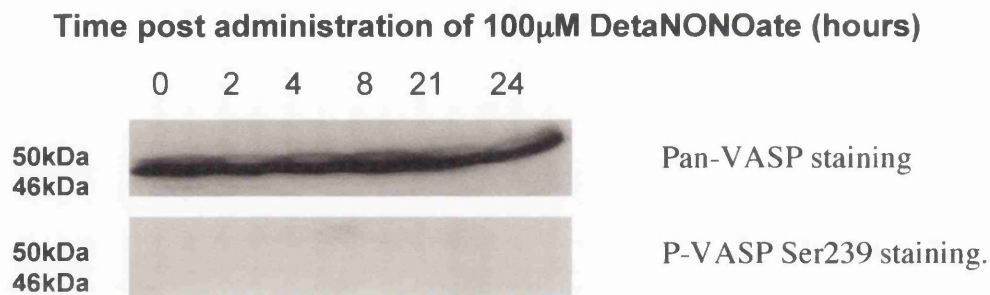


**Figure 2.6b.** Membrane stained for P-VASP239 phosphorylation following the administration of Spermine NONOate demonstrating an absence of Ser239 phosphorylation.

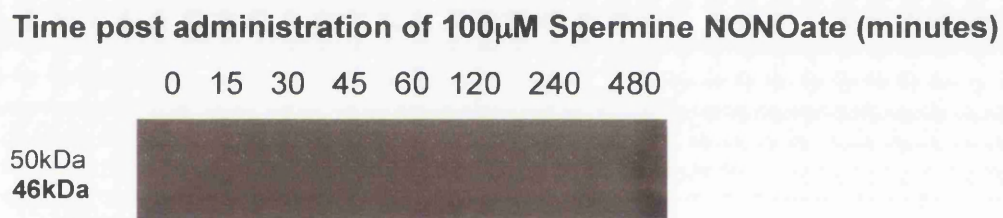


**Figure 2.6 VASP phosphorylation following the administration of NO donors to bronchial epithelial cells.** Membranes were stained with either a pan-VASP antibody, able to recognise all forms of VASP or with the 16C2 clone monoclonal antibody, only capable of recognising VASP that has undergone phosphorylation at the Ser239 site (P-VASP Ser239)

**Time post-administration of 8 Br-cGMP (hours)**

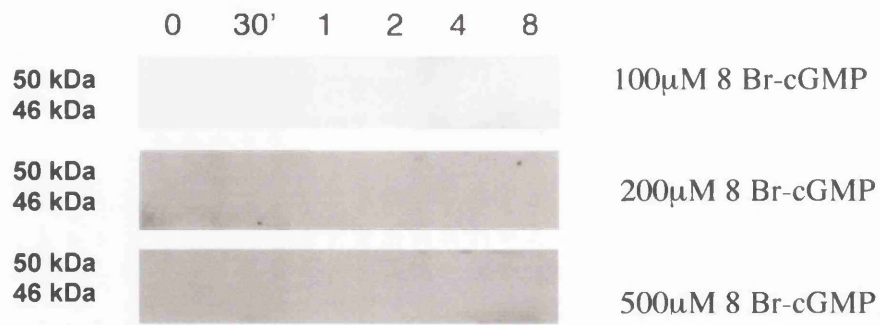


**Figure 2.7 VASP phosphorylation at Ser239 in bronchial epithelial cells following the administration of 8 Br-cGMP.** Following 8 Br-cGMP administration, samples were analysed for Ser239 phosphorylation using a phospho-specific antibody as before.

In most cell types, VASP exists in a mixture of both the 46kDa and 50kDa (Serine 157 phosphorylated) forms but levels of the Serine 239 phosphorylated form are not found. In NHBE cells prior to transfection, no phosphorylation of VASP at the Serine 239 site is detectable by immunoblotting – no band is seen either at the 46 or 50 kDa position (figure 2.8) in the first lane of the top right panel of the blot. In contrast, pan-VASP staining of the same membrane demonstrates two bands – at the 46 and 50 kDa positions. This shows that a percentage of VASP always exists in the Ser157 phosphorylated form at 50kDa. This was seen with all cell types used.

Following iNOS transfection, a rise in Ser239 phosphorylation was seen and is seen at both 4 and 8 hours post transfection (figure 2.8, right upper panel). By 20 hours post-transfection, this band is no longer visible. A Griess reaction to measure nitrite levels was performed in order to see whether this was due to a decrease in NO production. This showed that nitrite levels were still rising, 24 hours post transfection (figure 2.9) suggesting that another mechanism is involved in controlling the duration of phosphorylation and that this is able to block the effects of the continuing presence of NO.

When the membrane was stripped and reprobbed with pan-VASP antibody (figure 2.8, left hand panels), it was seen that Ser239 phosphorylated VASP is only detectable at the 50kDa position. This indicates that it must also be phosphorylated at Ser157 to have caused the observed mass shift.

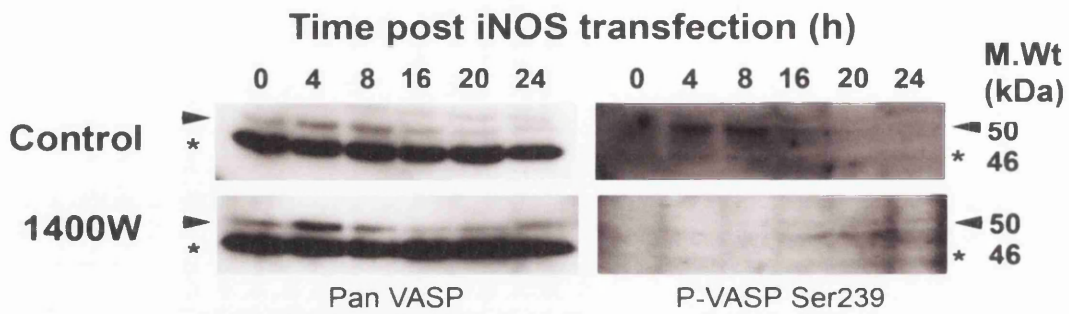


**Figure 2.8 VASP phosphorylation following iNOS transfection.** VASP phosphorylation at Ser157 is demonstrated by bands at 50kDa when stained with either antibody. Phosphorylation at Ser239 is detected by the use of a phospho-specific antibody. The appearance of a 50kDa band with Ser239 specific staining indicates that both Ser157 phosphorylation (to cause an apparent mass shift) and Ser239 phosphorylation must have occurred.

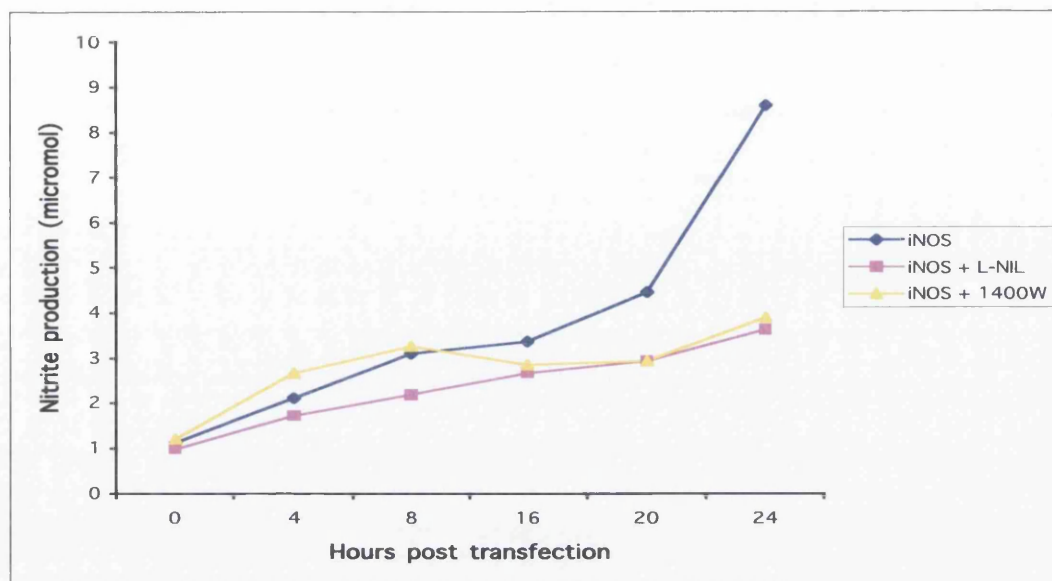


**Figure 2.9 Inhibition of nitrite production by iNOS inhibitors.** A Griess reaction to measure nitrite levels as a marker of NO production was used to detect the effects of the specific iNOS blockers L-NIL and 1400W on NO output following iNOS transfection in NHBEs.

The addition of 1400W prior to transfection, blocked Ser239 phosphorylation completely (figure 2.8, lower right hand panel) indicating that phosphorylation at this site is a nitric oxide-mediated process. The competitive iNOS inhibitor, L-NIL and 1400W successfully inhibited NO production when assessed by a Griess reaction. (Figure 2.9). The addition of 1400W failed to block an increase in Ser157 phosphorylation (Figure 2.8, lower left hand panel, second lane, upper band) suggesting an alternative method of activation of phosphorylation, not dependent on NO. This increase in Ser157 phosphorylation following transfection was not consistent and may reflect variability in transfection of these cells and their response to the transfection process.

In RAW cells a slightly different pattern of VASP phosphorylation was seen. In these cells, iNOS induction was produced by the use of LPS and IFN- $\gamma$  stimulation rather than by iNOS transfection. A rise in Ser157-phosphorylated VASP (50 kDa band) is seen with pan-VASP staining by 16 hours after stimulation and is still visible 12 hours later (figure 2.10). Ser239P-VASP is not detected until 24 hours after stimulation. In contrast to NHBEs, this form of VASP is visible as two bands at 46 and 50 kDa. This shows it is present both as the mono-phosphorylated form where it is only phosphorylated at Ser239 (46 kDa band), and as the bis-phosphorylated form (Ser239 and Ser157) shown by the 50kDa band, though at much higher levels as the bis-phosphorylated than the mono-phosphorylated form. In NHBEs, the mono-phosphorylated form was not detected (figure 2.8). In RAW cells, cytokine stimulation leads to very high levels of iNOS induction which may be sufficient to allow Ser239 phosphorylation alone even without accompanying Ser157 phosphorylation. Ser239 phosphorylation does appear to

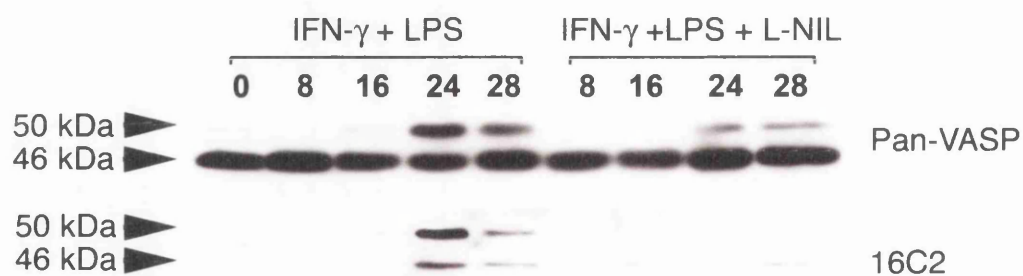


**Figure 2.10 VASP phosphorylation in RAW cells following iNOS induction.**

Raw cells were treated with IFN- $\gamma$  and LPS to induce iNOS. L-NIL was used as a selective blocker of iNOS in order to investigate the NO-mediated pathway of VASP phosphorylation. Membranes were blotted for P-VASP Ser239 (16C2 antibody) and for pan-VASP. The 50kDa band represents VASP that has undergone Ser157 phosphorylation.

be largely nitric oxide-dependent as the use of L-NIL completely abolishes the 50 kDa band and dramatically decreases the intensity of the 50 kDa band. In iNOS-transfected HPTEC, a rise in the proportion of P-VASP Ser157 phosphorylation was seen, starting at 4 hours and peaking at 21 hours following transfection (figure 2.11, upper panel). Phosphorylation at the Ser239 site was seen but only at very low levels, probably reflecting the high proportion of cell death and the relatively small amount of this form of the protein, compared to total cellular VASP levels. Phosphorylation at Ser239 (Figure 2.11, lower panel) appeared to occur earlier (at 4 hours post transfection) than the P-VASP157 but this result was inconsistent and difficult to confirm due to the variable and low levels of iNOS transfection seen in these cells.

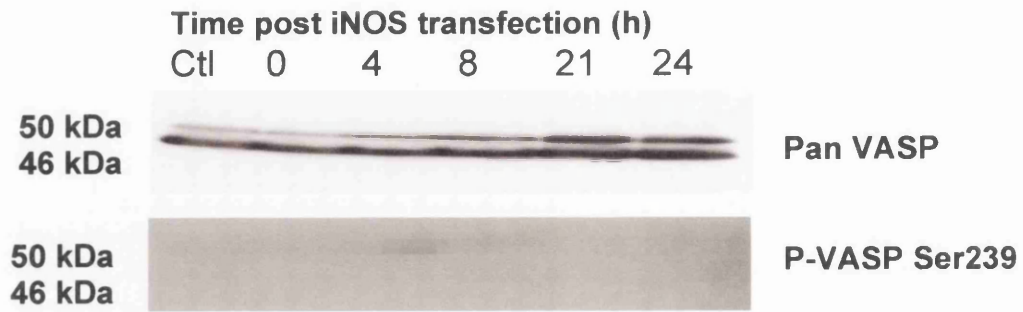


**Figure 2.11 VASP phosphorylation in HPTEC following iNOS transfection.**

Staining in the upper panel is with a pan-VASP antibody, capable of recognising all forms of VASP. In the lower panel, the same membrane has been stained with a monoclonal antibody only capable of recognising P-VASP Ser239.

### **2.3.6 The Effects of Addition of a cAMP Analog to iNOS-transfected cells**

As Ser239 phosphorylation was only detected at 50kDa, indicating that Ser157 phosphorylation had occurred, the effects of adding a cAMP analog were investigated. *In vitro* experiments suggest that Ser157 is preferentially phosphorylated by cAMP-dependent protein kinase (Halbrugge and Walter, 1989).

In NHBE cells treated with iNOS alone, P-VASP Ser239 was first seen at 4 hours post transfection and was no longer detectable by 6 hours (Upper left panel, figure 2.12a). Stripping of the membrane and reprobing for pan-VASP, demonstrated that this band was only present at the 50kDa position as before (Figure 2.12a, left lower panel), indicating that the VASP must also have been phosphorylated at Ser157 to induce the apparent mass shift. When 8 Br-cAMP was added 4 hours after iNOS transfection, the 50kDa band was also seen on staining for P-VASP Ser239 but persisted for much longer – it was still present at 8 hours post transfection (4 hours post 8-Br-cAMP) where it had disappeared in cells treated with iNOS alone (Upper right panel, figure 2.12a). This also appears to be mirrored by the persistence of a higher level of serine 157 phosphorylated-VASP at the 50kDa position seen with pan VASP staining. Thus, addition of a cAMP analog appears to be able to overcome dephosphorylation of P-VASP Ser239. When 8 Br-cAMP is added to cells that have not undergone iNOS transfection, no Ser239 phosphorylation of VASP is seen (Figure 2.12b), 8 Br-cAMP alone is unable to mediate Serine 239 phosphorylation of VASP. This suggests a potential synergistic mechanism between the cAMP and cGMP pathways, possibly via phosphorylation by cAMP at Ser157 leading to a conformational change, exposing the cGMP preferred Ser 239 site to phosphorylation (see figure 1.9, main introduction).

**Figure 2.12. iNOS transfection with or without costimulation with 8 Br-cAMP in NHBE cells: Effects on VASP phosphorylation**

**Figure 2.12a.** Effects of addition of Br-cAMP to NHBEs transfected with iNOS

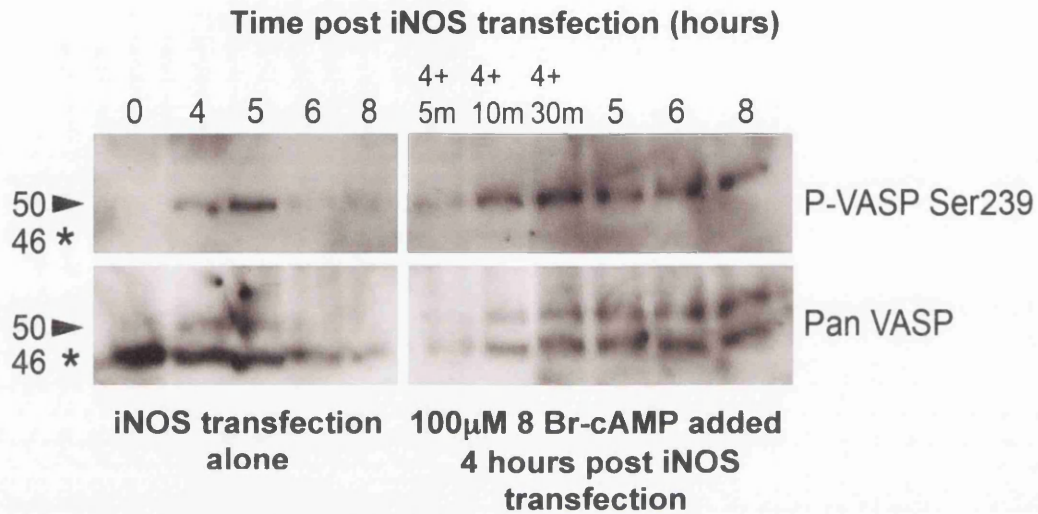
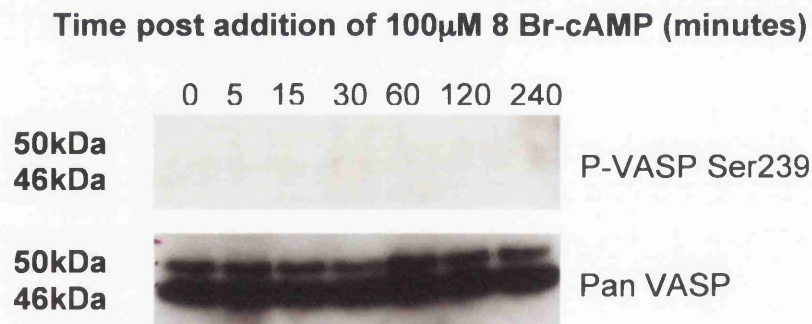


**Figure 2.12b.** Effects of addition of 8 Br-cAMP to untransfected NHBEs



### **2.3.7 Distribution of His-tagged VASP and Ser239-Ala VASP in HPTEC**

Use of the QuikChange site – directed mutagenesis kit allowed production of a mutant form of VASP in which the Ser239 residue was replaced by an Alanine residue. Alanine is not able to be phosphorylated. This mutation was confirmed by DNA sequencing. Transfection of this mutant in HPTECs was detected by staining for His-tagged VASP

Primary cells are difficult to transfect and less robust than cell lines. A high proportion of death was seen in transfected HPTEC, with less than 50% of cells surviving. His-tagged VASP was seen by 24 hours post-transfection. It localised in the same pattern as native VASP to the cell membranes at the ends of actin fibres (Figure 2.13a). As expected, VASP that had undergone mutation at the Ser239 residue to mutate it to alanine also localised in this pattern (Figure 2.13b).

In cells that had undergone co-transfection with VASP and iNOS, cell death was even higher, with less than 10% of cells surviving. Despite expression of His-tagged VASP in several of these cells, showing that transfection had occurred, iNOS co-expression could only be detected in very few cells. In cells where Ser239-AlaVASP mutant had been transfected with iNOS, no iNOS-expressing cells were seen.

Cells expressing iNOS and His-tagged VASP showed a different morphology to non-iNOS transfected cells. The cells were less spread out and no focal localisation of VASP was seen (Figure 2.13c).



**Figure 2.13a.** His-tagged VASP (red) and actin (green) distribution in HPTEC (Magnification x 630)



**Figure 2.13b.** His-tagged Ser239-Ala VASP (red) and actin (green) mutant distribution in HPTEC (Magnification x 630)



**Figure 2.13c.** Distribution of His-tagged VASP (green) and iNOS (red) in HPTEC (Magnification x 630)

**Figure 2.13. Distribution of VASP and the Ser239-Ala VASP mutant in HPTEC.** Cells were transfected with either VASP or Ser239-Ala VASP or co-transfected with iNOS and VASP and fixed and stained 24 hours later. No cells expressing the VASP mutant and iNOS were seen.

### **2.3.8 Transfection and Cloning of pTRE2hyg/iNOS in MDCK TetOff Cells**

We aimed to produce a stable MDCK TetOff clone containing a regulatable iNOS insert in order to allow us to investigate the effects of inducing iNOS expression at different points in epithelial sheet and tubule formation. Following successful production of the pTRE2hyg/iNOS construct, it was transfected into MDCK TetOff cells and examined after 24 hours. Cells grown in the presence of doxycycline showed no iNOS expression (Figure 2.14a) demonstrating tight control of expression by the TetOff system. In cells grown in the absence of doxycycline, iNOS expression was observed (figure 2.14b) but in a disappointingly low number of cells (less than 2%). This system was also used for transfection of dominant-negative VASP in chapter 4 with a much higher level of success. This suggests that it is the iNOS itself that is related to the low level of expression as all other experimental conditions are the same.

Construction of a hygromycin kill curve showed 100µg/ml to be a suitable hygromycin concentration to use in this experiment. In other attempts at cloning (Chapter 3.2.6), 200µg/ml was used.

Multiple attempts at cloning failed to produce a stable iNOS-expressing clone. The earliest time-point at which it was possible to test for iNOS expression was 2 weeks post-transfection. By this time, iNOS expression had already been lost. Further attempts at cloning were abandoned.

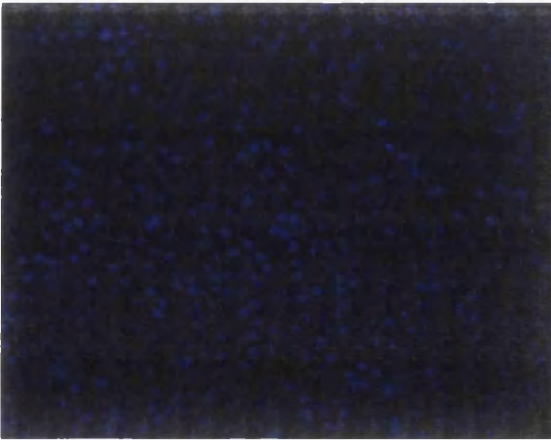


**Figure 2.14a.** MDCK TetOff cells transfected with pTRE2hyg/iNOS grown in the presence of doxycycline (Magnification x 100)



**Figure 2.14b.** MDCK TetOff cells transfected with pTRE2hyg/iNOS grown in the absence of doxycycline (Magnification x 100)

**Figure 2.14 Expression of iNOS in MDCK TetOff cells following transfection with pTRE2hyg/iNOS: Effects of Doxycycline Suppression.** Both sets of cells were transfected with pTRE2hyg/iNOS and allowed to continue growing for a further 24 hours before being fixed and stained. In the upper panel, no iNOS expression is seen. In the lower panel, in the absence of doxycycline suppression, a few iNOS-expressing (green) cells can be seen. (Nuclei stained blue with DAPI)

## 2.4 Discussion

The aim of the work described in this section was to find a mechanism by which nitric oxide causes shedding of epithelial cells. As described previously, VASP is a possible target due to its cGMP-dependent kinase site, situated near an actin-binding domain (Bachmann et al., 1999). We have shown VASP is normally localised at focal sites in the cell membrane, at the ends of actin fibres (figure 2.3) and that induction of iNOS is associated with loss of VASP from these sites (figure 2.4). These cells demonstrate altered morphology, tending to take up a more rounded shape and actin fibres are no longer seen. This suggests that the cells are no longer firmly attached to the extracellular matrix consistent with a redistribution of integrins away from the basolateral surface (Glynne et al., 2001), making them more prone to detachment and loss. This is the pattern also seen in ischaemic injury with disruption of actin filaments, a loss of cell polarity due to altered integrin:matrix interactions, cell shedding and tubule obstruction (Atkinson et al., 2004; Goligorsky et al., 1993; Molitoris et al., 1991; Molitoris and Wagner, 1996). The effects of iNOS on VASP distribution and the altered cell morphology associated with this are therefore a potential path by which cell loss in the proximal tubule during sepsis-induced pro-inflammatory cytokine release may occur.

We have also demonstrated that VASP phosphorylation at the Ser239 position in epithelial cells is seen following iNOS induction (Figure 2.8) and that inhibiting NO generation with the iNOS inhibitors L-NIL or 1400W stops this process. We have shown that in the epithelial cells studied, this phosphorylation is only seen on VASP that is already phosphorylated at the Ser157 position, a finding not previously reported. This is interesting in that it suggests that phosphorylation at the Ser157 residue,

preferentially phosphorylated by cAMP-dependent protein kinase (Halbrugge et al., 1990) is necessary in order for Ser239 phosphorylation to occur.

The mechanisms by which Ser157 phosphorylation may permit Ser239 phosphorylation have not yet been investigated. Phosphorylation at the 157 residue is known to cause a change in the electrophoretic mobility of VASP (Butt et al., 1994). This suggests that it may cause a conformational change in the protein, exposing the Ser239 residue and allowing it to be more easily phosphorylated by cGMP-dependent protein kinase. Another possible mechanism is that Ser157 phosphorylation may allow targeting of VASP to a cellular compartment in which it is more easily targeted by cGMP-dependent protein kinase. Finally, Ser157 phosphorylation may be involved in down regulation of protein phosphatase action at the Ser239 residue and therefore allow persistence of Ser239 phosphorylation. The latter explanation is interesting in the light of the results of combining iNOS transfection with a cAMP analog (Section 2.3.6). This causes persistence of the Ser239 phosphorylation signal that, without cAMP addition, is rapidly lost. The use of phosphatase inhibitors in this model would be a method of further investigation. X-ray crystallography or nuclear magnetic resonance (NMR) spectroscopy of phosphorylated VASP would also give an idea of the conformational changes caused by VASP phosphorylation and whether it alters the exposure of the Ser239 site.

The data discussed so far, suggests that there is a critical level of Ser157 phosphorylated VASP needed in order to allow the second Ser239 phosphorylation step to occur and that cAMP analogs prolong persistence of this form. This suggests an interplay between cAMP and cGMP-dependent pathways may be occurring with sequential

phosphorylation of the preferred cAMP-dependent protein kinase ser157 site followed by cGMP-dependent protein kinase Ser239 phosphorylation. Control of the cyclic-nucleotide dependent pathways occurs via substrate selective and stimulated phosphodiesterases (PDE) (Conti and Jin, 1999). The actions of cGMP are down regulated by its effects on PDE V. cGMP expression causes activation of this enzyme by binding to the GAF A domain of the enzyme (Rybalkin et al., 2003) which in turn increases the breakdown of cGMP to GMP (figure 1.9, main introduction). Cyclic AMP phosphorylation is controlled in a similar manner by PDE III and IV: a rise in cAMP levels increases activity of these enzymes (Scapin et al., 2004; Tilley and Maurice, 2002) resulting in increased breakdown to AMP. PDE III is also inhibited by cGMP leading to an elevation of cAMP levels as its breakdown is reduced (Zhang et al., 2001).

Nitric oxide itself appears to directly alter the response to the stimulus itself. NO causes a very rapid rise in cGMP levels which then rapidly decline despite guanylate cyclase remaining activated. NO appears to cause desensitisation of the cGMP pathway via phosphorylation and subsequent activation of PDE V (Mullershausen et al., 2003; Mullershausen et al., 2001). As shown in figure 2.8, Ser239 phosphorylation of VASP is present by 4 hours after transfection but is transient and is lost by 16 hours after iNOS transfection. This suggests that NO-induced activation of PDE V as discussed above may have been sufficient to down-regulate the cGMP-dependent pathway associated with phosphorylation of VASP at the Ser239 residue despite a continuing rise in NO levels (figure 2.9).

Synergy appears to occur between iNOS and cAMP in the experimental model detailed in section 2.3.6 in which persistence of VASP 239 phosphorylation is seen when the two stimuli are combined (figure 2.12). In this section, we saw persistence of high levels of P-VASP Ser239 at 8 hours in cells dually stimulated with iNOS transfection and 8-Br cAMP addition whilst in cells that had only undergone iNOS transfection, Ser239 phosphorylated VASP was undetectable by 6 hours. A possible explanation for this would be inhibition of phosphodiesterases by cAMP. PDE V has not been demonstrated to be affected by cAMP levels. However other enzymes may be involved. PDE Xa is a cAMP-inhibited cGMP PDE and could therefore be a potential mechanism by which this occurs (Fujishige et al., 1999). It is inhibited by dipyridamole which also inhibits PDE V making it difficult to isolate out the effects of PDE Xa alone. An alternative' though unlikely, explanation is that cAMP inhibits VASP dephosphorylation by regulation of protein phosphatases (PPs) (Abel et al., 1995). Cytostatin, an inhibitor of cell adhesion to the ECM inhibits PP2A (the protein phosphatase selective for Ser157 dephosphorylation) (Kawada M *et al* 1999) and may therefore be a potential method for exploring this aspect of control of VASP phosphorylation.

From our results, we suggest a model by which increased cAMP or cGMP activity leads to phosphorylation of VASP at the Ser157 site, causing a conformational change, thus exposing the Ser239 site to phosphorylation (Figures 2.8 and 2.12) by cGMP-dependent protein kinase. Phosphorylation at Ser239 is only seen at 50kDa (figures 2.8 and 2.11) therefore Ser157 phosphorylation must have occurred. As the level of Ser157 phosphorylation of VASP seems to be important in permitting Ser239 phosphorylation to occur, this could explain the effects of addition of 8-Br cAMP to iNOS transfected

cells. The cAMP analog could lead to higher levels of P-VASP Ser157 and therefore allow more P-VASP Ser239 to be produced.

RAW cells produce very high levels of iNOS when stimulated with pro-inflammatory cytokines, as well as changes in numerous other pathways. These lead to increases in cAMP dependent phosphorylation of VASP at Ser 157 (Fig 2.10). NO produces predominant phosphorylation of this Ser157 phosphorylated VASP, as observed in the 16HBE140- cells. However, there is a small amount of Ser239 phosphorylation alone (Fig 2.10) which is not abolished by NO inhibition. This may reflect Ser239 phosphorylation by cAMP dependent or other protein kinases.

Li *et al* (2003) suggested that cAMP-dependent protein kinase (PKA) is the predominant enzyme in cGMP-stimulated phosphorylation rather than cGMP-dependent protein kinase (PKG). They demonstrated that forskolin (a cell permeable adenylate cyclase activator) was able to induce Ser239 phosphorylation more rapidly than a cGMP analog, suggesting a possible indirect pathway for cGMP-induced Ser239 phosphorylation. They also showed that PKA inhibitors but not PKG inhibitors were able to block Ser239 phosphorylation. We would suggest a potential alternative explanation of these findings in the light of findings in epithelial cells. Using the pan VASP antibody we were able to show that Ser239 phosphorylation was only detectable at the 50kDa position, as discussed above, and that blocking the cGMP-dependent pathway with an iNOS inhibitor causes this to be lost (figure 2.8). We have suggested that Ser239 phosphorylation via the NO-induced PKG pathway requires initial phosphorylation at Ser157 (the PKA-preferred site), before it can occur. Therefore, blocking PKA-induced Ser157 phosphorylation would block Ser239 phosphorylation as

the initial, permissive step would not take place. The delay in Ser239 phosphorylation with a cGMP analog reported by Li *et al* may be due to activation of the cAMP dependent pathway by rising levels of cGMP, allowing Ser157 phosphorylation and then permitting Ser239 phosphorylation by cGMP.

Unexpectedly no changes in phosphorylation of VASP were seen when 8 Br-cGMP or NO donors were used to try and stimulate the cGMP-dependent kinase pathway. Different time points, concentrations and donors were used to try and stimulate phosphorylation without success. Phosphorylation at the Ser239 site can be difficult to detect due to low levels. However it would be expected that the use of supraphysiological concentrations of cGMP or NO in these experiments would be sufficient to allow activation of cGMP-dependent kinase. Nitric oxide is an unstable free radical and rapidly becomes oxidised. It is possible that it is rapidly metabolised before reaching the protein kinase/phosphatase complex located at specific subcellular locations (Sim and Scott, 1999). It is possible that iNOS may need to be co-localised with these complexes to allow direct localised NO production, permitting enzyme activation before NO is metabolised. Protein kinases can be targeted to the cytoskeleton by anchoring proteins such as A-kinase anchoring proteins (AKAPs). The assembly of complexes at the cytoskeleton appears to facilitate transmission of messages between membrane bound receptors and specific cytoskeletal sites (Diviani and Scott, 2001). The use of iNOS transfection may allow delivery of the enzyme to the correct compartment for it to have its effect. For example, previous work in Professor Evans' laboratory, demonstrated that iNOS is co-localised with the apical PDZ protein ezrin-radixin-moesin-binding Phosphoprotein 50 (EBP50) in a sub-membranous protein complex, bound to cortical actin. Apically localised iNOS directs vectorial NO

production at this site. This colocalisation of iNOS and EBP50 may allow modulation of function of EBP50-associated proteins within this compartment (Glynne et al., 2002). Phosphorylation of VASP could be tightly controlled within one compartment of the cell, for example, the leading edge. This may mean that looking at total P-VASP levels within the cell may not reflect the situation within these highly dynamic regions of actin turnover and could explain why only very low levels of phosphorylation could have a pronounced effect.

In summary, this section of work has demonstrated the normal localisation of VASP in renal epithelial cells and that iNOS causes this to be lost. We have also demonstrated that iNOS transfection induces VASP phosphorylation at the Ser239 residue but, in epithelial cells, only in the presence of Ser157 phosphorylation. In macrophages, some Ser239 phosphorylation alone is seen but that it is still predominantly seen in VASP that has also undergone Ser157 phosphorylation. We have also shown that Ser239 phosphorylation persists for longer in the presence of cAMP in addition to iNOS. We propose a mechanism by which VASP requires initial phosphorylation at Ser157 (the site preferentially phosphorylated by PKA *in vitro*) before Ser239 phosphorylation can occur.

## **Chapter 3. The Effects of Dominant-Negative VASP on Epithelial Sheet Formation.**

### 3.1 Introduction

Cell adhesion, both to the extracellular matrix and to other cells, is of fundamental importance in the assembly of individual cells into the organised 3-dimensional structures such as the proximal tubule of the kidney. Tubulogenesis involves many coordinated processes including cell differentiation, polarisation, changes in morphology, adhesion and reorganisation of the actin cytoskeleton. Prominent structures in cell:cell adhesion in epithelia are the adherens junctions (or *zona adherens*) containing a core of E-cadherins (Gumbiner, 1996; Nose *et al.*, 1988). The cytoplasmic domains of E-cadherin bind to  $\beta$ -catenin which in turn binds to  $\alpha$ -catenin which links to the actin cytoskeleton (Drubin and Nelson, 1996).  $\alpha$ -catenin also binds to other actin-binding proteins, amongst which is the related protein vinculin, to which VASP binds (Reinhard *et al.*, 1996). The actin cytoskeleton is essential in the formation of new cell:cell junctions and the stabilization of recently formed contacts (Vasioukhin *et al.*, 2000) though mature contacts are more stable in the face of cytoskeletal disruption.

We have used a canine renal epithelial cell line for this work, Madin-Darby canine kidney (MDCK) cells (briefly described in Chapter 2). We have used a specific clone of these cells for this work. MDCK TetOff cells are a stable clone containing the pTetOff regulator plasmid. These cells have been engineered to express a tetracycline-controlled regulatory protein which will allow controllable, high level gene expression. This has been created from amino acids 1-207 of the *E.coli* Tet repressor protein (TetR) and the c-terminal 127 amino acids of the Herpes simplex virus (HSV) VP-16 activation domain. The VP-16 domain converts the TetR from a transcriptional repressor to a transcriptional activator, the resultant protein being the tetracycline-controlled transactivator (tTA). tTA is encoded by the pTetOff regulator plasmid which also

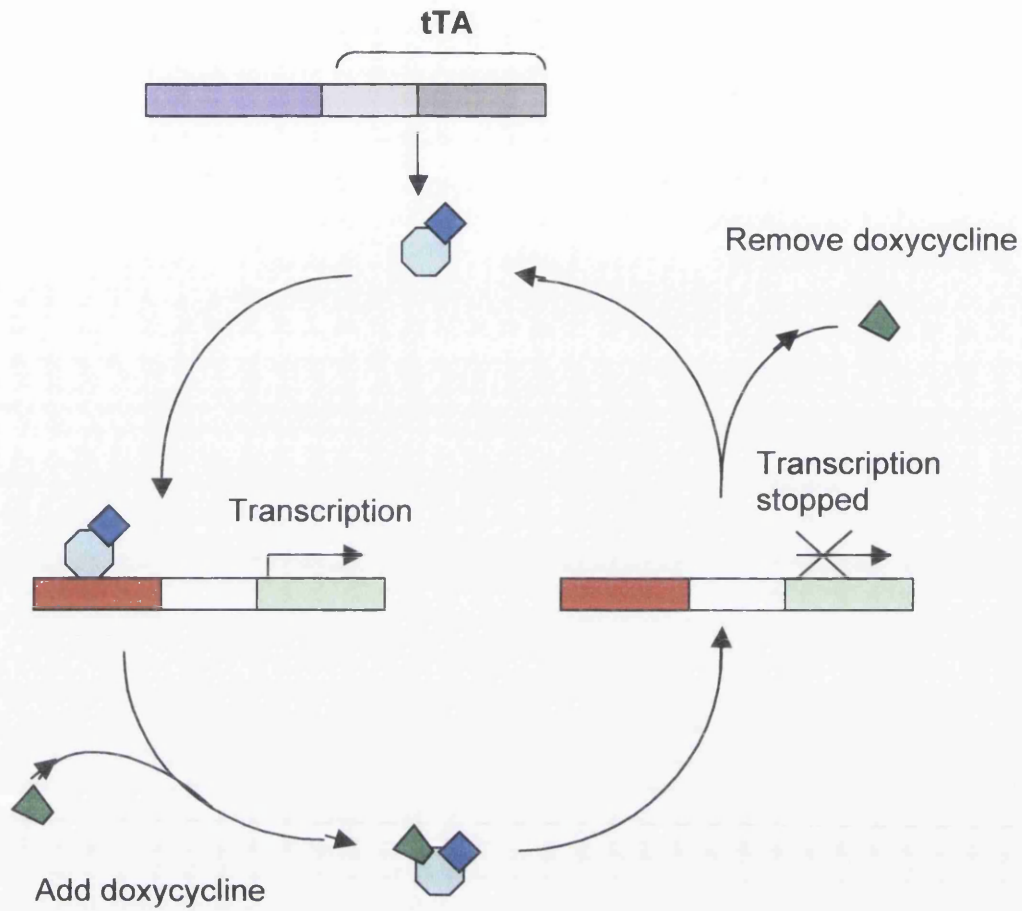
contains a puromycin resistance gene to maintain selection of a stable clone of transfected cells

The cells then require a second component – the Tetracycline response plasmid which expresses the gene of interest under the control of the tetracycline response element (TRE). This is contained in the pTRE2hyg plasmid that contains a multiple cloning site (MCS) for insertion of the gene of interest. The plasmid also contains a hygromycin resistance gene to allow selection and cloning of transfected cells. This system can therefore be used to control when the gene of interest is expressed by removal of tetracycline repression of transcription (Figure 4.2).

In this section of work, we have looked at the effects of actin cytoskeletal disruption on adhesion through the use of a dominant negative form of VASP (DN-VASP). The EVH2 domain of VASP, containing the regions essential for tetramerisation and coiled-coil formation (amino acids 277-383) acts in this manner (Bachmann *et al.*, 1999). DN-VASP does not contain the domains necessary for binding to other cytoskeletal proteins such as vinculin and zyxin, thereby disrupting the link between actin and cell: cell and cell: matrix junctions. It also does not include the F-actin and G-actin sites found in the central proline rich domain and the EVH2 domain.

In the formation of cell:cell junctions, epithelial cells from the epidermis initially form calcium-stimulated filopodia which penetrate into neighbouring cells. E-cadherin accumulates at the tips of the filopodia and bundles of actin filaments radiate back into the cell (Vasioukhin *et al.*, 2000). Cells grown in low calcium media will not form these structures. VASP, zyxin and vinculin also localise to focal contacts and puncta between

Figure 3.1 The TetOff System



**Key**

-  tTA (binds TRE and activates transcription in the absence of doxycycline)
-  Doxycycline
-  Gene of interest
-  Tetracycline Response Element (TRE)
-   $P_{CMV}$
-  TetR
-  VP-16 activation domain

the cells and act as a potential mechanism for the organised actin bundles radiating from these areas (Machesky and Insall, 1999). Studies using DN-VASP in order to interfere with this function show that membrane fusion between cells is inhibited (Vasioukhin *et al.*, 2000). Earlier studies of cell division and junction formation in MDCK cells suggested a slightly different mechanism with actin initially existing in a circumferential cable in these cells. As cells adhere, E-cadherin associates into puncta at cell:cell contacts which in turn leads to breakdown of the actin ring and insertion of actin fibres into these cables (Adams *et al.*, 1998). VASP localises to the *Zona adherens* via the assembled protein complex at the junction that contains the Ena/VASP-binding proteins zyxin and vinculin (Renfranz and Beckerle, 2002) and is involved in actin polymerisation (Walders-Harbeck *et al.*, 2002). We have used DN-VASP to investigate further the effects of cytoskeleton disruption on formation of a new epithelial sheet and on a pre-formed monolayer of MDCK cells. We have also gone on to investigate the use of a 3-dimensional model of tubule formation using MDCK cells.

Tubulogenesis is a developmental process seen in many organs of the body including the lungs, mammary and salivary glands and the kidney. Tubules are lined with polarised epithelial cells but during development polarity appears to be transiently lost as cells migrate (Pollack *et al.*, 1998). The different forms of cell: cell junctions appear to be differentially regulated during this process, with E-cadherins becoming distributed randomly across the cell surface whilst the tight junction protein ZO-1 remains at sites of cell:cell contact. MDCK cells grown in a 2-dimensional culture on a semi-permeable membrane support, form a well polarised monolayer approximately 10-15  $\mu\text{m}$  tall in contrast to when they are grown on a solid support when they are only 3-5  $\mu\text{m}$  high (Zegers *et al.*, 2003). When grown in a type I collagen matrix they organise to form a

fluid-filled cyst of a monolayer of cells. If treated with hepatocyte growth factor, they will then form branching tubules (Rosario and Birchmeier, 2003). Other growth factors such as transforming growth factor- $\beta$  (TGF- $\beta$ ) (Santos and Nigam, 1993) and epidermal growth factor (EGF) receptors (Kjelsberg *et al.*, 1997; Sakurai *et al.*, 1997) also appear to influence tubulogenesis though HGF appears to have the dominant effect in these cells (Barros *et al.*, 1995). Tubulogenesis is important as these mechanisms are similar to those needed for tubule repair post injury when cells must divide and move in 3 dimensions to recreate a polarised epithelial lining for the renal proximal tubule. HGF has been proposed as an agent which may be useful in the management of renal failure, both in the inhibition of fibrosis in chronic disease (Matsumoto and Nakamura, 2002; Negri, 2004) and in amelioration of damage in acute renal failure (Yamasaki *et al.*, 2002) though its role is, as yet, unclear (Reviewed in (Laping, 1999).

HGF acts via the c-met tyrosine kinase receptor and acts both as a growth factor, for example in hepatocytes where it was first characterised, and as a scatter factor stimulating cell dissociation and motility (Weidner *et al.*, 1993). Ligation of the receptor activates a host of signalling pathways that lead to reorganisation of the cytoskeleton and cell adhesion complexes. In particular, Rac1 and Cdc42 (Rho GTPases) are activated downstream of HGF and are required for adherens junction reorganisation, lamellopodia formation cell spreading and motility (Royal *et al.*, 2000). A potential role for VASP in this process via actin polymerisation and bundling is therefore likely. The distribution of VASP during tubulogenesis would be an interesting area to study to investigate its interactions with actin during this process.

## **3.2 Methods**

### **3.2.1 Immunofluorescent Staining of Native VASP in MDCK TetOff Cells**

MDCK TetOff cells were grown to 100% confluence on a 2 chamber tissue culture slide. They were then fixed and permeabilised as described previously before being blocked in 10% NGS. Following blocking they were incubated with the primary polyclonal anti-VASP antibody (1:500) for 1 hour at room temperature. Staining was visualised using a secondary fluorochrome linked anti-rabbit antibody. Nuclei were stained with DAPI.

### **3.2.2 Production of Dominant-Negative VASP (DN-VASP)**

The following additional reagents were used: VASP cDNA GeneStorm Expression ready clone RG00084 in pcDNA3.1/GS (Resgen); pCR2.1-TOPO vector, Zeocin, EcoR1, Mlu-1, Not-1, Bam-H1 restriction endonucleases, X-gal and TOP10 cells (all from Invitrogen, UK); Ligafast and Ligafast buffer, Taq polymerase and 10x Amplification buffer (all from Promega); Dimethylsulfoxide (DMSO) and agarose (electrophoresis grade) (Sigma, UK); Qiagen plasmid DNA Miniprep and Midiprep Kits, Qiagen Gel Purification Kit (Qiagen); Low Salt LB media (Tryptone 10g, NaCl 5g, Yeast extract 5g, distilled water to 1l).

#### **3.2.2.1 Polymerase Chain Reaction (PCR) Protocol**

cDNA VASP was extracted as in section 2.2.12.1. A dominant negative form of VASP (amino acids 277-380 of full length VASP) was amplified from full length VASP cDNA using the following oligonucleotide primers –

5' GCACGCGTATGACGCAAGTTGGGGAGAAAACC 3'

5' GCGCGGCCCGCCAGGGAGACCCCGCTTCC 3'

(Adapted from (Vasioukhin *et al.*, 2000)

(incorporating an ATG sequence to ensure the correct frame and Mlu-1 and Not-1 as restriction endonuclease sites) and VASP cDNA as detailed previously. Not-1 and Mlu-1 were chosen as restriction sites in order to be able to incorporate the protein into pTRE2Hyg vector which allows the production of a tetracycline-controllable construct for incorporation into MDCK-TetOff cells (see section 2.2.14).

The amplification protocol used was 95°C for 2 minutes, then 40 cycles of 95°C for 30 seconds, 55°C for 30 seconds and 72°C for 1 minute, finishing with 72°C for 10 minutes. VASP cDNA was used at concentrations of 1, 5 and 10ng as templates for the reaction. The presence of DNA of the expected size (approximately 350 base pairs) was confirmed by electrophoresis using a 2.5% agarose gel. The pcr product was excised from the gel and purified using a Qiagen gel purification kit.

### **3.2.2.2 Insertion of DN-VASP into a regulatable plasmid**

In order to increase the concentration of the dominant-negative VASP, it was initially TA cloned into pCR2.1-TOPO vector. TA cloning exploits the terminal transferase activity of Taq polymerase to add a 3A overhang to each end of the PCR product. It can then be cloned directly into a linearised cloning vector with 3T overhangs such as pCR2.1 TOPO. The PCR products are mixed with the vector in high proportion and ligated with T4 ligase.

The pcr amplification protocol detailed previously was repeated using non-proof reading taq polymerase in order to incorporate an AAA overhang. It was ligated into

linearised pCR2.1-TOPO and incubated at room temperature for 5 minutes. Following this, the DNA was chemically transformed into TOP10 cells. The cells were then spread onto LB-ampicillin plates pre-spread with 40mg/ml X-gal and incubated at room temperature overnight at 37°C. The following day a mixture of blue and white colonies were present. White colonies indicate incorporation of the DNA. White colonies were picked and grown overnight in LB-ampicillin (50µg/ml) liquid media. The following day, the cultures were spun down and the plasmid DNA extracted using a Qiagen minprep kit and run on a 2.5% agarose gel to look for incorporation of DN-VASP DNA. Samples of DNA from different colonies expressing the expected 2 bands were then sent for DNA sequencing to ensure incorporation of full length DN-VASP DNA had been successful. pCR2.1TOPO incorporates M13 primers which were used for sequencing.

DNA from a sample containing full length DN-VASP was the incorporated into the pTRE2hyg expression vector. PCR2.1 TOPO/DN-VASP and pTRE2hyg were both digested with Mlu-1 and Not1 at 37°C for 2 hours. Samples were run on a 2.5% and a 1% agarose gel respectively and the appropriate bands excised and gel purified using a Qiagen gel extraction kit. They were then ligated using the following quantities :-

- DN-VASP            7µl
- pTRE2hyg            1µl
- Ligafast buffer      10µl
- Ligafast              1µl

for 8 minutes at room temperature before being placed on ice to stop the reaction. The pTRE2/hyg/DN-VASP was electrically transformed into electrocompetent E.coli (100 Ohms resistance, 2.45kV charging voltage, 25µFD capacitance). Cultures were spread

onto LB-ampicillin agar plates and grown at 37°C overnight. The following day, colonies were picked and grown in 4ml LB-ampicillin liquid media overnight. Plasmid DNA was extracted as before and digested with Mlu-1 and Not-1. Samples were run on a 2.5% agarose gel in order to confirm incorporation of the DN-VASP insert.

### **3.2.3 Expression of DN-VASP in MDCK TetOff Cells**

The following reagents were used: VASP mouse monoclonal antibody (BD Transduction Laboratories); Novex 10-20% Tris-Glycine gels and SeeBlue Plus2 pre-stained proteins (Invitrogen).

#### **3.2.3.1 Detection with Immunoblotting**

MDCK TetOff cells were grown in 6 well plates to 80-90% confluence prior to transfection with pTRE2hyg/DN-VASP (protocol section 2.2.14.3, 4µg DNA and 20µl Lipofectamine 2000 per well). Cells were grown in the presence or absence of doxycycline (2µg/ml) for a further 24 hours before being harvested for assay. MDCK TetOff cells were washed twice with PBS then lysed in 200µl of SDS-lysis buffer. Samples were boiled at 95° C for 5 minutes and briefly sonicated before being loaded onto a 10-20% Tris-Glycine electrophoresis gel. 40µl of each sample was used. The gel was run at 20mA until the dye reached the base of the gel. The samples were then transferred onto a PVDF membrane at 400mA for 1 hour at 4°C. Transfer was checked by Ponceau S (Sigma, UK) staining. Following blocking, the membrane was stained using a VASP mAb (1:500 dilution in 5% non-fat milk) for 2 hours at room temperature on an orbital shaker. The membrane was washed before addition of the secondary biotinylated antibody for a further hour. The membrane was washed again before the addition of Streptavidin-HRP conjugate (1:3000) in 5% milk in PBS for 30 minutes.

Immunoreactive bands were detected using the ECL Plus detection system and visualised using autoradiography film.

### **3.2.3.2 Detection with Immunofluorescence**

The following additional reagents were used: VASP mAb (clone IE273) (Alexis Biochemicals); AlexaFluor 488-labelled Phalloidin and AlexaFluor 568 goat anti-mouse, 1:500 (Molecular Probes).

pTRE2hyg/DN-VASP was transfected into MDCK TetOff cells grown in Titretek 2 chamber slides using a standard protocol described previously. In one half of the cell chambers, in order to suppress DN-VASP expression, doxycycline was added to the media at a concentration of 2 $\mu$ g/ml. In the other chambers, no doxycycline was added in order to allow the protein to be expressed.

24 hours following transfection the cells were fixed and stained for DN-VASP and F-actin. The cells were fixed in 1%PFA, permeabilised in 0.2% Triton X-100 in PBS and blocked in 10% NGS as described previously. After blocking, cells were incubated with VASP mAb (IE273) at a 1:250 dilution in 10% NGS and FITC-labelled phalloidin at a 1:50 dilution for 2 hours at room temperature. Following washing, the secondary antibody and FITC-labelled phalloidin in 10% NGS were added and the cells incubated for a further hour. DAPI was added following washing to stain the nuclei. Cells were examined using immunofluorescent microscopy.

### **3.2.4 The Effects of DN-VASP Transfection on the Formation of an Epithelial Sheet and the Presence of Actin Fibres**

MDCK TetOff cells were cultured overnight in either 2 chamber slides or 6 well plates to approximately 90% confluence. They were then transfected with pTRE2Hyg/DN-VASP using Lipofectamine 2000 as before. Doxycycline was added at a concentration of 2 $\mu$ g/ml to half of the cells whilst the rest were cultured in the absence of doxycycline. 6 hours following transfection, the cells grown in 6 well plates were trypsinised and replated into 2 chamber slides. Slides were then fixed and stained at timepoints from 6 – 24 hours following transfection. Cells were stained with VASP mAb (IE273) for DN-VASP and either FITC-phalloidin (F-actin) or anti ZO-1 antibody to demonstrate cell: cell junctions (ZO-1 mAb, 1:100 dilution, Zymed). The cells were then examined using immunofluorescent microscopy with images being taken for deconvolution microscopy and z-stack images using Openlab software.

In order to assess the percentage of cells expressing DN-VASP at the various time points, random fields were photographed from each slide. The total number of cells present was counted and also the number of cells expressing DN-VASP. Means and standard deviations were then calculated. A Student's two tailed t-test was used to compare the percentage of cells expressing DN-VASP at equivalent time points between the two different growth conditions (Transfected in situ *vs* transfected and replated after 6 hours). A difference with  $p < 0.05$  was taken as a significant difference and  $p < 0.01$  as highly significant.

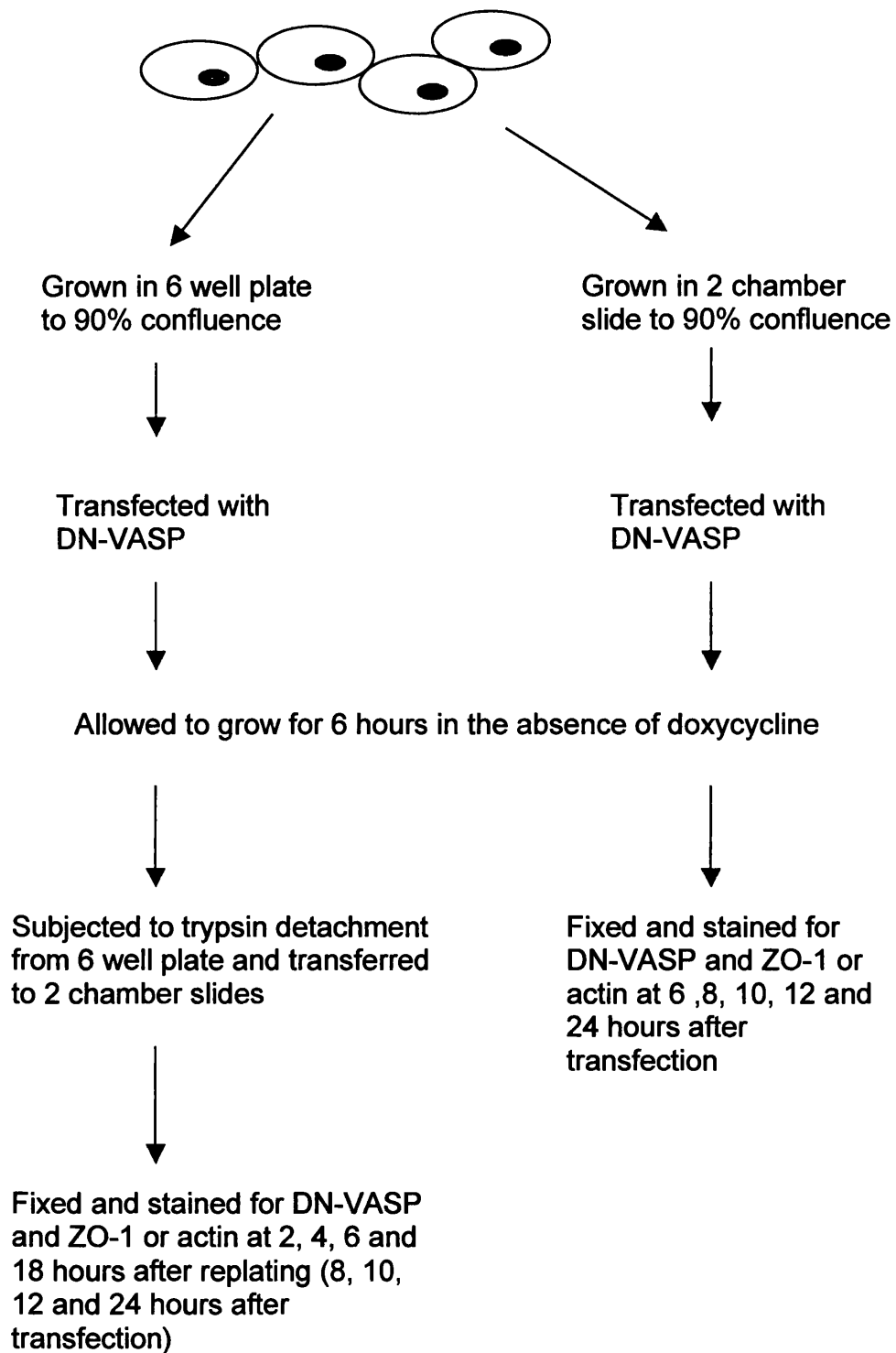


**Figure 3.2 Protocol for investigating the effects of replating DN-VASP transfected MDCK TetOff cells**

### **3.2.5 Establishment of a 3-Dimensional Tubule Model to Investigate VASP**

#### **Distribution**

##### **3.2.5.1 Culture of tubules**

The following reagents were used: Type I Rat Tail Collagen (Roche), RPMI powder (Gibco), sodium bicarbonate (Sigma), 1M HEPES (Gibco), hepatocyte growth factor (HGF) (Peprotech), 0.2µm pore Tissue Culture inserts (10mm Anopore membranes) (Nalge Nunc)

A sterile collagen matrix was prepared using 66% type I rat tail collagen, 1x RPMI media, sodium bicarbonate 2.35mg/ml, 0.02M HEPES and 12% sterile distilled water. MDCK cells were added to the matrix at a concentration of  $5 \times 10^4$  cells/ml. 0.25ml of the collagen/ cell mixture was placed onto 0.2µ anopore membrane inserts in a 24 well plate and allowed to set in a 37° incubator for approximately 20 minutes. Prewarmed media was then added above and below the membrane and the plates were incubated at 37° C, 5% CO<sub>2</sub> in a humidified incubator.

Media was changed daily. Approximately 1 week after seeding, cysts had formed and at this stage, HGF was added at a concentration of 20ng/ml. This was added daily in fresh media for 5 days until the formation of branching tubules was seen. Samples were fixed and stained at each stage of tubule growth.

##### **3.2.5.2 Immunostaining of Tubules in Collagen Matrices**

(Adapted from (Pollack et al., 1998) with unpublished modifications by Lucy O'Brien & Keith Mostov.)

Media was removed from above and below the samples which were then washed 3 times with PBS+ (Phosphate buffered saline supplemented with 1mM calcium chloride

and 0.5mM magnesium chloride). They were then incubated with 0.05units/ml collagenase (Liberase Blendzyme 3, Roche Pharmaceuticals) for 10 minutes at 37°C, washed a further 3 times in PBS+ before being fixed in 4% PFA for 30 minutes at room temperature. Following this, Quench solution (1.5ml 1M ammonium chloride, 0.4ml 1m glycine (pH8) made to 20ml with PBS+) was added for 10 minutes. The samples were washed again 3 times in PBS+ then blocked with PFS at 4° overnight.

The primary antibodies (Ezrin 1µg/ml (Transduction Laboratories) or  $\beta_1$  integrin 0.2µg/ml (Chemicon International)) were diluted in PFS (3.5g fish skin gelatin (Sigma), saponin (Sigma) 10% 1.25ml in PBS+ to 0.5l, 0.02% sodium azide) and added above and below the sample before being incubated for 24 hours on an orbital shaker at 4°C. The samples were washed in PFS before the secondary antibody, also diluted in PFS (AlexaFluor 488 goat anti mouse 1:500 dilution (Molecular Probes).) was added and the samples shaken for a further 24 hours at 4°C. Following washing in PFS (5 times) and PBS+ (twice), the samples were post-fixed in 4%PFA for 30 minutes before washing again in PBS+. The collagen gel was then removed from the filter insert and mounted in Vectashield on a microscope slide. The samples were allowed to harden at 4°C in the dark for 24 hours before being visualised using confocal microscopy.

### **3.2.6 Cloning of pTRE2hyg/DN-VASP Stable Transfectants**

MDCK TetOff cells were grown to 80% confluence in a 6 well tissue culture plate before being transfected with pTRE2hyg as described previously. The media was changed 4 hours after transfection and doxycycline 2µg/ml was added at this point. (Unless otherwise stated, doxycycline was always added to the media from now on in this experiment). 24 hours after transfection, cells were trypsinised and replated into 15cm Petri dishes. They were seeded into the plates at a 1:10, 1:20 and 1:50 dilutions.

Hygromycin was added as the selective antibiotic at a concentration of 200 $\mu$ g/ml from now on unless otherwise stated. The cells were then allowed to continue growing.

7 days after reseeding into the Petri dishes, small colonies began to appear. These clones were then replated into 24 well plates in order to keep the colonies separate. In order to replate clones individually without cross-contamination, the following method was employed. Tissue culture media was removed from the plates and the cells washed with HBSS. Sterile cloning discs (Sigma) were soaked in trypsin-EDTA and placed onto individual clones using sterile forceps. Cells were allowed to detach from the tissue culture plate. Discs were then removed to 24 well plates with detached cells adhering to them. 1ml of media was added to the wells of the 24 well plate and cells allowed to continue growing. By the following day, cells had detached from the disc and were now growing in the wells. Media was changed for fresh media and the discs removed. Clones were sequentially replated into 6 well and T25 tissue culture flasks to expand cell numbers.

### **3.2.7 DN-VASP Expression by Stable Transfectants.**

In order to assess DN-VASP expression in the clones, 2 aliquots of cells from each clone were grown in 2 chamber tissue culture slides, one in the presence of doxycycline and one in the absence of doxycycline, for 24 and 48 hours. They were then fixed, permeabilised, blocked and stained for DN-VASP as described in section 3.2.3.2. Immunofluorescent microscopy was used to assess DN-VASP expression.

### **3.3 Results**

#### **3.3.1 DNA sequencing of DN-VASP**

Sequencing of the PCR-amplified product confirmed that the DN-VASP sequence was present in its entirety and without errors. The product was therefore used in further experiments.

#### **3.3.2 Distribution of native VASP in MDCK TetOff Cells**

MDCK TetOff cells are a canine renal epithelial cell line. They were stained with polyclonal VASP in order to demonstrate normal distribution of the protein in these cells. VASP is known to localise to cell:cell and cell:matrix junctions. Figure 3.3 demonstrates localisation of VASP in focal sites at the cell membrane at cell:cell junctions. Contacts at the cell:matrix junction were not seen in this confluent monolayer as the plane imaged here is at a higher level within the cell. The antibody used in this experiment is a polyclonal antibody capable of recognising both human and canine VASP.

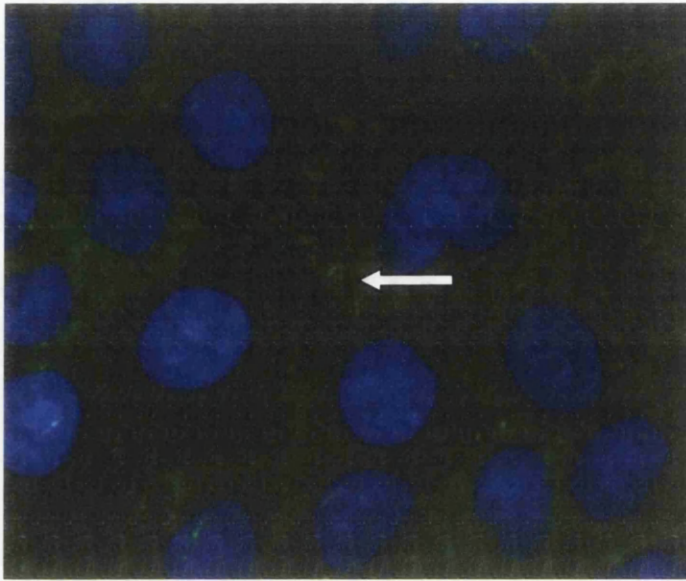


**Figure 3.3 Distribution of native VASP in MDCK TetOff cells.** VASP (green) is localised at cell; cell junctions in the epithelial monolayer (arrow). (Magnification x630)

### **3.3.3 Expression of DN-VASP in MDCK TetOff Cells**

DN-VASP expression was identified by the use of a monoclonal antibody against VASP. This commercially available antibody was raised against the EVH2 domain of human VASP and does not cross-react with canine VASP. Only cells expressing transfected DN-VASP, which is of human origin, will therefore stain with this antibody. The polyclonal antibody described in the previous section was not used as this is capable of staining both canine and human VASP. FITC-conjugated phalloidin was also used to stain F-actin in these cells. Stress fibres are visible in cells not expressing DN-VASP (figures 3.4a and b, black arrows)

Using immunofluorescent staining, it was possible to see DN-VASP expression by 4 hours post transfection. In the chambers in which expression was repressed by the addition of doxycycline, low level of DN-VASP expression was seen at all time-points (less than 1% by 24 hours) (figure 3.4a) demonstrating some leakiness of the tetracycline repression system. In the chambers to which doxycycline was not added, approximately 40% DN-VASP expression was seen by 24 hours post transfection (figure 3.4b). The control by tetracycline in this system appeared therefore to be effective in repressing gene transcription. Some leakiness of expression in the presence of DN-VASP is not unexpected but was present at a low enough level of expression to allow use of this model.

Cells expressing DN-VASP appear to be able to remain as part of the epithelial cell monolayer as seen in figure 3.4b. In this image, a relatively high number of cells (approximately 40%) are demonstrating DN-VASP expression (red) but appear to remain in the epithelial sheet, surrounded on all sides by other cells. No breakdown of

the epithelial sheet was seen and by 24 hours post transfection, 100% confluence had been reached as seen in figure 3.4b. DN-VASP appeared to be expressed throughout the cytoplasm of the cells, excluding the nuclei (best seen in the white-arrowed cells in figure 3.4b) and did not appear in a focal distribution at cell:cell contacts where native VASP is usually seen (Figure 3.3).

In summary, this experiment demonstrated DN-VASP was expressed in a regulatable fashion when transfected into MDCK TetOff cells. This experiment looked specifically at DN-VASP expression in cells that had already reached a high level of confluence before transfection. It suggested that expression of the dominant-negative protein did not appear to cause breakdown of the pre-formed cell monolayer, cells remained incorporated into the epithelial sheet.

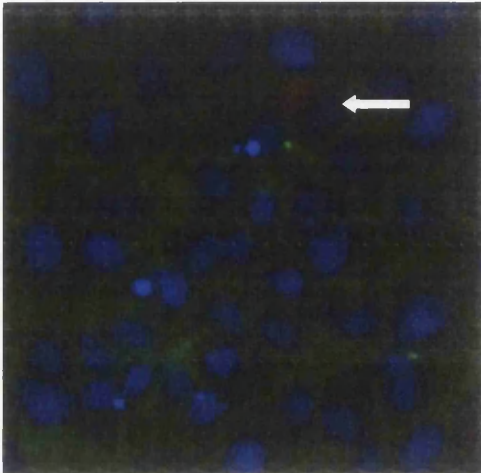


**Figure 3.4a** Expression of DN-VASP (red) in the presence of doxycycline showing a very low level of leaky expression (<1%).

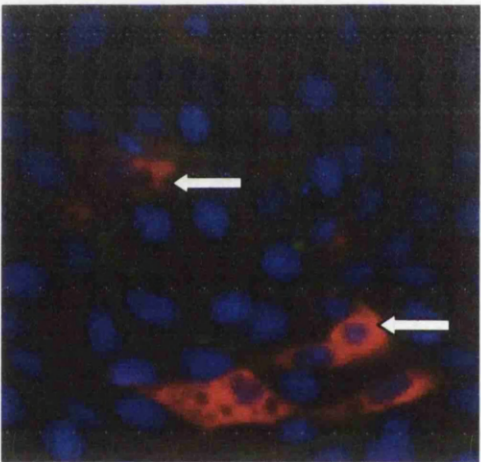


**Figure 3.4b** Expression of DN-VASP (red) in the absence of doxycycline repression.

Key	
Red	DN-VASP
Green	F-actin
Blue	Nuclei

**Figure 3.4 Detection of DN-VASP expression by Immunofluorescence.**

Slides were fixed and stained for DN-VASP (red) and F-actin (green) 24 hours after transfection with pTRE2hyg/DN-VASP. (Magnification x400)

### **3.3.4 Detection of DN-VASP by Immunoblotting**

In order to confirm the expression of DN-VASP, we prepared lysates of cells transfected with pTRE2hyg/DN-VASP at 24 and 48 hours after transfection, grown in either the presence or absence of doxycycline. These were then assayed for the presence of the dominant-negative protein by immunoblotting on high strength Tris-glycine gels to enhance detection of low molecular mass proteins.

DN-VASP was detected as a band at approximately 20kDA by immunoblotting 24 hours after transfection in cells grown in the absence of doxycycline. In samples where the cells had been grown in the presence of doxycycline, DN-VASP expression was suppressed to a sufficiently low level that it was undetectable by this method (Figure 3.5).

The level of DN-VASP expressed at 48 hours post transfection appears to be lower than at 24 hours. This may be due to cell shedding of MDCK cells due to a very high level of confluence. MDCK cells grow very rapidly and form an epithelial sheet several layers thick that is liable to detach easily from the tissue culture flask. This effect was also observed in non-transfected cells in this experiment.

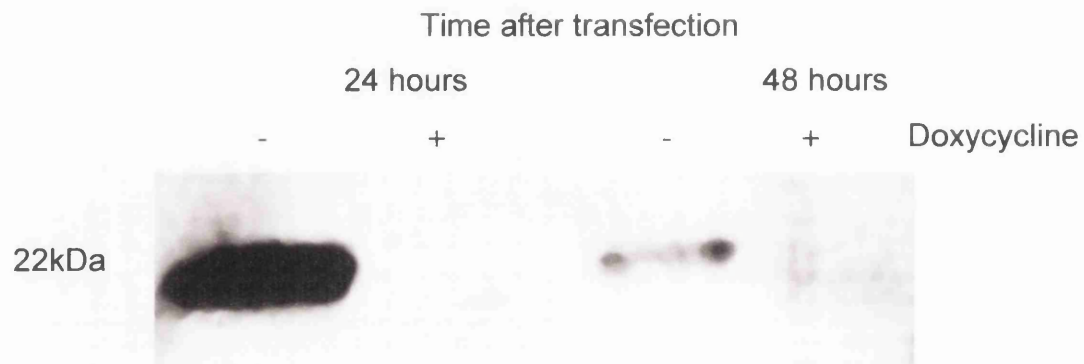


**Figure 3.5 DN-VASP expression in MDCK TetOff cells.** DN-VASP was detected at approximately 20kDa. The effects of addition of doxycycline, suppressing DN-VASP expression are clearly visible.

### **3.3.5 DN-VASP Expression Decreases Actin Fibre Formation.**

We next examined the effect of DN-VASP expression on the distribution of actin within MDCK TetOff cells. MDCK TetOff cells were transfected with pTRE2hyg/DN-VASP and grown in the absence of doxycycline in order to allow expression of the protein. We then stained cells for F-actin and DN-VASP expression.

In cells that do not express DN-VASP, typical actin stress fibres can be seen stretching across the cell (figure 3.6a, white arrow). Figure 3.6b shows the same microscopic field but in this image, staining for DN-VASP (red) has been included. In cells that do express the transfected protein, actin stress fibres are not visible. However, if these same cells are examined in figure 3.6a (black arrows), it can be seen that they do not demonstrate stress fibre formation as seen in adjacent cells. In these cells, DN-VASP is distributed throughout the cytoplasm, excluding the cell nuclei.

Whilst the distribution of F-actin within the cell has shown to be altered by the presence of DN-VASP, it was felt to be of less use to investigate the position of epithelial cells with respect to the plane of the monolayer as it is usually distributed throughout the cell. For the next series of experiments we therefore chose to study the effects of DN-VASP on distribution of ZO-1, a protein normally located at the *Zona occludens*.

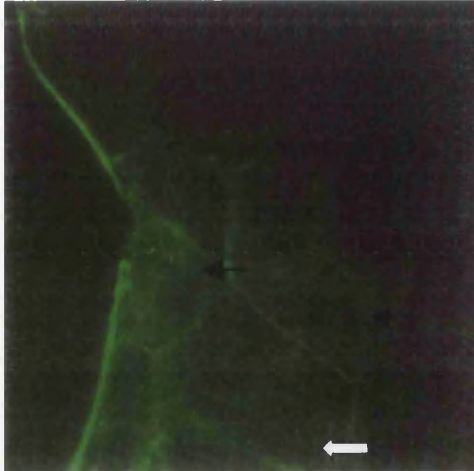


**Figure 3.6a.** Actin fibres in MDCK TetOff Cells

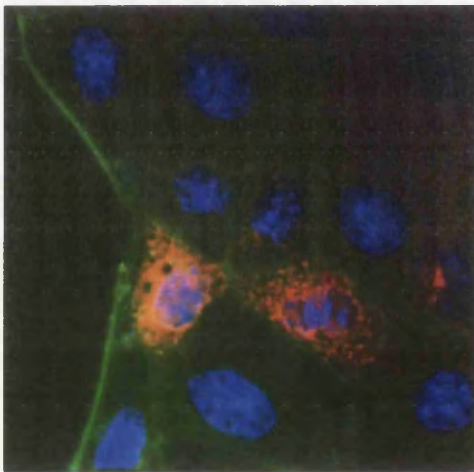


**Figure 3.6b.** Same microscope field as in figure 3.4a but including staining for DN-VASP expression (red).

**Figure 3.6 The presence of DN-VASP expression inhibits actin fibre formation.** Typical actin stress fibres (green stain, white arrow) are seen in cell not expressing DN-VASP. In DN-VASP expressing cells (red stain, black arrows), stress fibres are not seen. (Magnification x400)

### **3.3.6 Effects of DN-VASP Transfection on the Ability of Cells to Reattach to the Cell Sub-stratum**

The experiments described above showed that, although DN-VASP appeared to disrupt actin stress fibre formation, it had little apparent effect on the integrity of the epithelial sheet. To examine the effects on *de novo* epithelial sheet formation, cells were transfected with DN-VASP, allowed to recover for 6 hours before undergoing detachment from the tissue culture flask by the use of trypsin. They were then replated into 2 well tissue culture slides and allowed to continue growing. Following transfection, cells were allowed to grow in the absence of doxycycline in order to facilitate DN-VASP expression. This means that DN-VASP was being expressed by the time the cells were replated. Cells were then fixed and stained for DN-VASP at timepoints from 2-18 hours after replating. A control set of cells for each time-point used did not undergo replating but were allowed to grow *in situ* on the 2 chamber slides.

As a common starting point for both sets of growth conditions, one set of cells was fixed and stained at 6 hours following transfection, the time-point at which some of the cells underwent detachment and reattachment. By 6 hours after transfection, approximately 5% of cells expressed detectable DN-VASP using immunofluorescent microscopy. This shows that DN-VASP expression would therefore have started in the cells which then underwent replating at this point. By conventional phase contrast light microscopy, cells which were replated could be seen to be adhering to the slides by 2 hours after detachment and reattachment and this point was therefore taken as the next time-point for assessment.

By 8 hours after transfection (2 hours after replating), there was a statistically higher percentage of cells expressing DN-VASP seen in chambers where the cells had been allowed to remain growing in situ, compared to those that had undergone detachment and reattachment. This difference was observed at all the time-points measured in this experiment. In cells transfected in the 2 chamber slides and not replated, the percentage of cells expressing DN-VASP rose from 4.86 +/- 2.15 at 6 hours post transfection to 36.33 +/-11.1% at 24 hours post transfection. In cells that had undergone replating, by 18 hours after re-plating (24 hours after transfection), only 23 +/- 5.39% of cells were expressing DN-VASP. The difference between the two sets of cells was seen at all timepoints following transfection and reached statistical significance at 8, 10 and 12 hours after transfection (Figure 3.7).

In conclusion, this experiment suggests that expression of DN-VASP inhibits the ability of MDCK cells to adhere to the culture surface.

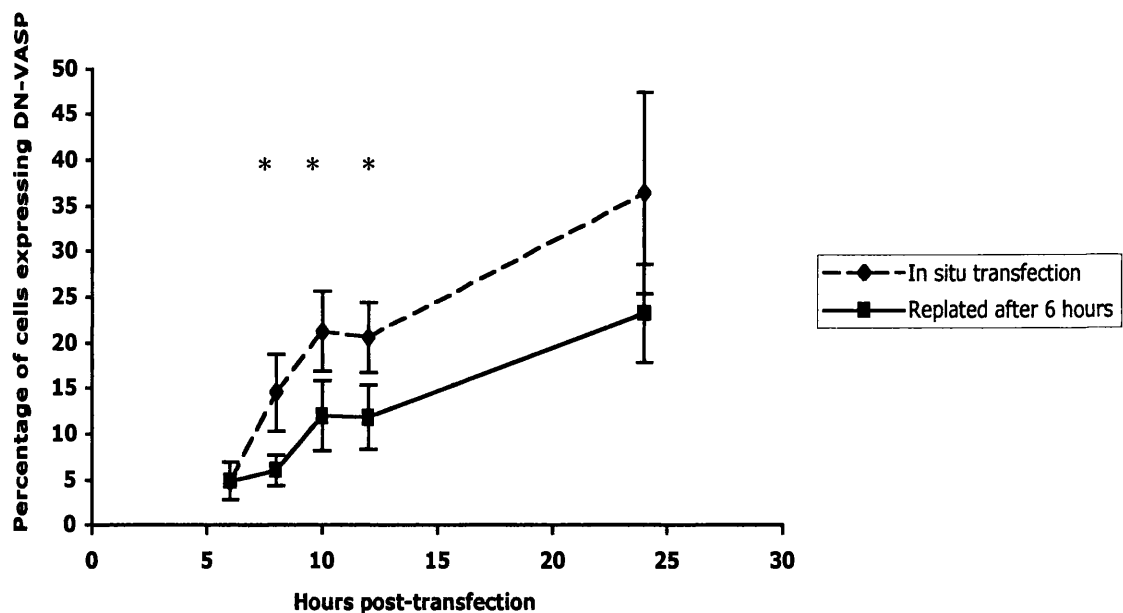


**Figure 3.7 The effects of replating cells transfected with DN-VASP.** In cells replated 6 hours after transfection, the percentage of cells expressing DN-VASP was significantly lower at timepoints 8, 10 and 12 hours after transfection – corresponding to 2, 4 and 6 hours after replating. (Error bars have been included and significant differences (\*  $p < 0.05$ ) calculated using a Student’s t-test,)

### 3.3.7 The Effects of DN-VASP Transfection on the Formation of an Epithelial Sheet

Previous experiments have shown that following replating, a lower percentage of DN-VASP expressing cells are seen than in cells that have undergone detachment and reattachment compared to cells left *in situ*. In this experiment, we looked at whether DN-VASP transfected cells could be incorporated into a newly forming monolayer and whether there were any differences in distribution.

In this experiment, as in the previous one, some cells were plated directly onto 2 chamber slides and transfected with pTRE2hyg/DN-VASP when nearly confluent. These cells were then grown in the absence of doxycycline in order to allow expression of DN-VASP. A second set of cells were grown in 6 well plates to approximately 80% confluence before undergoing DN-VASP transfection. They were then allowed to grow for a further 6 hours in the absence of doxycycline before undergoing replating onto 2 well slides as described in the previous experiment. Cells were then stained for DN-VASP expression and ZO-1 at timepoints between 10 and 24 hours following transfection (6 and 18 hours after replating). ZO-1 was chosen for staining in this experiment as it sits in a very localised area at cell:cell junctions at the *Zona occludens*. This therefore allowed us to look at whether cells expressing DN-VASP were found in the same plane as the rest of the monolayer where cells were not expressing DN-VASP.

In cells that were not replated (Figure 3.8), DN-VASP expressing cells appear to be fully incorporated into the cell monolayer. ZO-1 staining is seen around the cells suggesting that cell: cell junctions are forming at the *Zona Occludens*. The cells appear to be at the same level above the matrix as those that are not expressing DN-VASP (XY

images, all timepoints). This does not appear to alter between 6 and 24 hours post transfection (figure 3.8a and c).

In replated cells (Figure 3.9), 4 hours after replating (Figure 3.9a), the DN-VASP expressing cell can clearly be seen to be positioned above the level of the cell monolayer (0  $\mu\text{m}$  level). The lower set of images shown were taken 13 $\mu\text{m}$  above the level of the cells shown in the top panel but are from the same microscope field. Only in the images taken at this higher level, is the DN-VASP-expressing cell in focus. This is also noticeable if the XY section is viewed – this cell appears to be attached to other cells below it, not to the matrix. By 18 hours post-replating (Figure 3.8b), the DN-VASP cells appear to have been incorporated into an epithelial monolayer. However, some of these cells still appear to be located slightly above the main body of the monolayer. In an image taken at a level 5 $\mu\text{m}$  higher than the monolayer these cells appear more in focus, suggesting they are situated slightly higher than the surrounding cells. Whilst these cells appear to have made cell: cell contacts as demonstrated by ZO-1 staining this finding suggests that they may not be attached to the substratum but are being held in place by cell:cell contacts with cells that are not expressing DN-VASP.

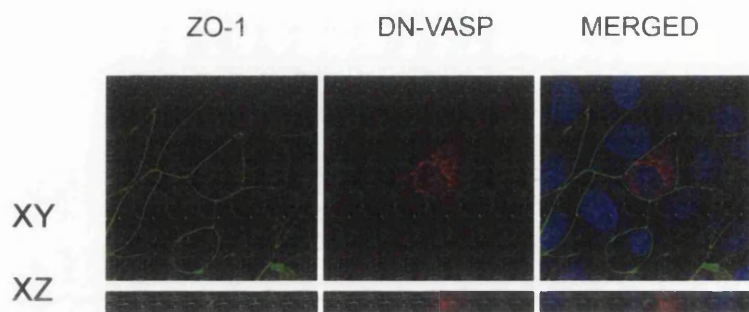


Figure 3.8a  
6 hours post transfection  
non-replated



Figure 3.8b  
10 hours post transfection  
non-replated

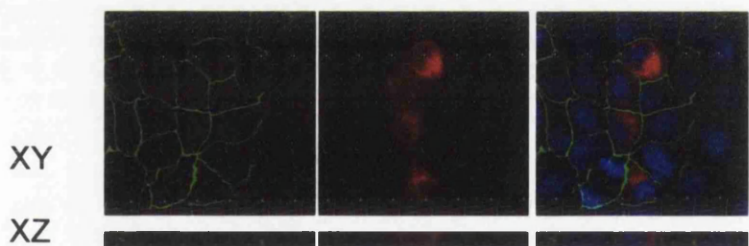


Figure 3.8c  
24 hours post transfection  
non-replated

**Figure 3.8 Distribution of MDCK TetOff Cells transfected *in situ* with DN-VASP.** DN-VASP expression is demonstrated by red staining in the above images. ZO-1 expression at cell:cell junctions is seen in green. Images were deconvolved and then reconstructed to create XZ images demonstrating the positions of the cells in a vertical slice through the image. (Magnification x400)

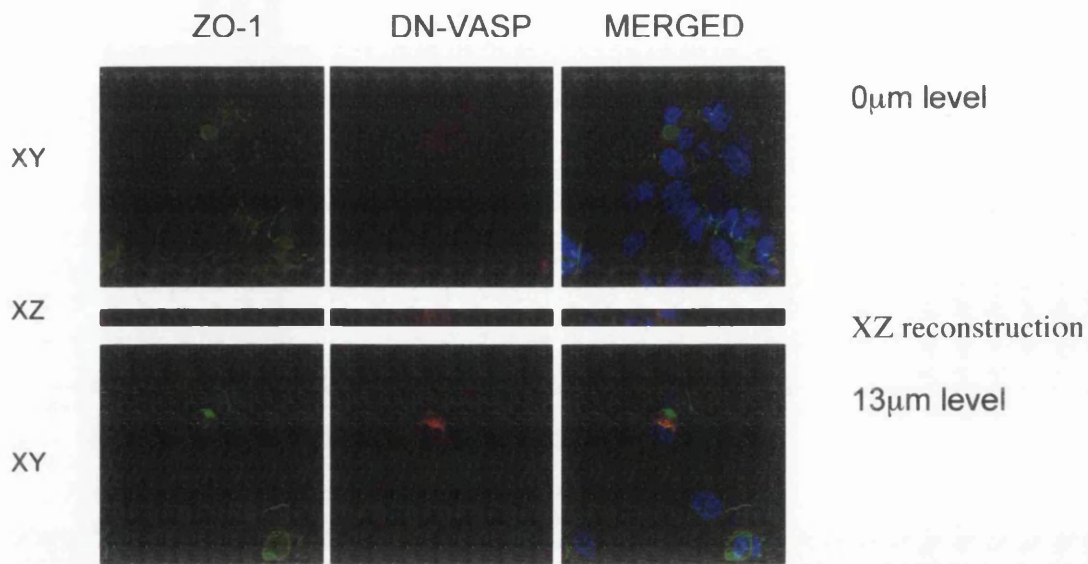


Figure 3.9a. 10 hours post transfection, 4 hours after replating

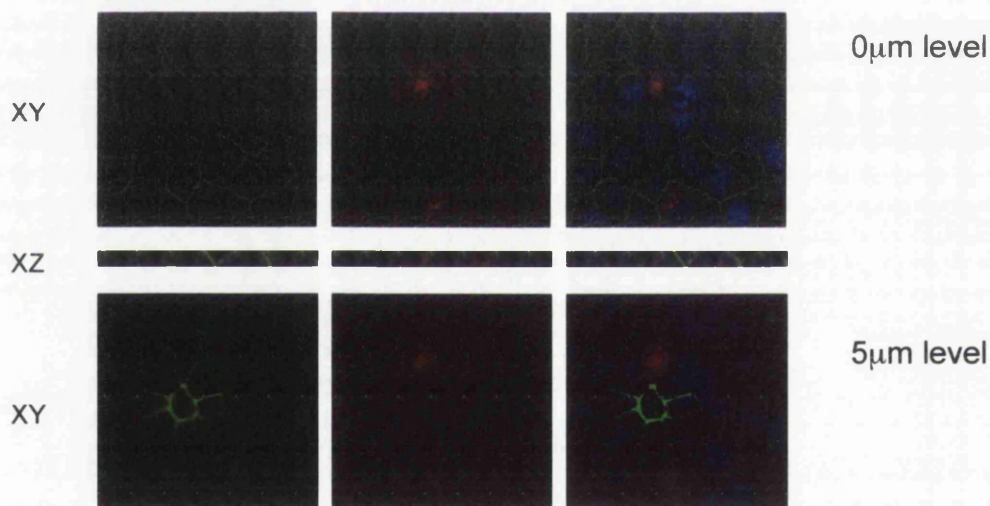


Figure 3.9b. 24 hours post transfection, 18 hours after replating

**Figure 3.9 Distribution of DN-VASP expressing MDCK TetOff cells subjected to detachment and reattachment 6 hours after transfection.**

As in figure 3.8, DN-VASP is stained red and ZO-1 green. The upper XY image in both 3.9 a and b is a deconvolved image at the level of the epithelial monolayer. The lower XY image is from the same microscope field but with the deconvolution carried out at either 13 or 5 µm above the monolayer, showing cells at an elevated plane. (Magnification x400)

### **3.3.8 Establishment of a 3D Tubule Model to Investigate Tubule Formation and Breakdown.**

The aim of this section of work was to establish a 3-dimensional model of tubules and then investigate the effects of allowing DN-VASP expression to be switched on at various stages of tubulogenesis. This could be used to investigate the effects of disrupting VASP function and its interaction with the actin cytoskeleton during these processes. This would give a clearer picture of how the actin cytoskeleton is altered during tubulogenesis and what alterations in cell polarity and morphology are necessary to allow formation of a new tubule. This has obvious implications then in the recovery of the proximal tubule following acute injury.

MDCK TetOff cells readily formed cysts when grown in a collagen matrix. These were easily visible by 3 days after seeding and continued to grow to day 7. Following the addition of 20ng/ml of HGF, spikes and projections were seen within 1-2 days (Figure 3.10a). With daily addition of HGF, these developed into cords (day 2-3) (Figure 3.10b), early tubules (day 3-4) (figure 3.10c) and complex branching tubules after 5 days (Figure 3.10d). Not all cysts responded, some remained at the cyst stage formation or regressed despite daily HGF addition. It is unknown why some were able to respond to HGF and others not.

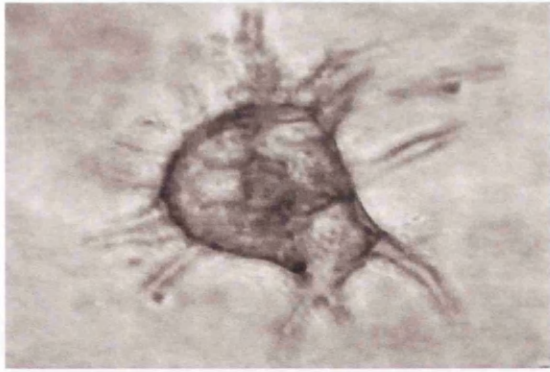


Figure 3.10a Spikes and projections

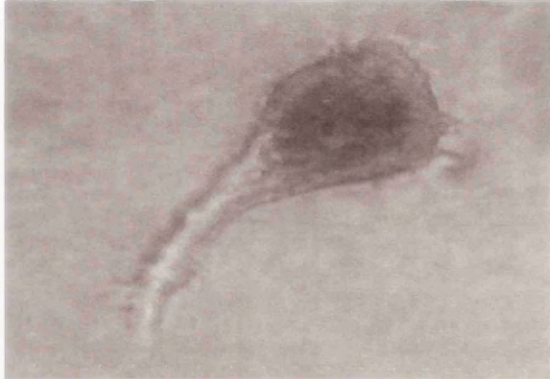


Figure 3.10b Cord – a chain of cells

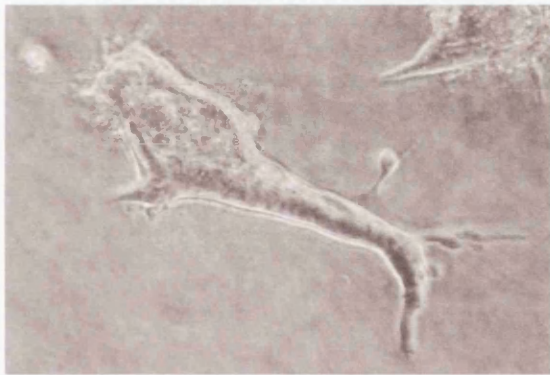


Figure 3.10c Early tubule

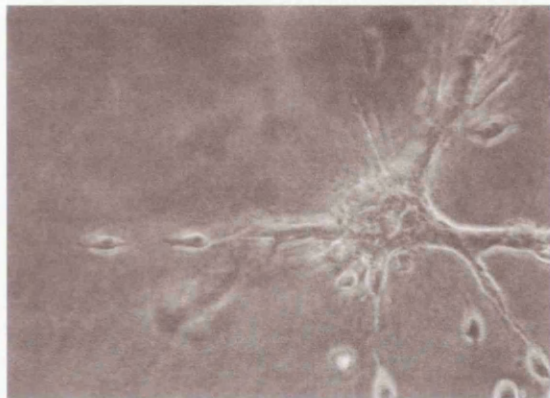


Figure 3.10d Branching tubule

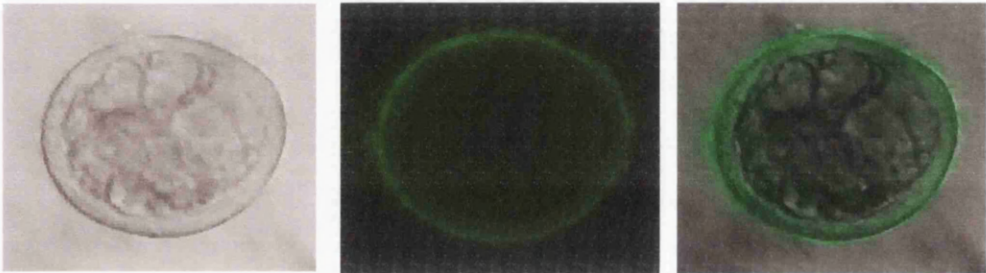
**Figure 3.10 MDCK Cells in Collagen Gels Following HGF Stimulation**

Light microscopy images, magnification x100)

Staining of the cells and examination by confocal microscopy revealed the polarised nature of these structures. This was present by the stage of cyst formation where  $\beta_1$  integrin can be seen to clearly localise to the basolateral aspects of the cells forming the cyst (figure 3.11a). In more complex tubules, the microvilli-associated protein Ezrin can be seen to localise to the apical aspects of the cells (Figure 3.11b), lining to tubule lumen demonstrating normal epithelial cell polarity.

It had been hoped to produce a stable clone of MDCK TetOff cells expressing DN-VASP under the control of tetracycline repression by transfecting with pTRE2hyg/DN-VASP and the use of selective antibiotics as described in section 3.2.6. Transient transfection demonstrated that transfection rates of at least 40% were possible (Section 3.3.4). Following cloning, we first tested for DN-VASP expression by immunofluorescent staining at 2 weeks following transfection by taking a sample of cells and growing them in the absence of the repressor antibiotic doxycycline. Unfortunately, by this time, we were already unable to detect any DN-VASP expression. Despite this, we continued with the cloning attempt and tested more samples when we had enough of a clone to grow in a T25 cell culture flask. 60 clones were tested for DN-VASP expression 24 hours after removal of doxycycline using the method described. No DN-VASP expression was seen in any of the clones. Approximately 25% of these clones were re-tested at 48 hours after doxycycline removal. Unfortunately, again, no DN-VASP expression was seen. In order to try and increase the chances of expression the histone deacetylase inhibitors, sodium butyrate and Trichostatin A were also added to the culture media following the removal of doxycycline. However, DN-VASP was still not detectable. This pathway of investigation was therefore discontinued.

**Figure 3.11 Confocal images of MDCK cells in collagen gels**

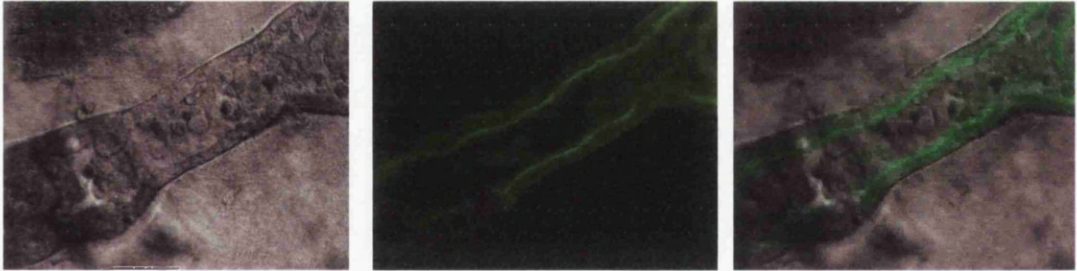


**Phase**

**$\beta_1$  Integrin**

**Merged**

Figure 3.11a MDCK cell cyst stained for the basolaterally-distributed protein  $\beta_1$  integrin



**Phase**

**Ezrin**

**Merged**

Figure 3.11b MDCK cell tubule stained for the microvilli-associated apically distributed, protein ezrin

### 3.4 Discussion

VASP is known to localise at both cell: cell and cell: extracellular matrix contacts and to act as a link to the actin cytoskeleton via subcellular targeting dependent on their EVH1 domains (Brindle *et al.*, 1996; Critchley *et al.*, 1999; Drees *et al.*, 2000). The exact role of VASP in maintenance of these contacts is yet to be fully evaluated. In this chapter we have presented evidence that VASP is of greater importance in newly forming epithelial sheets than in established monolayers. In section 3.3.6 we demonstrated that disruption of normal VASP function decreased the ability of cells to adhere to the extra-cellular matrix. A significantly decreased number of DN-VASP expressing cells were seen when they underwent replating at a time-point where we had demonstrated that the protein was being expressed. In cells that were not replated, a higher number of DN-VASP expressing cells were seen at all timepoints and this did not appear to interfere with sheet integrity. Cells that were expressing DN-VASP in the replated cells, appeared not to be forming contacts with the ECM but were instead seen above this level, attached to other cells. It is possible that the cells did not detach from their neighbouring cells during the trypsinisation process and were able to be transferred and stick in the new environment only because they had already formed stable attachments to other cells.

These findings are consistent with published literature in other cells. It has been noted previously that cells grown in low calcium media are unable to form normal cell: cell contacts until the calcium is replaced (Vasioukhin *et al.*, 2000). This is also seen with the use of cytochalasin D to disrupt the actin cytoskeleton. However, cytochalasin D is only effective at interrupting cell: cell contacts when they are either attempting to form or are less than 1 hour old. In contacts greater than 1 hour old, the contacts do not

disassemble with addition of cytochalasin D (Adams *et al.*, 1998). This suggests a role for the actin cytoskeleton in bringing together cells and forming new contacts but suggests it may not be so important in maintaining contacts. Our results (section 3.3) support this conclusion. In this section we demonstrated the effects of DN-VASP transfection on a pre-formed epithelial sheet. Despite 40% of the cells expressing DN-VASP, the monolayer has survived. This is despite disruption of actin fibre formation as demonstrated in figure 3.6.

The XZ reconstructions of replated cells expressing DN-VASP show that these cells are seen mainly above the monolayer. This was seen even 18 hours after replating when a sheet had reformed (Figure 3.9b). This could suggest that a more important role for VASP is in the formation of adhesions to the extracellular matrix, a process essential for cell motility in recovery after damage. Cell motility involves coordination of changes in cell polarity (Pollack *et al.*, 1998), membrane extension, alterations in adhesiveness and contractile mechanisms (Loureiro *et al.*, 2002). Ena/VASP proteins localise to dynamic regions of the cell with high rates of actin turnover such as lamellipodial and filopodial tips (Reinhard *et al.*, 1992; Rottner *et al.*, 1999). Studies in fibroblasts have demonstrated the necessity of the F-actin-binding domain of Ena/VASP proteins for whole cell motility (Loureiro *et al.*, 2002) These findings demonstrated that the EVH2 domain was sufficient to restore cell motility in Mena-deficient cells. Interestingly, the DN-VASP we used in our experiments did not contain F-actin binding portion of the EVH2 domain. It only contains the coiled-coil and tetramerisation domains of VASP. We used residues 277-380. The F-actin binding domain is at residues 259-276 of human VASP (Bachmann *et al.*, 1999). It would be interesting to repeat this work using a longer form of DN-VASP that also incorporated the F-actin domain.

In an earlier chapter we demonstrated that iNOS expression was sufficient to cause loss of VASP from focal adhesion sites in HPTECs. The presence of cyclic-nucleotide dependent phosphorylation sites has also been demonstrated to be essential for cell motility (Loureiro *et al.*, 2002). DN-VASP used in this experiment only contains the threonine 278 phosphorylation site, one that does not appear to be important in VASP function (Butt *et al.*, 1994) and is only very slowly phosphorylated. Again, it would be interesting to investigate the effects of other forms of truncated VASP including these sites to study cell motility. The Ser157 and 239 residues are phosphorylated in response to PKA and PKG (Haffner *et al.*, 1995). In sepsis, upregulation of both of these enzymes can occur. It is possible that ongoing, pro-inflammatory cytokine-induced upregulation of these pathways could disrupt the ability of tubules to reform after injury. However, transient phosphorylation to allow temporary rearrangement of actin to allow movement could be important in normal recovery.

A 3-D tubule model would provide a much more physiological model of tubule breakdown and formation as discussed in the main introduction (Section 1.3) (Zegers *et al.*, 2003). As demonstrated in this section (Figure 3.10), MDCK cells form polarised structures when grown in a type I collagen matrix with the expected distribution of apical and basolateral membrane-associated proteins. As it has been shown that cells need to lose polarity transiently to form tubules (Pollack *et al.*, 1998) this demonstrates that the actin cytoskeleton must undergo reorganisation and then reform to reproduce polarity. Cell:cell adhesion is maintained during this process but contacts with the extracellular matrix would need to be disrupted and focal adhesions formed to allow cell motility. With the findings discussed above that VASP appears to be more important in

these roles, the use of a regulatable DN-VASP-expressing clone of cells would have been of great interest as the effects of disrupting normal VASP function at different stages of development could have been investigated. Unfortunately, we were unable to produce a stable, DN-VASP expressing clone. The TetOff and TetOn systems are capable of producing highly regulatable systems by which expression of the gene of interest may be controlled (Gossen and Bujard, 1992; Kistner *et al.*, 1996) and we found we were able to obtain high levels of doxycycline-regulated transient transfection (Figures 3.4a and b). These systems have also been used in the production of transgenic mice (Ray *et al.*, 1997) in order to allow a lethal gene to be suppressed until the animals have reached a suitable stage of development, suggesting that long term suppression without loss of the gene of interest is feasible. There are a number of reasons why our cloning strategy may have failed. Whilst immunofluorescence is a very sensitive way of detecting protein expression, DN-VASP may have been expressed at levels too low for detection. We found that, even in the presence of doxycycline, some leakiness of the tetracycline repression occurred (Figure 3.3a). With the longer culture times involved in the production of a stable transfectant, this may have been sufficient to build up and have enough of an effect to stop these cells from binding to the substratum, thereby leading to the loss of successfully transfected cells. Another alternative explanation is that the gene of interest may have been incorporated into the cDNA in a location whereby its expression was repressed possibly due to the proximity of a repressor element. It is possible that by screening more clones we may have been able to find a stable, tetracycline regulated, DN-VASP expressing clone however it was not feasible to continue this process within the time limits of this project. If one could be found, it would provide a very interesting tool for future work involving the 3-D model.

## **Chapter 4. The Effects of Dominant–Negative VASP on T cell activation.**

## 4.1 Introduction

T cell activation and proliferation involves clustering of integrins (lymphocyte function related antigen (LFA)-1) around the T cell receptor (TCR) (van Kooyk, van Vliet et al. 1999) with an accompanying increase in their avidity for their ligands on the antigen-presenting cell (APC), intercellular adhesion molecules 1, 2 and 3 (ICAM 1, 2 and 3) (Griffiths and Penninger, 2002b; Sims and Dustin, 2002; van Kooyk et al., 1999). Conformational changes in the  $\alpha/\beta$  heterodimer are thought to be associated with the enhancement of binding (Lollo et al., 1993). T cell activation is associated with an increase in interleukin-2 (IL-2) and interferon- $\gamma$  (IFN- $\gamma$ ) production and the appearance on the cell surface of activation markers such as CD25 (IL-2 receptor  $\alpha$ ) and CD69. Changes in free intracellular calcium occur during T cell activation. The increase in calcium seen after TCR activation is one of the earliest biochemical responses to occur and happens within seconds (Sims and Dustin, 2002). The actin cytoskeleton undergoes rearrangement during T cell activation (Penninger and Crabtree, 1999; Valitutti et al., 1995). Upon binding to an APC, the T cell cytoskeleton rapidly polarises, forming a tight actin collar at the T cell; APC interface (Ryser et al., 1982; Valitutti et al., 1995). This reorganisation of the cytoskeleton is required for T cell activation. Disruption of the actin cytoskeleton with Cytochalasin D inhibits IL-2 gene transcription (Holsinger et al., 1998).

The adaptor protein ADAP has been suggested as a link between TCR activation and actin polarisation. The role of ADAP in actin cytoskeleton rearrangement remains unclear. ADAP has been shown to co-localise with F-actin, Ena/VASP proteins, the Arp 2/3 complex, Vav-I and WASP (Wiskott-Aldrich syndrome protein) (Barda-Saad et al., 2005) at the interface between Jurkat T cells and anti-CD3 coated beads. Blocking this

interaction by using transfected ActA repeats (the *Listeria* protein that binds EVH1 domains found in Ena/VASP proteins), inhibited TCR-induced actin rearrangement (Krause et al., 2000). Also, TCR-mediated integrin (LFA-1) clustering is deficient in ADAP-knockout mice (Griffiths et al., 2001; Peterson et al., 2001b). However, ADAP mutated in the EVH-1 bonding domain has no effect on LFA-1 avidity (Wang et al., 2004)

The Ena/VASP proteins are a potential pathway by which TCR stimulation and rearrangements of the actin cytoskeleton may be linked. VASP is capable of binding to integrins and polymerising actin and, in epithelial cells, forms an important part of focal adhesion formation. It is therefore a potential mechanism through which actin polarisation may occur following TCR stimulation and clustering of integrins. The ability to rearrange the actin cytoskeleton is known to be essential for full T cell activation (Barda-Saad et al., 2005; Valitutti et al., 1995). For example, in its non-active state, the T cell integrin, LFA-1 is tethered to the actin cytoskeleton. Release from this appears to allow motility, leading to LFA-1 clustering. Newly formed clusters then form stronger links with the actin cytoskeleton via proteins such as  $\alpha$ -actinin (Sampath et al., 1998) and recruit other molecules to form a functional adhesive unit, capable of transducing outside-in signals (van Kooyk et al., 1994).

Actin dynamics may also regulate other features of T cell activation, downstream of TCR clustering. Disruption of actin polymerisation is associated with a prolonged rise in elevation of intracellular calcium levels. This causes a persistent increase in NFAT (nuclear factor of activated T cells) activation and increased IL-2 promoter activity (Rivas et al., 2004). This suggests that actin polymerisation may have a negative regulatory role in this pathway normally, limiting calcium-induced NFAT activation.

There are other ways in which the actin cytoskeleton may play a role in downstream activation of T cells may be important. Components of the cytoskeleton may act as insulators, holding parts of a signal transduction apart until activation releases them from the cytoskeleton, allows them to move, contact each other and activate pathways such as MAP (mitogen-activated protein) kinases (Weston and Davis, 2001). They may act to target components of signalling pathways to specific sub-cellular compartments, controlling the dynamics of delivery of the components to upstream activators or downstream effectors (Burack et al., 2002). Many different signal transduction pathways are involved in T cell activation (Figure 4.1). The role of the actin cytoskeleton in control of these pathways has undergone little study.

In this chapter we present work investigating the effects of disruption of the actin cytoskeleton through the use of a dominant-negative form of VASP and how this alters aspects such as cell polarisation, cell adhesion, signal transduction pathways and expression of markers of activation. For this work we have used Jurkat cells to investigate the role of VASP in T cell activation. Jurkat Cells are a human cell line originally derived from a patient with acute lymphoblastic leukaemia (ALL) (Schneider et al., 1977). They are a non-adherent T cell line that grow singly or in clumps. Whilst they have proved a useful tool in the investigation of T cell activation, they are limited in how results can be interpreted and transferred to primary cells. Like all cell lines, they undergo spontaneous mutations the longer they are grown and also, unlike primary cells, exist in a state of low grade activation at all times (Astoul et al., 2001).

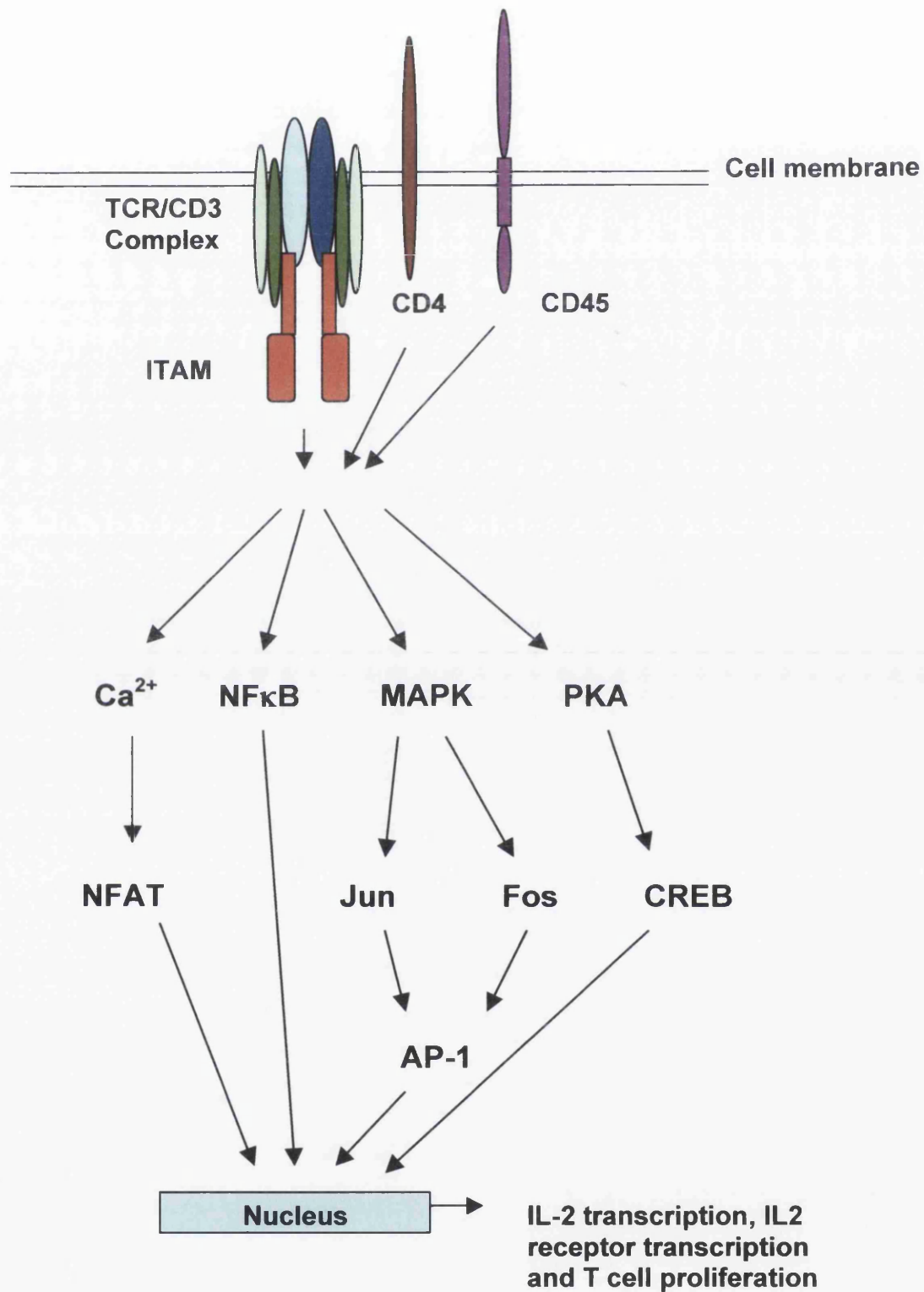


**Figure 4.1 T Cell Receptor Signalling Pathways.** This figure demonstrates some of the many pathways involved in T cell activation and proliferation. The role of VASP in these pathways has not yet been elucidated

We have used a specific clone of Jurkat cells for this work. Jurkat TetOff cells are a stable clone containing the pTetOff regulator plasmid as described in MDCK TetOff cells in the introduction to chapter 3. Jurkat TetOff cells require the presence of G-418 to maintain the clone whereas MDCK TetOff cells use puromycin.

We have used this system to transfect in dominant-negative VASP (DN-VASP) into Jurkat cells. This consists of the terminal portion of the EVH2 domain of VASP, the part associated with tetramerisation (Bachmann et al., 1999). As it does not include the EVH1 domain, it is unable to bind to proteins such as vinculin, zyxin and integrins, thereby altering its ability to anchor to transmembrane proteins (Carl et al., 1999; Reinhard et al., 1992). DN-VASP therefore provides an interesting way to look at the effects of Ena/VASP proteins and the actin cytoskeleton on T cell activation. It is particularly useful as it blocks the actions of all Ena/VASP proteins, not just VASP (Vasioukhin et al., 2000) and therefore has benefits over the techniques of siRNA or genetically engineered VASP knockouts where other members of the protein family could substitute for VASP.

## **4.2 Methods**

### **4.2.1 Culture of Jurkat TetOff Cells**

Jurkat TetOff cells (BD Clontech) were grown in the following media at 37°C, 5% CO<sub>2</sub>; DMEM supplemented with 4mM glutamine, 10% Tet-system approved Foetal bovine serum (FBS), Penicillin 10u/ml, streptomycin 10mg/ml and 100µg/ml G-418 (Sigma, UK). Stock cultures were sub-cultured at a 1:5 dilution when a cell density of 3x10<sup>6</sup> cells/ml was reached.

### **4.2.2 Optimisation of Jurkat TetOff Cell Transfection**

All transfections were carried out using an Amaxa Nucleofector (Amaxa, Germany). Nucleofector Kit V was used for transfection of Jurkat TetOff cells. pmaxGFP was supplied with the kit.

The Nucleofector allows delivery DNA into the cell nucleus, so called `nucleofection` and is used in conjunction with optimised solutions for individual cell types. Optimised protocols have been worked out by the company for different cell lines and clones. Whilst Jurkat TetOff cells do not have an optimised protocol, advice obtained from Amaxa was to use programmes C16 and G10 for initial experiments. Cell Line Nucleofector Kit V contains solutions and supplements optimised for Jurkat cell transfection and was used in the following experiments.

Jurkat TetOff cells were cultured in media as described above. The cells were counted using a haemocytometer and the required number were spun down at 1,000rpm for 10 minutes. For each transfection, 3x10<sup>6</sup> cells were used. All supernatant media was removed following centrifugation and the cells were resuspended in 100µl of

nucleofector solution with added nucleofector supplement per transfection reaction as per standard protocol. 2µg of pmaxGFP (Amaxa, supplied with kit) was added to the cell suspension and then transferred to a cuvette. The cuvette was placed into the Nucleofector and programs C-16 and G-10 were used to transfect individual samples. Following electroporation, the cells were then immediately transferred into prewarmed media in 12 well plates and the cells were incubated for 24 hours at 37°, 5% CO<sub>2</sub> before being harvested and prepared for FACS analysis for expression of GFP. The cells centrifuged at 1500rpm for 7 minutes, washed twice in FACS buffer (PBS plus 2% BSA) and resuspended in 800µl FACS buffer containing 2µg propidium iodide. FACS analysis was carried out using a FACSCalibur flow cytometer (BD Biosciences, San Jose, CA) and the data was analysed using FloJo software.

#### **4.2.3 Time Course of Expression of DN-VASP in Jurkat TetOff Cells**

Jurkat TetOff cells were transfected with either pTRE2hyg/DN-VASP or pTRE2hyg alone as described previously. (The production of pTRE2hyg/DN-VASP is described in section 3.2.2). Cells were cultured in 6 well tissue culture plates, each well holding 1.5x10<sup>6</sup> cells/well. Samples were taken for analysis at 2, 4, 6, 8 and 24 hours post transfection. The contents of one well were centrifuged at 200g for 10 minutes, washed twice in PBS and then lysed in 75µl of Laemelli lysis buffer. Samples were boiled at 95°C for 10 minutes and briefly subjected to sonication before being analysed by immunoblotting.

Samples were run on 10-20% Tris-glycine gels (Invitrogen, UK) at 20mA/gel to the bottom of the gel. 40µl of sample was added to each well. The proteins were then electrophoretically transferred onto a PVDF membrane as described previously.

Membranes were stained with primary antibody (Mouse mAB antiVASP, BD Transduction Labs, 1:500 dilution) and a biotinylated secondary antibody (Horse anti-mouse IgG (H+L), Vector Laboratories). was added for 1 hour. HRP-conjugated Streptavidin and the ECL Plus system were used to visualise immunoreactive bands. ECL film was used for autoradiography.

#### **4.2.4 The Effects of DN-VASP Transfection on Interleukin-2 and Interferon- $\gamma$ Expression in Jurkat Tet-Off Cells**

The following additional reagents were used: Purified mouse anti-human CD3 monoclonal antibody (No azide/ low endotoxin (NA/LE)) 1mg/ml and purified mouse anti-human CD28 monoclonal antibody (NA/LE) 1mg/ml (Both BD Biosciences Pharmingen, USA); DuoSet Elisa Development systems for human IL-2 and human IFN- $\gamma$  and Substrate Reagent Pack (Solution A H<sub>2</sub>O<sub>2</sub> and solution B tetramethylbenzidine (TMB)) (R&D Systems, USA).

##### **4.2.4.1 Transfection and stimulation**

Jurkat TetOff cells were transfected using Amaxa Nucleofector kit V in the Amaxa Nucleofector.(as described previously in section 4.2.2) with either pTRE2hyg or pTRE2hyg/DN-VASP and allowed to recover overnight. A 48 well plate was prepared for use in cell stimulation. Anti-CD3 antibody was diluted in PBS at a concentration of 5mg/ml and used to coat the bottom of the wells. The plate was incubated at 37°C for 2 hours before being washed twice in warm PBS. The plate was stored at 4°C until ready for use.

Transfected cells were counted and  $0.25 \times 10^6$  cells placed into each well of a 48 well plate. Cells for stimulation were placed into the CD3 coated plate. Those for dual stimulation were also treated with soluble anti-CD28 antibody (1mg/ml). Unstimulated cells were grown in uncoated 48 well plates and were also cultured in the presence or absence of  $2 \mu\text{g/ml}$  doxycycline. Each set of conditions was repeated in triplicate.

Samples were harvested at 48 hours for assay by ELISA. Samples were aspirated from the tissue culture well and placed into a microfuge tube. They were centrifuged at 200g for 5 minutes. The supernatant was removed and placed into a fresh microfuge tube before being stored at  $-20^\circ\text{C}$  until assayed.

#### **4.2.4.2 IL-2 and IFN- $\gamma$ Enzyme- Linked Immunosorbent Assay (ELISA)**

The assay was carried out using the DuoSet kits as described above. 96 well plates were coated with capture antibody (either IL-2 or IFN- $\gamma$  antibodies) and incubated at room temperature overnight. They were then washed and blocked with block buffer (BSA 1%, sucrose 5% in PBS with 0.05%  $\text{NaN}_3$ ) for at least 1 hour. Meanwhile IL-2 or IFN- $\gamma$  standards were prepared from 1000 pg/ml with 7 doubling dilutions. The standards were prepared in media which was also used as a blank. Each transfection and stimulation condition was assayed in triplicate.

After blocking, the plates were washed and the samples and standards added. The plates were covered and incubated for 2 hours at room temperature before further washing. Detection antibodies (biotinylated anti-IL-2 or IFN- $\gamma$ ) were then added to the plates which were again incubated at room temperature for 2 hours before washing. Following this Streptavidin-HRP (at the kit-recommended dilution of 1:200) was added for 20 minutes, before washing and addition of substrate solution (1:1 mixture of  $\text{H}_2\text{O}_2$  and

TMB) for a further 20 minutes. The reaction was then stopped with 1M sulphuric acid. Following this the plates were read on a Dynex MRX II microplate reader and Revelation software. The optical density of each well was determined at 450nm with 540nm wavelength correction.

Results were analysed using a Student's t test to look at significance;  $p < 0.05$  was considered significant and  $< 0.01$ , highly significant.

#### **4.2.5 The Effects of DN-VASP Transfection on CD69 and CD25 Expression by Jurkat TetOff Cells.**

The following additional reagents were used: Fluorescein isothiocyanate (FITC)-conjugated mouse anti-human monoclonal CD25 antibody, FITC-conjugated mouse monoclonal anti-human CD69 antibody and FITC-conjugated mouse IgG,  $\kappa$  monoclonal immunoglobulin isotype control (all BD Pharmingen); bovine serum albumin (BSA) and propidium iodide (Sigma, UK)

Jurkat TetOff cells were transfected with either DN-VASP or empty vector using the same protocols as described previously. They were allowed to recover overnight at 37°C, 5% CO<sub>2</sub>. The following day, they were stimulated with plate bound anti CD3 (5µg/ml) and soluble anti CD28 (1µg/ml) or left unstimulated. To assess CD69 expression, cells were harvested at 24 hours post transfection and for CD25 expression they were harvested at 48 hours post-transfection. Cells were centrifuged at 200g for 10 minutes, media removed, washed in 1% BSA in PBS three times and then resuspended in 0.5ml 1% BSA in PBS. FITC-conjugated antibody against either CD25 or CD69 was

added at a concentration of 20 $\mu$ l/0.5x10<sup>6</sup> cells. A control sample was incubated with a FITC conjugated-IgG control at the same concentration. The cells were then incubated on ice for 1 hour before being washed a further 3 times and analysed using FACs. Propidium iodide (25 $\mu$ l, 100 $\mu$ g/ml solution) was added just before analysis to allow exclusion of dead cells.

#### **4.2.6 The Effects of DN-VASP Transfection on Signal Transduction Pathways in Jurkat TetOff Cells.**

PathDetect in Vivo Signal Transduction Pathway *cis*-Reporting Systems, PathDetect in Vivo Signal Transduction Pathway *trans*-Reporting Systems and Luciferase Assay Kit were all obtained from Stratagene. For details of the vectors used in these experiments see Appendix 1)

Stratagene's PathDetect in Vivo Signal Transduction Pathway *cis* and *trans* Reporting Systems were used to assess the effects of DN-VASP on the activation of various signal transduction pathways. The *cis*-reporting systems (figure 4.2) are a series of inducible reporter plasmids containing the luciferase reporter gene driven by a basic reporter element. Expression of the luciferase gene is controlled by a synthetic promoter that contains direct repeats of the element under investigation (eg AP-1, NFAT). The effects of extracellular stimuli on these pathways can then be investigated. The *trans*-reporting systems are designed for assessment of the activation of transcription activators and upstream signal transduction pathways (Figure 4.3). Each *trans*-reporting system contains a fusion *trans*-activator plasmid that expresses a fusion protein which is a pathway-specific transcriptional activator. This fusion protein consists of the activation domain of the element of choice (e.g, CREB) fused with the yeast Gal4 DNA binding

domain. The transcriptional activator CREB is phosphorylated by protein kinase A (PKA) and activity reflects the activity of the signal transduction pathway.

In the *trans*-reporter systems as well as the *trans*-activator plasmid, the pFR-Luc plasmid is also transfected into the cells. This contains a synthetic promoter with 5 tandem repeats of the yeast Gal4 binding sites that control expression of the luciferase gene. The DNA-binding domain of the fusion *trans*-activator protein binds to the reporter plasmid at these sites. Phosphorylation of the transcription activation domain of the fusion protein due to cell stimulation will then activate transcription of the luciferase gene.

These systems can be used to investigate the effects of DN-VASP on Jurkat activation following stimulation by transfecting in the pTRE2hyg plasmid and investigating what effects it has on the activation of these pathways. The pathways investigated in Jurkat TetOff cells were AP-1 (Fos/Jun complex), NF- $\kappa$ B (nuclear factor - $\kappa$ B) and NFAT for *cis*-reporting systems and CREB (cAMP-response element binding factor) for *trans*-reporting systems

All transfections were carried out using  $3 \times 10^6$  cells/ transfection, Amaxa Nucleofector Kit V, DNA as indicated and programme G-10 with the Amaxa Nucleofector

Figure 4.2 PathDetect *cis*-Reporter System

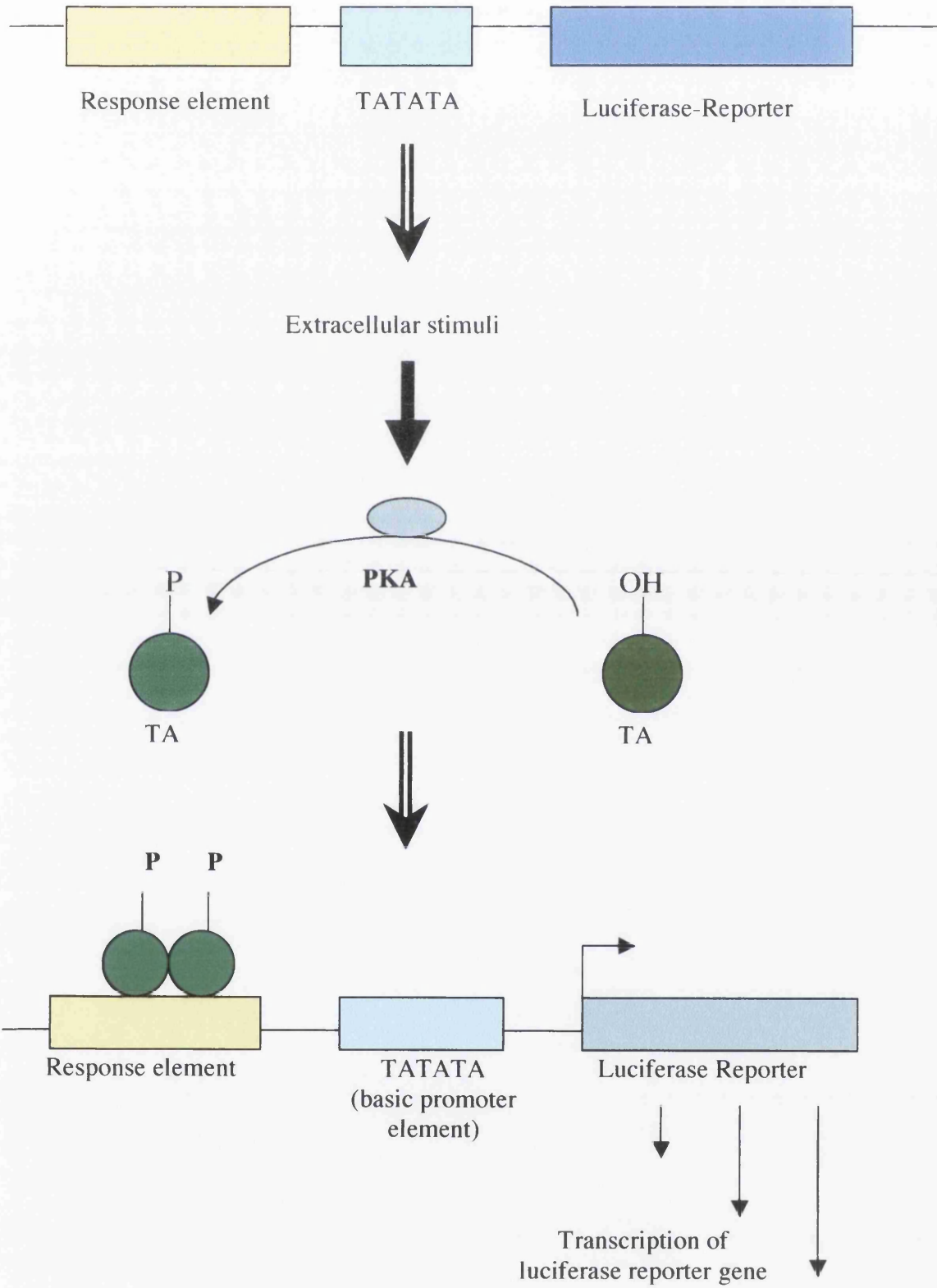
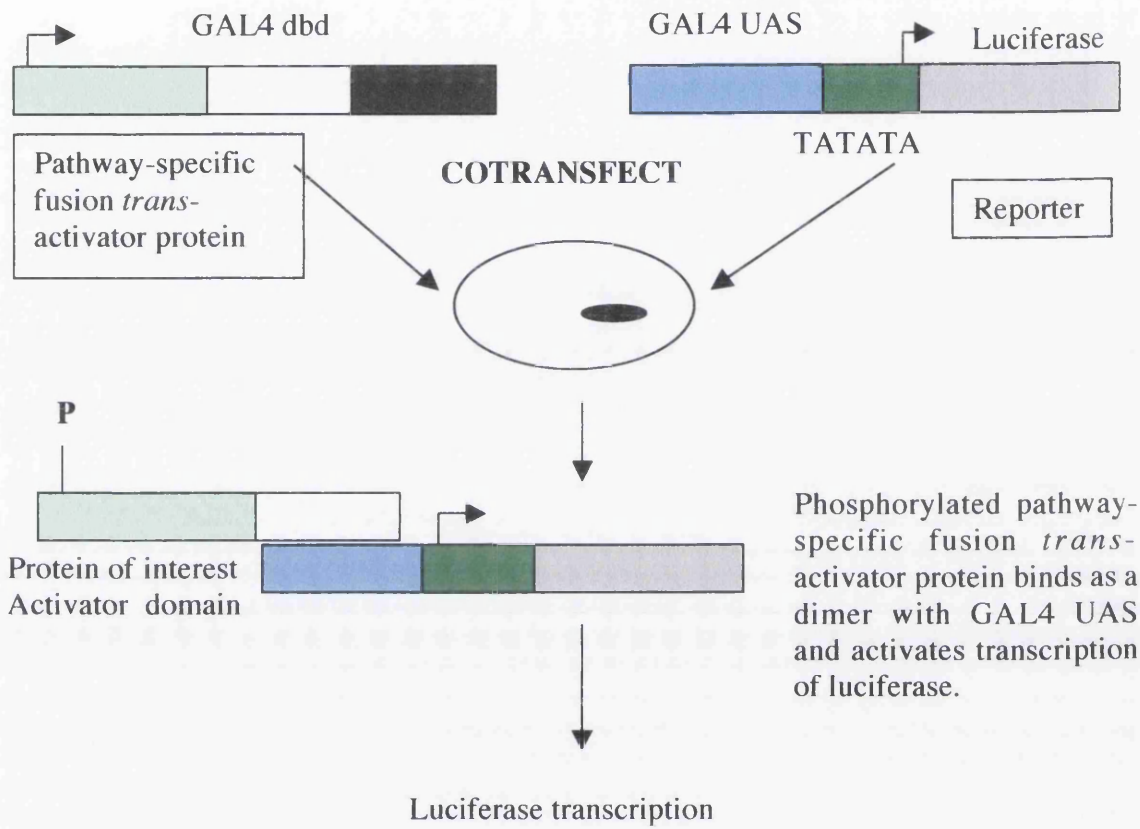


Figure 4.3 PathDetect *trans*-Reporter System



#### 4.2.6.1 Transfection protocols

(1) **Table 4.1 *cis*-reporting system plasmids** (for plasmid details see appendix 1)

Reporter Plasmid	Positive Control Plasmid	Negative Control Plasmid	Vector	Vector + insert	Carrier DNA
pAP-1-Luc	pFC-MEKK		pTRE2hyg	pTRE2hyg/ DN-VASP	pCI
pNF- $\kappa$ B-Luc	pFC-MEKK		pTRE2hyg	pTRE2hyg/ DN-VASP	pCI
pNFAT-Luc		pCIS-CK	pTRE2hyg	pTRE2hyg/ DN-VASP	

**Table 4.2 Protocol for *cis* system transfections**

Number	Reporter Plasmid	Negative Control Plasmid	Positive Control Plasmid	Vector + Insert	Empty Vector	Carrier DNA
1	1 $\mu$ g			1 $\mu$ g		
2	1 $\mu$ g				1 $\mu$ g	
3	1 $\mu$ g		50ng			950ng
4		1 $\mu$ g		1 $\mu$ g		

(2) **Table 4.3 *trans*-reporting system plasmids** (for plasmid details see appendix 1)

Reporter Plasmid	Fusion <i>trans</i> -Activator Plasmid	Negative Control Plasmid	Positive Control Plasmid	Empty Vector	Vector + Insert	Carrier DNA
pFR-Luc	pFA2-CREB	pFC2-dbd	pFC-PKA	pTRE2hyg	pTRE2hyg/ DN-VASP	pCI

**Table 4.4 Protocol for *trans* system transfections**

No	Report-er Plasmid	Fusion <i>trans</i> -Activat-or Plasmid	Negative Control Plasmid	Positive Control Plasmid	Empty Vector	Vector + Insert	Car-rier DNA
1	1µg	50ng				1µg	
2	1µg	50ng			1µg		
3	1µg	50ng		50ng			950ng
4	1µg		50ng				950ng

The Amaxa Nucleofector was used to transfect the cells, using Kit V,  $3 \times 10^6$  cells/transfection and programme G-10. Cells were transfected according to the protocols given above and then allowed to recover overnight in fresh media at 37°C, 5% CO<sub>2</sub>. For cells transfected with either pTRE2hyg or pTRE2hyg/DN-VASP, 2 transfections of  $3 \times 10^6$  cells were carried out. The cells were pooled and allowed to recover overnight.

The following day, cells were either stimulated with plate bound CD3 (5µg/ml) and soluble CD28 (1µg/ml) or remained unstimulated (table 4.5)

**Table 4.5 Transfection and stimulation conditions for signal transduction experiments**

Sample	DNA transfection	CD3/CD28 antibody Stimulation
<u>V</u> S	pTRE2hyg/DN-VASP	+
<u>E</u> S	pTRE2hyg	+
<u>V</u>	pTRE2hyg/DN-VASP	-
<u>E</u>	pTRE2hyg	-

Each experimental condition was repeated in triplicate. The cells were then incubated for a further 48 hours at 37°C, 5% CO<sub>2</sub>.

#### **4.2.6.2 Extraction of Luciferase**

Following 48 hours stimulation with CD3/CD28, the cells were lysed in order to extract luciferase for the assay. Cells were transferred into a microfuge tube and centrifuged at 200g for 10 minutes. The media was removed and the cells washed twice in PBS. The PBS was then removed and the cells lysed in 75µl 1x cell lysis buffer (25mM Tris-phosphate pH 7.8, 2mM DTT, 2mM 1,2-diaminocyclohexane-N,N,N',N',-tetraacetic acid, 10% glycerol, 1% Triton-X100) for 15 minutes at room temperature with occasional agitation. Following this, the lysates were vortexed for 15 seconds before being centrifuged at 12,000g for 2 minutes at 4°C. The supernatants were transferred into a fresh microfuge tube and assayed immediately for luciferase activity.

#### **4.2.6.3 Luciferase Activity Assay**

The luciferase substrate-assay buffer (from Luciferase Assay Kit) was prepared by adding the assay buffer to the vial containing the lyophilized luciferase substrate and mixing well. 100µl of buffer was then placed in a polystyrene tube. 20µl of supernatant was added to the tube which was then immediately placed into the luminometer (Lumat LB 9507 Luminometer, Berthold Technologies). The reading was taken using an integration time of 10 seconds. Results are a mean of triple determinants and were analysed using a Student's 2-tailed t test. The fold increase in pathway activity for either DN-VASP or empty vector transfectants after stimulation was calculated with respect to the non-stimulated samples.

#### **4.2.7 The Effects of DN-VASP on Calcium Flux in Jurkat TetOff Cells**

Changes in intracellular calcium can be followed using FACS analysis. We used two dyes, Fluo-4 and Fura red (both Molecular Probes) to follow these changes. Fluo-4 becomes brighter in the presence of calcium whereas Fura-red experiences quenching of fluorescence in response to a rise in calcium levels.

Jurkat TetOff cells were transfected with either pTRE2hyg/DN-VASP, pCI/DN-VASP (donated by Dr S. Lindsay) or pTRE2hyg vector alone using the Amaxa Nucleofector kit V as described previously, and allowed to recover overnight. The following day they were loaded with Fluo-4 (2.5 $\mu$ M) and Fura-red (2.5 $\mu$ M) and incubated for 60 minutes at 37°C in the dark. They were then removed from the incubator, washed in PBS, resuspended in fresh media and incubated for a further 30 minutes to allow de-esterification of the dyes. They were then washed and resuspended in 2% BSA in PBS to which anti CD3 antibody (5 $\mu$ g/ml) was added for 30 minutes to induce cell stimulation. Following this, the cells were washed twice and then resuspended in 2% BSA in PBS at a concentration of 1x10<sup>6</sup> cells/ml. Baseline FACs data was collected for dye fluorescence for 50 seconds before cross-linking was induced by the addition of 80 $\mu$ g/ml of anti mouse antibody. Further fluorescence data was immediately collected by FACs for a further 200 seconds. This was repeated for each sample.

Results were analysed by comparing alterations in the ratio of the fluorescence of the two dyes over time following cross-linking. Results were analysed using FloJo software.

#### **4.2.8 The Effects of DN-VASP Transfection on Phosphorylation of early MAP kinase signal pathways.**

Jurkat TetOff cells were transfected with either empty vector (pTRE2hyg) or DN-VASP (pTRE2hyg/DN-VASP) as described previously and were allowed to recover and express the protein overnight. The following day cells were either left untreated or stimulated with CD3 and CD28 antibodies as described previously, at a cell density of  $3 \times 10^6$  cells/ml. At time-points between 0-60 minutes, aliquots of  $1.5 \times 10^6$  cells were removed, washed with ice-cold PBS and then lysed in 100 $\mu$ l of Phosphosafe reagent (Novagen) for 15 minutes on ice. Nuclei were removed by centrifugation at 12,000g for 5 minutes. The supernatant was removed and mixed and mixed with an equal quantity of SDS-sample buffer.

In order to demonstrate phosphorylation, these samples were then assayed by immunoblotting. 30 $\mu$ l of lysate was loaded per lane of an 10-20% SDS-Page gel and separated electrophoretically. Gels were blotted onto PVDF membranes as described before and probed for various members of the MAP kinase family members as indicated (all antibodies were obtained from Cell Signalling and used at a 1:500 dilution).

#### **4.2.9 The Effects of DN-VASP Transfection on Actin Polymerisation in Jurkat TetOff Cells.**

Jurkat TetOff cells were transfected with either pTRE2hyg/DN-VASP, pTRE2hyg alone or left untransfected. Transfected cells were allowed to recover overnight. The following day, cells were centrifuged (200g for 10 minutes) and resuspended in PBS. Dynabead CD3/CD28 T cell expander beads (DynaL Biotech, Norway) were then added and the cells were incubated at 37°C for 10 minutes with occasional agitation. The beads are 4.5µm diameter magnetic, polystyrene beads coated with a mixture of mouse mAb to CD3 and CD28. Following this, the cells were washed in PBS containing 0.5% azide in order to stop any further actin polymerisation. They were resuspended in 50µl of PBS and pipetted onto poly-lysine coated slides (Sigma, UK) where they were allowed to settle and adhere for 15 minutes. They were then fixed in 4% PFA, permeabilised in 0.2% Triton X-100, blocked in 10% donkey serum (Sigma, UK) for 1 hour before staining with AlexaFluor – conjugated phalloidin 488 and goat αL polyclonal antibody (Santa Cruz laboratories, USA) against the integrins. Secondary donkey anti-goat AlexaFluor 588 conjugated secondary antibody (Molecular Probes) was then added. Cells were mounted in Vectashield and photographed using immunofluorescent microscopy and Improvision software to take z-stack images. Images were analysed using deconvolution microscopy.

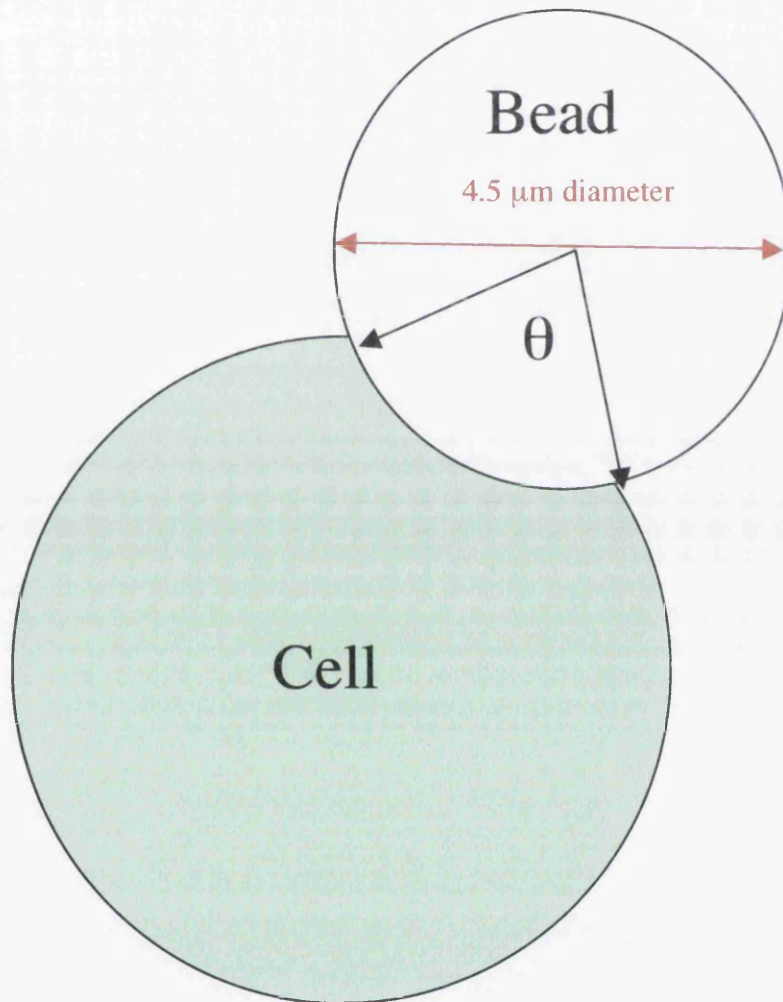
In order to measure the angle of contact between the cell and the bead, the arc transected by the cell: bead contact was measured and used to calculate the length of the contact between the cell and the bead (Figure 4.4). 20 cells for each condition (DN-VASP transfection, empty vector transfection and untransfected cells) were measured. The formula used to calculate the contact length was  $2\pi \times \theta/360$ . Differences in length

of contact were compared for significance using a Student's t-test with a result of  $<0.05$  considered significant and  $<0.01$  highly significant.

In order to assess whether actin polarisation at the site of bead: cell contact was present, 20 cells for each condition were photographed and assessed for polymerisation by an independent observer. The observer was blinded as to the transfection each cell had undergone.

Results were analysed using the Chi-squared test. A p value of  $< 0.05$  was taken as a significant value.

**Figure 4.4 Calculation of Contact Between Cell and Bead.** The length of contact between the Jurkat TetOff cell and the bead was calculated using measurements obtained as in the diagram below. Length of the arc of contact was calculated using the equation,  $\text{arc} = \theta/360 \times \pi \times \text{diameter}$ . 20 cells for each condition were measured.



#### **4.2.10 The effects of DN-VASP transfection on primary T cell binding**

The following reagents were used: Ficoll-Paque Plus (Amersham Biosciences); Pan T Cell Isolation Kit (Human) and autoMACS Separator (Miltenyi Biotec, Germany); MACS buffer (2% FBS in PBS, filter sterilised) and preservative-free heparin 1000 units/ml (Leo Pharmaceuticals);

##### **4.2.10.1 Isolation of Human T Cells**

60mls of blood was collected into heparinised tubes and diluted in a 50:50 ratio with HBSS. 20ml of Ficoll-Paque Plus was added to a 50ml centrifuge tube and 30ml of diluted blood carefully layered on top, avoiding mixing of the blood and Ficoll-Paque. The sample was then centrifuged at 400g for 30 minutes at 18°C. Following centrifugation, the upper layer (plasma) was removed without disturbing the layer below. This lower layer (containing platelets and lymphocytes) was then washed to remove platelets. Briefly, the lymphocyte/platelet layer was transferred to a clean centrifuge tube and had 3 volumes of HBSS added. The cells were resuspended by gentle pipetting and then centrifuged at 100g, 18°C for 10 minutes. The supernatant was removed and the cell pellet resuspended in HBSS. It was then re-centrifuged at 100g for 10 minutes and the supernatant removed once more. The pellet was resuspended in 500µl of HBSS and the cell count determined.

Following cell number determination, the cell suspension was centrifuged at 300 for 10 minutes. The supernatant was removed and the cell pellet resuspended in 40µl of MACS buffer/  $10^7$  cells. 10µl of Biotin-Antibody cocktail was added/ $10^7$  cells, the sample was mixed and incubated for 10 minutes at 4°C. 30µl of MACS buffer and 20µl of Anti-biotin MicroBeads/ $10^7$  cells were then added, mixed and incubated for a further

15 minutes at 4°C. 10x volume of buffer was then added and the sample centrifuged at 300g for 10 minutes. The supernatant was removed and the cells resuspended at a maximum concentration of  $10^8$  cells/ 500 $\mu$ l of MACS buffer.

In order to separate the cells, magnetic separation using an autoMACS separator was carried out. This involved passing the cells through a magnetic column to remove all cells labelled with magnetic beads. The non-labelled cells (negative fraction) were then collected as these were the T cell fraction.

Following collection, cell number was once again determined.

#### **4.2.10.2 Transfection of Primary T cells**

Cells were transfected using the Amaxa Nucleofector . To transfect primary human cells, the Human T Cell Nucleofector Kit (Amaxa) was used with programme U-14.  $3 \times 10^6$  cells and 2 $\mu$ g of DNA (either pTRE2hyg/DN-VASP or pTRE2hyg alone) were used per transfection. An equivalent number of cells was left un-transfected in order to act as a control sample.

Following transfection, cells were immediately transferred into pre-warmed media in 6 well plates. Jurkat TetOff media has been described previously. Human primary T cells were cultured in RPMI media, supplemented with 10% heat-treated FBS, 2mM glutamine and Penicillin-streptomycin. Cells were allowed to recover overnight.

#### **4.2.10.3 Binding assay**

Binding to LFA-1 on the surface of primary T cells was assayed by the use of fluorescent beads coated with ICAM-1 (Molecular Probes) (method adapted from Geijtenbeek et al., 1999). Following transfection with DN-VASP or empty vector and overnight recovery, the cells were activated by treatment with CD3 and CD28 antibodies (both at 10 µg/ml) for 30 minutes at 37°C and exposed to ICAM-1 coated beads (20 beads/cell) to allow binding. To confirm specificity of binding, an aliquot of cells was pre-incubated for 10 minutes with a blocking antibody to LFA-1 (BD Pharmingen) at a concentration of 20µg/ml prior to activation and exposure to the coated beads.

As a negative control and to confirm that transfection alone was not sufficient to stimulate ICAM-1:LFA-1 binding, an aliquot of cells was exposed to the beads without CD3/CD28 antibody exposure. As a positive control, a further aliquot of cells was fully activated using PMA at a concentration of 100nmol/L for 30 minutes.

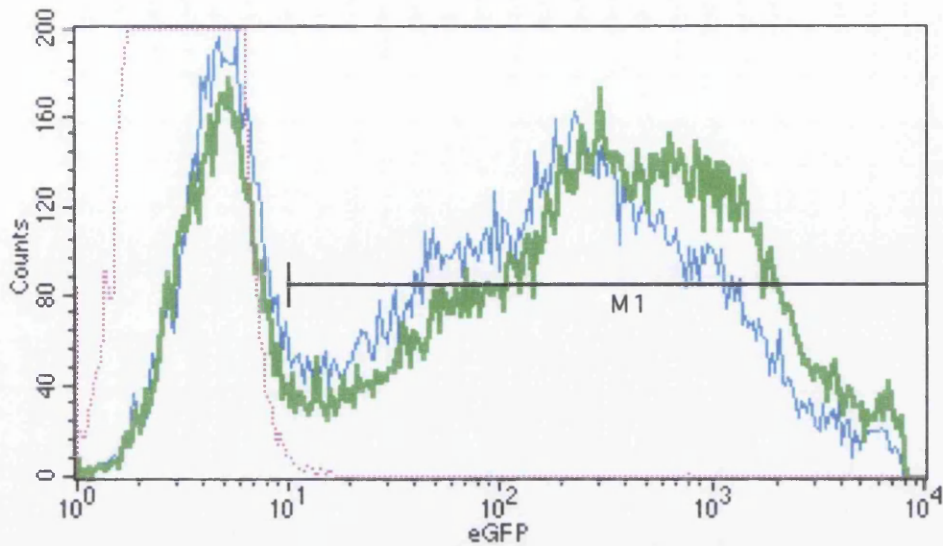
Binding of the fluorescent beads to the cells was then assayed using flow cytometry.

## 4.3 Results

### 4.3.1 Optimisation of Transfection

Two programmes (G-16 and C-10) were compared to a control sample in which the cells were electroporated using programme G-16 but without pmaxGFP. In the control sample, negligible levels of cells were detected within the set gate (0.3%). This gate was therefore used to analyse the results obtained with the two cell aliquots transfected using programmes G-10 and C-16 (Figure 4.5).

Both programmes showed approximately the same percentage cells lying within the set gates (73.57% with programme G-10 vs 78.96% with programme C-16). The percentage of eGFP positive cells within this was also similar (76.99 vs 73.69) between the two programmes. When the mean geometric fluorescence of cells transfected by these two programmes was compared, cells transfected using programme G-10 showed higher levels of fluorescence than with C-16 ((307.88 vs 201.85) (Table 4.6). This suggests better gene expression in cells transfected using this programme. This may be due to the different conditions leaving the cells in a healthier condition than those transfected with programme C-16. Programme G-10 was therefore selected for use in further transfections of Jurkat TetOff cells.



**Key**

- Pink** Control – no GFP
- Green** 2µg pmaxGFP, programme G-10
- Blue** 2µg pmaxGFP, programme C-16

**Figure 4.5 Electroporation of Jurkat TetOff Cells with pMaxGFP using the Amaxa Nucleofector – a comparison of Programmes G-10 and C-16. The gate (M1) is set to non-transfected cells.**

	<b>Control (no eGFP)</b>	<b>Programme G-10</b>	<b>Programme C-16</b>
<b>Events counted</b>	20025	20040	20037
<b>Percentage gated (live cells)</b>	0.3	73.57	78.96
<b>Percentage of gated cells positive</b>	0	76.99	73.69
<b>Percentage of total cells positive</b>	0	56.64	58.19
<b>Geometric mean fluorescence</b>	0	307.88	201.85

**Table 4.6 Transfection efficiency of Jurkat TetOff cells.** FACS results comparing nucleofection of Jurkat TetOff cells using programmes G-10 and C-16 on an Amaxa Nucleofector. (Live cells = PI negative)

### 4.3.2 Time Course of DN-VASP Expression

We used immunoblotting techniques to investigate the time course of DN-VASP expression following nucleofection with pTRE2hyg. Full length VASP has an apparent molecular weight on SDS-Page electrophoresis of 46-50kDa. DN-VASP is much smaller and therefore can be detected separately to the full-length protein. The monoclonal antibody used to detect DN-VASP will also detect full length, native VASP in Jurkat cells as they are both of human origin and the antibody has been raised against a sequence contained within the EVH2 domain.

A band representing full length VASP was seen at just above the 50kDa marker on the gel (figure 4.6) and was at the same intensity at each time point. Only one band is visible in most of these lanes at this weight, we have not been able to detect the 46 and 50 kDa forms of VASP in this experiment. This may be because the band is of sufficiently high intensity that it becomes impossible to distinguish between the two bands or because this cell line may not express both forms of VASP in its resting state. Transfection of DN-VASP has not altered the density of the band at 50kDa.

In several of the lanes, it is possible to see other, fainter bands just below the strong band representing VASP. This may be due to breakdown products of the protein or a cross-reaction with other proteins.

A second major band was detected at approximately 22kDa on the gel. This was not seen at time point 0 but was visible by 2 hours after transfection and continued to increase in intensity up to 24 hours post transfection. Whilst DN-VASP has an actual molecular weight of approximately 11kDa, this band represents the dominant-negative

protein. Full length VASP is also known to migrate at a higher molecular weight (50kDa) than its actual molecular weight (38kDa). Also, low molecular weight proteins are known to migrate in an aberrant fashion and are usually detected at a higher point than expected. This blot clearly demonstrates increasing levels of DN-VASP accumulating in the cells with time. High levels are present by 24 hours, making this a suitable time post-transfection to carry out experiments into the effects of DN-VASP on cell activation.

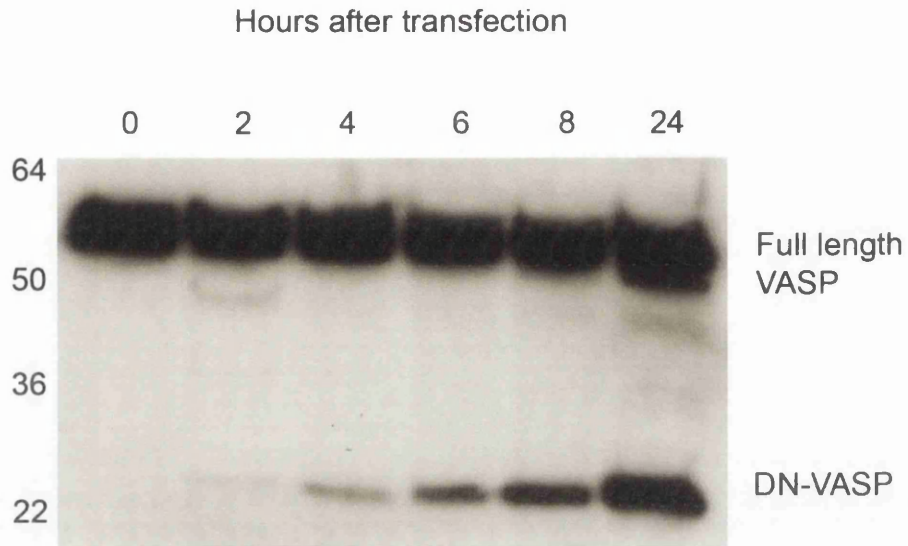


**Figure 4.6 Expression of DN-VASP following transfection in Jurkat TetOff cells.** The upper band represents full length native VASP, present at the same level in each lane. The lower band shows increasing levels of DN-VASP expression with time.

### **4.3.3 The effects of DN-VASP transfection on IL-2 and IFN- $\gamma$ production by Jurkat TetOff cells.**

Under basal conditions, Jurkat TetOff cells transfected with either pTRE2hyg/DN-VASP or empty vector alone produced minimal levels of IL-2 and IFN- $\gamma$  (Figures 4.7a and b) suggesting that transfection alone was not sufficient to cause activation of Jurkat cells. Following stimulation with plate-bound CD3 antibody alone, IL-2 levels were raised by 48 hours following stimulation. Levels were significantly different between DN-VASP and empty vector transfectants but the overall increases in IL-2 levels were so low as to make it difficult to assess this result.

When dual stimulation with plate-bound CD3 and soluble CD28 antibodies was carried out, a much greater increase in IL-2 expression was detected (figure 4.7a). In cells transfected with empty vector alone, levels of IL-2 detected rose to over 200 pg/ml. Cells transfected with DN-VASP also showed an increase in IL-2 output but the levels of IL-2 were significantly lower ( $p < 0.05$ ) than in the empty vector transfectants. The quantity of IL-2 produced by DN-VASP transfectants was approximately half that of empty vector transfectants. In earlier experiments to determine the level of transfection in these cells (section 4.3.1) we showed that only about 75% of cells are transfected using this protocol. Therefore, 25% of the surviving cells would not be expected to express DN-VASP and would not be subject to any inhibition of activation induced by the dominant negative protein. This suggests that the difference in output between DN-VASP transfected cells and cells not expressing this protein may be even greater. DN-VASP does appear to have a role in inhibiting T cell activation when assessed by IL-2 levels.

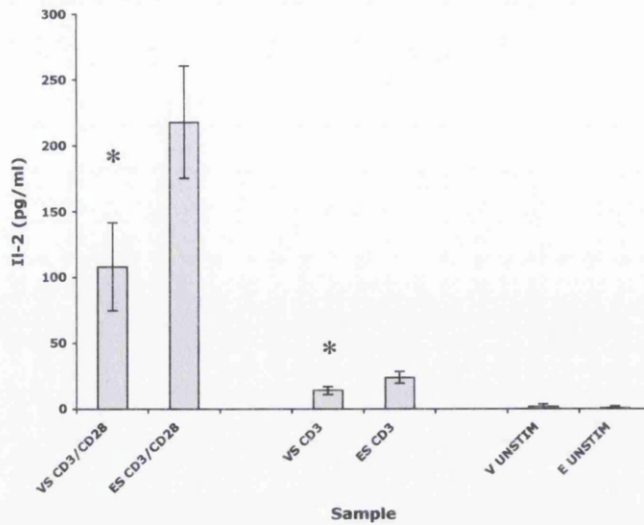


**Figure 4.7a** The effects of DN-VASP transfection on IL-2 production by Jurkat TetOff cells.

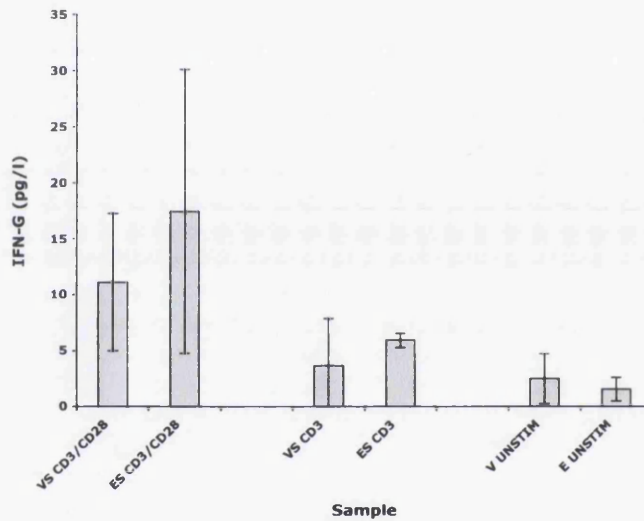


**Figure 4.7b** The effects of DN-VASP transfection on IFN- $\gamma$  production by Jurkat TetOff cells

**Figure 4.7 The effects of DN-VASP transfection on Interleukin-2 and Interferon- $\gamma$  production by Jurkat TetOff cells.** The data shows the effects of DN-VASP transfection (V) vs empty vector transfection (E) following either stimulation (S) with plate bound CD3 and soluble CD28 antibodies (CD3/CD28), plate bound CD3 alone (CD3) or no stimulation on IL-2 and IFN- $\gamma$  output. Shown are the means and standard deviations for the sample groups. (\*  $P < 0.05$  vs empty vector transfection).

Very low levels of IFN- $\gamma$  were detected in unstimulated cells transfected with either pTRE2hyg/DN-VASP or empty vector. Following CD3 stimulation alone, very little difference was seen in the levels of IFN- $\gamma$  detected in either set of cells (figure 4.8b). With combined CD3/CD28 stimulation levels of IFN- $\gamma$  did rise but again only by very little. No significant differences were seen between IFN- $\gamma$  levels under any conditions of stimulation. In this situation, IFN- $\gamma$  does not appear to be a useful marker to assess activation of Jurkat cells and the effect of DN-VASP.

The effects of doxycycline on stimulation of T cells were also assayed as the plasmid used contains a tetracycline-regulated element. In the presence of doxycycline, transcription should be switched off (TetOff system). Comparing DN-VASP transfected, CD3/CD28-stimulated cells grown in the presence and absence of doxycycline, no significant difference in IL-2 production was seen ( $p=0.35$ ) (Figure 4.8). Both sets of cells increased IL-2 production in response to antibody stimulation. Comparing CD3/CD28 stimulated cells, transfected with either DN-VASP or with empty vector and grown in the presence of doxycycline, a non-significant drop ( $p=0.08$ ) in IL-2 production was seen in the DN-VASP transfected cells. We have seen in epithelial cells transfected with DN-VASP that some leakiness of the system occurs in the presence of doxycycline (Section 3.3.2). In the T cell system used here, it may be that there was sufficient leak in the system such that overall, doxycycline did not suppress DN-VASP expression to allow a difference in results to be seen. However, the fact that there was a difference, though non-significant, between DN-VASP and empty vector transfected cell suggests that there is possibly a concentration-dependent effect of DN-VASP expression in IL-2 production. An additional complicating factor was that doxycycline alone in empty vector transfected cells seemed to influence IL-2 production

(Figure 4.8). Because of these effects of doxycycline, we did not attempt to use it further to control levels of DN-VASP expression. We used transfection with empty vector as a control for transfection with DN-VASP in the absence of doxycycline to allow maximal DN-VASP expression.

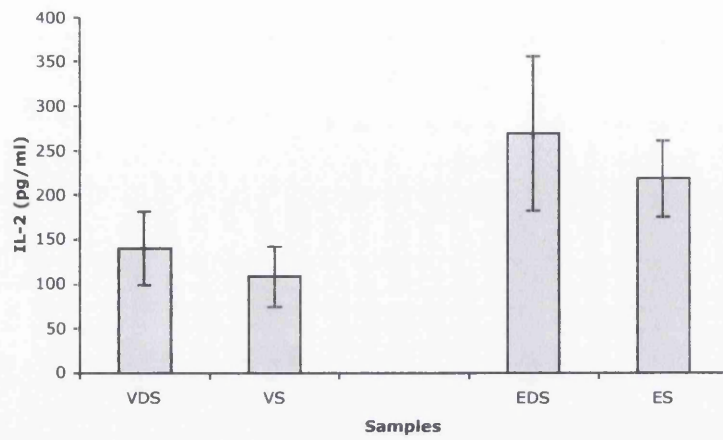


**Figure 4.8 The effects of doxycycline on IL-2 production by Jurkat TetOff cells following CD3/CD28 stimulation.** This graph shows the effects of CD3/CD28 stimulation (S) on DN-VASP transfectants (V) and empty vector transfectants (E) in the presence or absence of doxycycline (D) (2 $\mu$ g/ml).

#### **4.3.4 The Effects of DN-VASP Transfection on CD69 and CD25 Expression by Jurkat TetOff Cells.**

CD69 is a more rapidly appearing marker of T cell activation and expression was therefore examined at an earlier time-point stimulation than for CD25. On FACS analysis of unstimulated cells, low levels of CD69 expression (less than 10% of cells) were seen, probably reflecting the low grade activation of Jurkat TetOff cells, a feature they have as a cell-line developed from a leukaemia.

Following stimulation with combined CD3 and CD28 antibodies, the level of cells expressing CD69 rose to approximately 80%. This was seen both in cell that had been transfected with the pTRE2hyg/DN-VASP construct and the empty vector alone (Figure 4.9). No CD25 expression was detectable in unstimulated cells transfected with either DN-VASP or empty vector. 48 hours after stimulation with CD3 and CD28 antibodies, some CD25 expression was detectable but only at very low levels in both cell groups (figure 4.10).

The graphs shown in figure 4.10 are from a separate set of data but show a similar result. In these graphs, the gate was set on the IgG isotype control. In this set of data, some rise in CD25 expression was seen following CD3/CD28 stimulation but there was little difference between empty vector transfectants (12.6%) and DN-VASP transfectants (10.7%) in expression levels (figure 4.10.a.ii). When CD69 levels were examined in this set of data, following CD3/CD28 stimulation, levels rose to a similar degree in both groups (88.6% in empty vector transfectants vs 89.6% in DN-VASP transfectants).

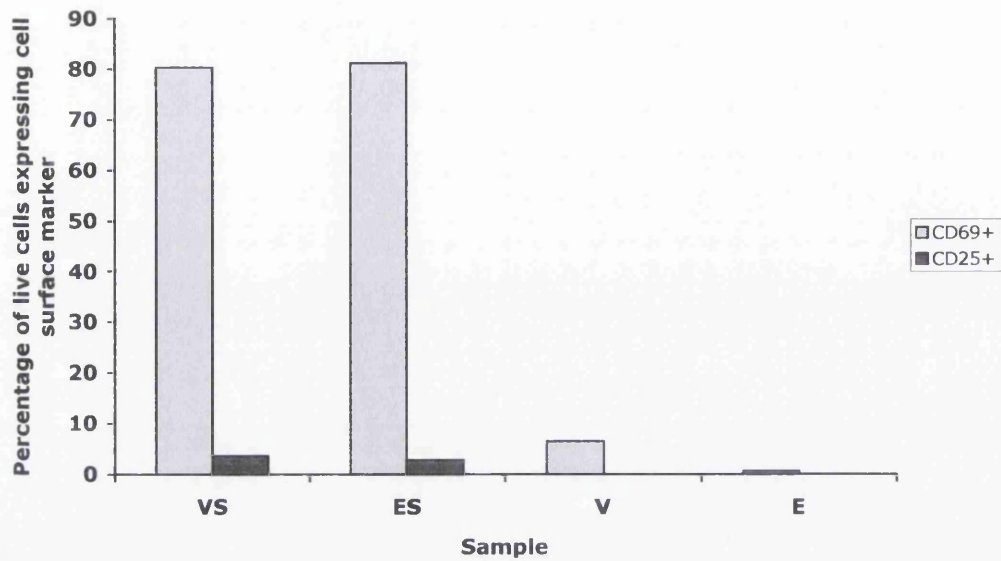
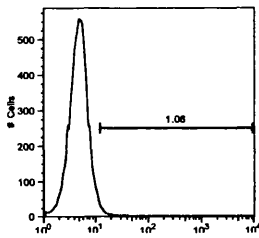


**Figure 4.9 The effects of DN-VASP transfection (V) vs empty vector transfection (E) on CD69 and CD25 expression.** Expression was analysed at 24hrs for CD69 expression and 48 hours for CD25 expression following CD3/CD28 antibody stimulation (S) of Jurkat TetOff cells.

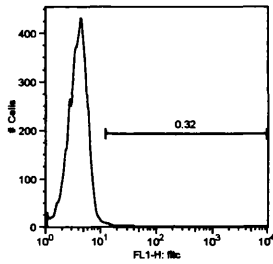
**Figure 4.10 Flow Cytometry data: Effects of DN-VASP Transfection on CD69 and CD25 Expression**



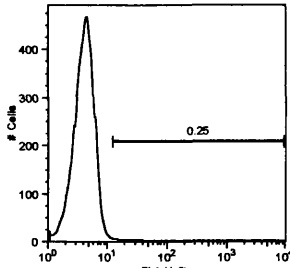
**Isotype Control.** The gate for analysis of results was set on this control sample

**a. CD25 Expression**

**(i) Unstimulated cells**

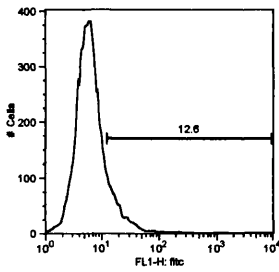


Empty vector

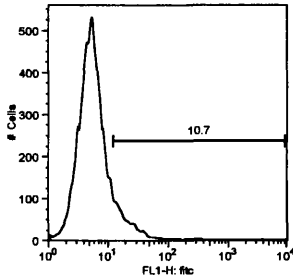


DN-VASP

**(ii) CD3/CD28 Stimulated cells**



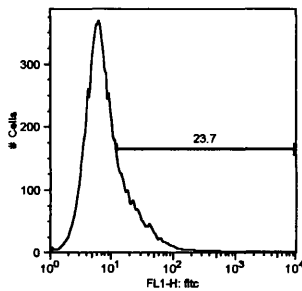
Empty vector



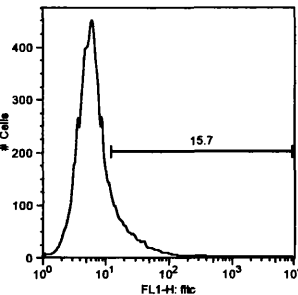
DN-VASP

**b. CD69 Expression**

**(i) Unstimulated cells**

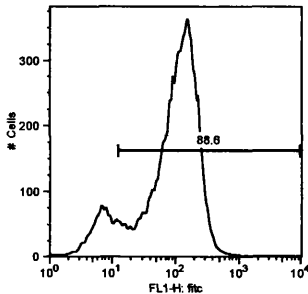


Empty vector

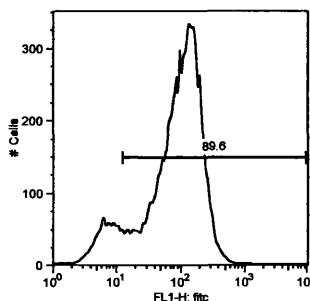


DN-VASP

**(ii) CD3/CD28 Stimulated cells**



Empty vector



DN-VASP

#### **4.3.5 The Effects of DN-VASP Transfection on Signal Transduction Pathways in Jurkat TetOff Cells.**

To determine which of the signal pathways triggered by the TCR are affected by DN-VASP, we utilised a reporter gene system specific for individual transcription factors. As cotransfection with the reporter genes are necessary for detection, only cells that have undergone transfection affect the result. This means that only cell transfected with DN-VASP are assayed and therefore any effects of DN-VASP on these pathways are easier to see. We have already demonstrated in section 4.3.3 that DN-VASP transfection significantly decreases IL-2 production following stimulation. This set of experiments was looking for what specific signals may be involved in this process.

Figure 4.11 shows the effects of DN-VASP transfection on the NF- $\kappa$ B and CREB pathways. CD3/CD28 stimulation of empty vector transfected cells leads to a dramatic increase in the activation of the pathway with relative luciferase unit (RLU) readings increasing from approximately 40,000 to 210,000 (5.25x increase). The magnitude of the NF- $\kappa$ B signal is reduced following DN-VASP transfection in both stimulated and un-stimulated cells but still shows a rise from 12,000 RLU to 90,000 RLU (7.5x increase). This is comparable to that seen in empty vector (EV) transfectants and suggests that DN-VASP does not alter the ability of this pathway to respond to antibody stimulation. NF- $\kappa$ B is activated via alterations in protein kinase C levels in T cells.

CREB activation occurs via phosphorylation following activation of a PKC/Ras/Raf-1/MEK and RSK2 signalling pathway upon TCR stimulation (Muthusamy and Leiden, 1998). Figure 4.11 shows that, prior to antibody stimulation, practically no CREB pathway activation was seen in either empty vector or DN-VASP transfected cells.

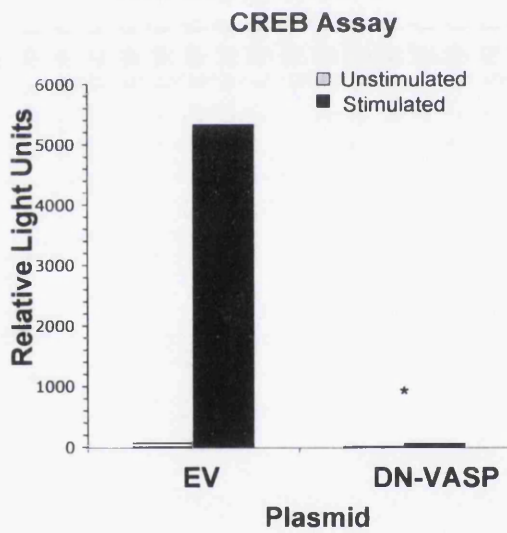
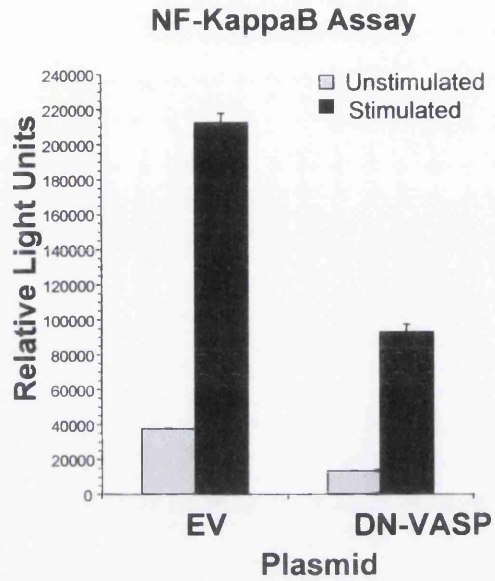


**Figure 4.11 The effects of DN-VASP transfection on the activation of NF-kB and CREB pathways**

Following CD3/CD28 stimulation, in empty vector transfectant cells showed pathway activation with a rise in RLU readings to >5,000. In contrast, DN-VASP transfected cells showed a significantly different result with basically no rise in activation observed. This pathway appears to have been completely blocked by DN-VASP.

The effects on NFAT and AP-1 pathways are shown in figure 4.12. In T cells, NFAT is activated by alterations in calcium flux. In this experiment, NFAT activation appears to be reduced by DN-VASP transfection following CD3/CD28 antibody stimulation whereas AP-1 activation is completely obliterated. Interestingly even the basal level of AP-1 activity seen in un-stimulated, empty vector transfected cells is not seen in DN-VASP transfected cells. The AP-1 complex is composed of the c-Jun and Fos components and is activated via MAP kinases. NFAT forms a complex with AP-1 to allow IL-2 transcription and T cell proliferation.

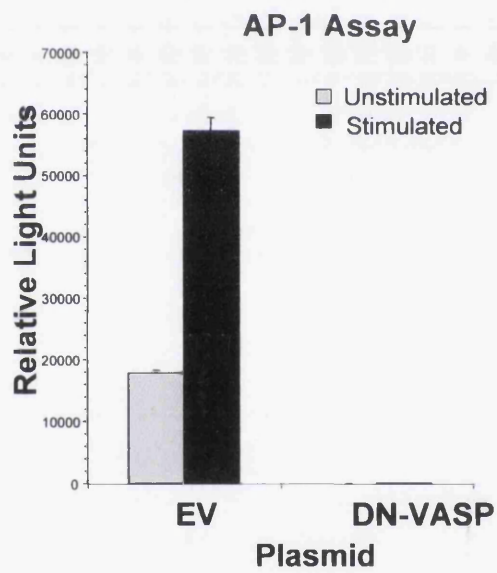
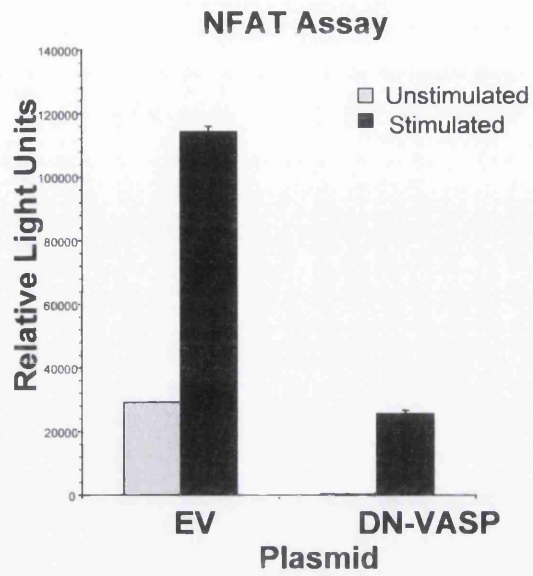


**Figure 4.12** The effects of DN-VASP on NFAT and AP-1 signal transduction pathway activation

#### **4.3.6 The Effects of DN-VASP Transfection on Calcium Flux in Jurkat Cells**

The effects of DN-VASP on calcium flux in Jurkat cells was assessed through the use of two dyes, Fluo-4 and Fura Red. The fluorescence intensity of Fluo-4 is increased in the presence of calcium whilst Fura-red is quenched (Burchiel et al., 2000). Analysis of changes in fluorescent intensity of the two dyes after cross-linking of CD3 with anti-mouse antibody were assessed using flow cytometry. We used 2 different expression vectors containing DN-VASP to ensure the results we obtained were not just a function of the tetracycline-regulated system.

Three groups of cells were used. The control cells were transfected with pTRE2hyg empty vector. Two other groups of cells were transfected with either pTRE2hyg/DN-VASP or pCI/DN-VASP. Baseline fluorescent intensity, prior to CD3 cross-linking was the same for each sample (Figure 4.13). Following cross-linking, the ratio of fluorescence intensity rose in all 3 groups, reaching a peak at about 50 seconds after addition of the antibody, and returning to near baseline values by 200 seconds. DN-VASP transfection in either vector, failed to have any effect on calcium flux. The change in the ratio of signal intensity was the same as seen in cells transfected with empty vector.

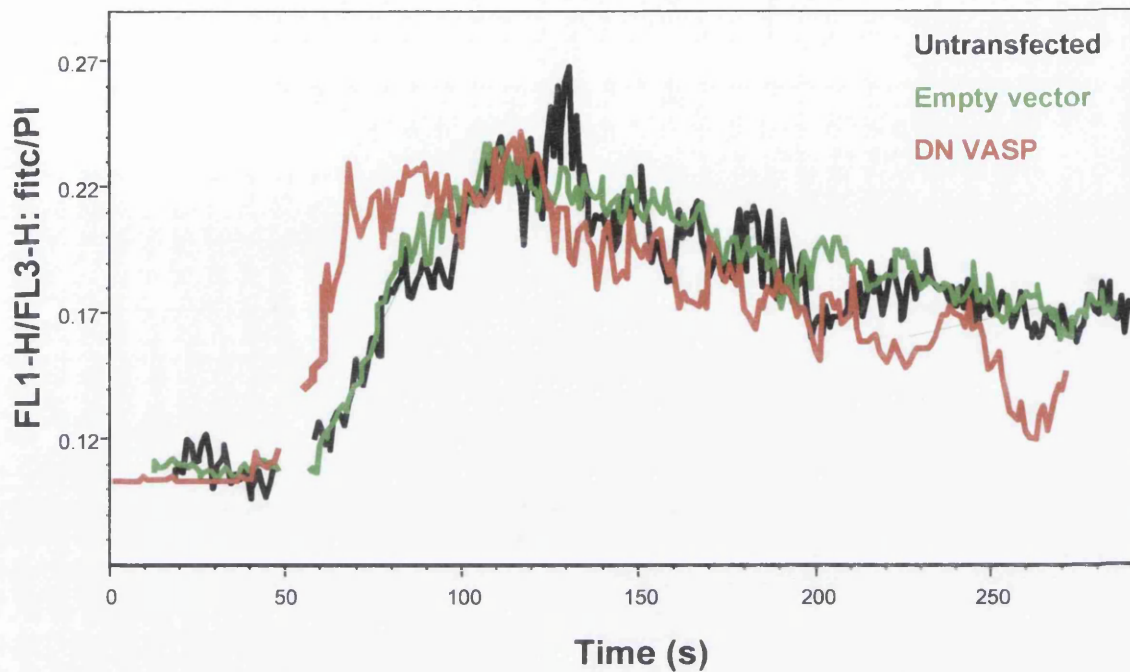


**Figure 4.13 The Effects of DN-VASP transfection on calcium flux in Jurkat TetOff Cells.** Two DN-VASP containing vectors were used pTRE2hyg/ DN-VASP and pCI-DN-VASP. Baseline data was collected for 50 seconds before CD3 was cross-linked by the addition of 80 $\mu$ g/ml anti-mouse antibody. Data was then collected for a further 200 seconds.

### **4.3.7 The effects of DN-VASP on early signal transduction pathways**

We looked at early signal transduction pathway activation and the effects of DN-VASP transfection (Figure 4.14). The images on the left are of empty vector transfected cells and those on the right of DN-VASP transfected cells. The lowest panel on the right demonstrates that equal levels of DN-VASP expression were seen at all timepoints under investigation. Phosphorylation of ERK and JNK occurs very rapidly after T cell receptor binding. Figure 4.14 shows a Western blot of p-ERK1/2, ERK 1/2 and p-JNK. No phosphorylation of either JNK or ERK is seen before antibody stimulation but is detectable by 5 minutes after antibody stimulation. By 30 minutes after stimulation, this has almost returned to baseline levels and no phosphorylation of either kinase is detectable by 60 minutes after stimulation. DN-VASP expression has no measurable effect on the level of phosphorylation. The same pattern of rapid phosphorylation followed by return to undetectable levels by 60 minutes is seen in both cell groups.

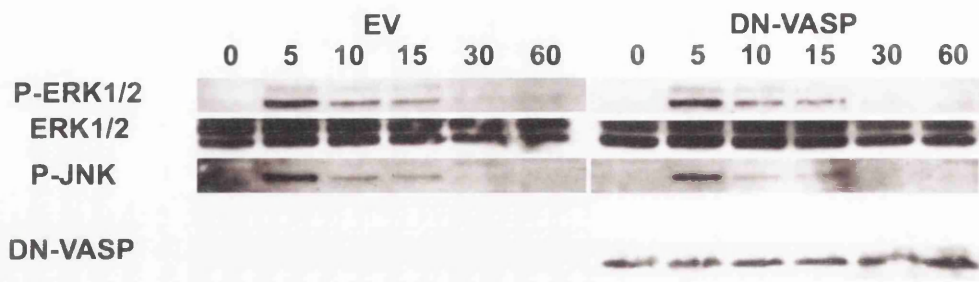


**Figure 4.14** The effects of DN-VASP transfection on early MAPK phosphorylation. EV = empty vector transfection.

#### **4.3.8 DN-VASP Transfection reduces actin collar formation and actin polarisation in Jurkat TetOff Cells**

Next, we examined the effects of DN-VASP expression on actin re-organization following T cell receptor crosslinking. We have previously shown that transfection in this system leads to approximately 75% transfection rates in surviving cells (section 4.3.1). We were unable to demonstrate by staining which cells contained the transfected vector and which did not. Therefore, in order to look for a difference, we examined 20 cells from each group, chosen randomly and assessed by an independent examiner, blinded to the sample group.

In non-transfected cells, a collar of actin was seen to form at the cell: bead contact. Leading away from this actin collar, fingers of F-actin were seen, protruding back into the cell, demonstrating polarisation of the actin cytoskeleton (Figure 4.15c). The actin cytoskeleton appeared to be directed towards the cell: bead junction, providing a support network to maintain the junction. This phenomenon was also seen in cells that had been transfected with pTRE2hyg empty vector (Figure 4.15b).

In cells transfected with pTRE2hyg/DN-VASP, reduced formation of actin collars and F-actin polarisation was seen (Figure 4.15a). Statistical analysis using the  $\chi^2$  test demonstrated significantly fewer cells with actin polarisation than in either non-transfected or empty vector transfected cells ( $p < 0.05$ ). This is likely to be even more significant if the fact that approximately 1/4 of the cells included in this group are likely not to be DN-VASP transfected as transfection efficiency has previously been demonstrated to be 75%.

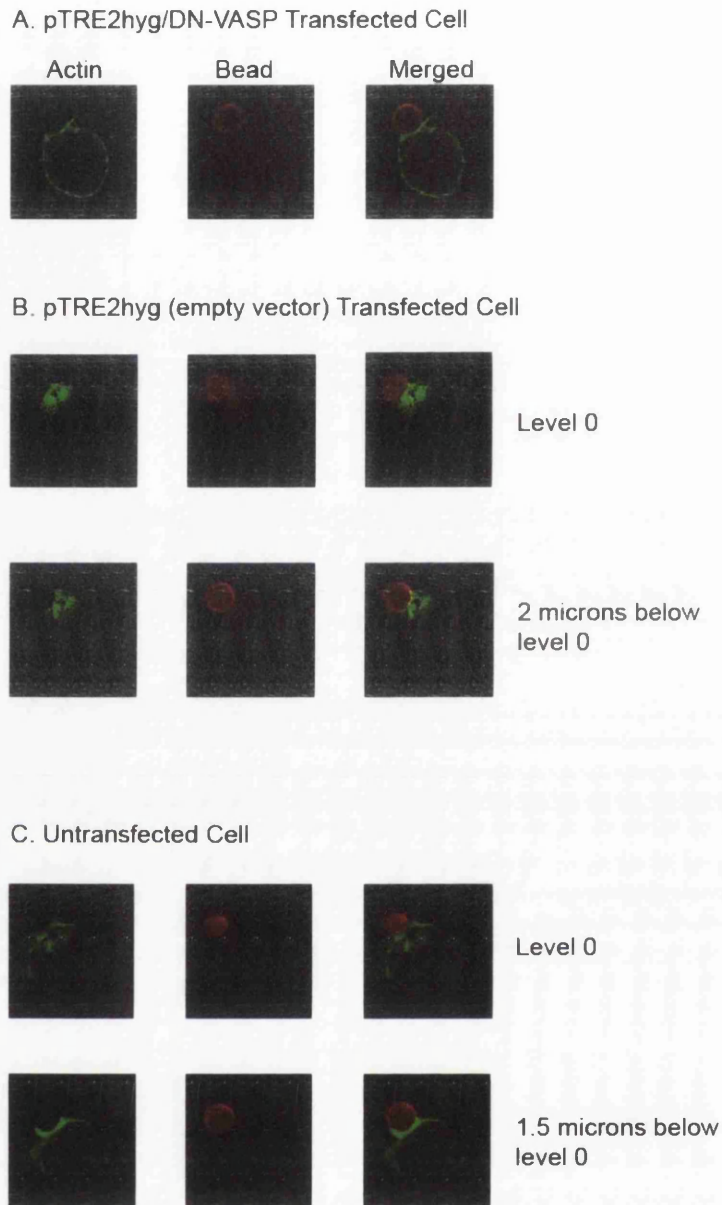


**Figure 4.15 The effects of DN-VASP transfection on actin cuff formation and cytoskeletal polarisation in Jurkat TetOff Cells.** Deconvolved immunofluorescent images of individual Jurkat cells interacting with a single CD3/CD28 antibody coated bead. Cells were stained with FITC-labelled phalloidin (green) to demonstrate F-actin polarisation. The beads are stained non-specifically (red). The images from a cell transfected with pTRE2hyg vector and an untransfected cell show two sets of images, one at an arbitrary level zero and one just below this.

### **4.3.9 DN-VASP Transfection Reduces the Contact Between CD3/CD28 antibody coated Beads and Jurkat TetOff Cells**

Following activation, T cells reorganise their actin cytoskeleton, polarising it towards the APC to allow contact to be maintained. We looked at whether transfection with DN-VASP, known to be an important regulator of actin polymerisation, would alter the ability of the cells to modify their cytoskeletons. We did this using CD3/CD28 antibody coated beads and measured the arc of contact between them.

In order to assess the contact length, 20 cells were photographed from each group and the angle between the two ends of cell: bead contact measured and used to calculate the length of the arc as described previously. We knew that the beads were 4.5 $\mu$ m in diameter and could therefore calculate the arc of the bead circumference in contact with the cell (see figure 4.4).

No difference in contact length was seen between cells from the non-transfected group, compared to those transfected with empty vector, suggesting that transfection itself does not have an effect. However, when the cells from the group transfected with the pTRE2hyd/DN-VASP construct were assessed, the arc of contact was seen to be significantly lower ( $p < 0.01$ ) than in those either untransfected or transfected with empty vector (figure 4.16). In view of the fact that approximately only 75% of the cells were likely to be transfected (section 4.2.2), if we had been able to distinguish and eliminate untransfected cells, it is likely the difference would have been greater.

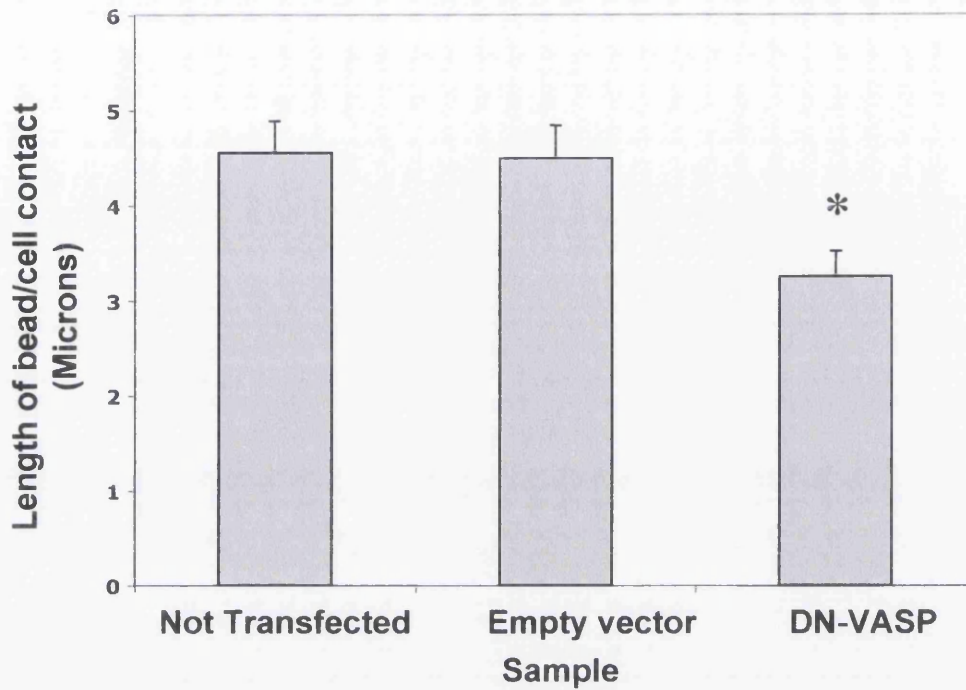


**Figure 4.16** The effects of DN-VASP transfection on the length of anti-CD3/CD28 coated bead: cell contact. The length of contact was compared from empty vector to non-transfected cells and from DN-VASP to empty vector transfected cells (\* $P < 0.01$ )

#### **4.3.10 The effects of DN-VASP on Primary T cell adhesion**

ICAM-1 is the ligand for the T cell integrin LFA-1. ICAM-1 coated beads were used to assess the ability of primary T cells to adhere following stimulation with CD3 and CD28 antibodies. Jurkat cells were not suitable for this study as they did not appear to express functional LFA-1. Use of the Amaxa Nucleofector to transfect primary T cells resulted in 60% survival and 60% transfection.

Binding was assayed using FACS analysis. Several peaks were seen in each assay; this represents the binding of one or more beads to a cell. Prior to antibody stimulation, only very low level binding was seen by T cells transfected with empty vector alone (figure 4.17). This increased after CD3/CD28 stimulation to nearly the same levels seen with full activation by PMA. This increase in binding was blocked by the LFA-1 antibody demonstrating that it was an integrin-dependent process.

In the presence of DN-VASP transfection (Figure 4.18) exactly the same response was seen. There was only a very low level of binding prior to stimulation. Addition of PMA or CD3/CD28 antibodies caused an increase in binding and this was blocked by LFA-1 antibody. DN-VASP transfection does not appear to alter the ability of LFA-1 to bind to its ligand ICAM-1

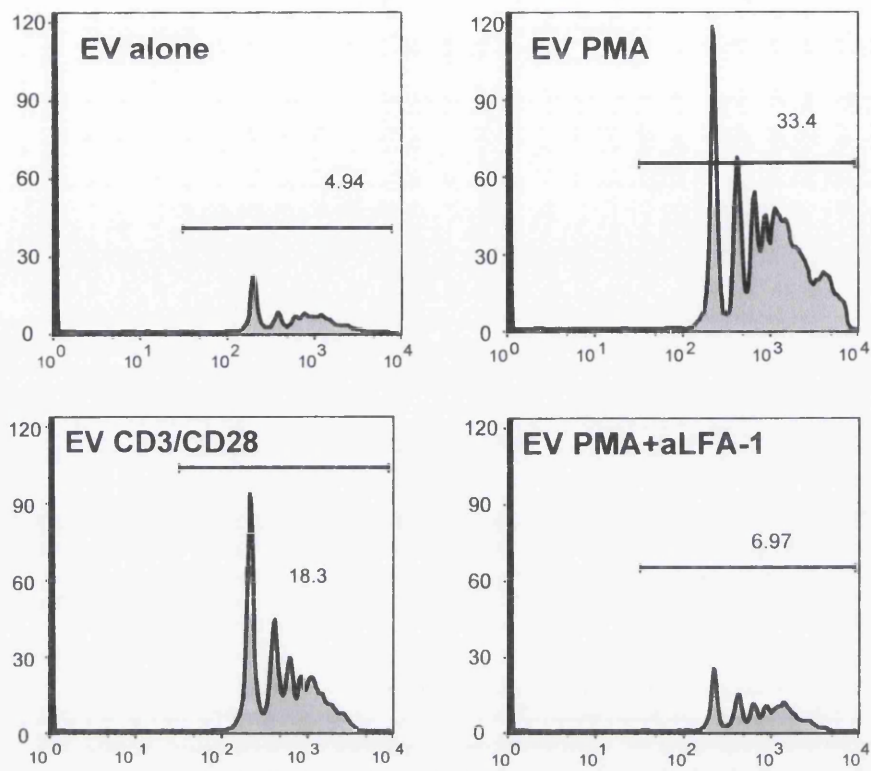


**Figure 4. 17 ICAM-1 coated bead binding by primary T cells .** The effects of empty vector alone (EV), stimulation with CD3 and CD28 antibodies, full activation with PMA and blocking with an LFA-1 antibody are demonstrated

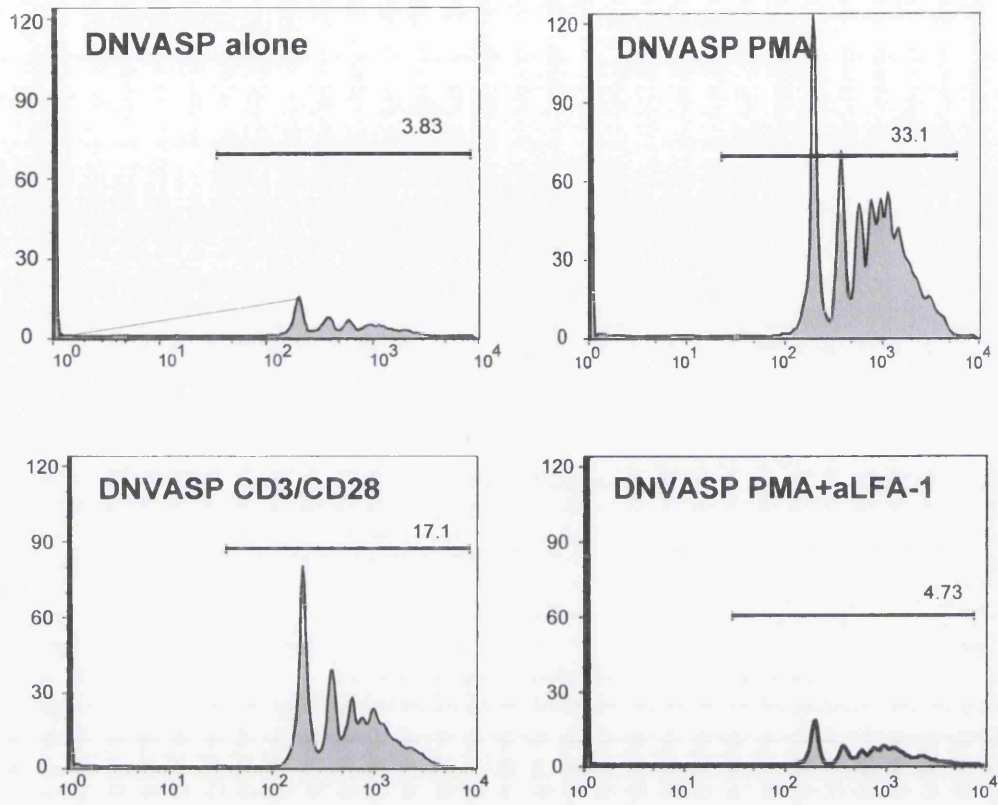


**Figure 4.18** The effects of DN-VASP on the ability of primary T cells to bind to ICAM-1 coated beads

#### **4.4 Discussion**

The ability of T cells to alter their cytoskeleton following TCR stimulation is vital to their full activation. If the actin cytoskeleton is disrupted by the use of the fungal metabolite Cytochalasin D IL-2 production and T cell proliferation is inhibited (Valitutti et al., 1995). The importance of a dynamic actin cytoskeleton for T cell activation has also been demonstrated by the use of genetically modified mice (Holsinger et al., 1998; Snapper et al., 1998) which have allowed study of the links between signalling cascades and the induction of cytoskeletal remodelling. For example, Vav is a gene that normally encodes a guanine-nucleotide-exchange factor (GEF) for the GTPase Rac, part of the Rho GTPase family and important in actin cytoskeleton regulation (Hall, 1998). Vav *-/-* T cells are deficient in IL-2 production and proliferation in response to TCR stimulation (Holsinger et al., 1998).

Most work has concentrated on cytoskeletal reorganisation and its effects on integrin clustering and avidity (Lub et al., 1997; Peterson, 2003; van der Merwe, 2002; van Kooyk et al., 1999). In resting T cells, antigen receptors appear to be distributed evenly throughout the cell surface. Activation of the T cell leads to the formation of supramolecular activation clusters (SMACs) with clustering of LFA-1 integrins in the peripheral zone (pSMAC) to enforce T cell: APC adhesion (Peter and O'Toole, 1995). F-actin has been shown to be able to both enhance and inhibit LFA-1-mediated ICAM-1 adhesion depending on the activation state of the T cells. In resting T cells, response to intracellular signals to bind the APC ligand ICAM-1 are poor unless the actin cytoskeleton is disrupted, allowing integrins to cluster. In activated T cells already demonstrating strong ligand binding, this is inhibited when the cytoskeleton is disrupted, allowing integrins to disperse (Lub et al., 1997). We were unable to

demonstrate any effect of DN-VASP on binding (using ICAM-1 coated beads) suggesting that however VASP functions in T cell activation, it is not via LFA1 clustering and avidity.

One of the pathways by which TCR triggering may be linked to cytoskeletal remodelling is via the recruitment and tyrosine phosphorylation of the adaptor protein ADAP (Fyb/SLAP). ADAP is found located in a complex at the activated TCR along with Evl (a member of the Ena/VASP family), WASP, SLP-76 and the Arp 2/3 complex. The use of ActA repeats to disrupt potential ADAP: EVH1 binding leads to impaired T cell binding to CD3 coated cells (Krause et al., 2000). Our experiments demonstrated that interrupting VASP function through use of DN-VASP had a similar effect. T cells were able to contact CD3/CD28 – coated beads but did not form the typical actin collar or demonstrate F-actin polarisation directed at the interface (section 4.3.8). Whilst ADAP contains an EVH1 binding domain, making it capable of binding to VASP, this may not be the mechanism involved in cytoskeletal reorganisation. In fact, ADAP deficient cells are still capable of forming actin caps and fibres (Griffiths and Penninger, 2002b). Also, mutation of the EVH1 binding domain of ADAP, abolishing the ability to bind VASP, appears to have no effect on LFA-1 avidity for its ligands (Wang et al., 2004). Put together, this suggests that whilst ADAP and VASP are capable of binding to each other, this is not the mechanism by which T cell cytoskeleton remodelling and activation occurs. ADAP and VASP may regulate independent signals for actin reorganisation with ADAP, potentially working through proteins such as WASP.

TCR ligation activates downstream signalling cascades leading to T cell activation. A central tyrosine kinase cascade is triggered. These early signals (that can also be induced by calcium ionophores such as Ionomycin), if sustained, lead to nuclear transcription of 3 families of transcription factor: NFAT, the AP-1 complex (Fos and Jun) and NFκB (Sims and Dustin, 2002). In our experiments, DN-VASP transfection was able to interfere with NFAT and AP-1 activation and to decrease IL-2 production following activation. NFAT forms a complex with AP-1. This complex then binds the IL-2 promoter and enhances transcription of the cytokine gene (Macian et al., 2000). The decrease in NFAT activity observed was different to that seen with in the AP-1 experiment. DN-VASP transfection completely eliminated even baseline AP-1 activity in contrast to empty vector transfected cells where measurable, baseline activity was observed. It is possible that this accounts for the effects seen in the NFAT pathway. As NFAT needs to complex with AP-1 for activation, the inhibitory effect of DN-VASP on AP-1 is probably enough to decrease NFAT activation. NFAT is activated via calcium flux alterations which we found to be unaltered by DN-VASP (figure 4.13) and we would therefore expect to see no alteration of activity in the luciferase assay if we were able to measure this pathway alone. A potential way to investigate this further would be to transfect in a constitutively active AP-1 at the same time in order to isolate the effect of DN-VASP on NFAT.

NFAT may be independently affected by cytoskeletal modification. As mentioned in the introduction to this chapter, calcium flux may play a role in limiting NFAT activation (Rivas et al., 2004) with actin cytoskeletal disruption leading to prolonged calcium flux and enhanced NFAT activation. We were unable to demonstrate any effect of disrupting VASP function by the use of DN-VASP on calcium but other proteins, capable of

altering actin polymerisation, such as WASP may be involved (Badour et al., 2004; Benesch et al., 2005; Volkman et al., 2002; Zhang et al., 2005). Interestingly, it has recently been shown that WASP has effects on NFAT and NF- $\kappa$ B distinct to its effects on the actin cytoskeleton (Huang et al., 2005). WASP appears to act via calcium regulated pathways. The combination of VASP and WASP may be necessary for full activation of signal transduction pathways following TCR ligation.

VASP and WASP may function by bringing together independent parts of the complex by cytoskeletal remodelling or holding them separate in the inactive state (an 'insulator' function (see (Burack et al., 2002; Davis, 2000) with activation leading to relaxation of the cytoskeleton, allowing them to move together.

CREB activation occurs downstream of the TCR via phosphorylation following activation of a PKC/Ras/Raf-1/MEK and RSK2 signalling cascade (Grady et al., 2004; Muthusamy and Leiden, 1998). We noted a decrease in CREB activation when DN-VASP was transfected into Jurkat cells (section 4.3.5), a process that we also showed disrupted normal actin cytoskeleton rearrangement (section 4.3.8). This suggests that the cytoskeleton may be important in this pathway, perhaps by allowing movement of the different factors, bringing them into contact with each other and facilitating signal transduction.

As all of these pathways are involved in IL-2 transcription, these effects would explain the decrease in IL-2 production following DN-VASP transfection observed in section 4.3.3. The differences observed for IL-2 production were not as strong as the differences seen in the CREB, AP-1 and NFAT luciferase assays. This is because the

luciferase reporter gene assays allow only transfected cells to be assayed, whereas the IL-2 ELISA assay also incorporates non-transfected cells (accounting for approximately 25% of live cells). However, the observed difference was still significant ( $p < 0.05$ )

NF- $\kappa$ B activation was increased in stimulated T cells regardless of transfection of DN-VASP or empty vector (section 4.3.5). A role for WASP, independent of its actions on the actin cytoskeleton in NFAT and NF- $\kappa$ B activation in natural killer (NK) cells has been suggested. Absence of WASP in these cells is associated with a decrease in calcineurin, WASP-interacting protein (WIP), ZAP70 and PLC- $\gamma$ 1 at the immune synapse (Huang et al., 2005). The use of DN-VASP, whilst potentially interfering with the ability of VASP to bind to ADAP, would not alter the ability of WASP to bind. Therefore WASP-associated activation of NF- $\kappa$ B could potentially be unaltered by DN-VASP transfection.

In signal transduction pathways therefore, VASP activity appears to be important in the MAP kinase activated pathways but not in the calcium flux mediated pathways where WASP may be active (Figure 4.17). This effect is not via modification of early phosphorylation steps such as ERK and JNK phosphorylation but occurs further down the cascade. Interfering with AP-1 and CREB but not NFAT or NF- $\kappa$ B is a potential way of inducing T cell anergy and could therefore be of interest as a new area for the development of immunosuppressive agents.

CD69 and CD25 (IL2R $\alpha$ ) are markers of T cell activation produced by early signal transduction pathways following T cell receptor signalling. CD69 is an early antigen

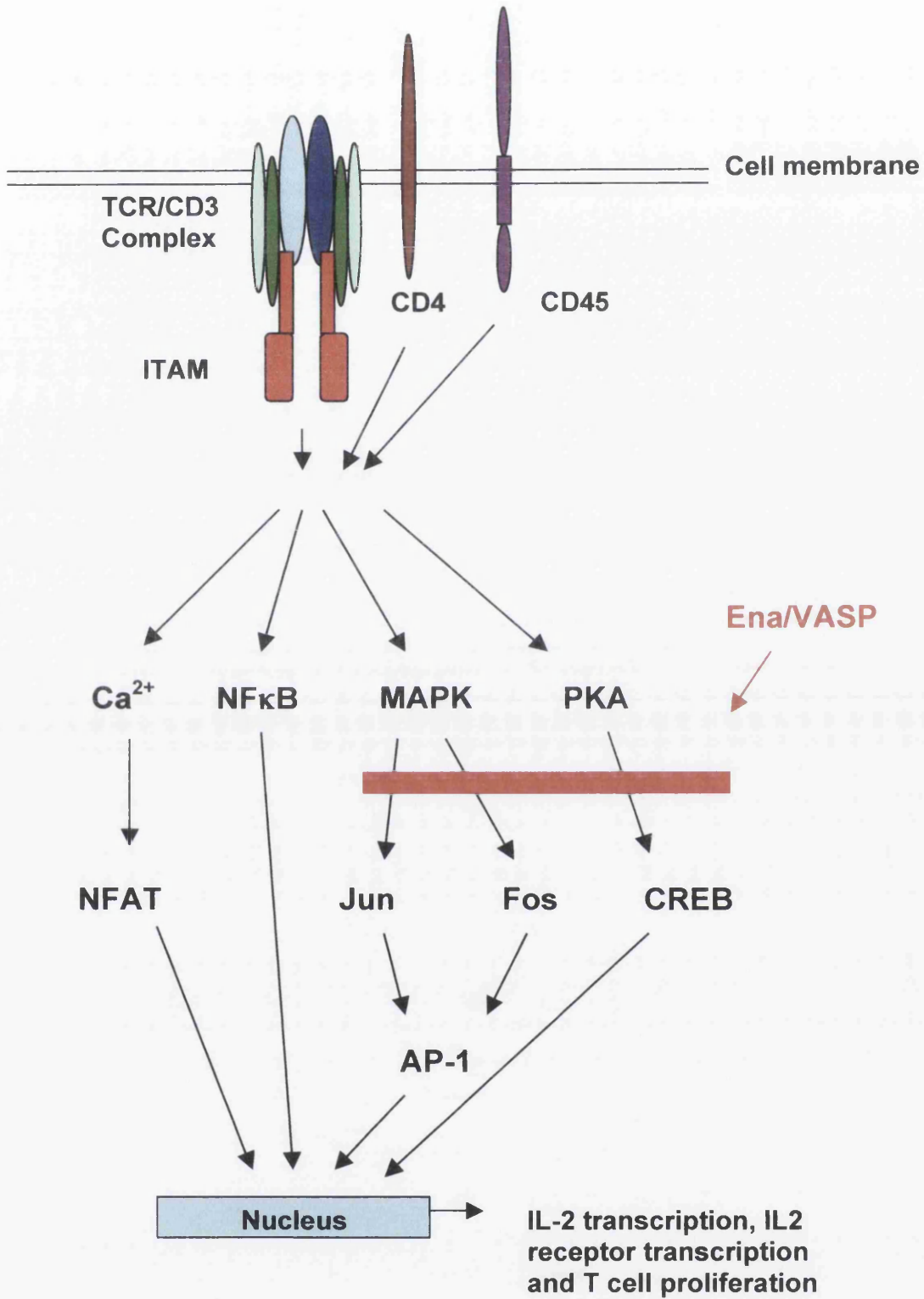


Figure 4.17 Potential site of VASP involvement in signal transduction in T cells following TCR ligation

activation marker and is expressed on the T cell surface earlier than CD25. In our experiments we saw very little CD25 expression following T cell stimulation but a marked increase in CD69 expression. The lack of CD25 activation may have been a function of Jurkat cells and it would be interesting to repeat this experiment in primary human lymphocytes. CD69 expression was not altered by DN-VASP transfection suggesting that T cell activation is not completely stopped by disruption of the actin cytoskeleton by DN-VASP and that other pathways are still functional.

Modifiers of T cell activation are still being sought for use in immunosuppression. Whilst we already have several (e.g. Cyclosporin, tacrolimus, OKT3) they all have limitations and side effects. The adaptor proteins present a future target for development of new agents able to modulate the interaction of various pathways in T cell activation (Rudd and Wang, 2003). It is interesting to note that in long-term surviving kidney transplants, T cell expression of CD69 is preserved, suggesting that immune regulation in these patients is preserved (Alvarez et al., 2004). Modifiers of the actin cytoskeleton may therefore be a system to explore further whilst looking for new immunosuppressant agents as the aim is to achieve long-term graft survival without impairing the host's immune system significantly.

There is a great deal of future work to be carried out in this interesting field. These experiments need to be carried out in primary cells as immortalised cell lines can show altered activities. Further elucidation of affected signal transduction pathways would help to clarify the exact positions at which VASP is acting. The effects of VASP phosphorylation in reaction to signals such as NO induction would be interesting as a potential mechanism for regulation of the T cell cytoskeleton *in vivo*. It would be useful to be able to create a tagged form of VASP in a stable clone of T cells to investigate the

effects of phosphorylation on location within the cell to allow changes in morphology, biochemistry and signal transduction to be studied in a coordinate fashion.

In summary, in this section of work we looked at the effects of interfering with VASP function by the use of a dominant-negative form of the protein in two major, interlinked areas

- Markers of T cell activation
- Effects on the actin cytoskeleton.

We showed that DN-VASP transfection was associated with down-regulation of some pathways but appeared to have no effect on others. Transfection of DN-VASP appeared to have no measurable effect on CD69 and CD25 expression or on the NF $\kappa$ B and c-Jun signal transduction pathways. It did however significantly alter T cell polarisation, binding to CD3/CD28 coated beads, IL-2 production and AP-1, and CREB signal transduction pathways following stimulation.

## Chapter 5. Conclusions

## 5.1 Summary of Results.

This study has investigated several different roles of VASP and the way its function is regulated. In epithelial cells we have demonstrated that VASP is phosphorylated at the Ser239 position in response to nitric oxide and that this is enhanced by the presence of Ser157 phosphorylation. The addition of a cyclic AMP analog to cells transfected with iNOS appears to have a synergistic effect on this phosphorylation. We have also shown that inducible nitric oxide is associated with a loss of VASP from focal sites at the cell membrane. We also used dominant-negative VASP in order to investigate the effects of disrupting VASP function in epithelial cells and showed that normal VASP function seems to be of much greater importance in the formation of new epithelial sheets than in the maintenance of existing sheets. Cells expressing DN-VASP appeared to have a diminished ability to adhere to the substratum but were still able to remain as part of an epithelial monolayer.

In the T cell line, Jurkat TetOff cells, disruption of VASP function using DN-VASP had a number of effects. DN-VASP transfection was associated with a significant decrease in interleukin-2 production, a loss of actin polarisation and decrease in the MAP kinase signal transduction pathways following stimulation with CD3 and CD28 antibodies. It did not alter calcium flux, CD69 or CD25 expression and did not appear to alter the NFAT signal transduction pathway. Its effects on NF- $\kappa$ B signal transduction were less clear but were probably related to its effects on AP-1. The effects on MAP kinases did not appear to be via early phosphorylation of the kinases but appear to occur at a later stage of the pathway activation.

## 5.2 Biological Implications and future work

Pro-inflammatory cytokines, acting via iNOS induction are able to produce PTEC shedding in an *in vitro* model (Glynne and Evans, 1999a) with disruption of the actin cytoskeleton and loss of cell polarity (Glynne *et al.*, 2001). Vasodilator-stimulated phosphoprotein is a potential mechanism by which this may occur. It binds to proteins situated at cell:cell and cell:matrix junctions via its EVH1 domain and to the actin cytoskeleton via its EVH2 domain. VASP contains a cGMP-dependent protein kinase phosphorylation site in close proximity to domains associated with G-actin binding and F-actin polymerisation. It is therefore an attractive proposition as a cytoskeletal protein that may later its ability to act as a link between the cytoskeleton and adjacent cells or the extracellular matrix. Our studies confirmed that iNOS induction was associated with a loss of VASP from focal membrane sites and with Ser239 phosphorylation. Interestingly, we found that the level of Ser239 phosphorylation appeared to be crucially dependent on the level of Ser157 phosphorylation. This Ser157 site, *in vitro*, is preferentially phosphorylated by cAMP-dependent protein kinase. As Ser 157 phosphorylation is known to be associated with a shift in the apparent molecular mass of VASP on western blotting, this suggests that it is associated with a conformational change, possibly exposing the Ser239 site and enabling phosphorylation.

Potentially, this suggests that there may be two possible pathways by which the effects of NO on VASP may be modulated, either by cGMP or cAMP-dependent protein kinase pathways and therefore two potential paths at which agents could be targeted. The activity of these pathways is regulated by phosphodiesterases (Conti and Jin, 1999; Feijge *et al.*, 2004; Murray *et al.*, 2002). We have several pharmacological agents available to us which act as phosphodiesterase inhibitors such as dipyridamole and

Zaprinast (Type V PDE inhibitors ) (Aktas et al., 2003; Matot and Gozal, 2004; Matsumoto and Nakamura, 2002) and Milrinone (type III PDE inhibitor). Milrinone, for example, has been noted to cause an increase in cAMP-mediated VASP Ser157 phosphorylation in platelets (Manns et al., 2002). From our results, we would expect this to allow a higher degree of Ser239 phosphorylation and potentially greater cell shedding. In fact, in an animal model, type III PDE inhibition has been associated with a greater degree of LPS-induced ARF (Jonassen et al., 2002).

To pursue this work further, it would be interesting to generate further VASP mutants, including an Ser157-Ala mutant to investigate whether Ser239 phosphorylation is still possible in this mutant and what effect this has on the response of a cell to nitric oxide. Use of PDE inhibitors would also allow further elucidation of the control of VASP phosphorylation and its effects on the cell. Further work should be directed at the investigating the effects in primary cells. The generation of fluorescence-labelled VASP mutants would allow the use of time-lapse photography to study the effects of NO donors and PDEs in the living cell.

Our studies also suggested that VASP is more important in forming cell:substratum adhesions and early cell:cell junctions rather than in the maintenance of cell:cell junctions. Interrupting VASP function with DN-VASP had a greater effect on the ability of cells to form a new epithelial monolayer but had relatively little effect on an established epithelial sheet. This is consistent with previously reported findings on the formation of cell:cell junctions (Adams et al., 1998; Adams and Nelson, 1998). Addition of cytochalasin D to disrupt the actin cytoskeleton, was only effective at disrupting cell:cell junctions either in newly forming junctions or those less than 1 hour

old. VASP may therefore play a role in cell motility, allowing cells to move close enough to adjacent cells to form an epithelial zipper (Vasioukhin et al., 2000) but once the junction is complete, other proteins may be involved in maintaining it. Indeed, VASP is generally located at highly dynamic areas of the cell membrane (Han et al., 2002). This may be important for example, in the recovery of the proximal tubule epithelium post-acute injury in forming a new epithelial sheet following cell shedding seen in ATN. As discussed above, phosphorylation of VASP is an important mechanism by which its actions may be modulated. Drugs which interfere with this such as milrinone may, in theory, prolong recovery via their actions on PDEs.

The final part of this study investigated the role of the actin cytoskeleton and the functions of VASP in T cell activation. The adaptor protein ADAP contains an EVH1 binding domain and has a role in the regulation of adhesion between the T cell and an APC (Wang et al., 2004) with ADAP knockout cells showing deficient LFA-1 clustering.. As VASP contains an EVH1 domain and is known to polymerise actin, it appeared an attractive pathway by which VASP could be involved in T cell activation. Our results demonstrated that DN-VASP transfection was associated with a loss of actin polarisation and cuff formation in response to TCR ligation by a CD3/CD28 coated bead. Previous studies (Griffiths and Penninger, 2002a) have shown that ADAP deficient cells are still capable of polarising actin and another approach using ActA repeats to block EVH-1 binding (Krause et al., 2000) suggested that actin polarisation does not occur through proteins such as VASP binding through this domain. Our work also suggested that VASP does not alter T cell activation through modulation of LFA-1 clustering and ligand avidity as we were unable to demonstrate any effect on ICAM-1 binding.

We therefore looked at other ways in which VASP may affect T cell activation. The effects we demonstrated on signal transduction via MAP kinases were striking. The AP-1 pathway appeared to be completely obliterated by DN-VASP with even base-line activation, prior to stimulation, being lost. The CREB pathway was also down-regulated. This is a potential method by which T cell anergy could be induced, with preservation of NFAT and NF- $\kappa$ B pathways but with a decreased ability of the cells to produce IL-2 and proliferate due to MAP kinase blockade. VASP could be involved in signal transduction by moving complexes into positions by which they can interact (Davis, 2000). Modulation of VASP's ability to interact with the actin cytoskeleton via modulation of its cyclic-nucleotide dependent protein kinase sites may be a model of manipulating T cell activation. The role of scaffold and adaptor proteins in the production of immunosuppressive agents has not yet been explored but may be a novel field for therapeutic agents.

The MAP kinases are involved in many other diseases such as tumour development (Johnson et al., 1996), wound healing by keratinocyte proliferation (Szabowski et al., 2000) Alzheimer's disease (AP-1 activation is associated with enhanced cerebral endothelial cell apoptosis (Yin et al., 2002) and chronic myeloid leukaemia (Yang et al., 2003). The role of modulation of VASP function in these diseases may be interesting both in terms of producing disease models and in therapeutic agents.

There is much more work to be done in these fields. The interaction between VASP and actin and the role by which NO has its effects is still to be fully clarified. It would be interesting to investigate the role of VASP on MAP kinase signalling in epithelial cells

and how this affects epithelial sheet integrity. The work in Jurkat cells needs to be repeated in primary cells as cell lines are known to mutate and may not mimic the situation in the body. DN-VASP appears to be a powerful tool in this work but the actions of NO on VASP in these situations may give more clues to the physiological control of these processes.

## References

- Abel, K., G. Mieskes, and U. Walter. 1995. Dephosphorylation of the focal adhesion protein VASP in vitro and in intact human platelets. *FEBS Lett.* 370:184-8.
- Aberle, H., S. Butz, J. Stappert, H. Weissig, R. Kemler, and H. Hoschuetzky. 1994. Assembly of the cadherin-catenin complex in vitro with recombinant proteins. *J Cell Sci.* 107 ( Pt 12):3655-63.
- Adams, C.L., Y.T. Chen, S.J. Smith, and W.J. Nelson. 1998. Mechanisms of epithelial cell-cell adhesion and cell compaction revealed by high-resolution tracking of E-cadherin-green fluorescent protein. *J Cell Biol.* 142:1105-19.
- Adams, C.L., and W.J. Nelson. 1998. Cyto mechanics of cadherin-mediated cell-cell adhesion. *Curr Opin Cell Biol.* 10:572-7.
- Ahern-Djamali, S.M., A.R. Comer, C. Bachmann, A.S. Kastenmeier, S.K. Reddy, M.C. Beckerle, U. Walter, and F.M. Hoffmann. 1998. Mutations in *Drosophila* enabled and rescue by human vasodilator-stimulated phosphoprotein (VASP) indicate important functional roles for Ena/VASP homology domain 1 (EVH1) and EVH2 domains. *Mol Biol Cell.* 9:2157-71.
- Aktas, B., A. Utz, P. Hoenig-Liedl, U. Walter, and J. Geiger. 2003. Dipyridamole enhances NO/cGMP-mediated vasodilator-stimulated phosphoprotein phosphorylation and signaling in human platelets: in vitro and in vivo/ex vivo studies. *Stroke.* 34:764-9.
- Alderton, W.K., C.E. Cooper, and R.G. Knowles. 2001. Nitric oxide synthases: structure, function and inhibition. *Biochem J.* 357:593-615.

- Allen, L.A., and A. Aderem. 1996a. Mechanisms of phagocytosis. *Curr Opin Immunol.* 8:36-40.
- Allen, L.A., and A. Aderem. 1996b. Molecular definition of distinct cytoskeletal structures involved in complement- and Fc receptor-mediated phagocytosis in macrophages. *J Exp Med.* 184:627-37.
- Alvarez, C.M., S.C. Paris, L. Arango, M. Arbelaez, and L.F. Garcia. 2004. Kidney transplant patients with long-term graft survival have altered expression of molecules associated with T-cell activation. *Transplantation.* 78:1541-7.
- Anane, D., P. Aegerter, M.C. Jars-Guinestre, and B. Guidet. 2003. Current epidemiology of septic shock: the CUB-Rea Network. *Am J Respir Crit Care Med.* 168:165-72.
- Arthur, W.T., N.K. Noren, and K. Burridge. 2002. Regulation of Rho family GTPases by cell-cell and cell-matrix adhesion. *Biol Res.* 35:239-46.
- Astoul, E., C. Edmunds, D.A. Cantrell, and S.G. Ward. 2001. PI 3-K and T-cell activation: limitations of T-leukemic cell lines as signaling models. *Trends Immunol.* 22:490-6.
- Aszodi, A., A. Pfeifer, M. Ahmad, M. Glauner, X.H. Zhou, L. Ny, K.E. Andersson, B. Kehrel, S. Offermanns, and R. Fassler. 1999. The vasodilator-stimulated phosphoprotein (VASP) is involved in cGMP- and cAMP-mediated inhibition of

agonist-induced platelet aggregation, but is dispensable for smooth muscle function.

*Embo J.* 18:37-48.

Atkinson, S.J., M.A. Hosford, and B.A. Molitoris. 2004. Mechanism of actin polymerization in cellular ATP depletion. *J Biol Chem.* 279:5194-9.

Auerbuch, V., J.J. Loureiro, F.B. Gertler, J.A. Theriot, and D.A. Portnoy. 2003. Ena/VASP proteins contribute to *Listeria monocytogenes* pathogenesis by controlling temporal and spatial persistence of bacterial actin-based motility. *Mol Microbiol.* 49:1361-75.

Bachmann, C., L. Fischer, U. Walter, and M. Reinhard. 1999. The EVH2 domain of the vasodilator-stimulated phosphoprotein mediates tetramerization, F-actin binding, and actin bundle formation. *J Biol Chem.* 274:23549-57.

Badour, K., J. Zhang, and K.A. Siminovitch. 2004. Involvement of the Wiskott-Aldrich syndrome protein and other actin regulatory adaptors in T cell activation. *Semin Immunol.* 16:395-407.

Ball, L.J., R. Kuhne, B. Hoffmann, A. Hafner, P. Schmieder, R. Volkmer-Engert, M. Hof, M. Wahl, J. Schneider-Mergener, U. Walter, H. Oschkinat, and T. Jarchau. 2000. Dual epitope recognition by the VASP EVH1 domain modulates polyproline ligand specificity and binding affinity. *Embo J.* 19:4903-14.

Barda-Saad, M., A. Braiman, R. Titerence, S.C. Bunnell, V.A. Barr, and L.E. Samelson. 2005. Dynamic molecular interactions linking the T cell antigen receptor to the actin cytoskeleton. *Nat Immunol.* 6:80-9.

Barros, E.J., O.F. Santos, K. Matsumoto, T. Nakamura, and S.K. Nigam. 1995. Differential tubulogenic and branching morphogenetic activities of growth factors: implications for epithelial tissue development. *Proc Natl Acad Sci U S A.* 92:4412-6.

Barzik, M., T.I. Kotova, H.N. Higgs, L. Hazelwood, D. Hanein, F.B. Gertler, and D.A. Schafer. 2005. Ena/VASP proteins enhance actin polymerization in the presence of barbed end capping Proteins. *J Biol Chem.*

Bear, J.E., M. Krause, and F.B. Gertler. 2001. Regulating cellular actin assembly. *Curr Opin Cell Biol.* 13:158-66.

Bear, J.E., T.M. Svitkina, M. Krause, D.A. Schafer, J.J. Loureiro, G.A. Strasser, I.V. Maly, O.Y. Chaga, J.A. Cooper, G.G. Borisy, and F.B. Gertler. 2002. Antagonism between Ena/VASP proteins and actin filament capping regulates fibroblast motility. *Cell.* 109:509-21.

Benesch, S., S. Polo, F.P. Lai, K.I. Anderson, T.E. Stradal, J. Wehland, and K. Rottner. 2005. N-WASP deficiency impairs EGF internalization and actin assembly at clathrin-coated pits. *J Cell Sci.* 118:3103-15.

Berdichevsky, F., D. Alford, B. D'Souza, and J. Taylor-Papadimitriou. 1994. Branching morphogenesis of human mammary epithelial cells in collagen gels. *J Cell Sci.* 107 ( Pt 12):3557-68.

Blank, C., A. Luz, S. Bendigs, A. Erdmann, H. Wagner, and K. Heeg. 1997. Superantigen and endotoxin synergize in the induction of lethal shock. *Eur J Immunol.* 27:825-33.

Bone, R.C., R.A. Balk, F.B. Cerra, R.P. Dellinger, A.M. Fein, W.A. Knaus, R.M. Schein, and W.J. Sibbald. 1992. Definitions for sepsis and organ failure and guidelines for the use of innovative therapies in sepsis. The ACCP/SCCM Consensus Conference Committee. American College of Chest Physicians/Society of Critical Care Medicine. *Chest.* 101:1644-55.

Bredt, D.S., and S.H. Snyder. 1994. Nitric oxide: a physiologic messenger molecule. *Annu Rev Biochem.* 63:175-95.

Brindle, N.P., M.R. Holt, J.E. Davies, C.J. Price, and D.R. Critchley. 1996. The focal-adhesion vasodilator-stimulated phosphoprotein (VASP) binds to the proline-rich domain in vinculin. *Biochem J.* 318 ( Pt 3):753-7.

Bubeck, P., S. Pistor, J. Wehland, and B.M. Jockusch. 1997. Ligand recruitment by vinculin domains in transfected cells. *J Cell Sci.* 110 ( Pt 12):1361-71.

Burack, W.R., A.M. Cheng, and A.S. Shaw. 2002. Scaffolds, adaptors and linkers of TCR signaling: theory and practice. *Curr Opin Immunol.* 14:312-6.

Burchiel, S.W., B.S. Edwards, F.W. Kuckuck, F.T. Lauer, E.R. Prossnitz, J.T. Ransom, and L.A. Sklar. 2000. Analysis of free intracellular calcium by flow cytometry: multiparameter and pharmacologic applications. *Methods*. 21:221-30.

Burrow, C.R., O. Devuyst, X. Li, L. Gatti, and P.D. Wilson. 1999. Expression of the beta2-subunit and apical localization of Na<sup>+</sup>-K<sup>+</sup>-ATPase in metanephric kidney. *Am J Physiol*. 277:F391-403.

Butt, E., K. Abel, M. Krieger, D. Palm, V. Hoppe, J. Hoppe, and U. Walter. 1994. cAMP- and cGMP-dependent protein kinase phosphorylation sites of the focal adhesion vasodilator-stimulated phosphoprotein (VASP) in vitro and in intact human platelets. *J Biol Chem*. 269:14509-17.

Buttery, L.D., T.J. Evans, D.R. Springall, A. Carpenter, J. Cohen, and J.M. Polak. 1994. Immunochemical localization of inducible nitric oxide synthase in endotoxin-treated rats. *Lab Invest*. 71:755-64.

Carl, U.D., M. Pollmann, E. Orr, F.B. Gertlere, T. Chakraborty, and J. Wehland. 1999. Aromatic and basic residues within the EVH1 domain of VASP specify its interaction with proline-rich ligands. *Curr Biol*. 9:715-8.

Carrier, M.F., S. Wiesner, C. Le Clairche, and D. Pantaloni. 2003. Actin-based motility as a self-organized system: mechanism and reconstitution in vitro. *C R Biol*. 326:161-70.

Conti, M., and S.L. Jin. 1999. The molecular biology of cyclic nucleotide phosphodiesterases. *Prog Nucleic Acid Res Mol Biol.* 63:1-38.

Coppolino, M.G., M. Krause, P. Hagendorff, D.A. Monner, W. Trimble, S. Grinstein, J. Wehland, and A.S. Sechi. 2001. Evidence for a molecular complex consisting of Fyb/SLAP, SLP-76, Nck, VASP and WASP that links the actin cytoskeleton to Fcγ receptor signalling during phagocytosis. *J Cell Sci.* 114:4307-18.

Cozens, A.L., M.J. Yezzi, K. Kunzelmann, T. Ohrui, L. Chin, K. Eng, W.E. Finkbeiner, J.H. Widdicombe, and D.C. Gruenert. 1994. CFTR expression and chloride secretion in polarized immortal human bronchial epithelial cells. *Am J Respir Cell Mol Biol.* 10:38-47.

Cramer, L.P. 1999. Role of actin-filament disassembly in lamellipodium protrusion in motile cells revealed using the drug jasplakinolide. *Curr Biol.* 9:1095-105.

Critchley, D.R., M.R. Holt, S.T. Barry, H. Priddle, L. Hemmings, and J. Norman. 1999. Integrin-mediated cell adhesion: the cytoskeletal connection. *Biochem Soc Symp.* 65:79-99.

da Silva, A.J., L. Zhuwen, C. de Vera, E. Canto, P. Findell, and C.E. Rudd. 1997. Cloning of a novel T-cell protein FYB that binds FYN and SH2-domain-containing leukocyte protein 76 and modulates interleukin 2 production. *Proc.Natl.Acad.Sci.USA.* 94:7493-7498.

Davis, R.J. 2000. Signal transduction by the JNK group of MAP kinases. *Cell*. 103:239-52.

Dinarello, C.A. 1992. The role of interleukin-1 in host responses to infectious diseases. *Infect Agents Dis*. 1:227-36.

Diviani, D., and J. Scott. 2001. AKAP signalling complexes at the cytoskeleton. *J.Cell.Sci*. 114:1431-1437.

Drees, B., E. Friederich, J. Fradelizi, D. Louvard, M.C. Beckerle, and R.M. Golsteyn. 2000. Characterization of the interaction between zyxin and members of the Ena/vasodilator-stimulated phosphoprotein family of proteins. *J Biol Chem*. 275:22503-11.

Drubin, D.G., and W.J. Nelson. 1996. Origins of cell polarity. *Cell*. 84:335-44.

Eigenthaler, M., C. Nolte, M. Halbrugge, and U. Walter. 1992. Concentration and regulation of cyclic nucleotides, cyclic-nucleotide-dependent protein kinases and one of their major substrates in human platelets. Estimating the rate of cAMP-regulated and cGMP-regulated protein phosphorylation in intact cells. *Eur J Biochem*. 205:471-81.

Eisen, R., D.R. Ratcliffe, and G.K. Ojakian. 2004. Modulation of epithelial tubule formation by Rho kinase. *Am J Physiol Cell Physiol*. 286:C857-66.

Evans, T.J., L.D. Buttery, A. Carpenter, D.R. Springall, J.M. Polak, and J. Cohen. 1996. Cytokine-treated human neutrophils contain inducible nitric oxide synthase that produces nitration of ingested bacteria. *Proc Natl Acad Sci U S A*. 93:9553-8.

Feijge, M.A., K. Ansink, K. Vanschoonbeek, and J.W. Heemskerk. 2004. Control of platelet activation by cyclic AMP turnover and cyclic nucleotide phosphodiesterase type-3. *Biochem Pharmacol*. 67:1559-67.

Fillingham, I., A.R. Gingras, E. Papagrigoriou, B. Patel, J. Emsley, D.R. Critchley, G.C. Roberts, and I.L. Barsukov. 2005. A vinculin binding domain from the talin rod unfolds to form a complex with the vinculin head. *Structure (Camb)*. 13:65-74.

Fischer, T.A., A. Palmethofer, S. Gambaryan, E. Butt, C. Jassoy, U. Walter, S. Sopper, and S.M. Lohmann. 2001. Activation of cGMP-dependent protein kinase I $\beta$  inhibits interleukin 2 release and proliferation of T cell receptor-stimulated human peripheral T cells. *J Biol Chem*. 276:5967-74.

Forstermann, U., E.I. Closs, J.S. Pollock, M. Nakane, P. Schwarz, I. Gath, and H. Kleinert. 1994. Nitric oxide synthase isozymes. Characterization, purification, molecular cloning, and functions. *Hypertension*. 23:1121-31.

Forstermann, U., I. Gath, P. Schwarz, E.I. Closs, and H. Kleinert. 1995. Isoforms of nitric oxide synthase. Properties, cellular distribution and expressional control. *Biochem Pharmacol*. 50:1321-32.

Forstermann, U., and H. Kleinert. 1995. Nitric oxide synthase: expression and expressional control of the three isoforms. *Naunyn Schmiedebergs Arch Pharmacol.* 352:351-64.

Fujishige, K., J. Kotera, H. Michibata, K. Yuasa, S. Takebayashi, K. Okumura, and K. Omori. 1999. Cloning and characterization of a novel human phosphodiesterase that hydrolyzes both cAMP and cGMP (PDE10A). *J Biol Chem.* 274:18438-45.

Geese, M., J.J. Loureiro, J.E. Bear, J. Wehland, F.B. Gertler, and A.S. Sechi. 2002. Contribution of Ena/VASP proteins to intracellular motility of listeria requires phosphorylation and proline-rich core but not F-actin binding or multimerization. *Mol Biol Cell.* 13:2383-96.

Geese, M., K. Schluter, M. Rothkegel, B.M. Jockusch, J. Wehland, and A.S. Sechi. 2000. Accumulation of profilin II at the surface of Listeria is concomitant with the onset of motility and correlates with bacterial speed. *J Cell Sci.* 113 ( Pt 8):1415-26.

Geijtenbeek, T.B., Y. van Kooyk, S.J. van Vliet, M.H. Renes, R.A. Raymakers, and C.G. Figdor. 1999. High frequency of adhesion defects in B-lineage acute lymphoblastic leukemia. *Blood.* 94:754-64.

Gertler, F.B., A.R. Comer, J.L. Juang, S.M. Ahern, M.J. Clark, E.C. Liebl, and F.M. Hoffmann. 1995. enabled, a dosage-sensitive suppressor of mutations in the Drosophila Abl tyrosine kinase, encodes an Abl substrate with SH3 domain-binding properties. *Genes Dev.* 9:521-33.

Gertler, F.B., K. Niebuhr, M. Reinhard, J. Wehland, and P. Soriano. 1996. Mena, a relative of VASP and Drosophila Enabled, is implicated in the control of microfilament dynamics. *Cell*. 87:227-39.

Glynnne, P.A., K.E. Darling, J. Picot, and T.J. Evans. 2002. Epithelial inducible nitric-oxide synthase is an apical EBP50-binding protein that directs vectorial nitric oxide output. *J Biol Chem*. 277:33132-8.

Glynnne, P.A., and T.J. Evans. 1999a. Inflammatory cytokines induce apoptotic and necrotic cell shedding from human proximal tubular epithelial cell monolayers. *Kidney Int*. 55:2573-97.

Glynnne, P.A., and T.J. Evans. 1999b. Inflammatory cytokines induce apoptotic and necrotic cell shedding from human proximal tubule epithelial cell monolayers. *Kidney Int*. 55:2573-97.

Glynnne, P.A., J. Picot, and T.J. Evans. 2001. Coexpressed nitric oxide synthase and apical beta(1) integrins influence tubule cell adhesion after cytokine-induced injury. *J Am Soc Nephrol*. 12:2370-83.

Goda, S., A.C. Quale, M.L. Woods, A. Felthausen, and Y. Shimizu. 2004. Control of TCR-mediated activation of beta 1 integrins by the ZAP-70 tyrosine kinase interdomain B region and the linker for activation of T cells adapter protein. *J Immunol*. 172:5379-87.

Goligorsky, M.S., W. Lieberthal, L. Racusen, and E.E. Simon. 1993. Integrin receptors in renal tubular epithelium: new insights into pathophysiology of acute renal failure. *Am J Physiol.* 264:F1-8.

Gomez, T.M., and E. Robles. 2004. The great escape; phosphorylation of Ena/VASP by PKA promotes filopodial formation. *Neuron.* 42:1-3.

Goncz, K.K., L. Feeney, and D.C. Gruenert. 1999. Differential sensitivity of normal and cystic fibrosis airway epithelial cells to epinephrine. *Br J Pharmacol.* 128:227-33.

Gossen, M., and H. Bujard. 1992. Tight control of gene expression in mammalian cells by tetracycline-responsive promoters. *Proc Natl Acad Sci U S A.* 89:5547-51.

Grady, G.C., S.M. Mason, J. Stephen, J.C. Zuniga-Pflucker, and A.M. Michie. 2004. Cyclic adenosine 5'-monophosphate response element binding protein plays a central role in mediating proliferation and differentiation downstream of the pre-TCR complex in developing thymocytes. *J Immunol.* 173:1802-10.

Grakoui, A., S.K. Bromley, C. Sumen, M.M. Davis, A.S. Shaw, P.M. Allen, and M.L. Dustin. 1999. The immunological synapse: a molecular machine controlling T cell activation. *Science.* 285:221-7.

Greenberg, S., K. Burrridge, and S.C. Silverstein. 1990. Colocalization of F-actin and talin during Fc receptor-mediated phagocytosis in mouse macrophages. *J Exp Med.* 172:1853-6.

Grenklo, S., M. Geese, U. Lindberg, J. Wehland, R. Karlsson, and A.S. Sechi. 2003. A crucial role for profilin-actin in the intracellular motility of *Listeria monocytogenes*. *EMBO Rep.* 4:523-9.

Griffiths, E.K., C. Krawczyk, Y.Y. Kong, M. Raab, S.J. Hyduk, D. Bouchard, V.S. Chan, I. Kozieradzki, A.J. Oliveira-Dos-Santos, A. Wakeham, P.S. Ohashi, M.I. Cybulsky, C.E. Rudd, and J.M. Penninger. 2001. Positive regulation of T cell activation and integrin adhesion by the adapter Fyb/Slap. *Science.* 293:2260-3.

Griffiths, E.K., and J.M. Penninger. 2002a. ADAP-ting TCR signaling to integrins. *Sci STKE.* 2002:RE3.

Griffiths, E.K., and J.M. Penninger. 2002b. Communication between the TCR and integrins: role of the molecular adapter ADAP/Fyb/Slap. *Curr Opin Immunol.* 14:317-22.

Groeneveld, A.B. 1994. Pathogenesis of acute renal failure during sepsis. *Nephrol Dial Transplant.* 9 Suppl 4:47-51.

Groeneveld, A.B., D.D. Tran, J. van der Meulen, J.J. Nauta, and L.G. Thijs. 1991. Acute renal failure in the medical intensive care unit: predisposing. complicating factors and outcome. *Nephron.* 59:602-10.

Groeneveld, P.H., J. Ringers, and J.T. van Dissel. 1994. Effect of nitric oxide on renal function in septic shock. *N Engl J Med.* 330:1620.

Gumbiner, B.M. 1996. Cell adhesion: the molecular basis of tissue architecture and morphogenesis. *Cell*. 84:345-57.

Haffner, C., T. Jarchau, M. Reinhard, J. Hoppe, S.M. Lohmann, and U. Walter. 1995. Molecular cloning, structural analysis and functional expression of the proline-rich focal adhesion and microfilament-associated protein VASP. *Embo J*. 14:19-27.

Halbrugge, M., M. Eigenthaler, C. Polke, and U. Walter. 1992. Protein phosphorylation regulated by cyclic nucleotide-dependent protein kinases in cell extracts and in intact human lymphocytes. *Cell Signal*. 4:189-99.

Halbrugge, M., C. Friedrich, M. Eigenthaler, P. Schanzenbacher, and U. Walter. 1990. Stoichiometric and reversible phosphorylation of a 46-kDa protein in human platelets in response to cGMP- and cAMP-elevating vasodilators. *J Biol Chem*. 265:3088-93.

Halbrugge, M., and U. Walter. 1989. Purification of a vasodilator-regulated phosphoprotein from human platelets. *Eur J Biochem*. 185:41-50.

Halbrugge, M., and U. Walter. 1990. Analysis, purification and properties of a 50,000-dalton membrane-associated phosphoprotein from human platelets. *J Chromatogr*. 521:335-43.

Hall, A. 1998. Rho GTPases and the actin cytoskeleton. *Science*. 279:509-14.

Han, Y.H., C.Y. Chung, D. Wessels, S. Stephens, M.A. Titus, D.R. Soll, and R.A.

Firtel. 2002. Requirement of a vasodilator-stimulated phosphoprotein family member

for cell adhesion, the formation of filopodia, and chemotaxis in dictyostelium. *J Biol Chem.* 277:49877-87.

Hannappel, E., and F. Wartenberg. 1993. Actin-sequestering ability of thymosin beta 4, thymosin beta 4 fragments, and thymosin beta 4-like peptides as assessed by the DNase I inhibition assay. *Biol Chem Hoppe Seyler.* 374:117-22.

Harbeck, B., S. Huttelmaier, K. Schluter, B.M. Jockusch, and S. Illenberger. 2000. Phosphorylation of the vasodilator-stimulated phosphoprotein regulates its interaction with actin. *J Biol Chem.* 275:30817-25.

Hazan, R.B., L. Kang, S. Roe, P.I. Borgen, and D.L. Rimm. 1997. Vinculin is associated with the E-cadherin adhesion complex. *J Biol Chem.* 272:32448-53.

Hikita, C., S. Vijayakumar, J. Takito, H. Erdjument-Bromage, P. Tempst, and Q. Al-Awqati. 2000. Induction of terminal differentiation in epithelial cells requires polymerization of hensin by galectin 3. *J Cell Biol.* 151:1235-46.

Hobbs, A.J. 1997. Soluble guanylate cyclase: the forgotten sibling. *Trends Pharmacol Sci.* 18:484-91.

Holsinger, L.J., I.A. Graef, W. Swat, T. Chi, D.M. Bautista, L. Davidson, R.S. Lewis, F.W. Alt, and G.R. Crabtree. 1998. Defects in actin-cap formation in Vav-deficient mice implicate an actin requirement for lymphocyte signal transduction. *Curr Biol.* 8:563-72.

Horstrup, K., B. Jablonka, P. Honig-Liedl, M. Just, K. Kochsiek, and U. Walter. 1994. Phosphorylation of focal adhesion vasodilator-stimulated phosphoprotein at Ser157 in intact human platelets correlates with fibrinogen receptor inhibition. *Eur J Biochem.* 225:21-7.

Huang, W., H.D. Ochs, B. Dupont, and Y.M. Vyas. 2005. The Wiskott-Aldrich syndrome protein regulates nuclear translocation of NFAT2 and NF-kappa B (RelA) independently of its role in filamentous actin polymerization and actin cytoskeletal rearrangement. *J Immunol.* 174:2602-11.

Huttelmaier, S., B. Harbeck, O. Steffens, T. Messerschmidt, S. Illenberger, and B.M. Jockusch. 1999. Characterization of the actin binding properties of the vasodilator-stimulated phosphoprotein VASP. *FEBS Lett.* 451:68-74.

Ibarra-Alvarado, C., J. Galle, V.O. Melichar, A. Mameghani, and H.H. Schmidt. 2002. Phosphorylation of blood vessel vasodilator-stimulated phosphoprotein at serine 239 as a functional biochemical marker of endothelial nitric oxide/cyclic GMP signaling. *Mol Pharmacol.* 61:312-9.

Ignarro, L.J., R.E. Byrns, G.M. Buga, and K.S. Wood. 1987. Endothelium-derived relaxing factor from pulmonary artery and vein possesses pharmacologic and chemical properties identical to those of nitric oxide radical. *Circ Res.* 61:866-79.

Jiang, S.T., S.J. Chiu, H.C. Chen, W.J. Chuang, and M.J. Tang. 2001. Role of alpha(3)beta(1) integrin in tubulogenesis of Madin-Darby canine kidney cells. *Kidney Int.* 59:1770-8.

Jiang, S.T., W.J. Chuang, and M.J. Tang. 2000. Role of fibronectin deposition in branching morphogenesis of Madin-Darby canine kidney cells. *Kidney Int.* 57:1860-7.

Johnson, R., B. Spiegelman, D. Hanahan, and R. Wisdom. 1996. Cellular transformation and malignancy induced by ras require c-jun. *Mol Cell Biol.* 16:4504-11.

Jonassen, T.E., M. Graebe, D. Promeneur, S. Nielsen, S. Christensen, and N.V. Olsen. 2002. Lipopolysaccharide-induced acute renal failure in conscious rats: effects of specific phosphodiesterase type 3 and 4 inhibition. *J Pharmacol Exp Ther.* 303:364-74.

Kaissling, B., and W. Kriz. 1979. Structural analysis of the rabbit kidney. *Adv Anat Embryol Cell Biol.* 56:1-123.

Kellerman, P.S., and R.T. Bogusky. 1992. Microfilament disruption occurs very early in ischemic proximal tubule cell injury. *Kidney Int.* 42:896-902.

Kelley TJ, a.-N.L.D.M. 1995. CFTR-mediated chloride permeability is regulated by type III phosphodiesterases in airway epithelial cells. *Am.J.Respir.Cell.Mol.Biol.* 13:657-664.

Kistner, A., M. Gossen, F. Zimmermann, J. Jerecic, C. Ullmer, H. Lubbert, and H. Bujard. 1996. Doxycycline-mediated quantitative and tissue-specific control of gene expression in transgenic mice. *Proc Natl Acad Sci U S A.* 93:10933-8.

Kjelsberg, C., H. Sakurai, K. Spokes, C. Birchmeier, I. Drummond, S. Nigam, and L.G. Cantley. 1997. Met <sup>-/-</sup> kidneys express epithelial cells that chemotax and form tubules in response to EGF receptor ligands. *Am J Physiol.* 272:F222-8.

Knowles, R.G., and S. Moncada. 1994. Nitric oxide synthases in mammals. *Biochem J.* 298 ( Pt 2):249-58.

Koesling, D., and A. Friebe. 1999. Soluble guanylyl cyclase: structure and regulation. *Rev Physiol Biochem Pharmacol.* 135:41-65.

Kolanus, W., and B. Seed. 1997. Integrins and inside-out signal transduction: converging signals from PKC and PIP3. *Curr Opin Cell Biol.* 9:725-31.

Kone, B.C. 1997. Nitric oxide in renal health and disease. *Am J Kidney Dis.* 30:311-33.

Kone, B.C. 2000. Protein-protein interactions controlling nitric oxide synthases. *Acta Physiol Scand.* 168:27-31.

Koukouritaki, S.B., E.A. Vardaki, E.A. Papakonstanti, E. Lianos, C. Stournaras, and D.S. Emmanouel. 1999. TNF-alpha induces actin cytoskeleton reorganization in glomerular epithelial cells involving tyrosine phosphorylation of paxillin and focal adhesion kinase. *Mol Med.* 5:382-92.

Krause, M., J.E. Bear, J.J. Loureiro, and F.B. Gertler. 2002. The Ena/VASP enigma. *J Cell Sci.* 115:4721-6.

Krause, M., A.S. Sechi, M. Konradt, D. Monner, F.B. Gertler, and J. Wehland. 2000. Fyn-binding protein (Fyb)/SLP-76-associated protein (SLAP), Ena/vasodilator-stimulated phosphoprotein (VASP) proteins and the Arp2/3 complex link T cell receptor (TCR) signaling to the actin cytoskeleton. *J Cell Biol.* 149:181-94.

Krawczyk, C., and J.M. Penninger. 2001. Molecular controls of antigen receptor clustering and autoimmunity. *Trends Cell Biol.* 11:212-20.

Kwiatkowski, A.V., F.B. Gertler, and J.J. Loureiro. 2003. Function and regulation of Ena/VASP proteins. *Trends Cell Biol.* 13:386-92.

Lambrechts, A., A.V. Kwiatkowski, L.M. Lanier, J.E. Bear, J. Vandekerckhove, C. Ampe, and F.B. Gertler. 2000. cAMP-dependent protein kinase phosphorylation of EVL, a Mena/VASP relative, regulates its interaction with actin and SH3 domains. *J Biol Chem.* 275:36143-51.

Laping, N.J. 1999. Hepatocyte growth factor in renal disease: cause or cure? *Cell Mol Life Sci.* 56:371-7.

Larson, R.S., A.L. Corbi, L. Berman, and T. Springer. 1989. Primary structure of the leukocyte function-associated molecule-1 alpha subunit: an integrin with an embedded domain defining a protein superfamily. *J Cell Biol.* 108:703-12.

Lauffenburger, D.A., and A.F. Horwitz. 1996. Cell migration: a physically integrated molecular process. *Cell.* 84:359-69.

Laurent, V., T.P. Loisel, B. Harbeck, A. Wehman, L. Grobe, B.M. Jockusch, J.

Wehland, F.B. Gertler, and M.F. Carrier. 1999. Role of proteins of the Ena/VASP family in actin-based motility of *Listeria monocytogenes*. *J Cell Biol.* 144:1245-58.

Lebrand, C., E.W. Dent, G.A. Strasser, L.M. Lanier, M. Krause, T.M. Svitkina, G.G. Borisy, and F.B. Gertler. 2004. Critical role of Ena/VASP proteins for filopodia formation in neurons and in function downstream of netrin-1. *Neuron.* 42:37-49.

Levy, E.M., C.M. Viscoli, and R.I. Horwitz. 1996. The effect of acute renal failure on mortality. A cohort analysis. *JAMA.* 275:1489-94.

Li, Z., J. Ajdic, M. Eigenthaler, and X. Du. 2003. A predominant role for cAMP-dependent protein kinase in the cGMP-induced phosphorylation of vasodilator-stimulated phosphoprotein and platelet inhibition in humans. *Blood.* 101:4423-9.

Lieberthal, W., J.S. Koh, and J.S. Levine. 1998. Necrosis and apoptosis in acute renal failure. *Semin Nephrol.* 18:505-18.

Ling, H., P.E. Gengao, P.Y. Martin, A. Wangsiripaisan, R. Nemenoff, and R.W. Schrier. 1998. Effect of hypoxia on proximal tubules isolated from nitric oxide synthase knockout mice. *Kidney Int.* 53:1642-6.

Lollo, B.A., K.W. Chan, E.M. Hanson, V.T. Moy, and A.A. Brian. 1993. Direct evidence for two affinity states for lymphocyte function-associated antigen 1 on activated T cells. *J Biol Chem.* 268:21693-700.

- Loureiro, J.J., D.A. Rubinson, J.E. Bear, G.A. Baltus, A.V. Kwiatkowski, and F.B. Gertler. 2002. Critical roles of phosphorylation and actin binding motifs, but not the central proline-rich region, for Ena/vasodilator-stimulated phosphoprotein (VASP) function during cell migration. *Mol Biol Cell*. 13:2533-46.
- Lozano, E., and A. Cano. 1998. Cadherin/catenin complexes in murine epidermal keratinocytes: E-cadherin complexes containing either beta-catenin or plakoglobin contribute to stable cell-cell contacts. *Cell Adhes Commun*. 6:51-67.
- Lub, M., Y. van Kooyk, S.J. van Vliet, and C.G. Figdor. 1997. Dual role of the actin cytoskeleton in regulating cell adhesion mediated by the integrin lymphocyte function-associated molecule-1. *Mol Biol Cell*. 8:341-51.
- Lucas, C.E. 1976. The renal response to acute injury and sepsis. *Surg Clin North Am*. 56:953-75.
- Machesky, L.M., and A. Hall. 1996. Rho: a connection between membrane receptor signalling and the cytoskeleton. *Trends Cell Biol*. 6:304-10.
- Machesky, L.M., and R.H. Insall. 1999. Signaling to actin dynamics. *J Cell Biol*. 146:267-72.
- Machner, M.P., C. Urbanke, M. Barzik, S. Otten, A.S. Sechi, J. Wehland, and D.W. Heinz. 2001. ActA from *Listeria monocytogenes* can interact with up to four Ena/VASP homology 1 domains simultaneously. *J Biol Chem*. 276:40096-103.

Macian, F., C. Garcia-Rodriguez, and A. Rao. 2000. Gene expression elicited by NFAT in the presence or absence of cooperative recruitment of Fos and Jun. *Embo J.* 19:4783-95.

Maddox, D.A., and F.J. Gennari. 1987. The early proximal tubule: a high-capacity delivery-responsive site. *Am.J.Physiol.* 252:F573-84.

Madsen, K.M., and C.H. Park. 1987. Lysosome distribution and cathepsin B and L activity along the rabbit proximal tubule. *Am J Physiol.* 253:F1290-301.

Mangoo-Karim, R., M. Uchic, C. Lechene, and J.J. Grantham. 1989. Renal epithelial cyst formation and enlargement in vitro: dependence on cAMP. *Proc Natl Acad Sci U S A.* 86:6007-11.

Manns, J.M., K.J. Brenna, R.W. Colman, and S.B. Sheth. 2002. Differential regulation of human platelet responses by cGMP inhibited and stimulated cAMP phosphodiesterases. *Thromb Haemost.* 87:873-9.

Markewitz, B.A., J.R. Michael, and D.E. Kohan. 1993. Cytokine-induced expression of a nitric oxide synthase in rat renal tubule cells. *J Clin Invest.* 91:2138-43.

Matot, I., and Y. Gozal. 2004. Pulmonary responses to selective phosphodiesterase-5 and phosphodiesterase-3 inhibitors. *Chest.* 125:644-51.

Matsumoto, K., and T. Nakamura. 2002. Renotropic role and therapeutic potential of HGF in the kidney. *Nephrol Dial Transplant.* 17 Suppl 9:59-61.

McKeithan, T.W. 1995. Kinetic proofreading in T-cell receptor signal transduction.

*Proc Natl Acad Sci U S A.* 92:5042-6.

McLay, J.S., P. Chatterjee, A.G. Nicolson, A.G. Jardine, N.G. McKay, S.H. Ralston, P.

Grabowski, N.E. Haites, A.M. MacLeod, and G.M. Hawksworth. 1994. Nitric oxide production by human proximal tubular cells: a novel immunomodulatory mechanism?

*Kidney Int.* 46:1043-9.

Mitchison, T.J., and L.P. Cramer. 1996. Actin-based cell motility and cell locomotion.

*Cell.* 84:371-9.

Miyamoto, Y.J., B.F. Andruss, J.S. Mitchell, M.J. Billard, and B.W. McIntyre. 2003.

Diverse roles of integrins in human T lymphocyte biology. *Immunol Res.* 27:71-84.

Molitoris, B.A., A. Geerdes, and J.R. McIntosh. 1991. Dissociation and redistribution of

Na<sup>+</sup>,K<sup>(+)</sup>-ATPase from its surface membrane actin cytoskeletal complex during

cellular ATP depletion. *J Clin Invest.* 88:462-9.

Molitoris, B.A., and J. Marrs. 1999. The role of cell adhesion molecules in ischemic

acute renal failure. *Am J Med.* 106:583-92.

Molitoris, B.A., and M.C. Wagner. 1996. Surface membrane polarity of proximal

tubular cells: alterations as a basis for malfunction. *Kidney Int.* 49:1592-7.

Monks, C.R., B.A. Freiberg, H. Kupfer, N. Sciaky, and A. Kupfer. 1998. Three-dimensional segregation of supramolecular activation clusters in T cells. *Nature*. 395:82-6.

Montesano, R., K. Matsumoto, T. Nakamura, and L. Orci. 1991a. Identification of a fibroblast-derived epithelial morphogen as hepatocyte growth factor. *Cell*. 67:901-8.

Montesano, R., G. Schaller, and L. Orci. 1991b. Induction of epithelial tubular morphogenesis in vitro by fibroblast-derived soluble factors. *Cell*. 66:697-711.

Mullershausen, F., A. Friebe, R. Feil, W.J. Thompson, F. Hofmann, and D. Koesling. 2003. Direct activation of PDE5 by cGMP: long-term effects within NO/cGMP signaling. *J Cell Biol*. 160:719-27.

Mullershausen, F., D. Koesling, and A. Friebe. 2005. NO-sensitive guanylyl cyclase and NO-induced feedback inhibition in cGMP signaling. *Front Biosci*. 10:1269-78.

Mullershausen, F., M. Russwurm, W.J. Thompson, L. Liu, D. Koesling, and A. Friebe. 2001. Rapid nitric oxide-induced desensitization of the cGMP response is caused by increased activity of phosphodiesterase type 5 paralleled by phosphorylation of the enzyme. *J Cell Biol*. 155:271-8.

Murray, F., M.R. MacLean, and N.J. Pyne. 2002. Increased expression of the cGMP-inhibited cAMP-specific (PDE3) and cGMP binding cGMP-specific (PDE5) phosphodiesterases in models of pulmonary hypertension. *Br J Pharmacol*. 137:1187-94.

Muthusamy, N., and J.M. Leiden. 1998. A protein kinase C-, Ras-, and RSK2-dependent signal transduction pathway activates the cAMP-responsive element-binding protein transcription factor following T cell receptor engagement. *J Biol Chem.* 273:22841-7.

Myers, B.D., and S.M. Moran. 1986. Hemodynamically mediated acute renal failure. *N Engl J Med.* 314:97-105.

Nath, K.A., and S.M. Norby. 2000. Reactive oxygen species and acute renal failure. *Am J Med.* 109:665-78.

Nathan, C. 1992. Nitric oxide as a secretory product of mammalian cells. *Faseb J.* 6:3051-64.

Nathan, C. 1997. Inducible nitric oxide synthase: what difference does it make? *J Clin Invest.* 100:2417-23.

Nathan, C., and Q.W. Xie. 1994. Nitric oxide synthases: roles, tolls, and controls. *Cell.* 78:915-8.

Negri, A.L. 2004. Prevention of progressive fibrosis in chronic renal diseases: antifibrotic agents. *J Nephrol.* 17:496-503.

Neveu, H., D. Kleinknecht, F. Brivet, P. Loirat, and P. Landais. 1996. Prognostic factors in acute renal failure due to sepsis. Results of a prospective multicentre study. The French Study Group on Acute Renal Failure. *Nephrol Dial Transplant.* 11:293-9.

Niebuhr, K., F. Ebel, R. Frank, M. Reinhard, E. Domann, U.D. Carl, U. Walter, F.B. Gertler, J. Wehland, and T. Chakraborty. 1997. A novel proline-rich motif present in ActA of *Listeria monocytogenes* and cytoskeletal proteins is the ligand for the EVH1 domain, a protein module present in the Ena/VASP family. *Embo J.* 16:5433-44.

Nobes, C.D., and A. Hall. 1999. Rho GTPases control polarity, protrusion, and adhesion during cell movement. *J Cell Biol.* 144:1235-44.

Nogawa, H., and T. Mizuno. 1981. Mesenchymal control over elongating and branching morphogenesis in salivary gland development. *J Embryol Exp Morphol.* 66:209-21.

Noiri, E., A. Nakao, K. Uchida, H. Tsukahara, M. Ohno, T. Fujita, S. Brodsky, and M.S. Goligorsky. 2001. Oxidative and nitrosative stress in acute renal ischemia. *Am J Physiol Renal Physiol.* 281:F948-57.

Nose, A., A. Nagafuchi, and M. Takeichi. 1988. Expressed recombinant cadherins mediate cell sorting in model systems. *Cell.* 54:993-1001.

Osinski, M.T., and K. Schror. 2000. Inhibition of platelet-derived growth factor-induced mitogenesis by phosphodiesterase 3 inhibitors: role of protein kinase A in vascular smooth muscle cell mitogenesis. *Biochem Pharmacol.* 60:381-7.

Palmer, R.M., A.G. Ferrige, and S. Moncada. 1987. Nitric oxide release accounts for the biological activity of endothelium-derived relaxing factor. *Nature.* 327:524-6.

Penninger, J.M., and G.R. Crabtree. 1999. The actin cytoskeleton and lymphocyte activation. *Cell*. 96:9-12.

Peter, K., and T.E. O'Toole. 1995. Modulation of cell adhesion by changes in alpha L beta 2 (LFA-1, CD11a/CD18) cytoplasmic domain/cytoskeleton interaction. *J Exp Med*. 181:315-26.

Peterson, E.J. 2003. The TCR ADAPts to integrin-mediated cell adhesion. *Immunol Rev*. 192:113-21.

Peterson, E.J., M.L. Woods, S.A. Dmowski, G. Derimanov, M.S. Jordan, J.N. Wu, P.S. Myung, Q. Liu, J.T. Pribila, B.D. Freedman, Y. Shimizu, and G.A. Koretsky. 2001a. Coupling of the TCR to integrin activation by SLAP-130/Fyb. *Science*. 293:2263-2265.

Peterson, E.J., M.L. Woods, S.A. Dmowski, G. Derimanov, M.S. Jordan, J.N. Wu, P.S. Myung, Q.H. Liu, J.T. Pribila, B.D. Freedman, Y. Shimizu, and G.A. Koretzky. 2001b. Coupling of the TCR to integrin activation by Slap-130/Fyb. *Science*. 293:2263-5.

Piepenhagen, P.A., and W.J. Nelson. 1998. Biogenesis of polarized epithelial cells during kidney development in situ: roles of E-cadherin-mediated cell-cell adhesion and membrane cytoskeleton organization. *Mol Biol Cell*. 9:3161-77.

Pistor, S., T. Chakraborty, U. Walter, and J. Wehland. 1995. The bacterial actin nucleator protein ActA of *Listeria monocytogenes* contains multiple binding sites for host microfilament proteins. *Curr Biol*. 5:517-25.

Pittet, D., S. Rangel-Frausto, N. Li, D. Tarara, M. Costigan, L. Rempe, P. Jebson, and R.P. Wenzel. 1995. Systemic inflammatory response syndrome, sepsis, severe sepsis and septic shock: incidence, morbidities and outcomes in surgical ICU patients. *Intensive Care Med.* 21:302-9.

Pollack, A.L., R.B. Runyan, and K.E. Mostov. 1998. Morphogenetic mechanisms of epithelial tubulogenesis: MDCK cell polarity is transiently rearranged without loss of cell-cell contact during scatter factor/hepatocyte growth factor-induced tubulogenesis. *Dev Biol.* 204:64-79.

Puddicombe, S.M., R. Polosa, A. Richter, M.T. Krishna, P.H. Howarth, S.T. Holgate, and D.E. Davies. 2000. Involvement of the epidermal growth factor receptor in epithelial repair in asthma. *Faseb J.* 14:1362-74.

Puls, A., A.G. Eliopoulos, C.D. Nobes, T. Bridges, L.S. Young, and A. Hall. 1999. Activation of the small GTPase Cdc42 by the inflammatory cytokines TNF(alpha) and IL-1, and by the Epstein-Barr virus transforming protein LMP1. *J Cell Sci.* 112 ( Pt 17):2983-92.

Racusen, L.C. 1995. The histopathology of acute renal failure. *New Horiz.* 3:662-8.

Rahilly, M.A., and S. Fleming. 1993. The specificity of integrin-ligand interactions in cultured human renal epithelium. *J Pathol.* 170:297-303.

Rangel-Frausto, M.S., D. Pittet, M. Costigan, T. Hwang, C.S. Davis, and R.P. Wenzel. 1995. The natural history of the systemic inflammatory response syndrome (SIRS). A prospective study. *Jama*. 273:117-23.

Ray, P., W. Tang, P. Wang, R. Homer, C. Kuhn, 3rd, R.A. Flavell, and J.A. Elias. 1997. Regulated overexpression of interleukin 11 in the lung. Use to dissociate development-dependent and -independent phenotypes. *J Clin Invest*. 100:2501-11.

Reinhard, M., K. Giehl, K. Abel, C. Haffner, T. Jarchau, V. Hoppe, B.M. Jockusch, and U. Walter. 1995. The proline-rich focal adhesion and microfilament protein VASP is a ligand for profilins. *Embo J*. 14:1583-9.

Reinhard, M., M. Halbrugge, U. Scheer, C. Wiegand, B.M. Jockusch, and U. Walter. 1992. The 46/50 kDa phosphoprotein VASP purified from human platelets is a novel protein associated with actin filaments and focal contacts. *Embo J*. 11:2063-70.

Reinhard, M., M. Rudiger, B.M. Jockusch, and U. Walter. 1996. VASP interaction with vinculin: a recurring theme of interactions with proline-rich motifs. *FEBS Lett*. 399:103-7.

Renfranz, P.J., and M.C. Beckerle. 2002. Doing (F/L)PPPPs: EVH1 domains and their proline-rich partners in cell polarity and migration. *Curr Opin Cell Biol*. 14:88-103.

Ridley, A.J., and A. Hall. 1992. The small GTP-binding protein rho regulates the assembly of focal adhesions and actin stress fibers in response to growth factors. *Cell*. 70:389-99.

Rivas, F.V., J.P. O'Keefe, M.L. Alegre, and T.F. Gajewski. 2004. Actin cytoskeleton regulates calcium dynamics and NFAT nuclear duration. *Mol Cell Biol.* 24:1628-39.

Rogers, K.K., T.S. Jou, W. Guo, and J.H. Lipschutz. 2003. The Rho family of small GTPases is involved in epithelial cystogenesis and tubulogenesis. *Kidney Int.* 63:1632-44.

Rosario, M., and W. Birchmeier. 2003. How to make tubes: signaling by the Met receptor tyrosine kinase. *Trends Cell Biol.* 13:328-35.

Rottner, K., B. Behrendt, J.V. Small, and J. Wehland. 1999. VASP dynamics during lamellipodia protrusion. *Nat Cell Biol.* 1:321-2.

Royal, I., N. Lamarche-Vane, L. Lamorte, K. Kaibuchi, and M. Park. 2000. Activation of cdc42, rac, PAK, and rho-kinase in response to hepatocyte growth factor differentially regulates epithelial cell colony spreading and dissociation. *Mol Biol Cell.* 11:1709-25.

Rudd, C.E., and H. Wang. 2003. Hematopoietic adaptors in T-cell signaling: potential applications to transplantation. *Am J Transplant.* 3:1204-10.

Rybalkin, S.D., C. Yan, K.E. Bornfeldt, and J.A. Beavo. 2003. Cyclic GMP phosphodiesterases and regulation of smooth muscle function. *Circ Res.* 93:280-91.

Ryser, J.E., E. Rungger-Brandle, C. Chaponnier, G. Gabbiani, and P. Vassalli. 1982.

The area of attachment of cytotoxic T lymphocytes to their target cells shows high motility and polarization of actin, but not myosin. *J Immunol.* 128:1159-62.

Sakurai, H., T. Tsukamoto, C.A. Kjelsberg, L.G. Cantley, and S.K. Nigam. 1997. EGF receptor ligands are a large fraction of in vitro branching morphogens secreted by embryonic kidney. *Am J Physiol.* 273:F463-72.

Salerno, J.C., D.E. Harris, K. Irizarry, B. Patel, A.J. Morales, S.M. Smith, P. Martasek, L.J. Roman, B.S. Masters, C.L. Jones, B.A. Weissman, P. Lane, Q. Liu, and S.S. Gross. 1997. An autoinhibitory control element defines calcium-regulated isoforms of nitric oxide synthase. *J Biol Chem.* 272:29769-77.

Sampath, R., P.J. Gallagher, and F.M. Pavalko. 1998. Cytoskeletal interactions with the leukocyte integrin beta2 cytoplasmic tail. Activation-dependent regulation of associations with talin and alpha-actinin. *J Biol Chem.* 273:33588-94.

Santos, O.F., and S.K. Nigam. 1993. HGF-induced tubulogenesis and branching of epithelial cells is modulated by extracellular matrix and TGF-beta. *Dev Biol.* 160:293-302.

Sariola, H., and K. Sainio. 1997. The tip-top branching ureter. *Curr Opin Cell Biol.* 9:877-84.

Saxen, L., and H. Sariola. 1987. Early organogenesis of the kidney. *Pediatr Nephrol.* 1:385-92.

Scapin, G., S.B. Patel, C. Chung, J.P. Varnerin, S.D. Edmondson, A. Mastracchio, E.R. Parmee, S.B. Singh, J.W. Becker, L.H. Van der Ploeg, and M.R. Tota. 2004. Crystal structure of human phosphodiesterase 3B: atomic basis for substrate and inhibitor specificity. *Biochemistry*. 43:6091-100.

Schmidt, A., and M.N. Hall. 1998. Signaling to the actin cytoskeleton. *Annu Rev Cell Dev Biol*. 14:305-38.

Schneider, U., H.U. Schwenk, and G. Bornkamm. 1977. Characterization of EBV-genome negative "null" and "T" cell lines derived from children with acute lymphoblastic leukemia and leukemic transformed non-Hodgkin lymphoma. *Int J Cancer*. 19:621-6.

Schnermann, J. 1998. Juxtaglomerular cell complex in the regulation of renal salt excretion. *Am J Physiol*. 274:R263-79.

Sechi, A.S., and J. Wehland. 2004. ENA/VASP proteins: multifunctional regulators of actin cytoskeleton dynamics. *Front Biosci*. 9:1294-310.

Shultz, P.J., and L. Raij. 1992. Endogenously synthesized nitric oxide prevents endotoxin-induced glomerular thrombosis. *J Clin Invest*. 90:1718-25.

Sim, A.T., and J.D. Scott. 1999. Targeting of PKA, PKC and protein phosphatases to cellular microdomains. *Cell Calcium*. 26:209-17.

Sims, T.N., and M.L. Dustin. 2002. The immunological synapse: integrins take the stage. *Immunol Rev.* 186:100-17.

Skoble, J., V. Auerbuch, E.D. Goley, M.D. Welch, and D.A. Portnoy. 2001. Pivotal role of VASP in Arp2/3 complex-mediated actin nucleation, actin branch-formation, and *Listeria monocytogenes* motility. *J Cell Biol.* 155:89-100.

Small, J.V., I. Kaverina, O. Krylyshkina, and K. Rottner. 1999a. Cytoskeleton cross-talk during cell motility. *FEBS Lett.* 452:96-9.

Small, J.V., K. Rottner, and I. Kaverina. 1999b. Functional design in the actin cytoskeleton. *Curr Opin Cell Biol.* 11:54-60.

Smolenski, A., C. Bachmann, K. Reinhard, P. Honig-Liedl, T. Jarchau, H. Hoschuetzky, and U. Walter. 1998. Analysis and regulation of vasodilator-stimulated phosphoprotein serine 239 phosphorylation in vitro and in intact cells using a phosphospecific monoclonal antibody. *J Biol Chem.* 273:20029-35.

Snapper, S.B., F.S. Rosen, E. Mizoguchi, P. Cohen, W. Khan, C.H. Liu, T.L.

Hagemann, S.P. Kwan, R. Ferrini, L. Davidson, A.K. Bhan, and F.W. Alt. 1998.

Wiskott-Aldrich syndrome protein-deficient mice reveal a role for WASP in T but not B cell activation. *Immunity.* 9:81-91.

Solez, K., L. Morel-Maroger, and J.D. Sraer. 1979. The morphology of "acute tubular necrosis" in man: analysis of 57 renal biopsies and a comparison with the glycerol model. *Medicine (Baltimore).* 58:362-76.

Sponsel, H.T., R. Breckon, W. Hammond, and R.J. Anderson. 1994. Mechanisms of recovery from mechanical injury of renal tubular epithelial cells. *Am J Physiol.* 267:F257-64.

Springer, T.A. 1990. Adhesion receptors of the immune system. *Nature.* 346:425-34.

Sriskandan, S., and J. Cohen. 1995. The pathogenesis of septic shock. *J Infect.* 30:201-6.

Stanley, P., P.A. Bates, J. Harvey, R.I. Bennett, and N. Hogg. 1994. Integrin LFA-1 alpha subunit contains an ICAM-1 binding site in domains V and VI. *Embo J.* 13:1790-8.

Stuehr, D.J. 1997. Structure-function aspects in the nitric oxide synthases. *Annu Rev Pharmacol Toxicol.* 37:339-59.

Szabowski, A., N. Maas-Szabowski, S. Andrecht, A. Kolbus, M. Schorpp-Kistner, N.E. Fusenig, and P. Angel. 2000. c-Jun and JunB antagonistically control cytokine-regulated mesenchymal-epidermal interaction in skin. *Cell.* 103:745-55.

Taub, M., Y. Wang, T.M. Szczesny, and H.K. Kleinman. 1990. Epidermal growth factor or transforming growth factor alpha is required for kidney tubulogenesis in matrigel cultures in serum-free medium. *Proc Natl Acad Sci U S A.* 87:4002-6.

Thiemermann, C., C. Szabo, J.A. Mitchell, and J.R. Vane. 1993. Vascular hyporeactivity to vasoconstrictor agents and hemodynamic decompensation in hemorrhagic shock is mediated by nitric oxide. *Proc Natl Acad Sci U S A.* 90:267-71.

Thiery, J.P., and B. Boyer. 1992. The junction between cytokines and cell adhesion. *Curr Opin Cell Biol.* 4:782-92.

Tilley, D.G., and D.H. Maurice. 2002. Vascular smooth muscle cell phosphodiesterase (PDE) 3 and PDE4 activities and levels are regulated by cyclic AMP in vivo. *Mol Pharmacol.* 62:497-506.

Tisher, C.C., S. Rosen, and G.B. Osborne. 1969. Ultrastructure of the proximal tubule of the rhesus monkey kidney. *Am J Pathol.* 56:469-517.

Tominaga, T., K. Sugie, M. Hirata, N. Morii, J. Fukata, A. Uchida, H. Imura, and S. Narumiya. 1993. Inhibition of PMA-induced, LFA-1-dependent lymphocyte aggregation by ADP ribosylation of the small molecular weight GTP binding protein, rho. *J Cell Biol.* 120:1529-37.

Valitutti, S., M. Dessing, K. Aktories, H. Gallati, and A. Lanzavecchia. 1995. Sustained signaling leading to T cell activation results from prolonged T cell receptor occupancy. Role of T cell actin cytoskeleton. *J Exp Med.* 181:577-84.

van der Merwe, P.A. 2002. Formation and function of the immunological synapse. *Curr Opin Immunol.* 14:293-8.

van Kooyk, Y., S.J. van Vliet, and C.G. Figdor. 1999. The actin cytoskeleton regulates LFA-1 ligand binding through avidity rather than affinity changes. *J Biol Chem.* 274:26869-77.

van Kooyk, Y., P. Weder, K. Heije, and C.G. Figdor. 1994. Extracellular Ca<sup>2+</sup> modulates leukocyte function-associated antigen-1 cell surface distribution on T lymphocytes and consequently affects cell adhesion. *J Cell Biol.* 124:1061-70.

van Lambalgen, A.A., A.A. van Kraats, G.C. van den Bos, H.V. Stel, J. Straub, A.J. Donker, and L.G. Thijs. 1991. Renal function and metabolism during endotoxemia in rats: role of hypoperfusion. *Circ Shock.* 35:164-73.

Vasioukhin, V., C. Bauer, M. Yin, and E. Fuchs. 2000. Directed actin polymerization is the driving force for epithelial cell-cell adhesion. *Cell.* 100:209-19.

Volkman, B.F., K.E. Prehoda, J.A. Scott, F.C. Peterson, and W.A. Lim. 2002. Structure of the N-WASP EVH1 domain-WIP complex: insight into the molecular basis of Wiskott-Aldrich Syndrome. *Cell.* 111:565-76.

Walders-Harbeck, B., S.Y. Khaitlina, H. Hinssen, B.M. Jockusch, and S. Illenberger. 2002. The vasodilator-stimulated phosphoprotein promotes actin polymerisation through direct binding to monomeric actin. *FEBS Lett.* 529:275-80.

Walker, J.F., A.D. Cumming, R.M. Lindsay, K. Solez, and A.L. Linton. 1998. The renal response produced by non-hypotensive crisis in a large animal model. *American Journal of Kidney Disease.* 8:88-97.

Walter, U., M. Eigenthaler, J. Geiger, and M. Reinhard. 1993. Role of cyclic nucleotide-dependent protein kinases and their common substrate VASP in the regulation of human platelets. *Adv Exp Med Biol.* 344:237-49.

Walter, U., J. Geiger, C. Haffner, T. Markert, C. Nehls, R.E. Silber, and P. Schanzenbacher. 1995. Platelet-vessel wall interactions, focal adhesions, and the mechanism of action of endothelial factors. *Agents Actions Suppl.* 45:255-68.

Wang, F., V.M. Weaver, O.W. Petersen, C.A. Larabell, S. Dedhar, P. Briand, R. Lupu, and M.J. Bissell. 1998. Reciprocal interactions between beta1-integrin and epidermal growth factor receptor in three-dimensional basement membrane breast cultures: a different perspective in epithelial biology. *Proc Natl Acad Sci U S A.* 95:14821-6.

Wang, H., F.E. McCann, J.D. Gordan, X. Wu, M. Raab, T.H. Malik, D.M. Davis, and C.E. Rudd. 2004. ADAP-SLP-76 binding differentially regulates supramolecular activation cluster (SMAC) formation relative to T cell-APC conjugation. *J Exp Med.* 200:1063-74.

Wange, R.L., and L.E. Samelson. 1996. Complex complexes: signaling at the TCR. *Immunity.* 5:197-205.

Weidner, K.M., G. Hartmann, M. Sachs, and W. Birchmeier. 1993. Properties and functions of scatter factor/hepatocyte growth factor and its receptor c-Met. *Am J Respir Cell Mol Biol.* 8:229-37.

Welch, M.D., J. Rosenblatt, J. Skoble, D.A. Portnoy, and T.J. Mitchison. 1998.

Interaction of human Arp2/3 complex and the *Listeria monocytogenes* ActA protein in actin filament nucleation. *Science*. 281:105-8.

Weston, C.R., and R.J. Davis. 2001. Signal transduction: signaling specificity- a complex affair. *Science*. 292:2439-40.

Wilkinson, B., H. Wang, and C.E. Rudd. 2004. Positive and negative adaptors in T-cell signalling. *Immunology*. 111:368-74.

Wiseman, J.W., C.A. Goddard, D. McLelland, and W.H. Colledge. 2003. A comparison of linear and branched polyethylenimine (PEI) with DCCchol/DOPE liposomes for gene delivery to epithelial cells in vitro and in vivo. *Gene Ther*. 10:1654-62.

Witke, W., J.D. Sutherland, A. Sharpe, M. Arai, and D.J. Kwiatkowski. 2001. Profilin I is essential for cell survival and cell division in early mouse development. *Proc Natl Acad Sci U S A*. 98:3832-6.

Woodhall, P.B., C.C. Tisher, C.A. Simonton, and R.R. Robinson. 1978. Relationship between para-aminohippurate secretion and cellular morphology in rabbit proximal tubules. *J Clin Invest*. 61:1320-9.

Woods, M.L., and Y. Shimizu. 2001. Signaling networks regulating beta1 integrin-mediated adhesion of T lymphocytes to extracellular matrix. *J Leukoc Biol*. 69:874-80.

Xie, Q.W., H.J. Cho, J. Calaycay, R.A. Mumford, K.M. Swiderek, T.D. Lee, A. Ding, T. Troso, and C. Nathan. 1992. Cloning and characterization of inducible nitric oxide synthase from mouse macrophages. *Science*. 256:225-8.

Yamasaki, N., T. Nagano, I. Mori-Kudo, A. Tsuchida, T. Kawamura, H. Seki, M. Taiji, and H. Noguchi. 2002. Hepatocyte growth factor protects functional and histological disorders of HgCl<sub>2</sub>-induced acute renal failure mice. *Nephron*. 90:195-205.

Yang, M.Y., T.C. Liu, J.G. Chang, P.M. Lin, and S.F. Lin. 2003. JunB gene expression is inactivated by methylation in chronic myeloid leukemia. *Blood*. 101:3205-11.

Yaqoob, M., C.L. Edelstein, E.D. Wieder, A.M. Alkhunaiza, P.E. Gengaro, R.A. Nemeroff, and R.W. Schrier. 1996. Nitric oxide kinetics during hypoxia in proximal tubules: effects of acidosis and glycine. *Kidney Int*. 49.

Yin, K.J., J.M. Lee, S.D. Chen, J. Xu, and C.Y. Hsu. 2002. Amyloid-beta induces Smac release via AP-1/Bim activation in cerebral endothelial cells. *J Neurosci*. 22:9764-70.

Zegers, M.M., L.E. O'Brien, W. Yu, A. Datta, and K.E. Mostov. 2003. Epithelial polarity and tubulogenesis in vitro. *Trends Cell Biol*. 13:169-76.

Zhang, W., H. Ke, A.P. Tretiakova, B. Jameson, and R.W. Colman. 2001. Identification of overlapping but distinct cAMP and cGMP interaction sites with cyclic nucleotide phosphodiesterase 3A by site-directed mutagenesis and molecular modeling based on crystalline PDE4B. *Protein Sci*. 10:1481-9.

Zhang, W., Y. Wu, L. Du, D.D. Tang, and S.J. Gunst. 2005. Activation of the Arp2/3 complex by N-WASp is required for actin polymerization and contraction in smooth muscle. *Am J Physiol Cell Physiol.* 288:C1145-60.

Zuk, A., and K.S. Matlin. 1996. Apical beta 1 integrin in polarized MDCK cells mediates tubulocyst formation in response to type I collagen overlay. *J Cell Sci.* 109 ( Pt 7):1875-89.

## Appendix

<b>Plasmid</b>	<b>Source</b>	<b>Plasmid content</b>
pFC-MEKK	Stratagene	Mitogen-activated protein/ERK kinase kinases gene.
pFC-PKA	Stratagene	cAMP-dependent protein kinase A gene (transcriptional activator of CREB)
pFC2-dbd	Stratagene	GAL-4 DNA binding domain
pAP-1-Luc	Stratagene	Activator Protein-1 gene linked to luciferase gene
pNFκB-Luc	Stratagene	Nuclear factor-κB (NFκB) linked to luciferase gene
pNFAT-Luc	Stratagene	Nuclear factor of activated T cells (NFAT) linked to luciferase gene
pFR-Luc	Stratagene	Luciferase reporter plasmid
pFA2-CREB	Stratagene	Activation domain of CREB (cAMP-response element binding protein)
pTRE2hyg	BD Clontech	Tetracycline regulatable, empty vector
pTRE2hyg/DN-VASP	BD Clontech/Produced in Laboratory	Tetracycline regulatable vector, containing sequence for expression of DN-VASP
pCI	Promega	Carrier DNA, empty vector
pCIS-CK	Stratagene	Negative control plasmid

**Appendix 1. Plasmids used in signal transduction pathway experiments in Jurkat TetOff cells** (section 4.2.6)